Impacts of Climate Change on Irrigated Agriculture in the Eastern Nile Region

Special Study – Final Report

Jeremy S Pal

Table of Contents

1 Executive Summary

In this special study, the potential impacts of climate change on irrigation and agriculture in the Eastern Nile basin are investigated. The specific objectives are to quantify the potential impacts of climate change on potential evaporation and crop yields; and to address the impact of climate change on cropping patterns. These objectives are met by (1) determining, quantifying, and assessing both climate change in recent decades and projections of end of century climate in the Eastern Nile basin; and (2) by determining the present day and future crop suitability and water needs.

The former is conducted through an extensive literature survey addressing past and future climate change; an extensive analysis of recent climate change using observational data; and an extensive analysis end of century high resolution nested regional climate model projections of climate change based on both a high and low IPCC greenhouse gas emissions scenarios. The latter is conducted applying the observations and climate change projections from the former to determine crop suitability (operative and optimal) for the basic five crop groups and to determine the water needs for a variety of crops typical to the Eastern Nile region using the FAO Crop Coefficient method. Of important note, terrain characteristics, such as soil type and slope, are not considered in the analysis and would likely result in significant reductions on regions suitable for cultivation.

The findings show that Eastern Nile basin temperatures and precipitation have increased by more than 1° C and 100 mm in the past 30 years. Both these values are well over the global average of 0.16 C per decade and 1.1 mm per decade. End of century projected changes of mean surface temperature are up to 4.5° C in the lower emissions scenario and up to 9° C in the higher emissions scenario. In regions where irrigated agriculture is prevalent such as in the Gazira region, feedbacks from evaporative cooling would likely result in a reduction of the projected warming by a degree or two. Precipitation changes are regionally dependent especially in the low emissions scenario. Of particular note, in the high emissions scenario precipitation and resulting water availability increases in the wettest months (July and August) and decreases in the surrounding months (April through June; September and October).

The projected changes in temperature, regardless of the emissions scenario result in considerable changes in crop suitability. In general, there are both spatial and temporal shifts in suitability. Crops suited for cooler climates shift north and south out of Sudan and southern Egypt to higher elevations such as the Ethiopian Highlands and north to the Nile Delta. In addition, crops suitable in warmer months shift to the cooler winter months. The largest decreases are to Group I crops (e.g., wheat, barley, oats, and potatoes) and Group II crops (e.g., rice, cotton, cassava, and groundnut), which become unsuitable in much of the region due to their lower temperature suitability range. On the contrary, Group III crops (e.g., maize, sorghum, and millet) tend to benefit in terms total area suitable for cultivation due to their higher temperature suitability range.

Although the Eastern Nile region remains suitable for crop growth, the areas of optimal growth reduce considerably regardless of whether or not farmers shift to crops better suited for warmer climates and shift the growing season to cooler periods. The resulting decrease in productivity with a warmer climate would to some extent likely be compensated by improvements in agricultural technologies and by the fertilization effect from the increased atmospheric carbon dioxide. However, populations are also expected to grow substantially, which would increase agricultural demand.

Crop evapotranspiration increases substantially over the entire region due to the increases in projected temperatures and resulting increases in reference evapotranspiration. This results in a substantial increase in irrigation required to meet the crops needs (except in summer in the Ethiopian Highlands where rainfall increases). Shifting the primary growing season to cooler periods can help compensate the additional irrigation requirements; however Nile flows are lowest during the cooler portions of the year. As a result, additional storage (e.g., reservoirs) in the upstream portions of the basin would be required.

2 ENTRO and Special Study Background

Set up in February, 1999 NBI is a cooperative transitional mechanism of the ten riparian countries[1] designed to promote basin-wide cooperation for sustainable socio-economic development of, and benefit from, the common Nile Basin water resources. The NBI seeks to develop the river in a cooperative manner, share substantial socioeconomic benefits, and promote regional peace and security. Its Strategic Action Program is made up of two complementary programs: the basin-wide *Shared Vision Program* to build confidence and capacity across the basin, and *Subsidiary Action Programs* to initiate concrete investments and action on the ground at sub-basin levels. The programs are reinforcing in nature. The Shared Vision Program, which focuses on building regional institutions, capacity, and trust, lays the foundation for unlocking the development potential of the Nile, which can be realized through the Subsidiary Action Program (SAP). At present there are two SAPs at the sub-basin levels of the Eastern Nile (ENSAP) and the Nile Equatorial Lakes (NELSAP). ENSAP is served by the Eastern Nile Technical Regional Office (ENTRO), located in Addis Ababa, Ethiopia, while NELSAP Coordination Unit is in Kigali, Rwanda.

ENSAP seeks to realize the NBI Shared Vision for the Eastern Nile region, and is aimed at the reduction of poverty, achieve economic growth, and the reversal of environmental degradation in the Eastern Nile Region.

There is general agreement that climate change will increase the vulnerability in Africa as a whole, including in the Eastern Nile region (IPCC, 2007). As such, the 2006-2010 Strategy of ENTRO addresses the immediacy of the threats of climate change. The individual ENSAP projects accordingly sought to address their respective project-specific climate change issues, but only to realize the need for a coordinated ENSAP level climate change programmatic approach and strategy.

In 2009 ENTRO laid down the foundation of its systematic response to climate change issues. Through Netherlands Support, it commissioned a study to develop an Approach Paper as base for formulation of the requisite strategy. The Approach Paper recommended a comprehensive five-pillar Climate Change Strategy to respond to the challenges and opportunities associated with climate change in Eastern Nile cooperation. It was widely disseminated, and the draft strategy was reviewed in a series of consultations at various levels prior to its finalization and adoption.

In 2010 ENTRO took the Strategy further and commissioned the formulation of a Climate proofing Consolidated Action Plan, to identify a list of specific activities to climate-proof ENSAP projects. This Action Plan has been finalized through a consultative and review and quality assurance process.

ENTRO's climate change strategy has five pillars strategy of Prediction, Adaptation, Mitigation, Education, and Financing opportunities. Among these five pillars adaptation comes first as water resources is the first and the hardest to be impacted by climate change and mainstreaming climate change adaptation will be complementing country

[1] Member countries include: Burundi, DRC, Egypt, Ethiopia, Kenya, Rwanda, Tanzania and Uganda. Eritrea is an observer.

efforts in adaptation actions specially from the transboundary river basin perspective. For example, efficient water management and water use is better addressed from a transboundary perspective and this will complement national efforts in adaptation to climate change at large and especially in water resources.

While it is virtual certain climate change resulting from anthropogenic greenhouse gas emissions will occur in the Eastern Nile region via an increase in surface temperature, considerable uncertainty regarding the direction and magnitude on hydrological variables remains (IPCC, 2007). For example, it is unknown how Nile River mean flow, flow extremes, and seasonal variations will respond to climate change. In case of a decrease in mean flow (and/or large population increase), the demand-supply gap will need to be closed and large-scale efforts to increase productivity, manage demand and augment flow may be required to adapt to climate change. In the case of an increase in flow, flood control measures may be required.

Agriculture is a key focus due to its obvious links to weather and climate, as well as the inelastic demand for staple food commodities. Although there is some consensus that warming will likely be harmful to agriculture in Africa and the Eastern Nile region, active debate continues about whether warming will result in a net gain or loss mainly due to uncertainties in changes to precipitation, evapotranspiration and runoff. However, it is expected that such warming will have substantial impacts on agricultural yields by the end of the century. This impact will vary by region and crop type.

3 Objectives and Methodology

ENTRO has commissioned this special study to identify these impacts on irrigation and agriculture and potential adaptation measures. The specific objectives of the special study are:

1. Quantify the potential impacts of *climate change* on *potential evaporation* and *crop yields* over the Eastern Nile region
2. Address the impact of *climate change* on *cropping patterns* in the region.

To address the special study objectives, the following are quantified and determined based on the existing literature and latest projections of climate change in the Eastern Nile region:

1. The role of anthropogenic climate change versus natural variability in the Eastern Nile region and potential impacts on hydrology and agriculture;
2. Climate change impacts on potential evapotranspiration in the Eastern Nile different climatic regions and with varying vegetation covers and cropping patterns;
3. Impacts of climate change on various crop yields including addressing feasibility, productivity and water requirements for crops such as wheat, cotton, sorghum, Coffee Arabica as well as other crops that may become more suitable for this region under future climates.

These are achieved by conducting a series of tasks including a literature review; an analysis of past observations; an analysis of climate change projections; and a crop suitability analysis for both present climate and future projections of climate. At the end of the project, recommendations are provided.

3.1 Literature Review

An extensive survey of existing documents on climate change is performed to aid in the quantification past and future climate change as well as potential impacts of climate change on hydrology and agriculture in the Eastern Nile basin. The primary sources of information to be surveyed are the IPCC Fourth Assessment Report, peer-reviewed literature, and other credible documents such as those published by the Food and Agriculture Organization of the United Nations. By surveying the literature, insight in the Eastern Nile basin should be gained into recent changes climate, as well as, the latest projections of climate change and associated uncertainties.

3.2 Recent Climate Change

In this phase of the study, an extensive analysis of recent climate change is performed using observational data from various sources (see Table 1). The purpose is to gain an understanding of climate variability under present day conditions for the entire Eastern Nile basin and the four major sub-basins. The primary variables to be analyzed are mean, minimum and maximum temperature (T_{mean}, T_{min}, T_{max}, respectively);

precipitation (P); evapotranspiration (ET); and potential evapotranspiration (PET). The analyses are performed for each of the four Eastern Nile subbasins as well as on a 0.5-degree resolution grid for the entire basin.

3.3 Climate Change Projections

In this phase of the special study, end of century projections of climate change based on two IPCC greenhouse gas emissions scenarios are assessed from high-resolution nested regional climate model simulations. The primary variables to be analyzed are the same as those of the analysis of observations: mean, minimum and maximum temperature; precipitation; evapotranspiration; potential evapotranspiration; and discharge. The aim this phase is to develop an understanding of changes to mean climate and its variability.

3.4 Crop Suitability and Scenarios

The potential impacts of climate change on agriculture in the Eastern Nile basin include those on irrigation water requirements. Under a warmer climate and an atmosphere that is richer in carbon dioxide, both potential evaporation and crop coefficients are likely to change. General speaking, potential evaporation is expected to increase due to the increase in temperature, while crop coefficients may decrease because of the carbon dioxide fertilization effect; however, the are other competing factors that impact both the signs and magnitudes of the changes. Depending on the relative magnitudes of these two changes, the overall magnitude of evaporative demand by crops may increase or decrease.

The goal in this phase of the study is to determine crop suitability in the Eastern Nile region on the 0.5 degree grid established in the observational analysis and the modeled climate change projections (Sections 5 and 6, respectively). Suitability of the primary crops types of the Eastern Nile region are determined based on the FAO (1985) optimal crop suitably temperature range (see Table 3). This is done using the temperature data from both CRU datasets for each year and growing season. The number of years in the period 1980 through 2009 that each crop is suitable are determined as part of the analysis. The future climate is determined by computing the differences between the simulated future and present day climates. The simulated changes in climate are then added to the observations.

3.5 Recommendations

In this final phase, recommendations are made based on the above findings. This includes possible adjustments in crop types and cropping patterns as well as other measures to adapt to these impacts.

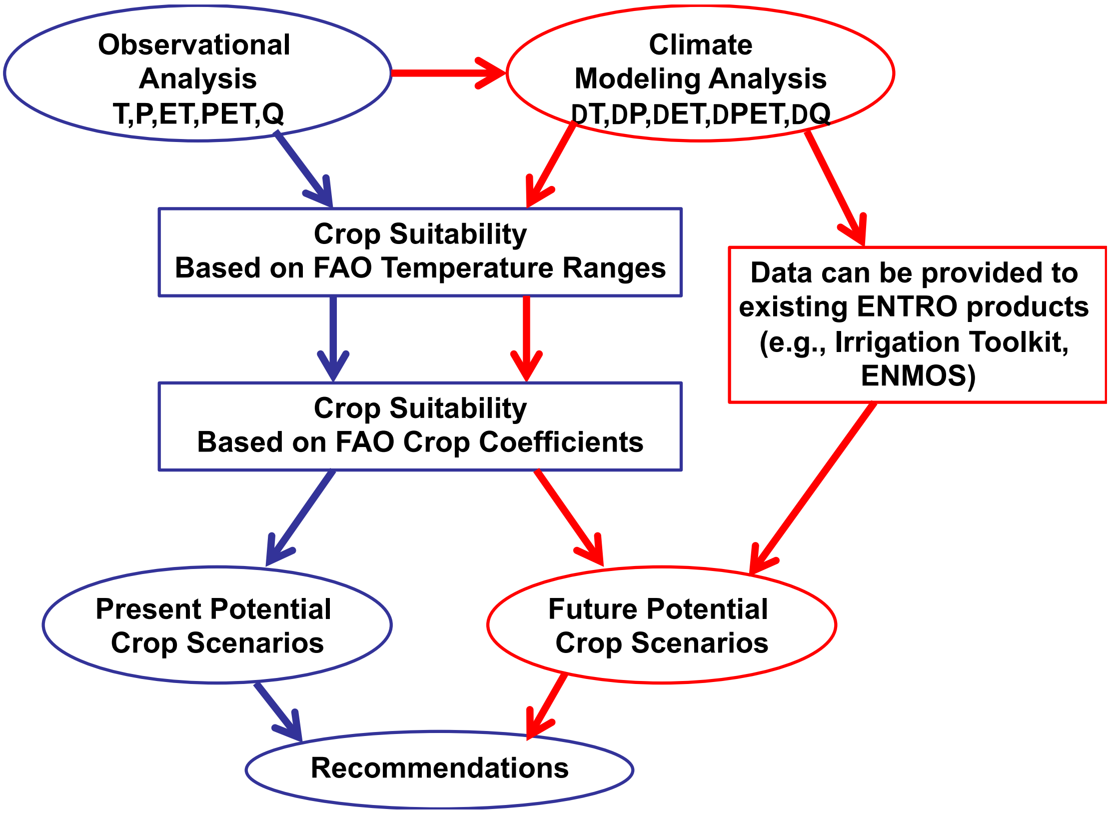

Figure 1: Summary of the methodology to be applied in this study.

4 Literature Review

Climate change is undeniably occurring and poses significant risks to a wide range of societies and natural systems (IPCC 2007). The latest report by the Intergovernmental Panel on Climate Change (IPCC) states global average surface air and ocean temperatures are increasing at rates unequivocal to any other period on record including paleo records (IPCC 2007; Figure 2).

In the last few decades, droughts have become more common, especially in the tropics and subtropics and increases have occurred in the number of heavy precipitation events. These extreme conditions, expected to be exacerbated in the future, have already caused substantial flooding and food shortage, and constitute significant threats to water resource and public health management (Parry et al. 2007). For Africa, based on climate model results, warming is very likely (90 to 99% probability) to be larger than the globally average in all seasons by the end of the 21st century, particularly in drier subtropical regions. Africa is thus one of the most vulnerable continents to such changes; a situation aggravated by different interactions between population and ecosystems and low adaptive capacity.

This is particularly true for East Africa where agriculture is the prominent instrument for spurring growth, enhancing food security, and overcoming poverty (Boko 2007). This is also a region that experiences high water stress and faces recurrent and localized drought and increased food shortage. It is thus not surprising that in recent decades competition for Nile River water utilization has become a matter of major interest for the countries sharing the basin (Evans 1990; Adar et al. 2007).

The Nile River is the world's longest river flowing from south to north with an estimated length of 6800 km spanning more than 30 degrees of latitude. The Eastern Nile (EN) basin, depicted in Figure 3, spans a variety of hydro-climatic zones ranging from tropical wet climate to semi-arid and arid climates (Elshamy et al. 2009). It encompasses four countries (Ethiopia, South Sudan, Sudan, and Egypt) and provides a wide variety of resources that include hydropower, irrigation and domestic water, fisheries, and wetland agriculture (Ibrahim 1984; Dumont 2009).

The majority of the Nile water supply originates through rainfall upstream in the Blue Nile in the Ethiopian highlands and the White Nile at the Equatorial Lake Plateau. The Blue Nile contributes up to 60% of the Nile mean annual flow and is characterized by its seasonal flow due to summer monsoon rains. The White Nile arises in the headwaters of Lake Victoria, a region of heavy, year-round rainfall (Arnell 1999).

The changes in riverflow in upstream countries are of major importance to the sustainable development of downstream countries such as Egypt and Sudan where most of the Nile water is consumed (Yates and Strzepek 1998; Tafesse 2001). The agriculture activities in the Eastern Nile region, especially in Egypt, depend on rainfall in the upper reaches of the Nile such as in the Ethiopian Highlands and Lake Victoria (Gornall et al. 2012). Water resources and agriculture over the Nile basin are therefore potentially vulnerable to climate change (Yates et al. 1998, Conway 2005).

4.1 Observed Changes

In this subsection, a literature review of climate change in recent decades is performed for the EN basin. The studies reviewed are based on observations of surface temperature, precipitation, and riverflow.

4.1.1 Surface Temperature

At current, IPCC (2007) states that global surface temperatures have risen by more than 0.75° C since 1850. Temperatures in EN basin have increased considerably less over the same period. Since 1979, however, temperature in the EN region has increased by approximately of 0.4 per decade, well above the global average of 0.16° C per decade.

The spatial and temporal patterns of recent temperature change vary substantially across the Basin. For instance, Conway et al. (2004) show that minimum daily temperatures have increased slightly faster than maximum daily temperatures in Ethiopia. King'uyu et al. (2000) observe decreasing temperature trends in most parts of eastern Africa, especially in the Great Lakes region. For Egypt, decreasing maximum and increasing minimum temperature trends are observed for the period 1941-2000 during winter. In contrast, during the summer season, increasing trend prevailed for both maximum and minimum temperature (Domroes and El-Tantawi 2005; Hasanean and Basset 2006). Generally, the majority of these studies reveal warming trends in the EN basin in the last 50 years; however, the patterns of warming vary spatially and temporally, but are becoming gradually more evident in recent last decades.

4.1.2 Precipitation

While it is expected that a warmer climate will result in an increase in global average precipitation, due to increased evaporation and resulting atmospheric water vapor, the direction of change in average precipitation (increase or decrease) will depend on the region (IPCC 2007). Changes due to climate patterns such as El Nino-Southern Oscillation (ENSO) and northern and southern hemisphere annual modes control the direction of precipitation changes.

Rainfall in the EN basin exhibits significant spatial and temporal variability embedded in patterns more complex than those observed for temperature (Hulme et al. 2005; Conway et al. 2007). Conway (2005) concludes that significant fluctuations in rainfall have occurred in the humid headwaters of the EN over decadal timescales with marked consequences on the Nile flows. Earlier studies show mixed precipitation trends over the Nile basin (Flohn H. 1987; Conway and Hulme 1993; Beltrando and Camberlin, 1993; Seleshi and Demaree 1995; Camberlin 1997).

More recent studies have identified a clear decreasing trend in precipitation amount in most of the basin. For example, Conway (2000) analyze a basin-wide time series of annual rainfall constructed from 11 gauges for the period 1900 to 1998 and find that precipitation over the basin shows a marked decrease between the mid-1960s and the late 1980s. Osman and Sauerborn (2002) indicate that the second half of the 20th century suffered predominantly negative rainfall anomalies over Ethiopia, supporting the results of Conway (2000). In another study, Seleshi and Zanke (2004) report that the annual and the June-September total rainfalls for the period 1965-2002 show a significant decline since around 1982 over most of the eastern basin. Camberlin (2009), based on Climate Research Unit precipitation data for the period 1950-2000, find that most the Nile basin has undergone a downward rainfall trend. This trend is much more pronounced in northern Sudan, the Darfur region, and southwestern Ethiopia with a decrease ranging from 35 to 50%. According to the IPCC (2007), since 1901 parts of the Eastern Nile region have experienced significant drying. Since 1979, however, no statistical change has been observed in the region.

4.1.3 Riverflow

These climate fluctuations have dramatically changed both the structure and the regime of the Nile River (Said 1993) and suggest that small changes in climate conditions can result in relatively large changes in runoff and water availability. This is supported by Conway and Hulme (1996) who show based on experiments over the Blue Nile and Lake Victoria that runoff response is greater than the size of the precipitation anomaly. Along the same lines, Elshamy et al. (2009) show that runoff is more sensitive to precipitation changes than to potential evapotranspiration changes and that the sensitivity increases with the aridity of the catchment. Such sensitivity to precipitation along with the increasing water demand led to prolonged period of low flows during the 1970s and 1980s, and flow high flows during 1990s (Abu-Zeid and Bisway 1991; Conway and Hulme 1996).

Overall, recent literature analyzing precipitation and riverflow records during the 20th century reveal a generally downward trend embedded in high interannual and interdecadal variability over the EN basin. The variability is not only observed locally in the headwater regions (e.g., humid Ethiopian and East African highlands) but also regionally through its effects downstream in Sudan, South Sudan, and Egypt (e.g., Gleick 1991; Conway and Hulme 1993, Yates and Strzepek 1998, Conway 2005; Beyene et al. 2007; Tesemma et al. 2010). The effects of these climate conditions are manifested through droughts and famine, floods, and substantial changes in the flow of the Nile River.

4.2 Climate Change Projections

In this subsection, a literature review of climate change projections for the EN basin is performed. The studies reviewed are based on results from climate models with varying levels of anthropogenic greenhouse gas levels.

4.2.1 Surface Temperature

The IPCC (2007) report indicates for the A1B Special Report on Emissions Scenarios (SRES; IPCC, 2000), which is considered a mid-range emissions scenario, end of century annual temperature increase by 3.0 to greater than 3.5° C with the greatest increase at the Egypt-Sudan border (Figure 4). Seasonally, increases of 2.5 to 3.5° C are projected for the months of December, January, February (DJF) and 3.0 to 4.0° C for the months of June, July and August (JJA). The intermodel variability around the temperature projections is typically ±0.5° C.

4.2.2 Precipitation

The drying trend which affect most parts of the EN, occurring from the second half of the 20th Century along with the potential impact of global change associated with increasing GHGs, have prompted speculations about future climate of the Nile basin.

Most of the climate change projections based on anthropogenic greenhouse gas emissions scenarios for the Nile basin are based on results from few Global Climate Models (GCMs). For instance, Strzepek et al. (1996) use three GCMs (UKMO, GISS and GFDL) to evaluate future changes in the Nile basin under a doubled pre-industrial atmospheric carbon dioxide concentration scenario and predict an increase in the basin-averaged rainfall by approximately 5-17%.

Future climate change projections applying the IPCC SRES emission scenarios show complex and variable patterns for precipitation. For example, Elshamy (2000) use 16 transient experiments from seven different GCMs participating to the IPCC Third Assessment Report (TAR; IPCC 2001) and find that some of the models exhibit up to an 18% increase in precipitation over the basin while others project up to a 22% reduction. Hulme et al. (2001), on the contrary, analyzing 10 experiments from seven atmosphere-ocean GCMs (AOGCMs or coupled GCMs) under the SRES B1 scenario B1 (a relatively low emissions scenario) and A2 (a relatively high emissions scenario), find that the majority of the models predict precipitation decreases for much of the EN.

According to the IPCC (2007) Fourth Assessment report, climate model projections of annual precipitation from the A1B SRES emissions scenario in the EN basin range from -25% in Egypt to +20% in Sudan and only a slight increase in Ethiopia. In DJF, the projections range from -40% in Egypt and Sudan to +50% in Ethiopia; while in JJA, they range from -40% in Egypt to +25% in Sudan and little change in Ethiopia. However, similar to the findings of Elshamy (2000), there is little model agreement with these projections as about half of the models project an increase in precipitation and half a decrease over the region.

4.2.3 Riverflow

Strzepek et al. (2001) show that eight out of the nine climate change scenarios analyzed result in reductions of Nile flows during the 21st century as consequence of precipitation decreases. Furthermore, Sayed (2004), evaluating four GCMs, suggest that rainfall will increase in the Blue and White Nile basins by approximately 1 to 11% by 2030.

In studies specific to the Nile basin, many studies attempt to estimate changes in runoff and riverflow based on projections of future climate over the basin. For instance, Tate et al. (2004) analyze the sensitivity of the water balance of Lake Victoria to climate change using HadCM3 forced by the A2 and B2 SRES scenarios. Their results reveal that changes in annual rainfall and evaporation result in a decrease in lake water levels during the 2021-2050 time period and an increase in levels during the 2021-2050 time period. More recently, Elshamy et al. (2009) run an ensemble of climate change scenarios using the Nile Forecasting Model with bias corrected precipitation and temperatures from 17 coupled GCMs for the 2081-2098 period and find that the upper Blue Nile is very sensitive to precipitation and moderately sensitive to temperature. On average, a 10% precipitation change leads to a 30% streamflow change and a 1°C temperature change leads to a 4% streamflow change.

Beyene et al. (2010) assess the impacts of climate change on the hydrology and water resources of the Nile basin using bias corrected and spatially downscaled simulations from 11 GCMs forced by two IPCC SRES scenarios and a macro-scale hydrological model. Their multi-model ensemble suggests an increase Nile riverflow during the period 2010-2039 due to overall increase in precipitation and a decrease during the periods 2040-2069 and 2070-2099 due to both a decrease in precipitation and increase in evaporation.

Overall, model projections of the potential hydrological impacts of climate change over the Nile basin display differing trends in both sign and magnitude over the basin.

4.2.4 Agriculture

Changes in climate due to increased emissions of anthropogenic greenhouse gases are expected to have widespread impacts on agriculture and food production in many regions over East Africa (Lobell et al. 2008; Burke et al. 2009). Therefore, the threat of food security due to climate change is of serious concern for the EN. The aforementioned uncertainties of precipitation and riverflow presented in the previous sections, however, make it difficult to unambiguously assess the associated changes in agriculture. The uncertainties should be accounted for when projecting impacts of climate change on agriculture.

Conway and Hulme (1996) find from their experiments of possible future Nile riverflow ranging from a 30% increase to a 77% decrease. These diverse changes lead to a wide range of agricultural yield changes. Yates and Strzepek (1998a, b) establish that under doubled pre-industrial atmospheric carbon dioxide concentrations that agriculture is negatively affected by climate change as a result of impacts associated with changes in local and regional biophysical systems. In a later study, however, Strzepek and Yates (1999) use dry and wet climate scenarios to examine the future conditions in water resources along with the possible impacts on agriculture. They find that, under the wet climate scenario, there is a surplus of annual water amount, which remains unused suggesting possible expansion of future irrigation as suggested by (Conway 2005). For the drier scenarios, water availability becomes less common and thus constrains agricultural production into the 21st century. As a result, they suggest that the water resources should be allocated to less water demanding crops, livestock, and non-agricultural sectors.

Projected warming of surface temperatures may also lead to increased flood and drought in EN basin (Funk et al. 2005). Such extremes can have serious impacts on agriculture including land degradation from topsoil erosion and nutrient leaching. Additional studies investigating crop yields attempt to estimate the impact of climate change on food production over East Africa (Pearce et al. 1996; McCarthy et al. 2001; Parry et al. 2004; Stern 2007). Davidson et al. (2003), for example, reveal that although the food demand is predicted to double over the next three decades, agriculture yields and food production per capita have been steadily decreasing. Yields in millet and sorghum are predicted to decline in Sudan due to increasing climate variability, decreases in annual precipitation, and a possible southward shift of humid agro-climatic zones.

Increasing variability in the rain season start, duration, and rainfall amount can substantially disrupt subsistence agricultural production and food security. Thornton et al. (2008), in comparing current and future production over part of the Nile basin, find that if all the highlands areas were cropped, the regional production of beans and maize would decline by 1-3% for the lower emission scenario and by 11-15% for the higher-emission scenario by 2050s. In addition, their results show that crop yield responses to the changing rainfall amounts and patterns and the generally increasing temperatures vary by crop type, location, and climate model used.

It is, however, recognized that spatial and temporal changes in precipitation and temperature patterns shift agro-ecological zones (Kurukulasuriya and Mendelsohn 2008) and thus have major impacts on the viability of both dryland (Challinor et al. 2005) and irrigated farming (Knox et al. 2010) in the EN basin. Jaramillo et al. (2011) suggest that, although coffee production has already benefited from the temperature rise in East Africa, production is projected to decrease in the future in region over the Nile Basin, especially over Ethiopia.

It is thus evident, that there is a growing consensus in the scientific literature that over the coming decades, higher temperatures and changing precipitation levels caused by climate change will reduce crop yields in much of the EN basin. Climate change is therefore projected to compromise agricultural production, especially in smallholder systems with little adaptive capacity, as is currently prevalent in many parts of the EN basin.

4.3 Summary

The range of uncertainties in the change of climate change and the related impacts on water resources and agriculture over the EN basin tend to be wide with no consensus even on the sign and magnitude (Buontempo et al. 2009). Beyene et al. (2010) state that most of these studies are limited by the coarse spatial resolution of the GCMs used and the small number of GCMs that can be evaluated. The use of regional climate models (RCMs) to dynamically downscale GCM projections and drive impact models over the EN basin is starting to emerge. Only a few studies, however, are available in the literature (Mohamed et al. 2005; Anyah et al. 2006; Moore et al. 2012).

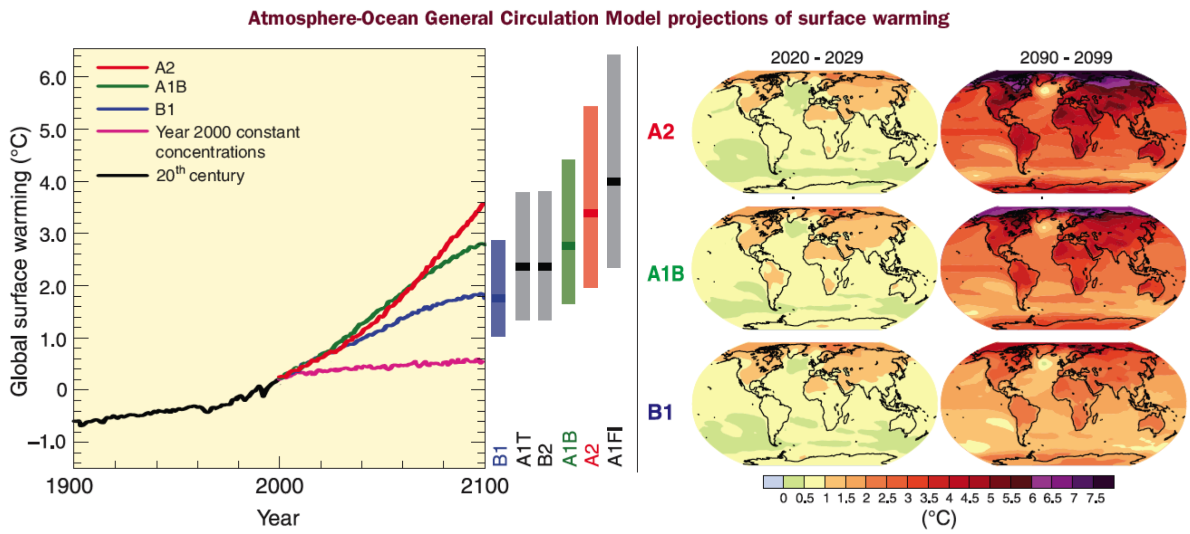

Figure 2: Global Temperature Projections from State-of-the-Science Climate Models. Figure adapted from IPCC (2007).

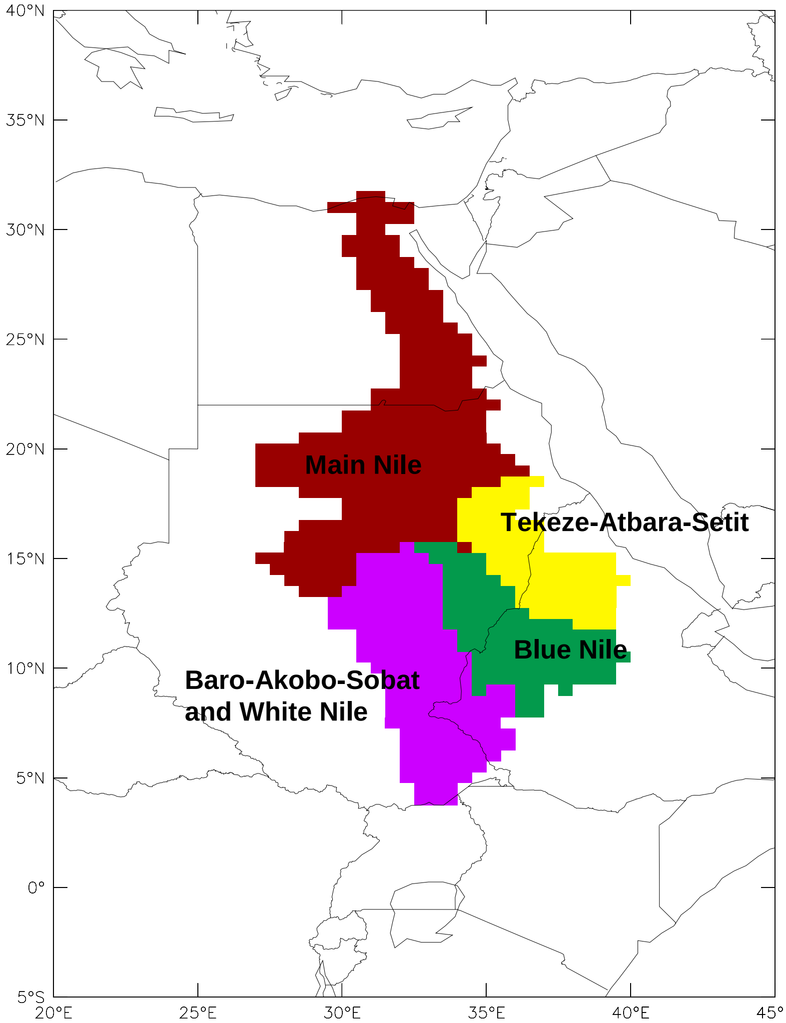

Figure 3: Eastern Nile Basin interpolated to a 0.5 degree grid. The different colors represent the different subbasins.

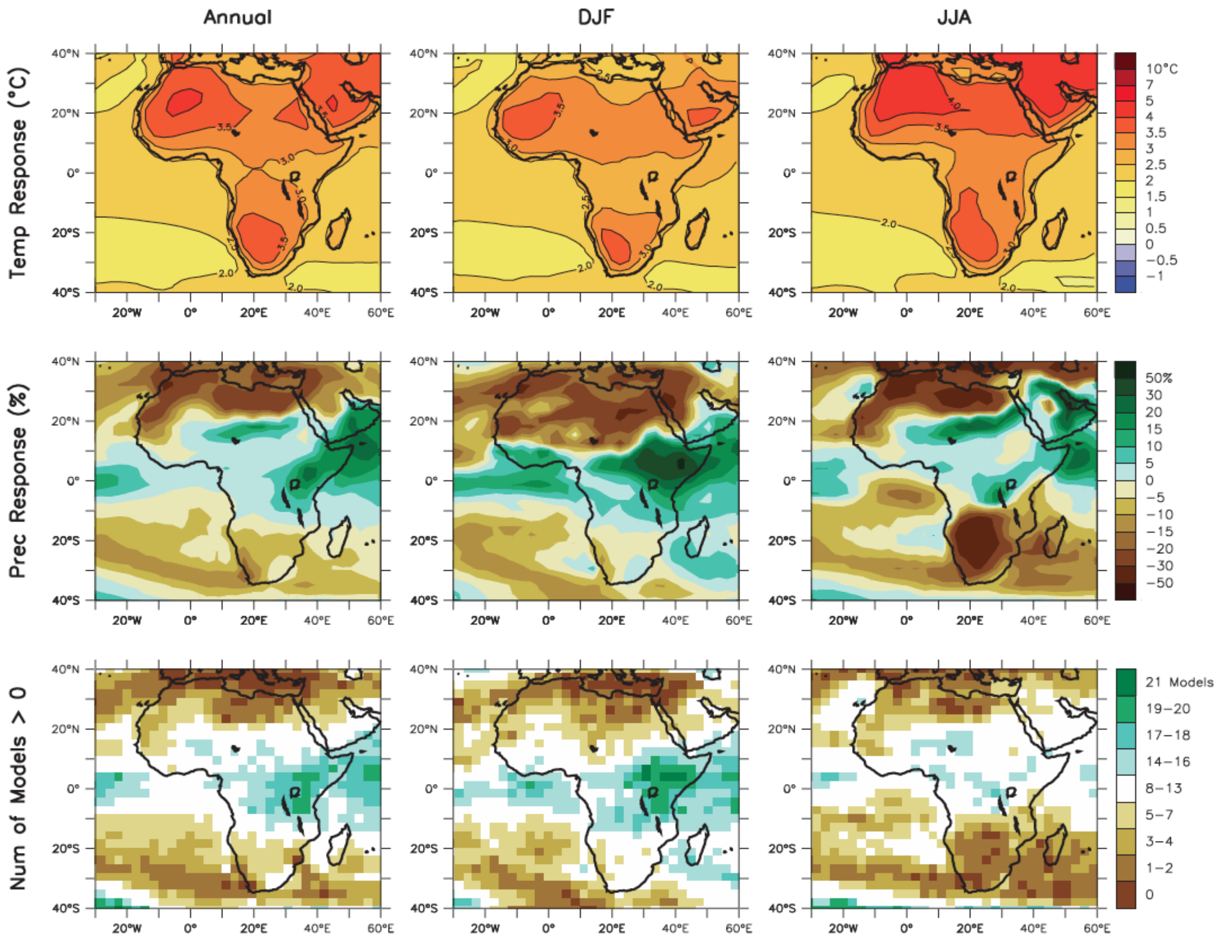

Figure 4: IPCC AR4 Projections of Temperature and Precipitation. Adapted from IPCC (2007).

5 Recent Climate Change

In this phase of the study, an extensive analysis of recent climate change is performed using observational data from various sources (see Table 1). The purpose is to gain an understanding of climate variability under present day conditions for the Eastern Nile basin sub-basins. The primary variables to be analyzed are mean, minimum and maximum temperature (T_{mean}, T_{min}, T_{max}, respectively); precipitation (P); evapotranspiration (ET); potential evapotranspiration (PET); and aridity index (AI=ET/PET). The analysis is performed for each of the four Eastern Nile subbasins as well as on a 0.5-degree resolution grid for the entire basin.

A climatology and trends in mean, minimum and maximum temperature; precipitation, potential evapotranspiration, and aridity index is analyzed for the past 30 years (1980-2009) using the 0.5-degree resolution global gridded datasets of the Climate Research Unit (CRU; Mitchell, et al, 2003) and the University of Delaware (UDEL; Willmott and Matsuura, 2001). Both of these datasets provide monthly data from the beginning of last century to present. The UDEL dataset additionally includes evapotranspiration, which used to compute the aridity index, both of which are included in the analysis.

The deliverables for this phase are provided below:

1. 0.5° resolution maps of seasonal T_{mean}, T_{min}, T_{max}, P, PET and AI;
2. Basin average time series plots of annual T_{mean}, T_{min}, T_{max}, P, PET and AI;
3. Annual trends of T_{mean}, T_{min}, T_{max}, P, PET and AI.
4. Basin average plots of monthly T_{mean}, T_{min}, T_{max}, P, PET and AI;

5.1 Monthly Climatology

In this subsection, monthly climatologies based on the period 1980 to 2009 are computed for the aforementioned variables using the aforementioned datasets.

5.1.1 Precipitation

Figure 5 and Figure 6 depict the monthly precipitation climatology for the EN basin from January through December for the CRU and UDEL datasets, respectively. Precipitation during January, February, and March (JFM) in both products is mostly limited to Ethiopia and southern South Sudan. From April, the amount increases and extends northward to cover most of eastern Sudan. Maxima are located in northern Ethiopia during July, August, and September (JAS) with accumulated rainfall reaching 400 mm. It should be noted that UDEL provides slightly higher precipitation amounts than CRU around regions of maxima, a feature that may be related to the differences in the number of rain gauges considered and interpolation procedures. In October, the rainband starts to retreat southward and in December, it is again confined in Ethiopia. It should be emphasized that throughout the whole year and in both observational datasets, Egypt receives very little rainfall and thus depends largely on the Nile riverflow originating from Ethiopia for agriculture.

5.1.2 Surface Temperature

The mean (Figure 7 and Figure 8), minimum (Figure 9) and maximum temperatures (Figure 10) display similar spatial patterns. Throughout the whole year, the Ethiopian Highlands and Mediterranean Egypt experience the cooler temperatures and the continental Sudan and South Sudan. However, during July, August, and September, Ethiopia is considerably cooler than Egypt, primarily due to higher rainfall amounts and elevation. For both mean and minimum temperature, the warmest months are June, July, August, and September while for the maximum temperature, the largest warmest months, in terms of magnitude and spatial extent, occur in May and June.

5.1.3 Surface Moisture

Potential evapotranspiration (*PET*) from CRU observations (Figure 11) does not follow the patterns of minimum, maximum and mean temperatures. The maxima are located just north of the warmest temperatures. This is particularly true for the July, August, and September and generally true from May through September when *PET* is lowest upstream regions of the basin and largest in downstream regions implying higher irrigation demand in northern regions. It should be emphasized that UDEL exhibits lower values compared to CRU suggesting existence of uncertainty in the methods used to compute *PET* (Figure 12). The corresponding monthly UDEL evapotranspiration (*ET*) values closely follow the pattern of precipitation (Figure 13). *ET* tends to follow the seasonality of precipitation. Values are lowest during the dry season (November through March), with any significant values limited to Ethiopia. As the rainband migrates northward into South Sudan and Sudan during the summer, so does the *ET*.

Surplus of water occurs only in Ethiopia in the summer season suggesting potentials for extension of irrigation (Figure 14). Unlike the surplus, the spatial distribution of deficit exhibits a clear annual cycle closely related to *PET* (Figure 15). Thus, the highest deficit is experienced during the summer season in northern Sudan and most of Egypt. Such distribution may suggest less water-demanding irrigated crops upstream. The aridity index, defined as the ratio between *ET* and *PET*, exhibits a similar pattern than *ET* and is confided in the lower part of the EN basin where *ET* is greater than zero (Figure 16). *ET* is much lower than *PET* around northern Ethiopia during JFM. However, as the summer approaches, the aridity index increases to values slightly greater than one and extends toward central Sudan, suggesting that ET tends to be equal to, and over Ethiopia sometimes exceeds PET. During the last three months of the year, although the highest values retreat southward, values are closer to one in Ethiopia. This indicates that South Sudan and Ethiopia hold ample water resources that may be sufficient for irrigated agriculture throughout the year. In contrast, northern Sudan and many parts of Egypt display an extremely low aridity index suggesting indicating that irrigation is required for successful for agriculture, consistent to the deficit of water resources discussed above.

In summary, the EN basin exhibits two regions with different hydro-climatological characteristics: a wetter region in Ethiopia and South Sudan experiencing higher precipitation and lower *PET* maintaining a surplus of water availability which make it suitable for agricultural activities (assuming good terrain and soil conditions); and an arid region in Sudan and Egypt primarily on the Nile river irrigation for agricultural activities.

5.2 Annual Trends

In this context, it is interesting to analyze trends in the different hydro-climatic variables to seek out and examine systematic historical patterns over the different region of the EN basin. The majority of the studies available in literature analyze trends in the EN basin for a period ending before or up to the year 2000 (Flohn 1987; Conway and Hulme 1993; Beltrando and Camberlin, 1993; Seleshi and Demaree 1995; Conway and Hulme 1996; Camberlin 1997; Conway 2000; Hulme 2001; Osman and Sauerborn 2002; Seleshi and Zanke 2004; Hulme et al. 2005; Camberlin 2009). A few of them include years between 2001 and 2005 in their analysis (Conway et al. 2007; Elshamy et al. (2009) Bayene et al. 2010; Tessema et al. 2010). It is thus useful to extend the analyses to the current climate (up to 2009) and specifically to the EN basin. Computed trends based are based on annual means from CRU and UDEL for the entire EN basin and for the Main Nile (MN), Tezeke-Setite-Atbara (TSA), Baro-Akobo-Sobat-White Nile (BASWN) and the Blue Nile (BN) sub-basins.

5.2.1 Precipitation

Precipitation in both datasets display increasing trends over the Nile basin except for in the southern portion of the basin in Ethiopia (Figure 17 and Figure 18). The trend from the UDEL observations is more pronounced, especially in central Sudan and southern Sudan/Ethiopia border. This is confirmed considering the trends in the different sub-basins. For example, the entire EN basin displays a trend of 19 mm per decade with the CRU data versus 34 mm per decade with the UDEL data. A common feature is that precipitation is highly variable with a clear positive trend in all sub-basins and BASWN experiences the largest change per decade (48 mm/decade with CRU and 63 mm/decade with UDEL).

5.2.2 Temperature

The corresponding temperature trends for mean, minimum and maximum temperature over the entire basin and the same sub-regions mentioned above derived from CRU (mean, minimum and maximum) and UDEL (mean only) exhibit a generally positive trend (Figure 19 through Figure 22). This indicates that temperature has risen in most parts of the EN basin except in gezira region in Sudan where evaporative cooling due to irrigation may be damping the climate change signal. Consistent with IPCC (2007), the regions that display the most warming include northern Sudan and Egypt. This general warming is a result of increasing trends in both maximum and minimum temperatures. In Egypt, however, minimum temperature has risen more than maximum temperature narrowing the diurnal temperature range. This suggests that Egypt has experienced lesser cold nights in the recent decades. In northern Sudan and most parts of Ethiopia, maximum temperature has increased more than minimum temperature indicating that the region has been affected by hotter days. In the Gezira region of Sudan, both minimum and maximum temperatures have undergone a cooling trend consistent with mean temperature.

The general increase in temperature trends can also be detected in the sub-basins. Mean, minimum, and maximum temperatures increase in all subbasins expect in the BN where most of the warming accounts only for maximum temperature. The highest warming rate per decade occurs in the MN. An interesting feature is that in the MN along with the TSA, minimum temperature has risen faster than maximum by approximately 0.2 to 0.6 degree Celsius per decade. This suggests, as indicated above, this region has encountered more warm nights than the rest of the EN basin. The positive temperature trends should strongly impact *PET* and *ET*.

5.2.3 Surface Moisture

PET in both observational datasets exhibits a substantial increasing trend of about 20-60 mm per decade each of the subbasins (Figure 23 and Figure 24). Most of the trends between the datasets are similar. The lone exception is TSA where the UDEL trends is approximately twice that of CRU.

The spatial distribution of *ET* trend closely follows that of precipitation with an increase in most part of the basin and a decrease in northern Egypt (Figure 25). The highest increase is observed in central Sudan and South Sudan, where the lowest temperature trend is observed. Thus, this increasing trend in *ET* may be caused by strong cloud-radiation feedback and elevated evaporative cooling. While the entire EN basin undergoes a positive change of only 29 mm per decade embedded in a low-level variability, BASWN exhibits high inter-annual variations and a trend with a slope of more than 56 mm per decade indicating that *ET* trends in the EN sub-basin are highly heterogeneous.

This heterogeneity is considerably more evident in the surplus trend in Ethiopia (Figure 26). In fact, while most of the EN basin displays a slight increase of surplus of water, Ethiopia exhibits a mixed trend of alternating increases and decreases from the southwest to the northeast. As a consequence, the surplus in the entire EN basin is highly variable with no marked trend observed. This result is also observed in the different subbasins.

Contrary to the surplus trends, water deficit reveal significant trends that substantially vary across the basin in both sign and magnitude leading to no significant change once average over the entire EN basin (Figure 27). A decreasing water deficit trend is only detected in central Sudan and South Sudan, while Egypt, northern Sudan and northeastern Ethiopia exhibit a positive trend in water deficit, which potential threaten agricultural activities in these regions. Consistent to the spatial distribution, the highest decrease occurs in BASWN (approximately -2.5 mm per decade) while the highest increase occurs over MN with a slope of about 1.6 mm per decade.

The aridity index closely matches the evapotranspiration (Figure 28). It tends to increase in almost all the EN and subbasins with a net slope of about 2-3 percent per decade. This indicates that *ET* relative to *PET* has been increasing in recent decades, suggesting less stressed moisture conditions.

In general, the EN basin experienced significant and widespread precipitation fluctuations, and exhibits a marked increasing trend of about 19 – 31 mm per decade since 1980. In addition, while Egypt has been experiencing less cold nights, northern Sudan and most part of Ethiopia have been affected by warmer summer days. The region has become less arid as indicated by increasing precipitation and aridity index, despite the increasing trend of *PET*. Furthermore, the water resources deficit has decreased in South Sudan, but increased in northeastern Ethiopia, northern Sudan and Egypt.

Table 1: Datasets, variables and temporal and spatial resolution to be used in this study.

Dataset	Time Period	Temporal Resolution	Spatial Resolution	P	T_{mean}	T_{max}	T_{min}	ET	PET	AI
CRU	1901-2010	Monthly	0.5°	X	X	X	X		X	
UDEL	1900-2009	Monthly	0.5°	X	X			X	X	X

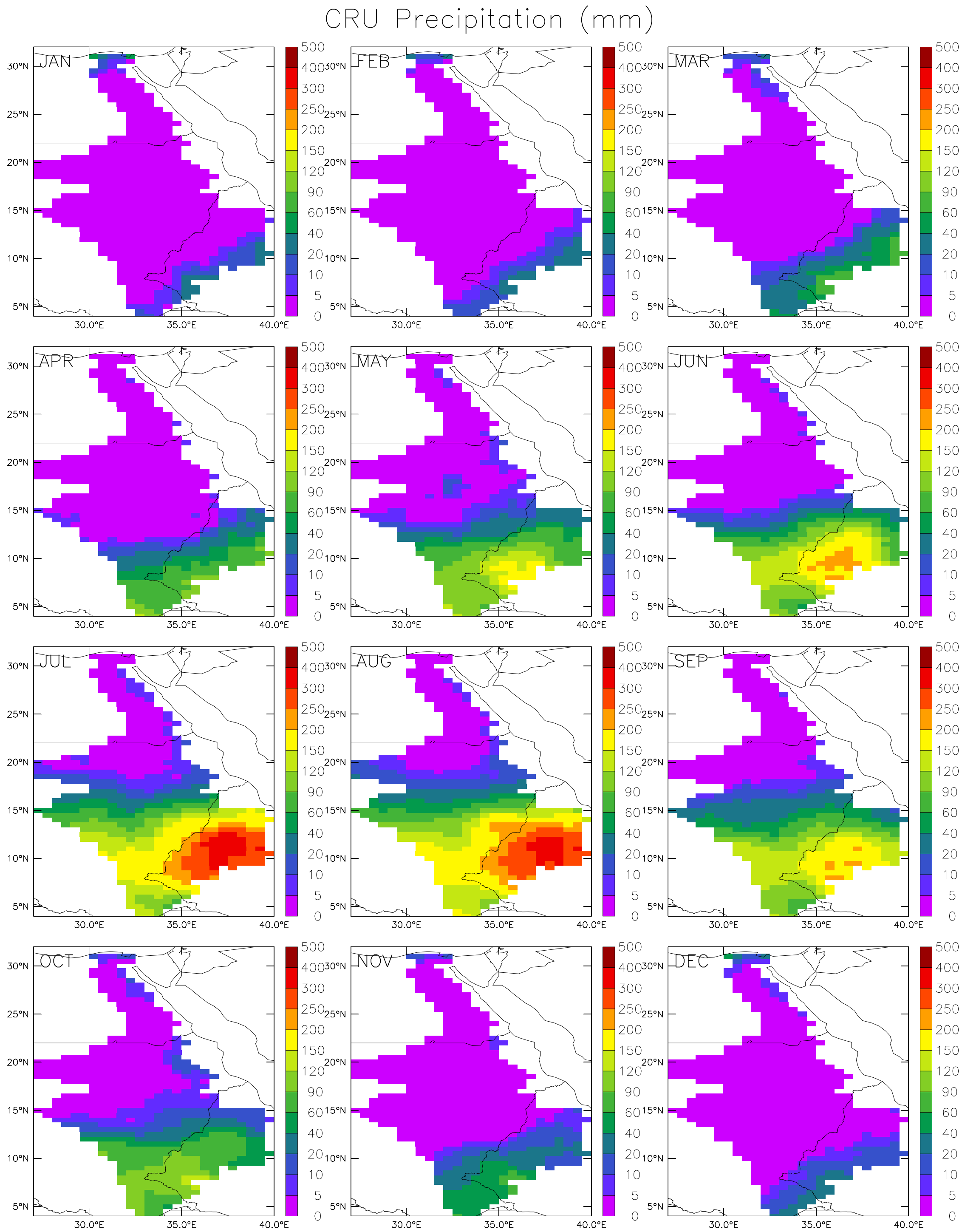

Figure 5: Monthly CRU Precipitation (mm/month).

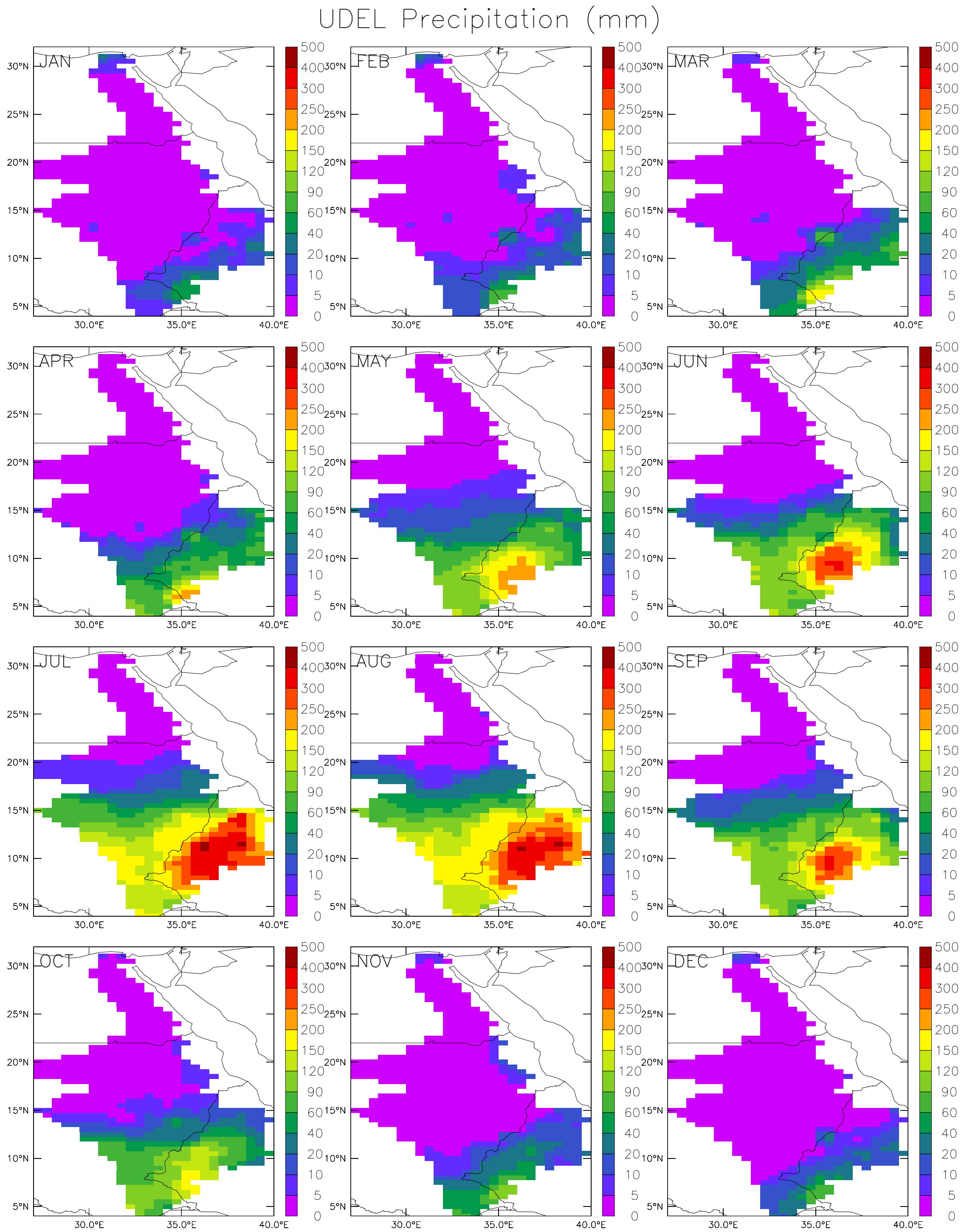

Figure 6: Monthly UDEL Precipitation (mm/month).

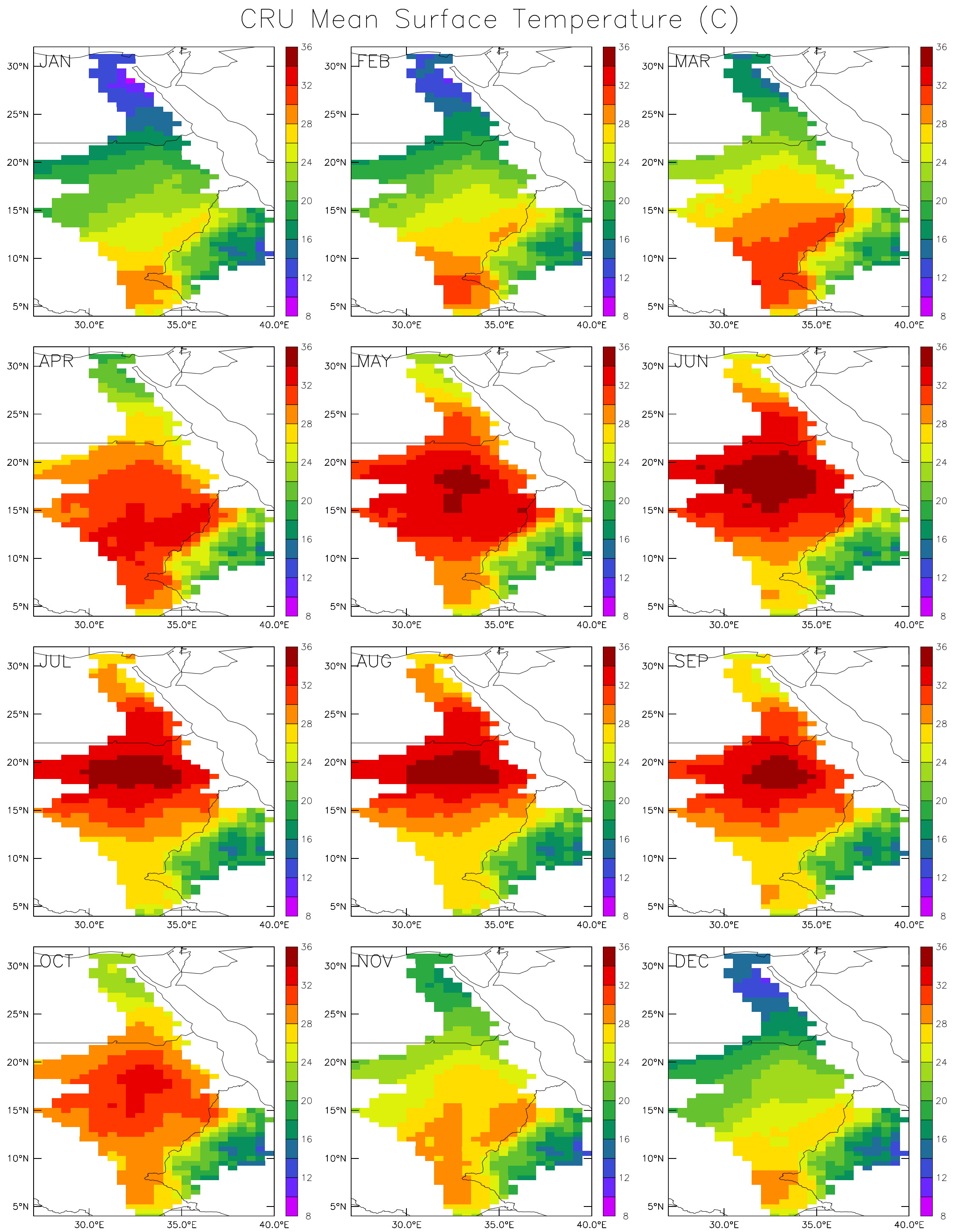

Figure 7: CRU monthly mean temperature (C).

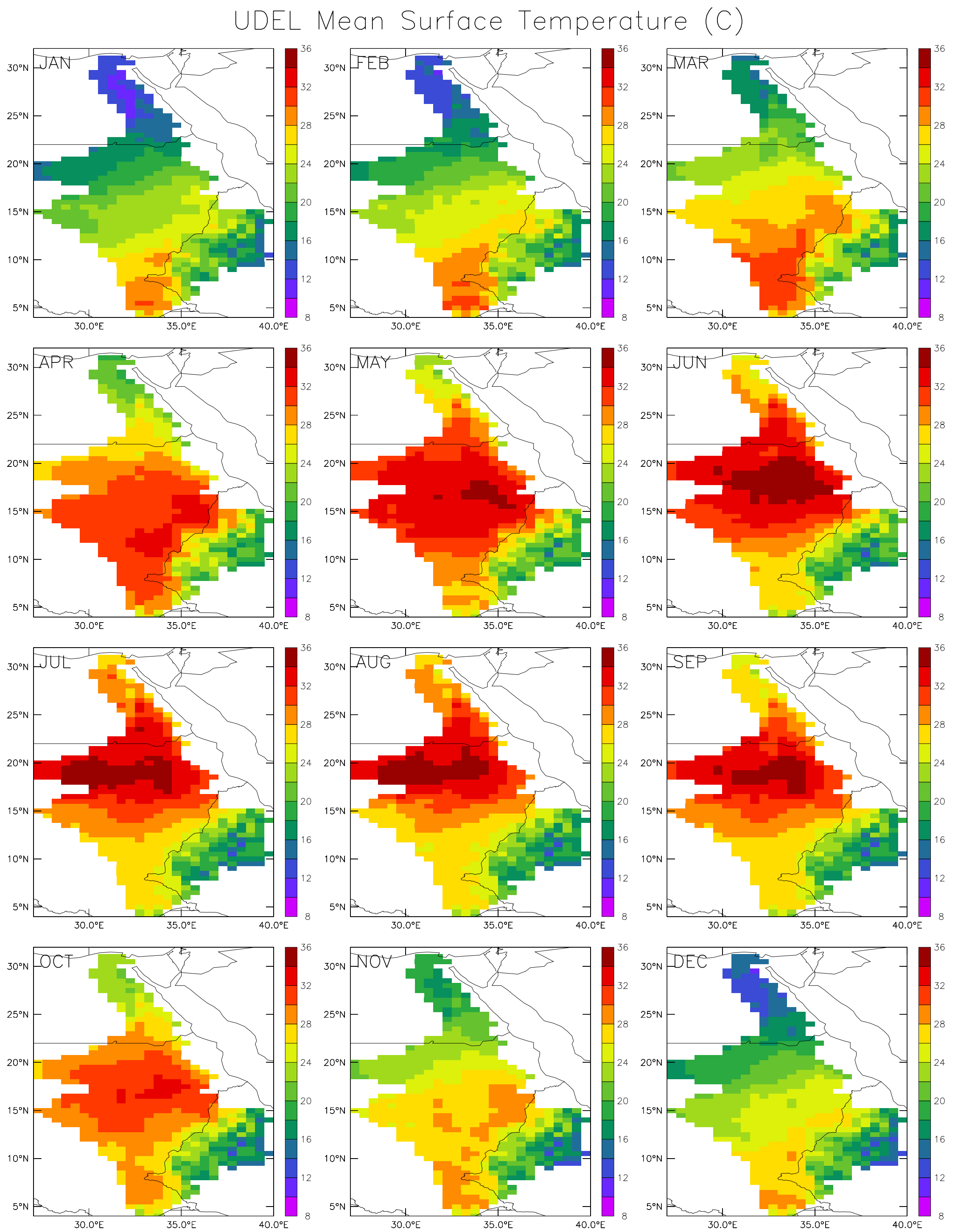

Figure 8: UDEL monthly mean temperature (C).

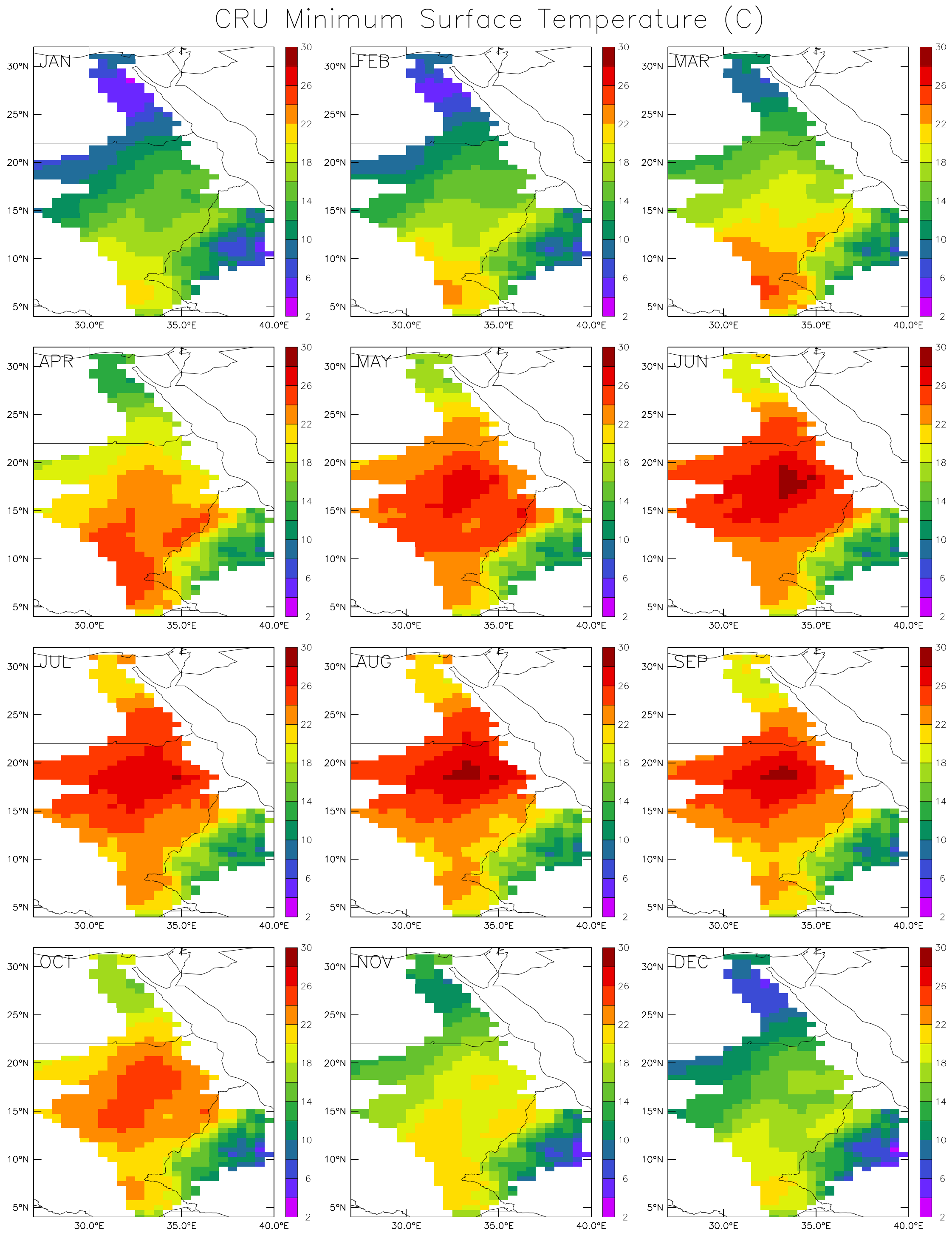

Figure 9: CRU minimum monthly temperature (C).

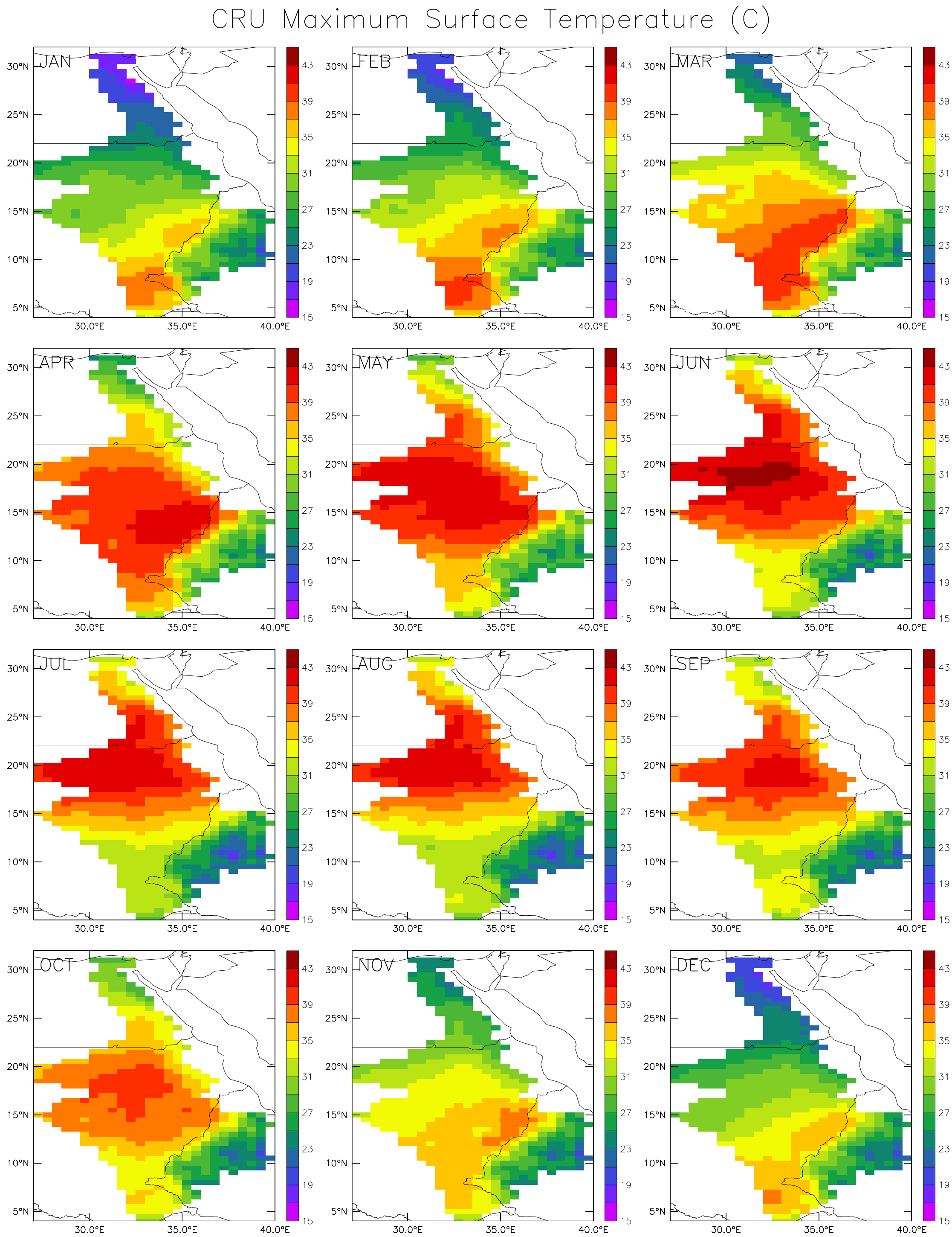

Figure 10: CRU monthly maximum temperature (C).

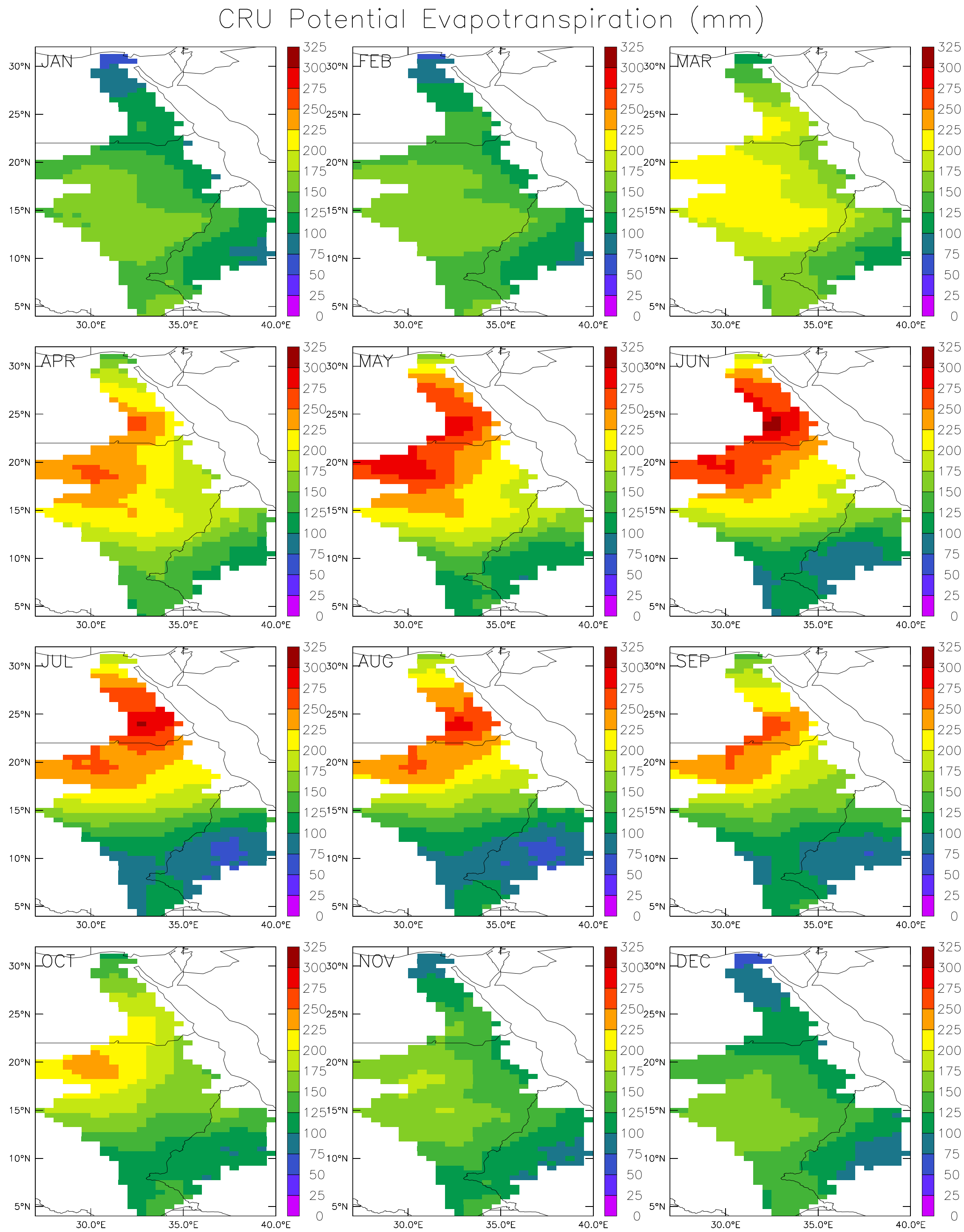

Figure 11: CRU monthly potential evapotranspiration (mm/month).

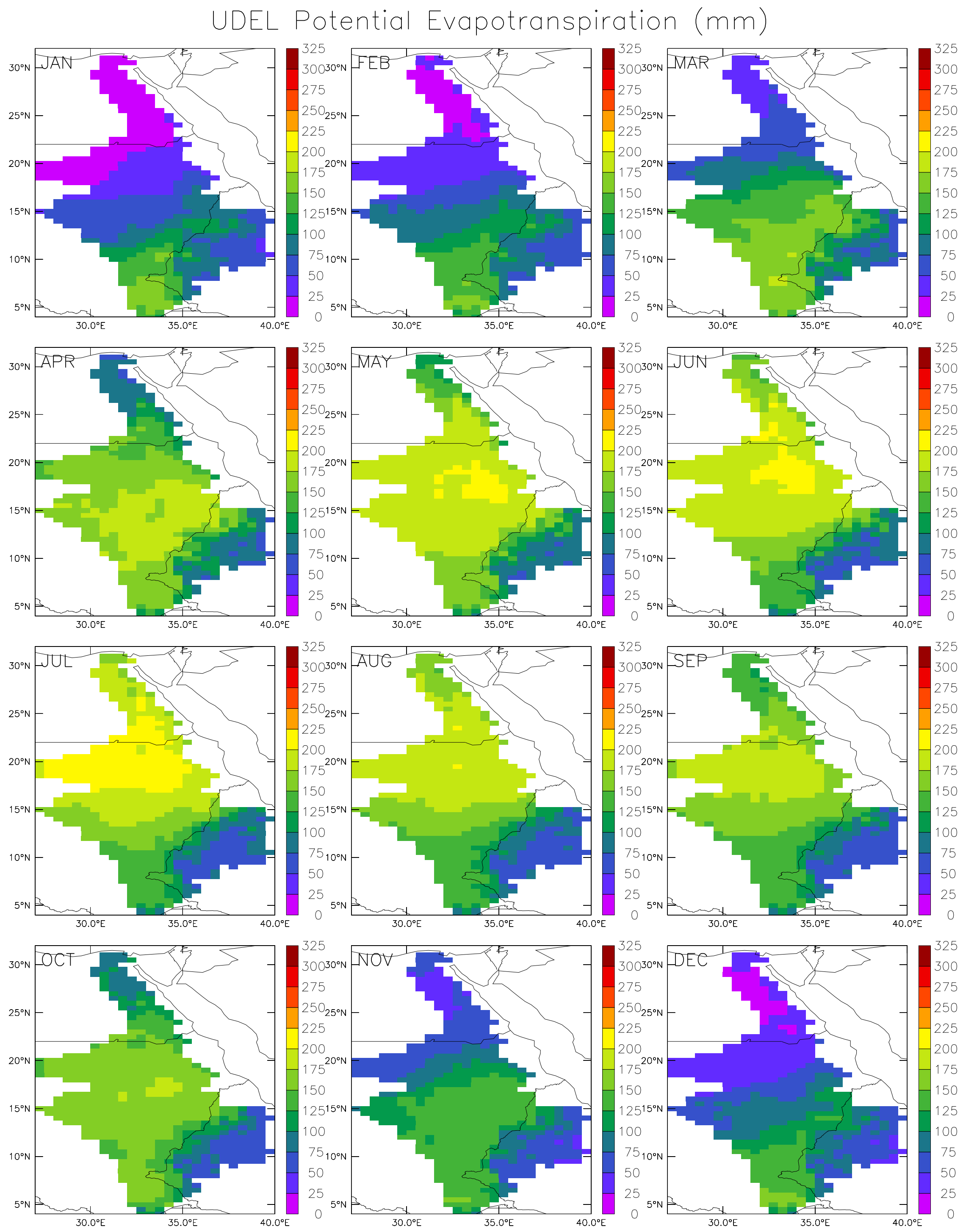

Figure 12: UDEL monthly potential evapotranspiration (mm/month).

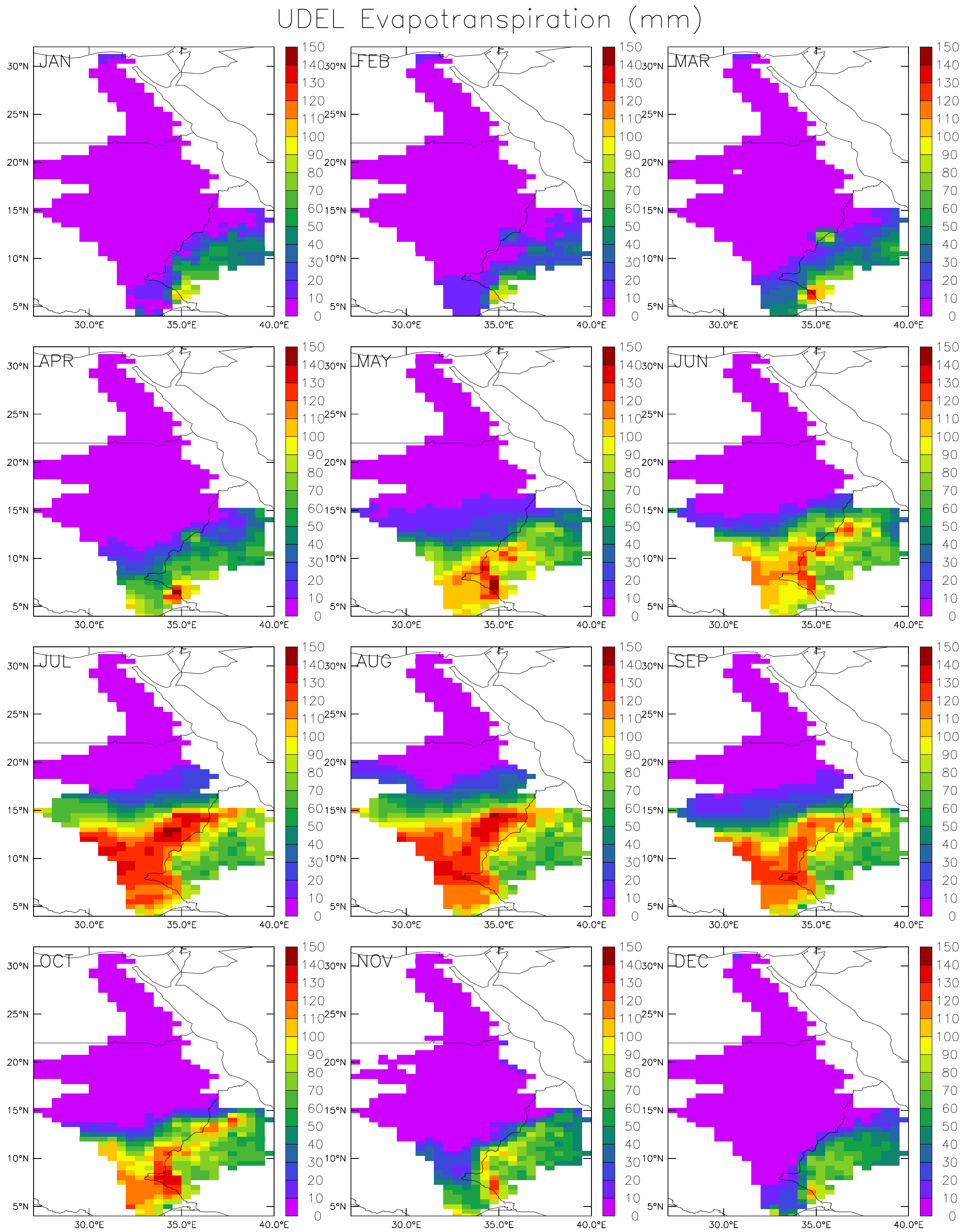

Figure 13: UDEL monthly evapotranspiration (mm/month).

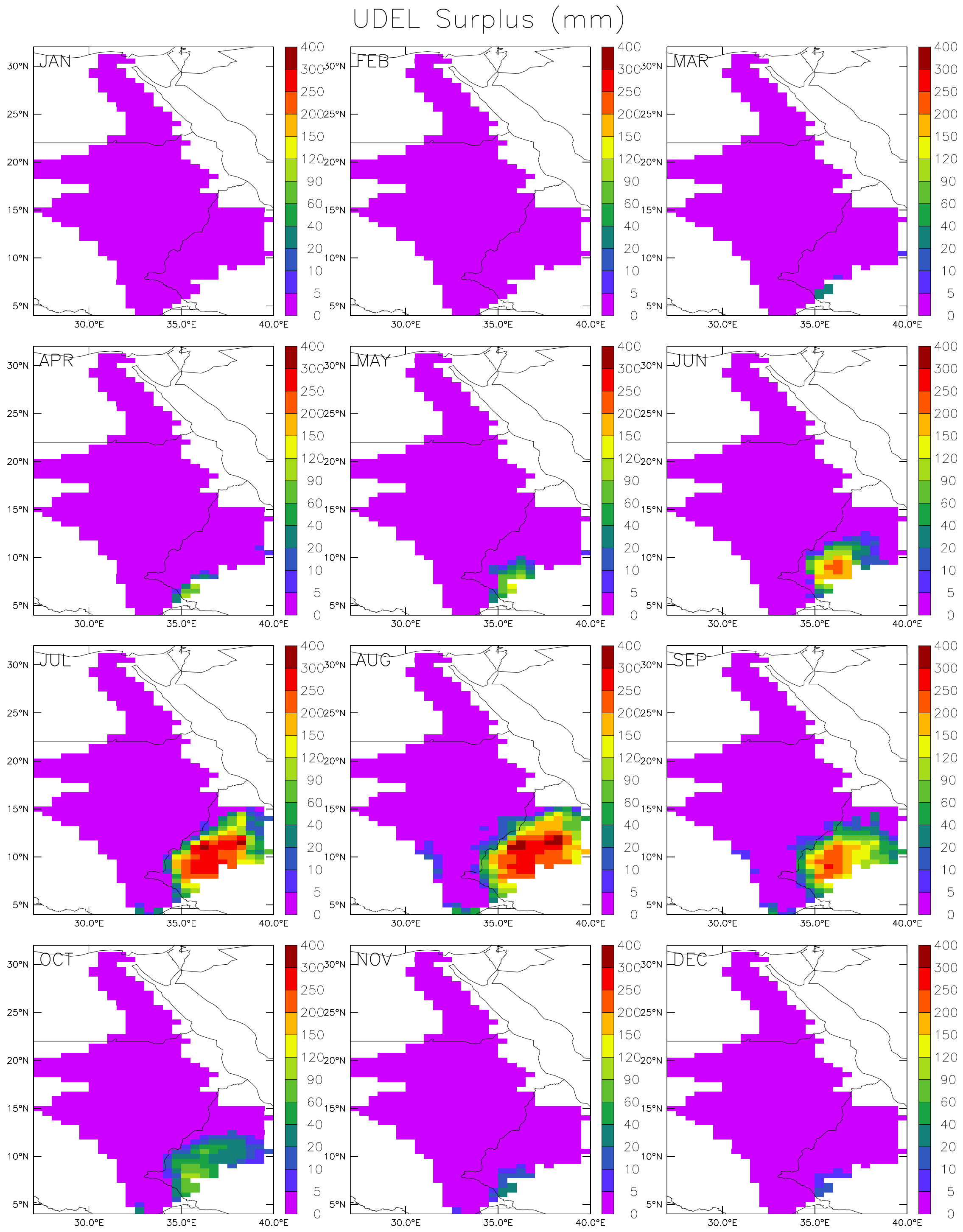

Figure 14: UDEL monthly surplus (mm/month).

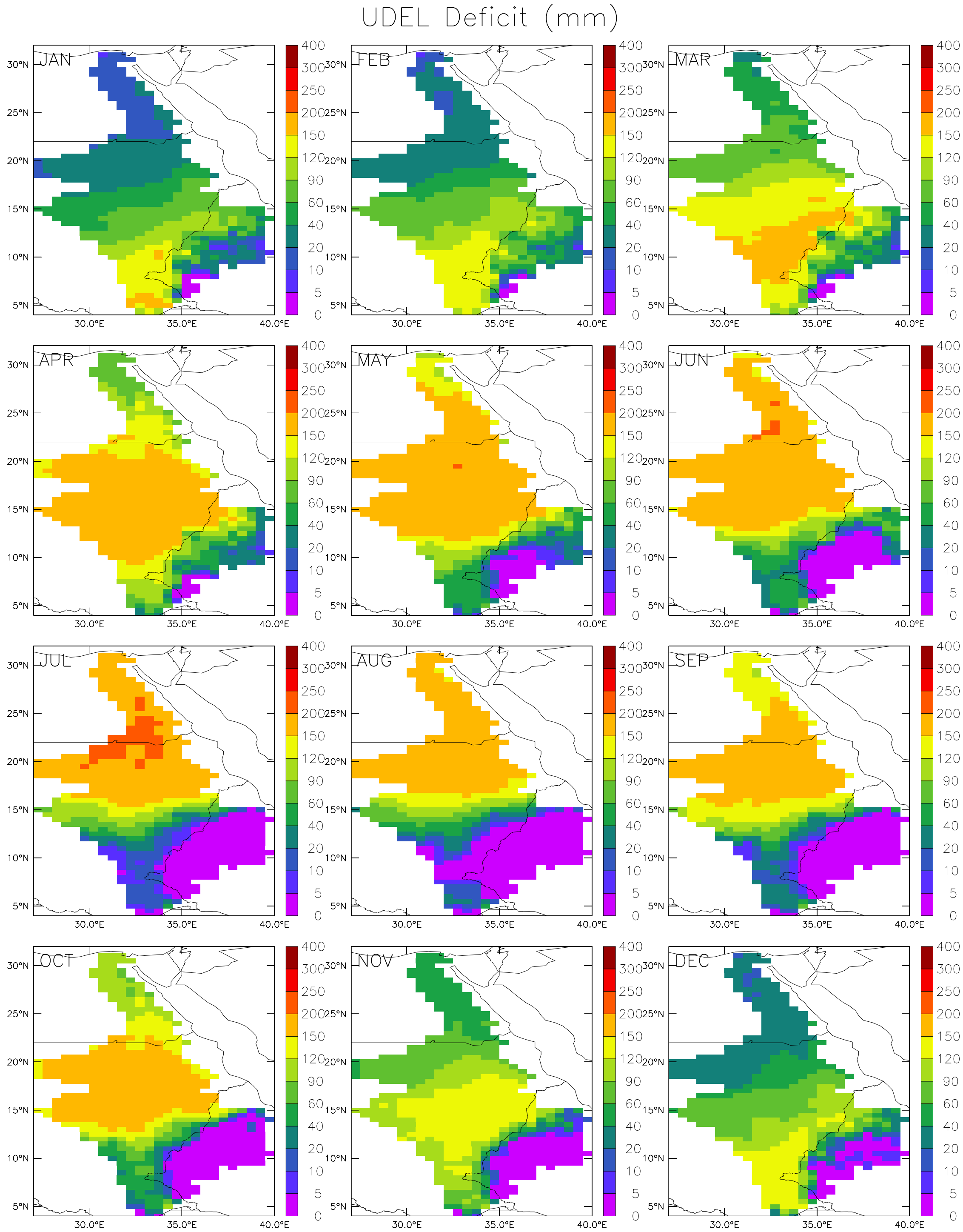

Figure 15: UDEL monthly deficit (mm/month).

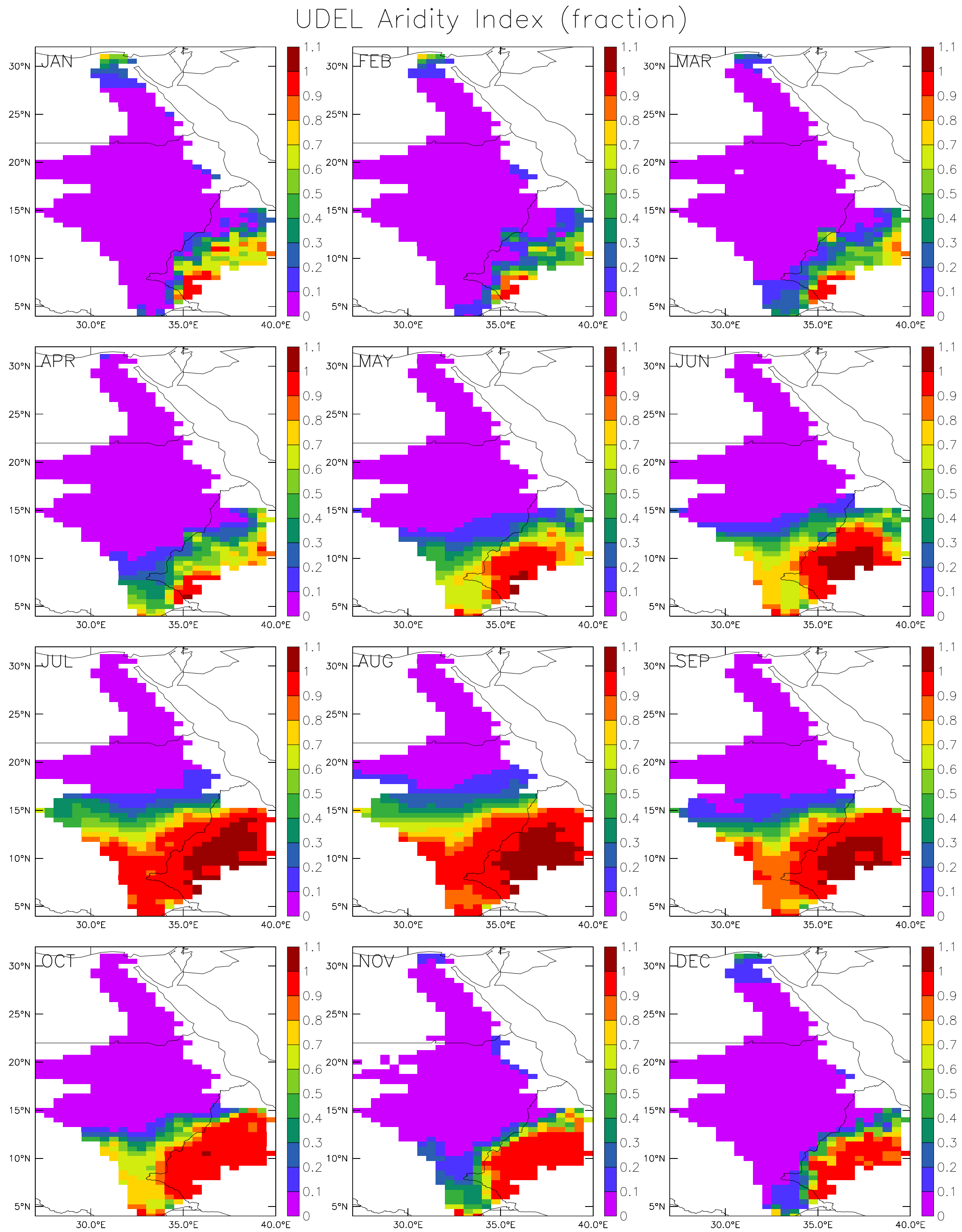

Figure 16: UDEL monthly aridity index (ET/PET).

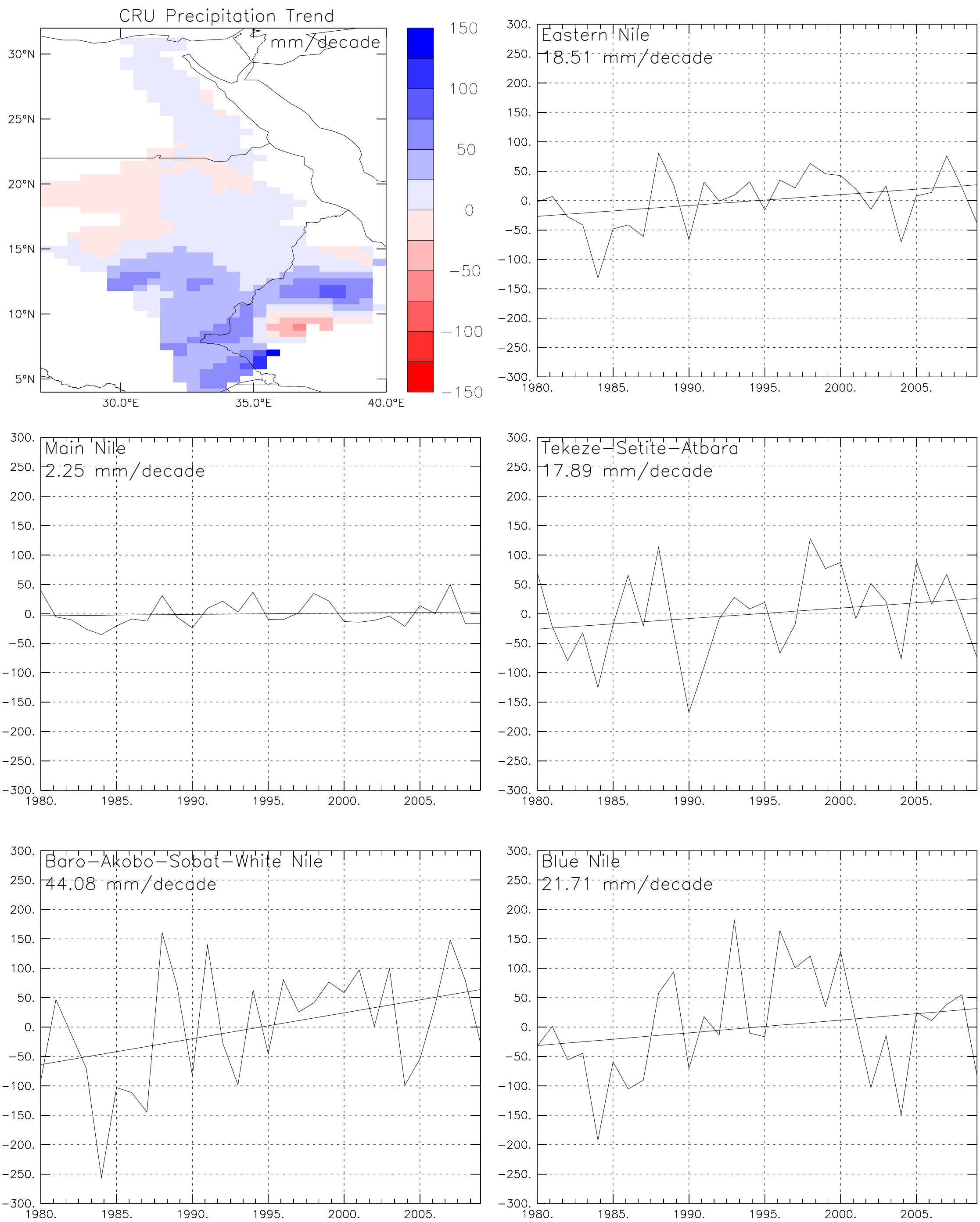

Figure 17: CRU annual precipitation trends (mm/decade).

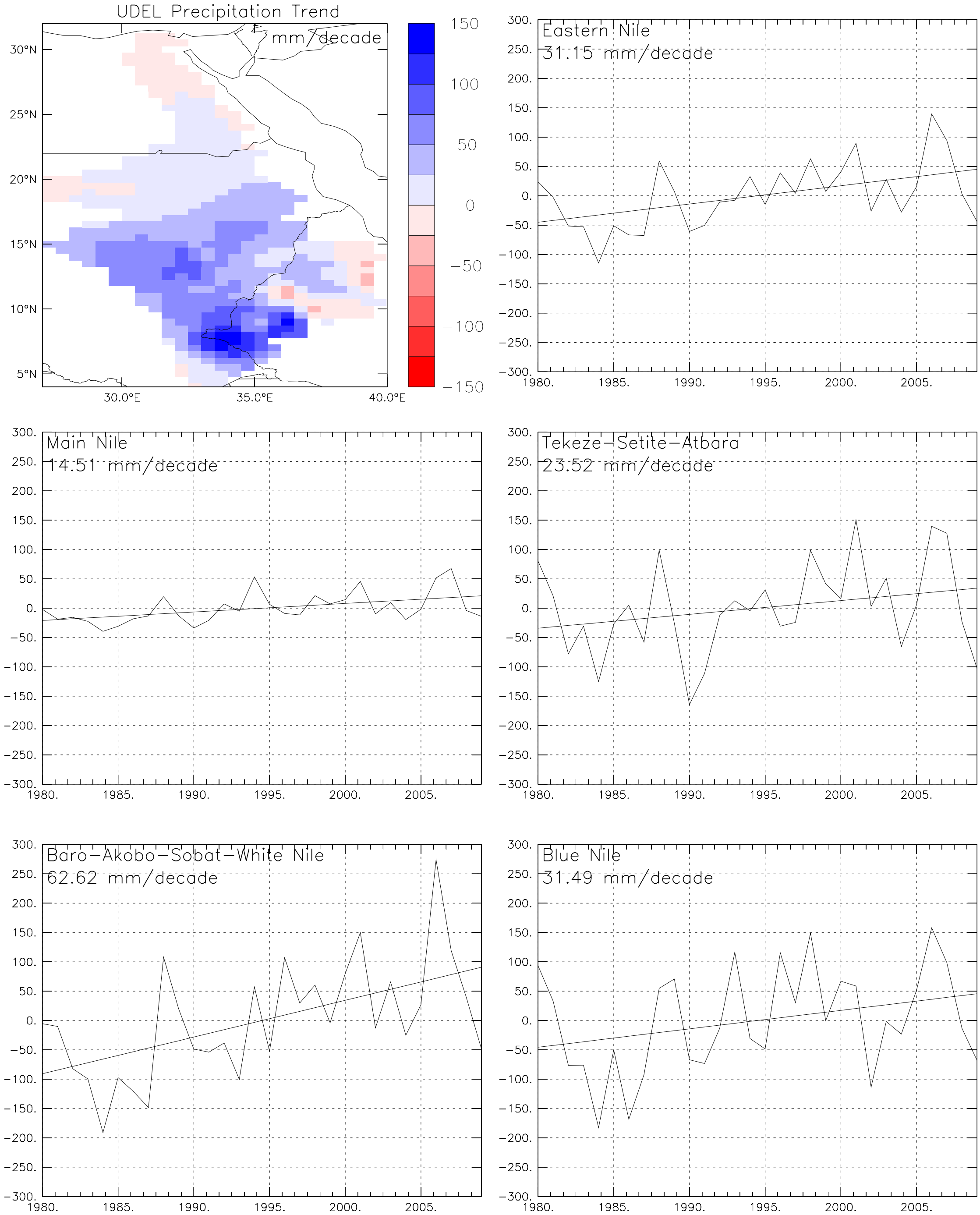

Figure 18: UDEL annual precipitation trends (mm/decade).

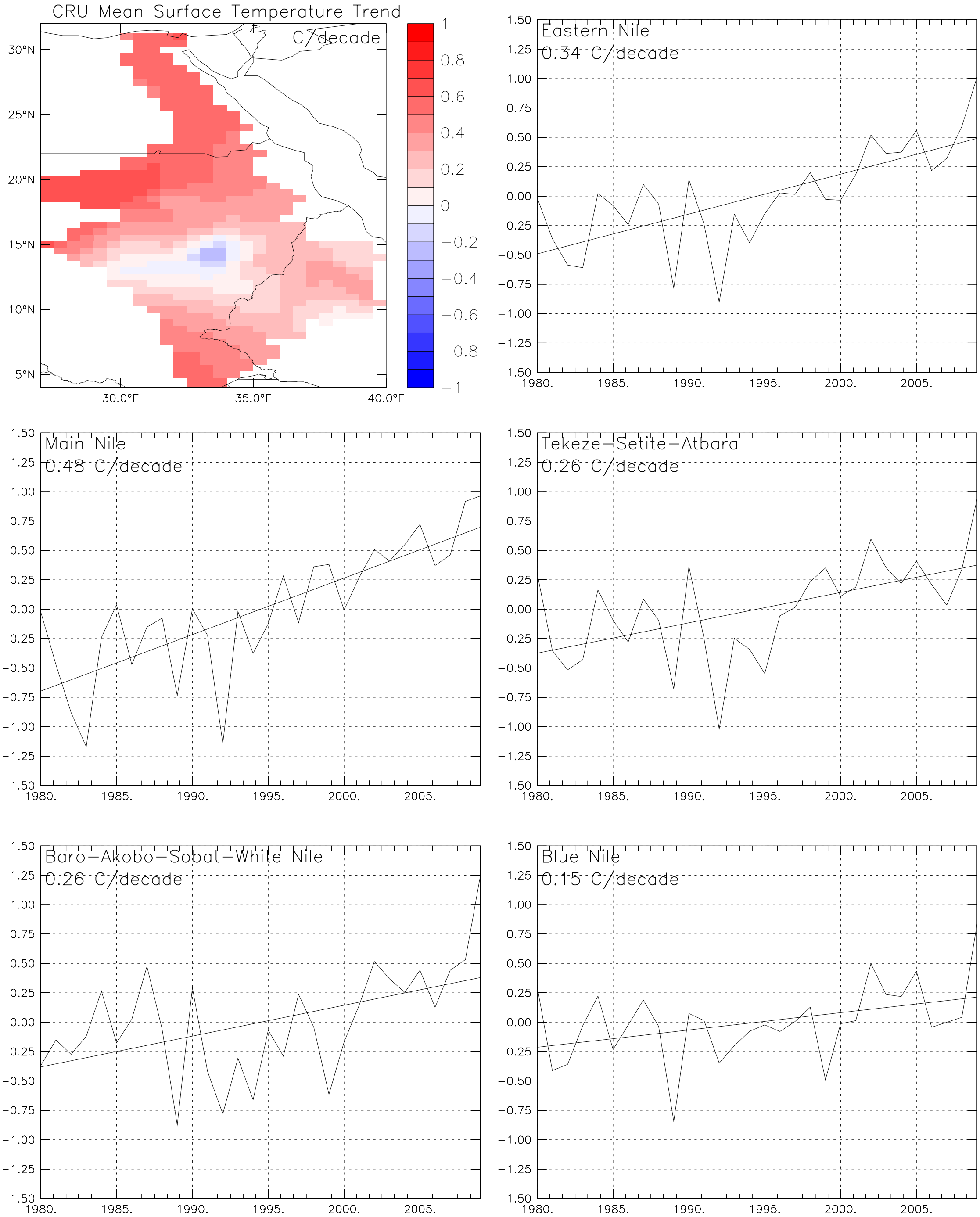

Figure 19: CRU mean surface temperature trends (°C/decade).

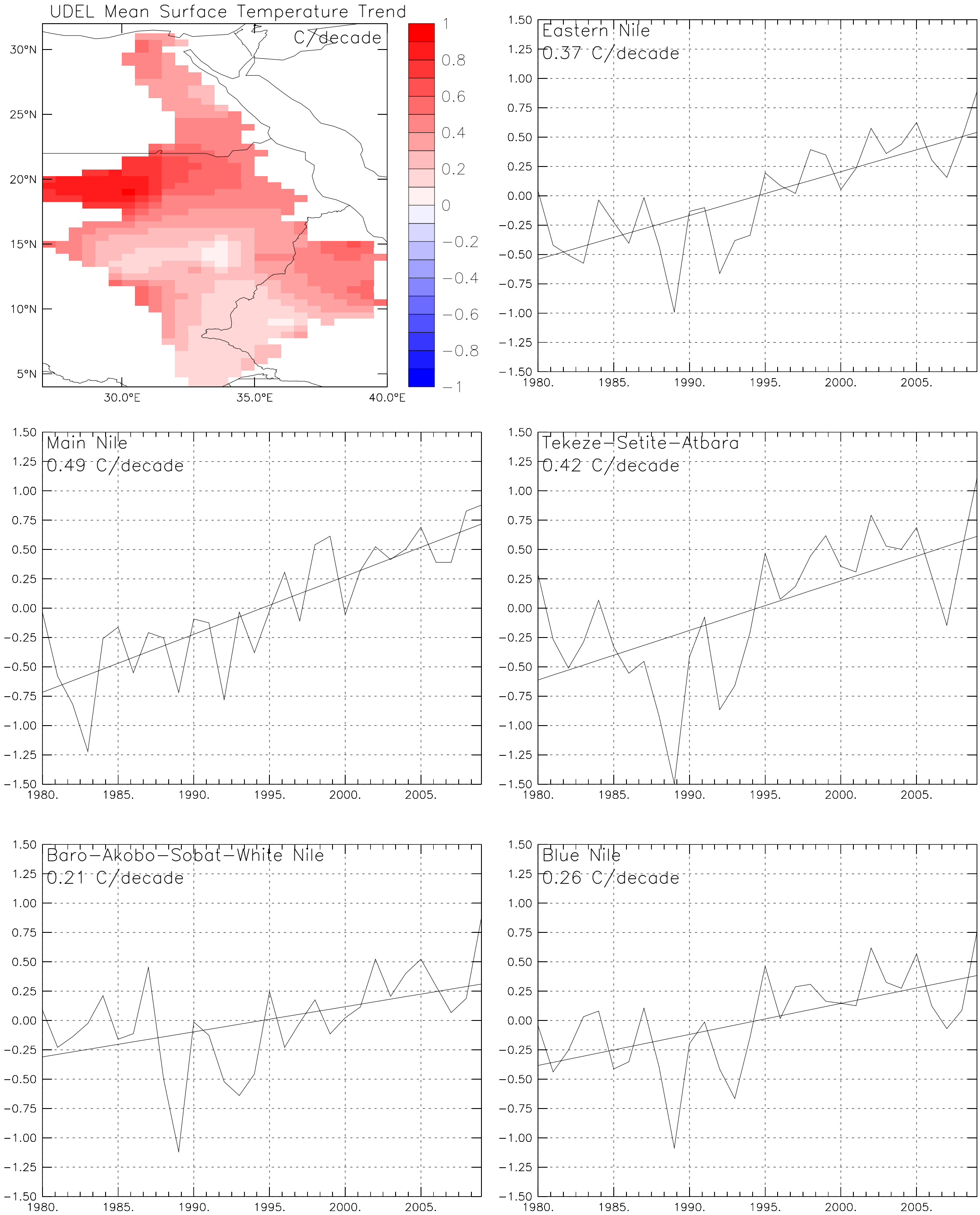

Figure 20: UDEL mean surface temperature trends (°C/decade).

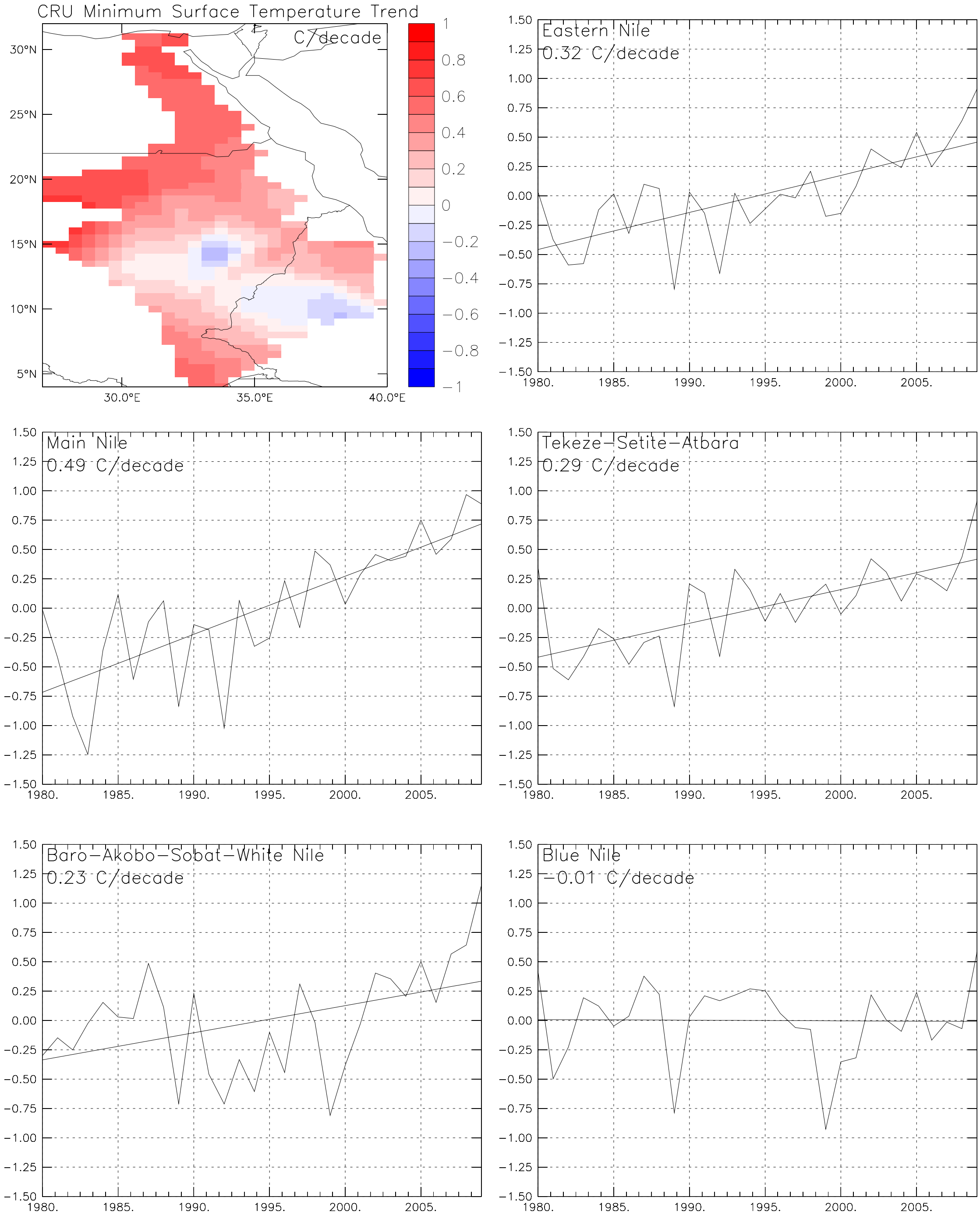

Figure 21: CRU minimum surface temperature trends (°C/decade).

Figure 22: CRU maximum surface temperature trends (°C/decade).

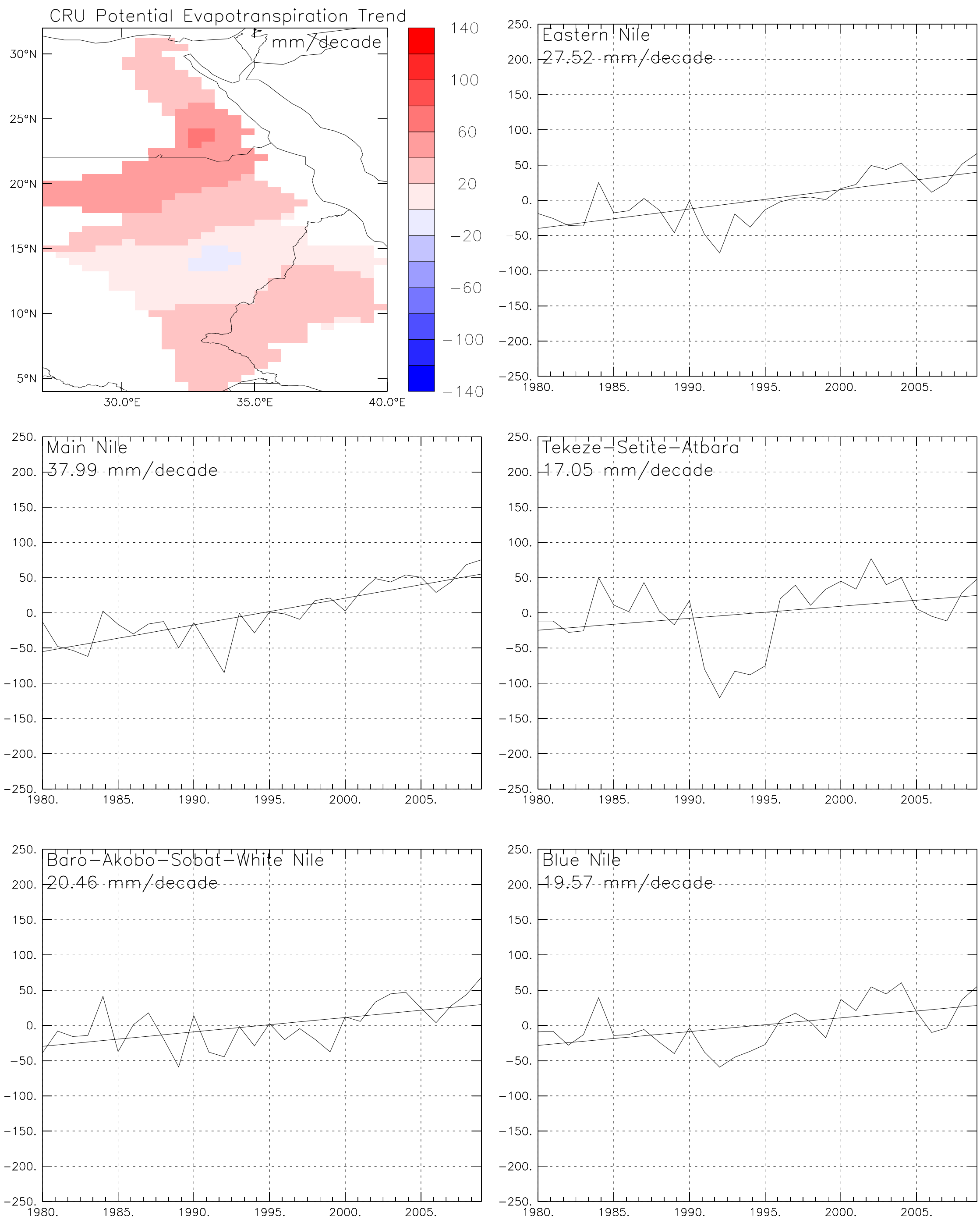

Figure 23: CRU potential evapotranspiration trends (mm/decade).

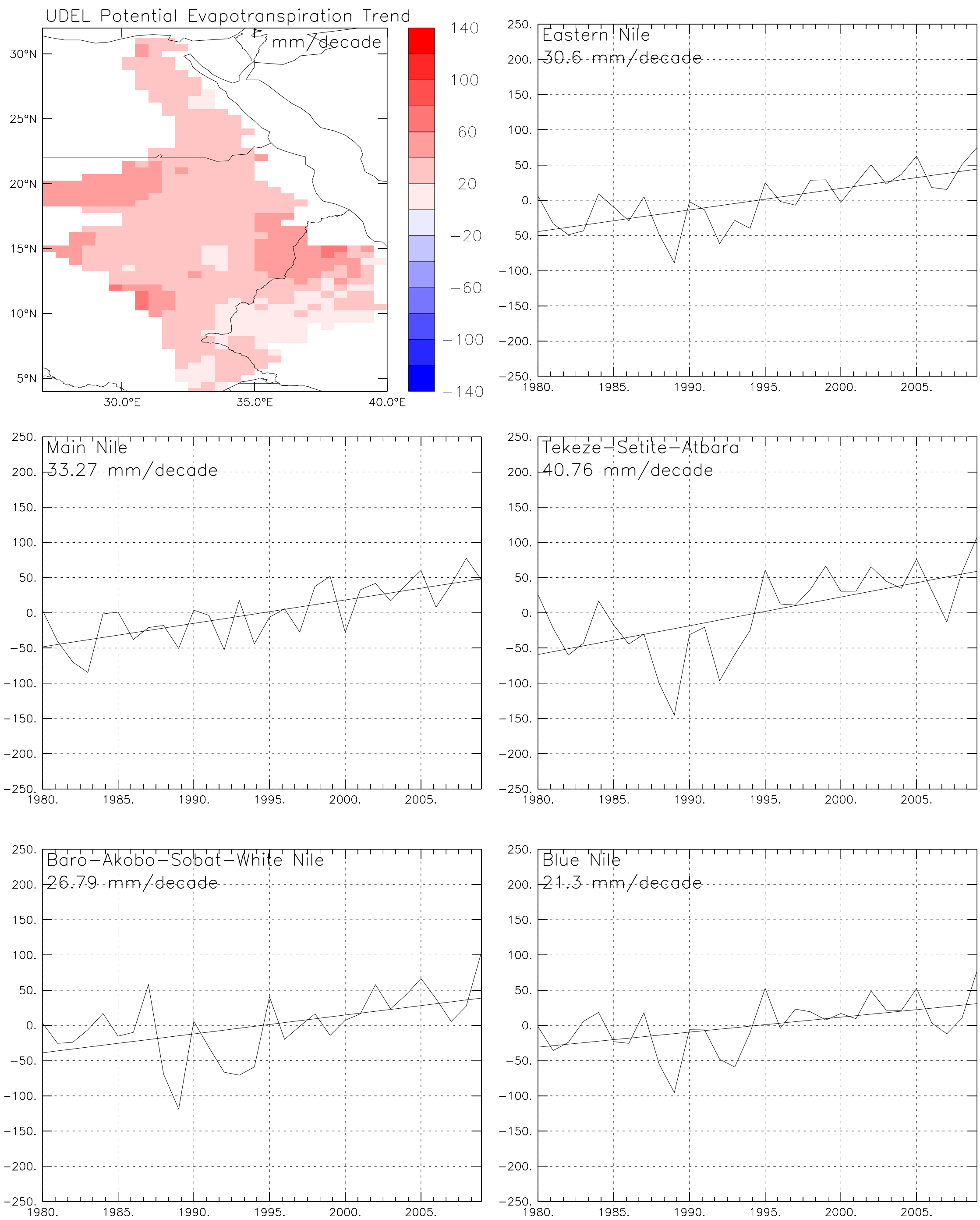

Figure 24: UDEL potential evapotranspiration trends (mm/decade).

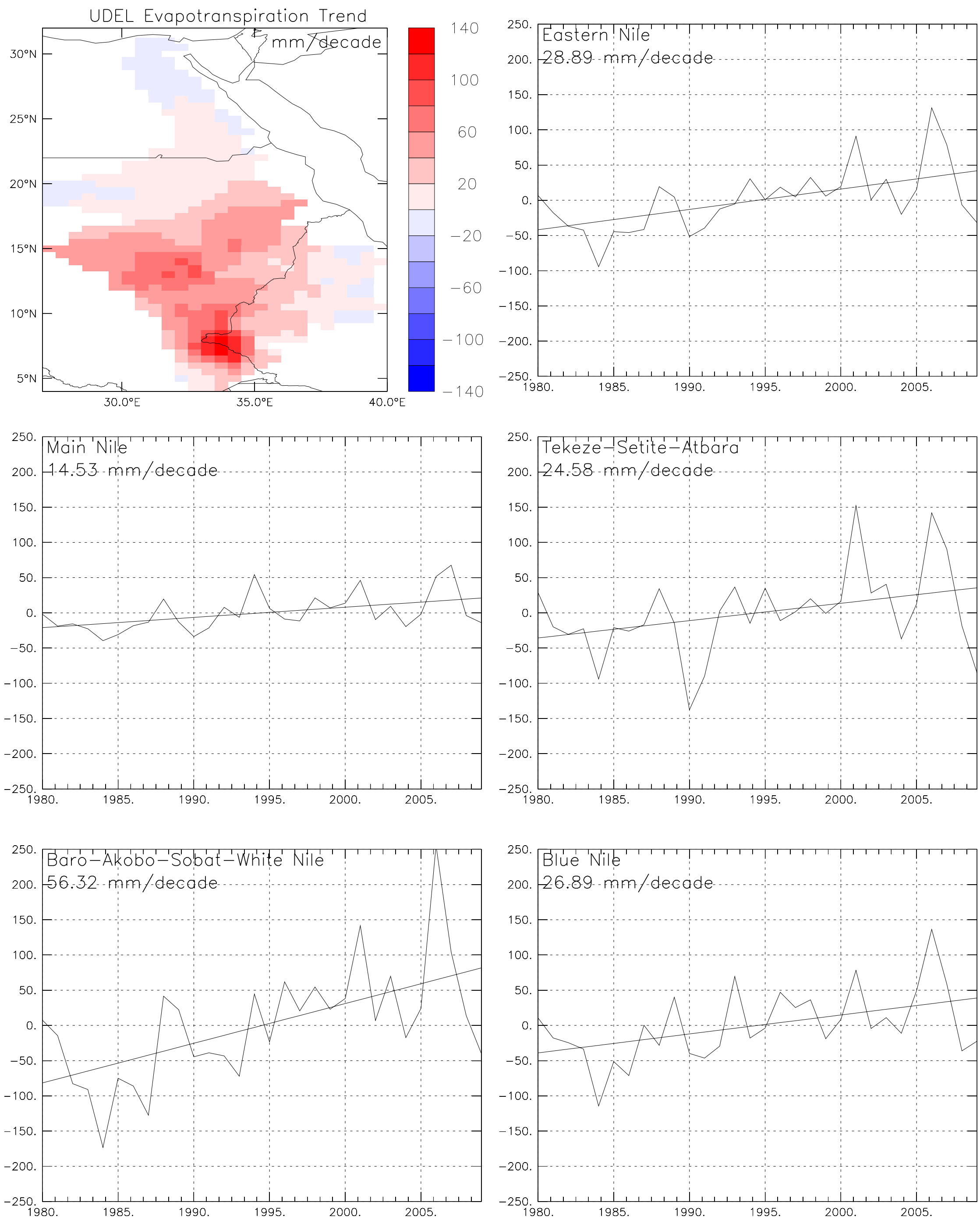

Figure 25: UDEL evapotranspiration trends (mm/decade).

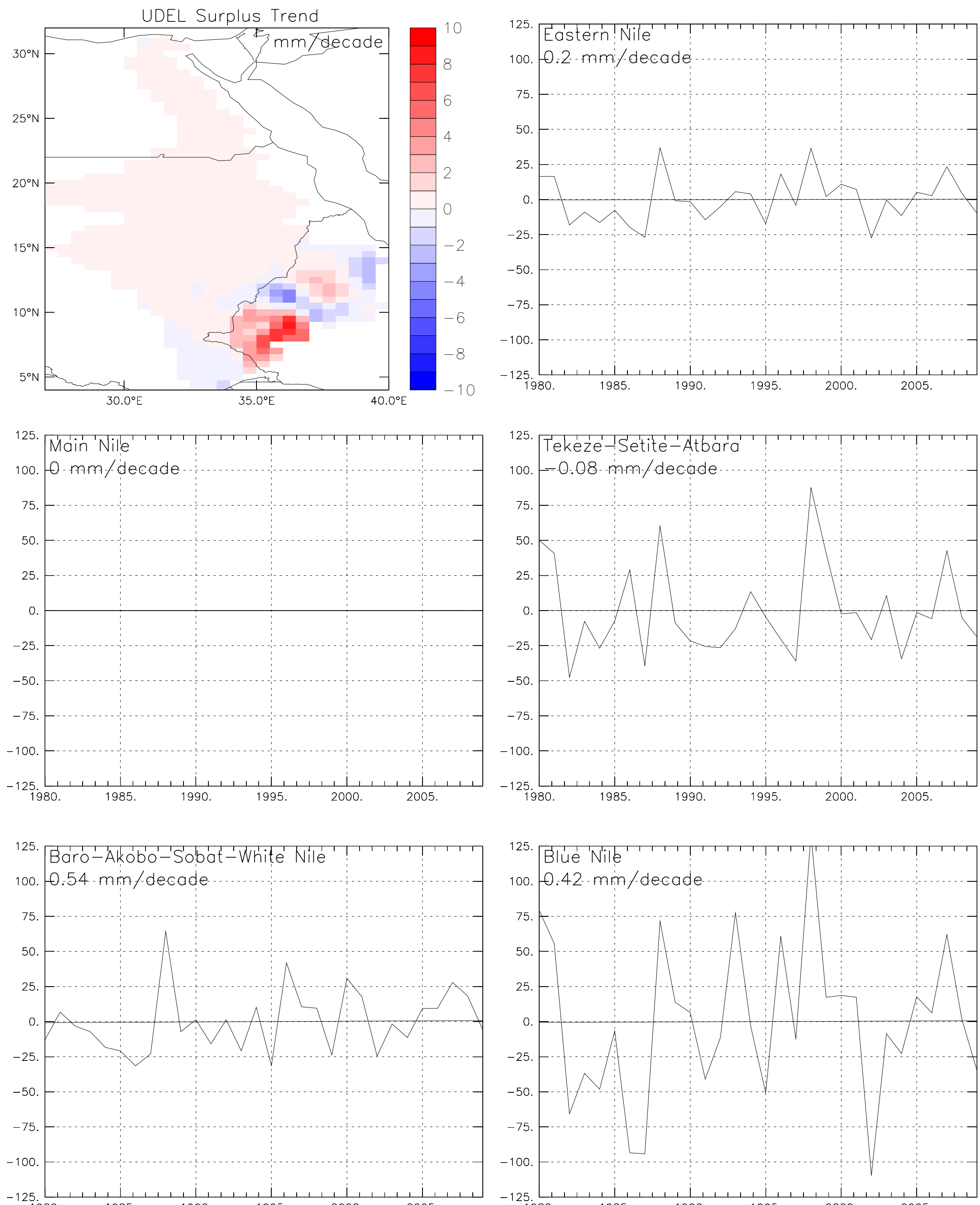

Figure 26: UDEL surplus trends (mm/decade).

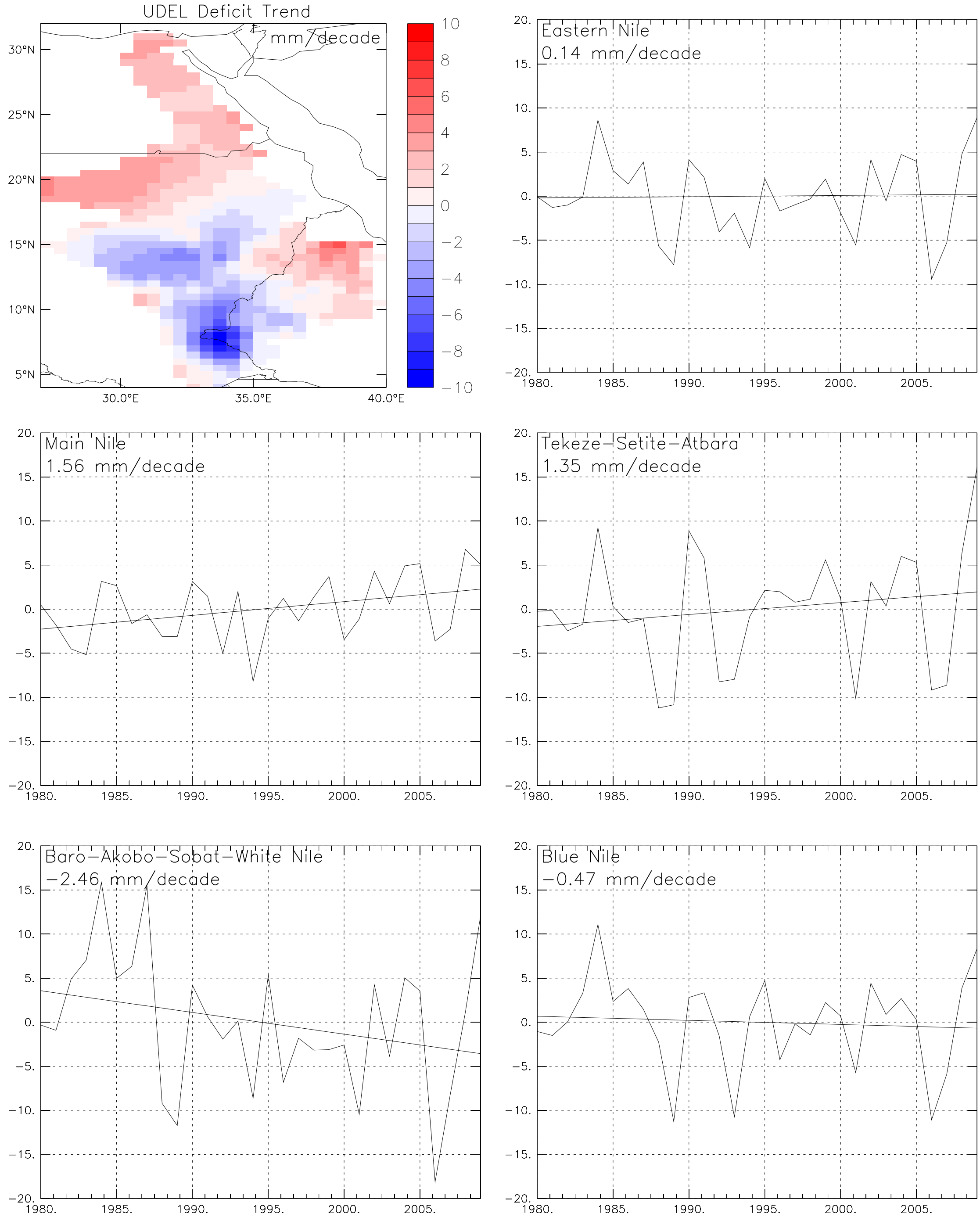

Figure 27: UDEL deficit trends (mm/decade).

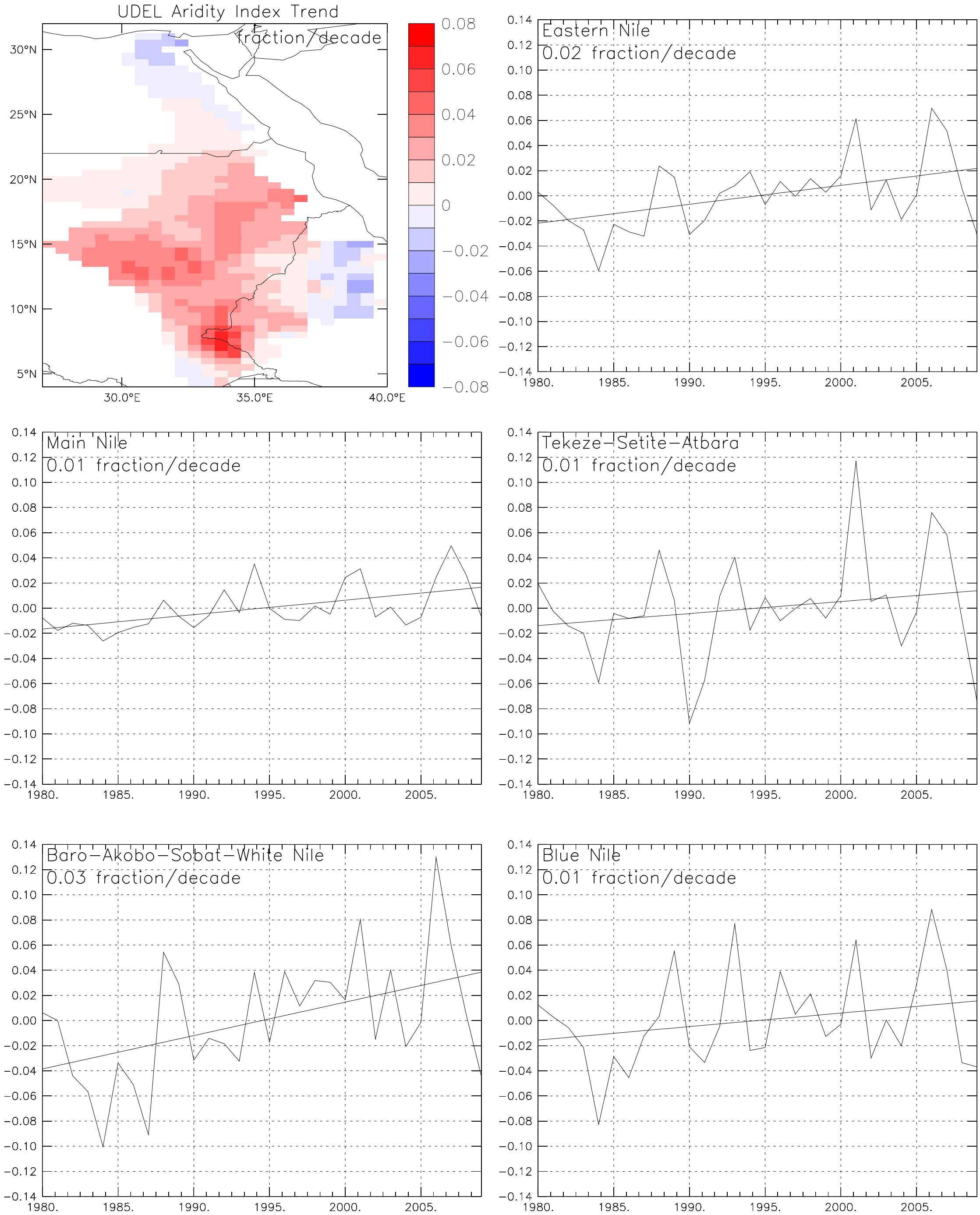

Figure 28: UDEL aridity index trends (fraction/decade).

6 Climate Change Projections

Addressing climate change over EN basin is a significant challenge for understanding the effects of greenhouse gas (GHG) warming in the EN basin. Such assessment is critical because the basin encompasses different hydro-climatological zones ranging from wet to semi-arid to arid. Changes in future climate may pose significant threats to the region already subject to recurrent drought episodes in the recent decades.

Climate change projections for the region have been often derived using Global Climate Models (GCMs; e.g., Hulme et al. 2001; Sayed 2004; Elshamy et al. 2009). Despite the significant progress, GCMs projections over the EN basin are limited by at least two factors. First, the precipitation response to anthropogenic climate change is uncertain because the spread among the GCM projections is quite large. Second, the typical grid spacing of GCMs is in the range of 100-300 km and is not sufficient to account for land surface heterogeneities such as vegetation variations, lakes, complex topography, and coastlines (Figure 30). These heterogeneities are important aspects of the physical response governing the local and regional climate change signal (Paeth et al. 2006; Rummukainen 2010; Sylla et al. 2012). Regional Climate Models (RCMs) can be used to dynamically downscale GCMs output in order to account for the fine-scale forcings and provide climate change information at the local and regional level needed for impact assessments (Giorgi and Mearns 1999; Paeth et al. 2008; Philipon et al. 2009).

For Africa, based on climate model results, warming is very likely (90 to 99% probability) to be larger than the globally average warming in all seasons by the end of the 21st century, particularly in drier subtropical regions. For the A1B Special Report on Emissions Scenarios (SRES) emissions scenario (IPCC, 2000), which is considered a mid-range emissions scenario, end of century annual temperatures are projected to increase by 3.0 to greater than 3.5° C with the greatest increase at the Egypt-Sudan border. Seasonally, increases of 2.5 to 3.5° C are projected for the months of December, January, February (DJF) and 3.0 to 4.0° C for the months of June, July and August (JJA). The intermodel variability around the temperature projections is typically ±0.5° C indicating a high signal to noise ratio.

Climate model projections of annual precipitation for the A1B SRES emissions scenario in the Eastern Nile region range from -25% in Egypt to +20% in Sudan and only a slight increase in Ethiopia. In DJF, the projections range from -40% in Egypt and Sudan to +50% in Ethiopia; while in JJA, they range from -40% in Egypt to +25% in Sudan and little change in Ethiopia. It is important to note that there is little model agreement with these projections as about half of the models project an increase in precipitation and half a decrease over the region (low signal to noise ratio). It is essential to account for this uncertainty in precipitation projections when modeling the impacts of climate change on agriculture in the Eastern Nile region.

In this phase of the special study, mid-century and end of century projections of climate change are assessed based on high resolution nested regional climate model simulations. The primary variables to be analyzed are the same as those of the analysis of observations: mean, minimum and maximum temperature; precipitation; evapotranspiration; potential evapotranspiration; and discharge. Additionally, soil moisture are analyzed. The aim this phase is to develop an understanding of changes to mean climate and its variability. In addition, an assessment of the uncertainty of the projections are performed.

The deliverables for this phase are provided below:

1. 0.5° resolution maps of projected mid and end of century climate changes in seasonal T_{mean}, T_{min}, T_{max}, P, PET and Q;
2. Basin average time series plots of projected mid and end of century climate changes in annual T_{mean}, T_{min}, T_{max}, P, PET and Q;
3. Basin average time series plots of projected mid and end of century climate changes in growing season T_{mean}, T_{min}, T_{max}, P, PET and Q;
4. Basin average plots of projected mid and end of century climate changes in monthly T_{mean}, T_{min}, T_{max}, P, PET and Q;
5. Basin average tables of projected mid and end of century climate changes in growing season T_{mean}, T_{min}, T_{max}, P, PET and Q.

6.1 Regional Climate Model Projections

The International Centre for Theoretical Physics (ICTP) Regional Climate Model version 4.3.4 (RegCM-4.3.4; Giorgi et al. 2012) is used downscale the United Kingdom Meteorological Office (UKMO) Hadley Centre Global Environment Model version 2 (HadGEM2; Collins et al. 2008) climate change projections. HadGEM2 is forced by two of the latest IPCC emission scenarios (Moss et al. 2010) named Representative Concentration Pathways (RCP). The scenarios considered have a radiative forcing of 4.5 (RCP4.5) and 8.5 (RCP8.5) (Figure 29).

The standard version RegCM-4.3.4 employed in this study does not substantially differ from that of RegCM3 (Pal et al. 2007). The RegCM3 version has been thoroughly evaluated over all of Africa by Sylla et al. (2010) when driven by the European Center Interim Reanalysis (also called ERA-Interim) at 50 km. The regional climate model exhibits a good performance in locating the observed temperature minima and maxima during both winter and summer seasons in the EN basin (Figure 31). Similarly, the seasonal precipitation, along with the prevailing wind fields, is well represented in the regional climate model over Eastern Africa (Figure 32). The mean annual cycle of precipitation, including single and multiple rainy seasons, along with the observed interannual variability are well reproduced over most regions, mostly following, and sometimes improving, the quality of the ERA-interim reanalysis (not shown for brevity). In general, the performance of this model over the entire African domain is of sufficient quality for application to the study of climate change and climate variability over the African continent.

Two 20-year time periods are analyzed for both the RCP4.5 and RCP8.5 emissions scenarios: Present day (1985-2004) and late 21st century (2080-2099). The analysis is performed for each of the time periods for the entire Eastern Nile region and for each of the subbasin, and interpolated to the 0.5-degree resolution grid used in the observational analysis (Section 5). The differences between the two projections and the present day simulation provide a measure of potential changes in climate under a lower and higher greenhouse gas emissions scenario. To provide a measure of uncertainty, the results are placed in the context of the IPCC AR4 global climate model projections run a much coarser resolution.

The standard version of RegCM-4.3.4 is used to derive climate change projections by dynamically downscaling HadGEM2 at very high resolution (25 km) to account for land surface heterogeneity in the EN basin as shown in Figure 30. The changes between the future and present day simulations considering RCP4.5 and RCP8.5 are respectively denoted by F45 and F85.

6.1.1 Precipitation

RCP4.5 exhibits a complex pattern of precipitation annual cycle (Figure 33). Precipitation changes during the first semester are not significant and range mostly between -5 mm and 5 mm compared to present day longterm monthly means. A significant pattern starts to emerge in April and May when northeastern Ethiopia and South Sudan, which experience decreased and increased precipitation of more than 25 mm, respectively. The decreasing precipitation is covers the entire EN basin in June. It should be emphasized that these changes are not uniform. This tendency is reversed in July over southern Sudan and around the South Sudan. However, the wettest month is August when the regional climate model projects significant positive changes of more than 50 mm over much of the EN basin except in northern Egypt and a small portion of northeastern Ethiopia. This pattern, however, is not persistent throughout the summer season. From August to October the wetting transitions to drying. Changes in November and December are not significant.

The future climate projection using the higher RCP8.5 radiative forcing scenario tends to amplify the drying, although it exhibits a dipole pattern from April and September (Figure 34). This dipole pattern displays significant negative changes in the north and positive changes southward. The projected drier future is more intense (greater than 75 mm) and more extensive in June and September leaving very few wet areas in South Sudan. In July and August, the projected wetter conditions expand and affect most parts of Ethiopia and South Sudan. An interesting feature is that in the month of October, the regional climate model projects almost similar pattern and magnitudes as in the RCP4.5 over the entire EN basin. This suggests that natural variability is dominant in October and drives most of the predicted changes.

6.1.2 Surface Temperature

Projected surface air temperature changes reveal that the EN basin will be considerable warmer in the future if anthropogenic greenhouse gas emissions continue (Figure 35 and Figure 36). The temperature change in RCP4.5 approaches 5° C in some regions (Figure 35). Throughout the whole year, except during the summer, while Sudan experiences the temperature changes of up to 4.5° C, Egypt and Ethiopia warm 2 to 3 degree Celsius compared to the present day. During the summer season, this trend is reversed. In fact, in June, July, and August, the wetter South Sudan and Ethiopia undergo less warming (less than 2° C) indicating that the increased cloud cover along with the surface evaporative cooling tends to dampen the warming.

The general warming in the EN basin is amplified by more than 5° C over the entire basin in the RCP8.5 scenario (Figure 36). The drier months sustain a general warming of more than 6-7° C. However, a more complex spatial pattern is projected during the summer. As in RCP4.5, July, August, and September exhibit a dampened warming in region experiencing increased rainfall (South Sudan and Ethiopia), whereas in northern Sudan and Egypt, the temperature change is intensified and reaches 9° C.

The minimum and maximum surface temperature changes in both scenarios closely follow the corresponding change in mean temperature (Figure 37 through Figure 40). Both minimum and maximum temperature changes are intensified in RCP8.5 compared to RCP4.5 due to the greater greenhouse gas forcing. The changes in minimum temperature are greater than the changes in maximum temperature for RCP4.5, especially in July, August, and September over the southern EN basin. This difference is larger and more extensive in most of the basin and throughout the entire year in RCP8.5, suggesting that global warming affects minimum temperature more than maximum temperature, at least in the EN basin. This decreases the diurnal temperature range and thus indicates that the EN basin will be prone to more warm nights.

6.1.3 Surface Moisture

Changes in evaporation in both RCP4.5 and RCP8.5 exhibit similar patterns to those of precipitation (Figure 41 and Figure 42). In the first three months of the year, RCP4.5 shows small evaporation changes alternating in sign from South Sudan and Ethiopia to Egypt. As with precipitation, the largest projected decreases in evaporation are projected in June and the largest increases in August. In September and October, while precipitation was projected to decrease, more moisture evaporates. A similar behavior is observed in RCP8.5 where the changes in evaporation are much more intense. The increase is extended over all of Ethiopia and South Sudan particularly during the July, August, and September, including even areas where precipitation changes are negative. This suggests that although precipitation is the primarily driver for evaporation in the sense that it enhances moisture availability, temperature and other atmospheric dynamics also an important role.

6.2 Summary

Overall, it is thus evident that increasing anthropogenic greenhouse gas concentrations will further increase warming over the EN basin. Northern Sudan and most parts of Egypt already experience the warmest climates and are projected to experience the greatest warming, especially during the summer. Also during that period, changes in minimum temperature are projected to be larger than that of maximum temperature, thus indicating a reduction in the diurnal temperature range.

Projected precipitation changes reveal more common drier in most parts of the EN basin. Such changes are much more intense in the highest radiative forcing scenario (RCP8.5). In South Sudan and western Ethiopia, wetter conditions prevail during the wettest summer months. Evaporation changes primarily follow precipitation changes, except in a few locations in Ethiopia suggesting that other atmospheric dynamics may be important.

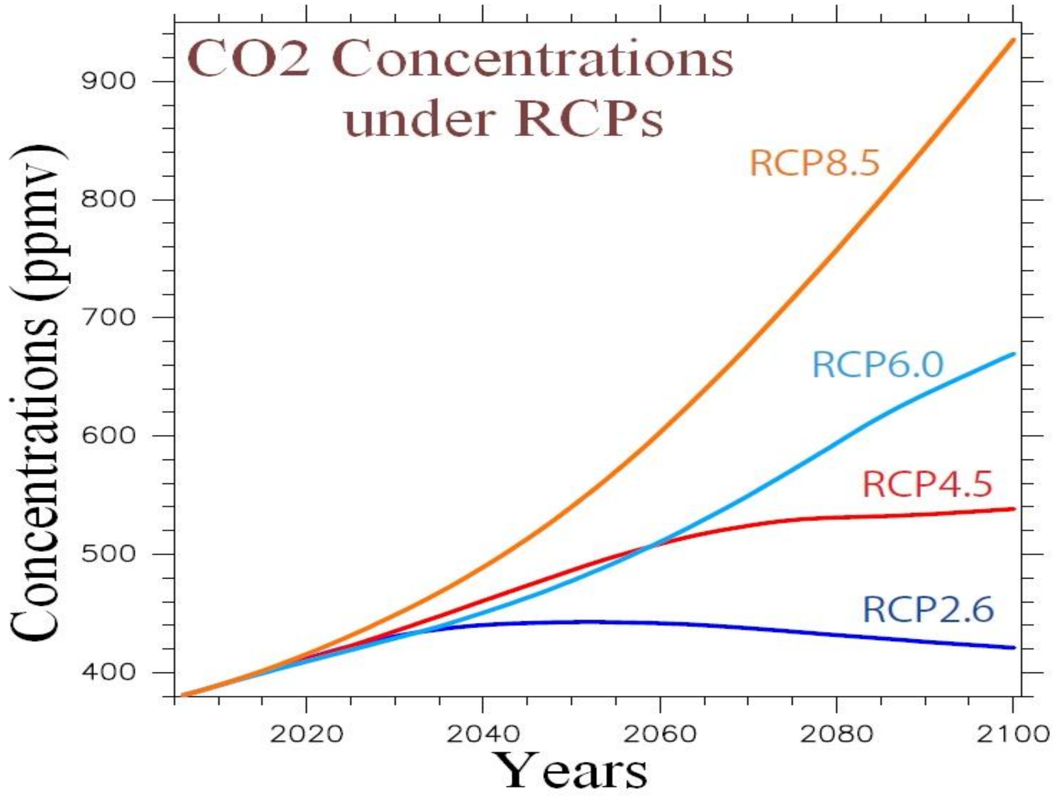

Figure 29: The greenhouse gas concentrations associated with the latest IPCC emissions scenarios.

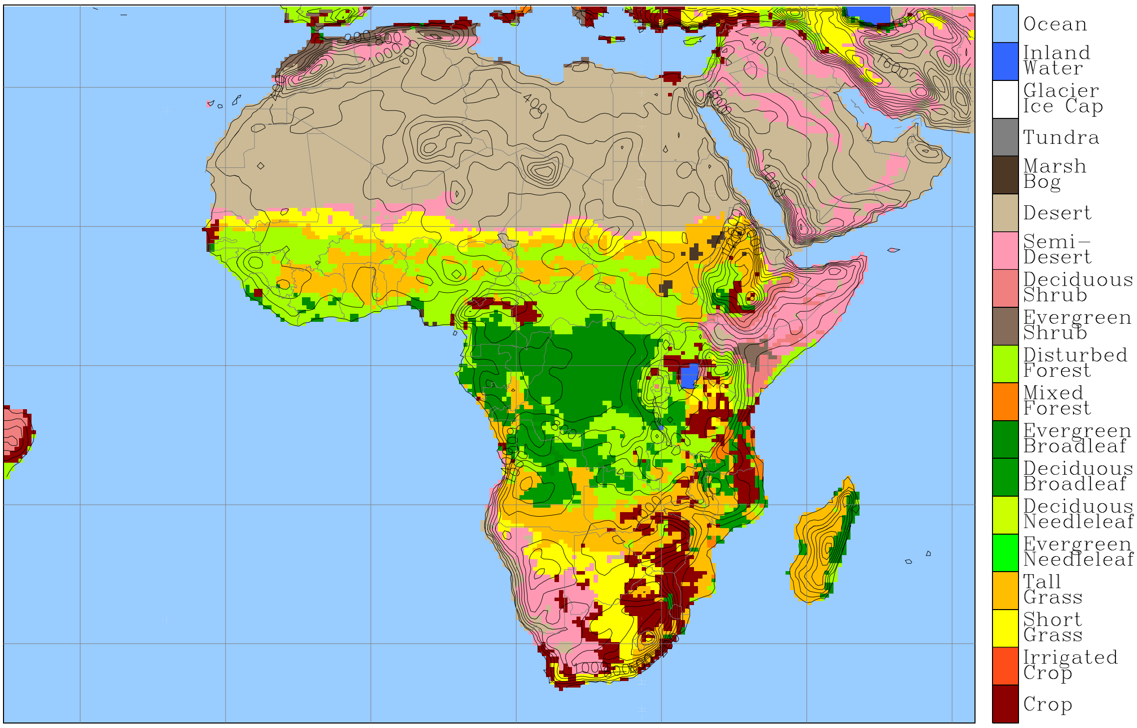

Figure 30: Map of land cover and topography for the climate change simulations to be analyzed as part of this study.

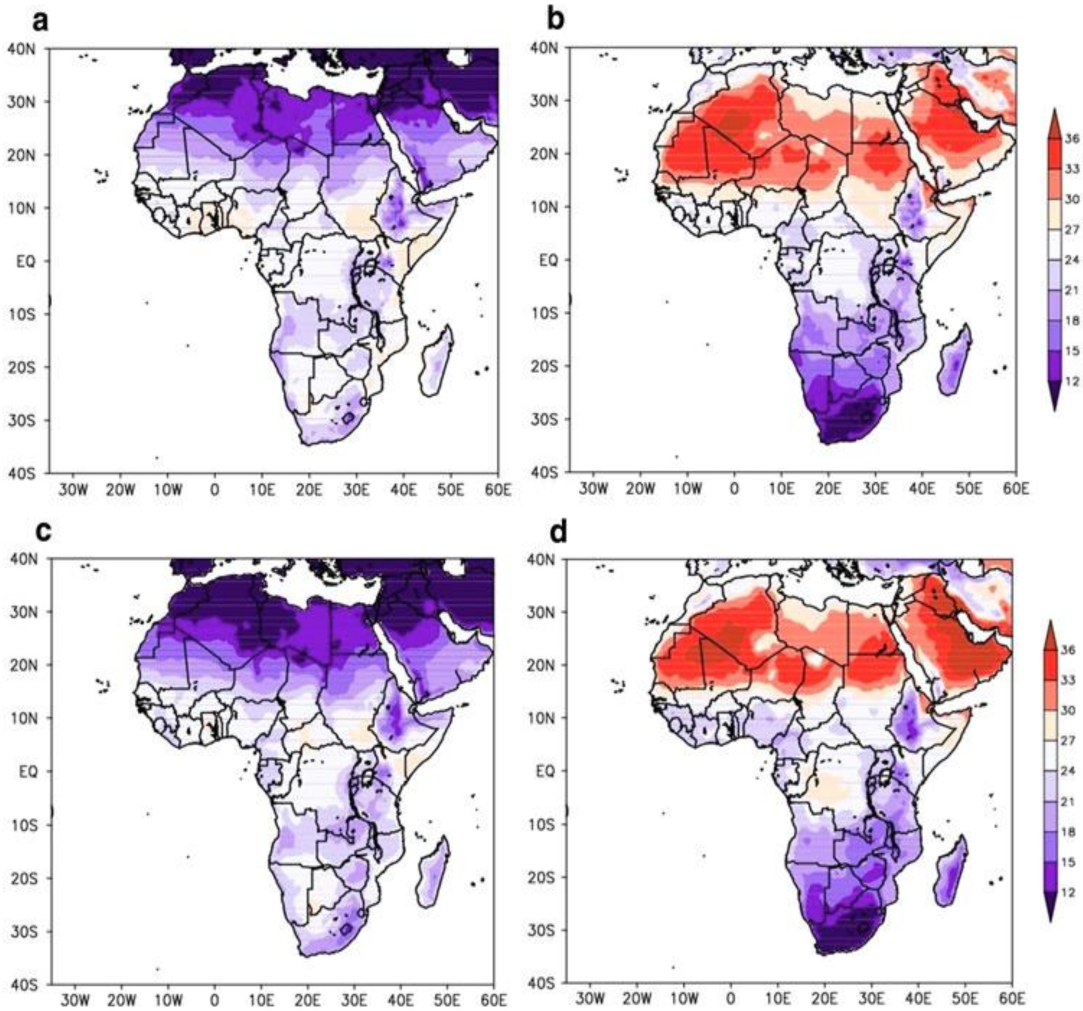

Figure 31: Averaged 1989–2002 2-meter Air Temperature (in o C) in DJF (left panels) and JJA (right panels) from CRU (a and b) and RegCM (c and d) adopted from Sylla et al. (2010).

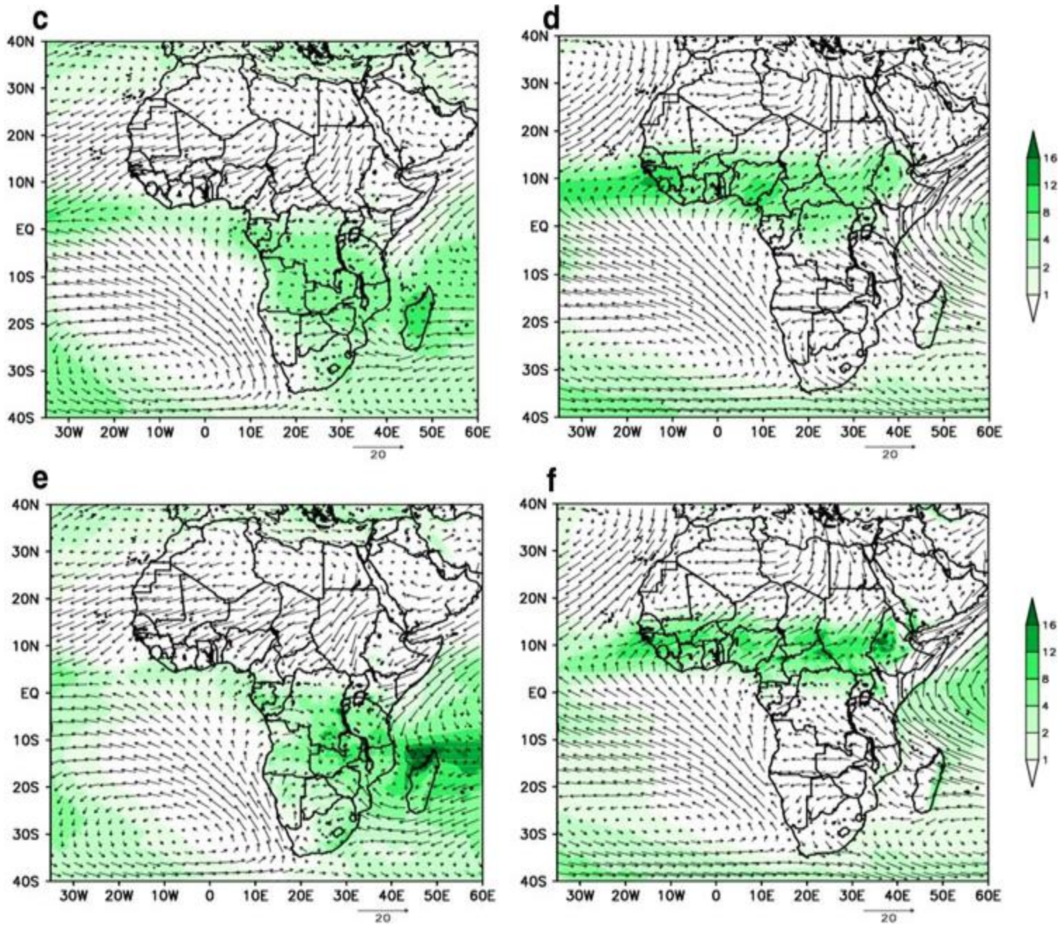

Figure 32: Averaged 1989–2007 Precipitation (mm/day) in DJF (left panels) and JJA (right panels) from CRU (c and d) and RegCM (e and f) from Sylla et al. (2010).

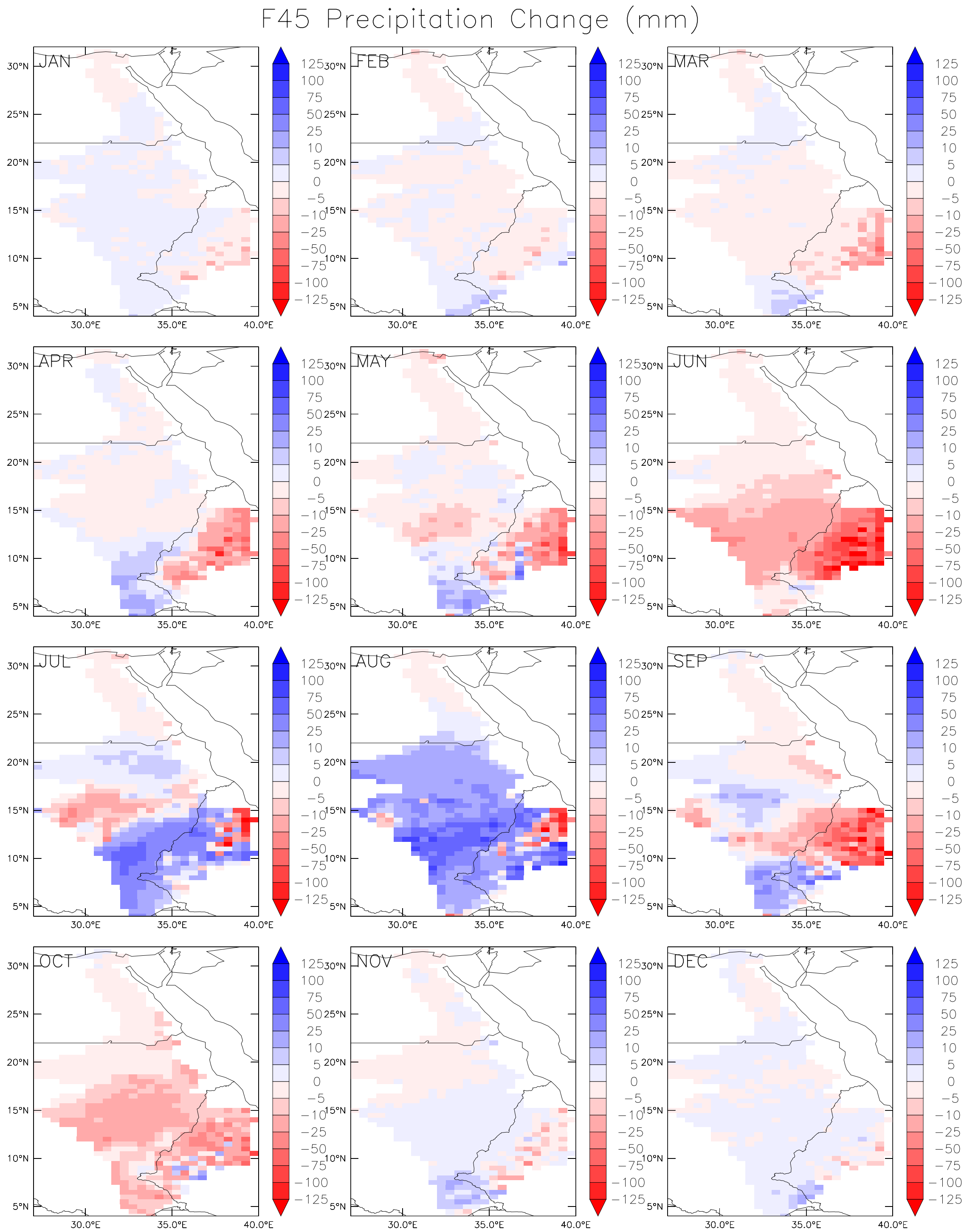

Figure 33: RCP4.5 precipitation change (mm/month).

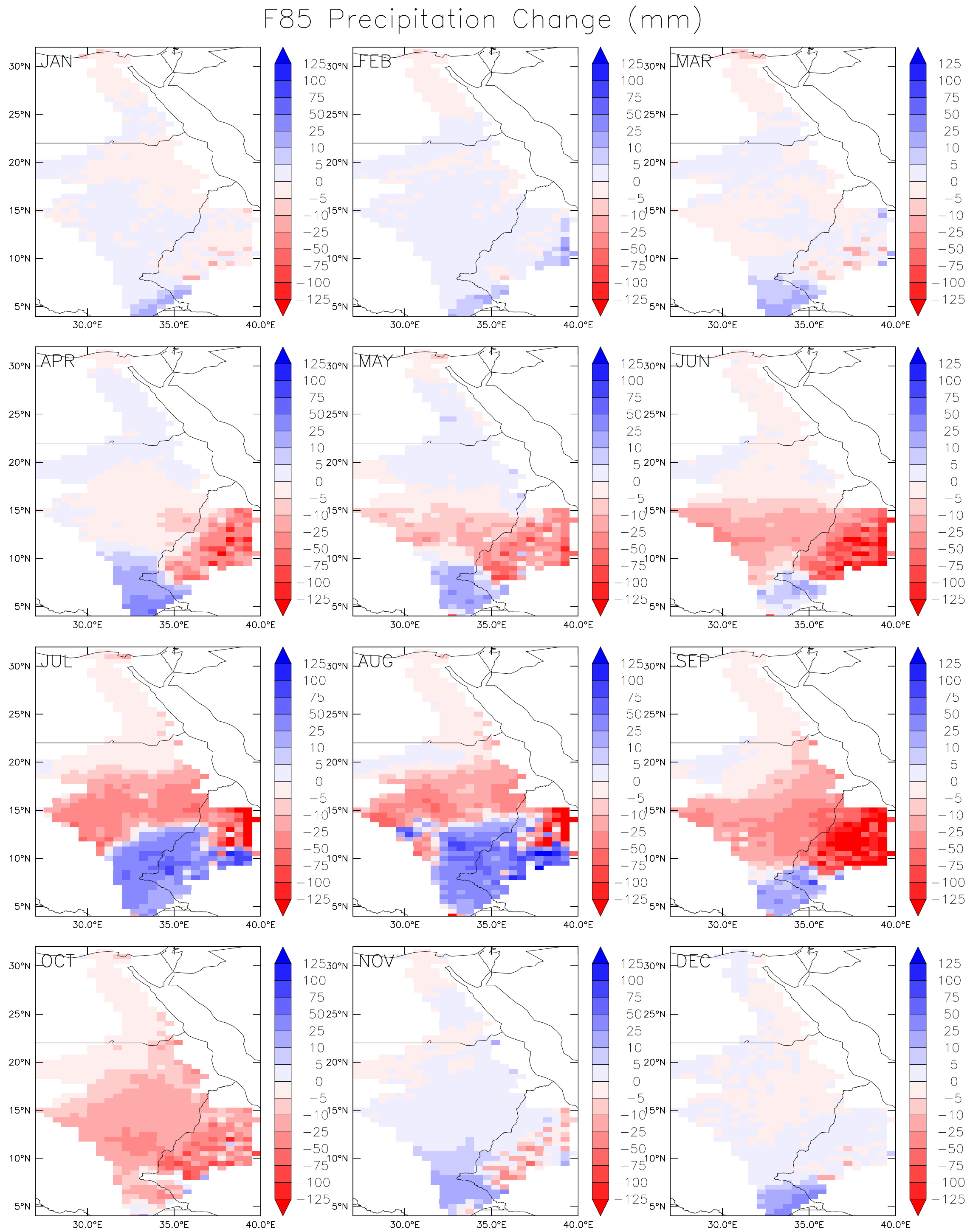

Figure 34: RCP8.5 precipitation change (mm/month).

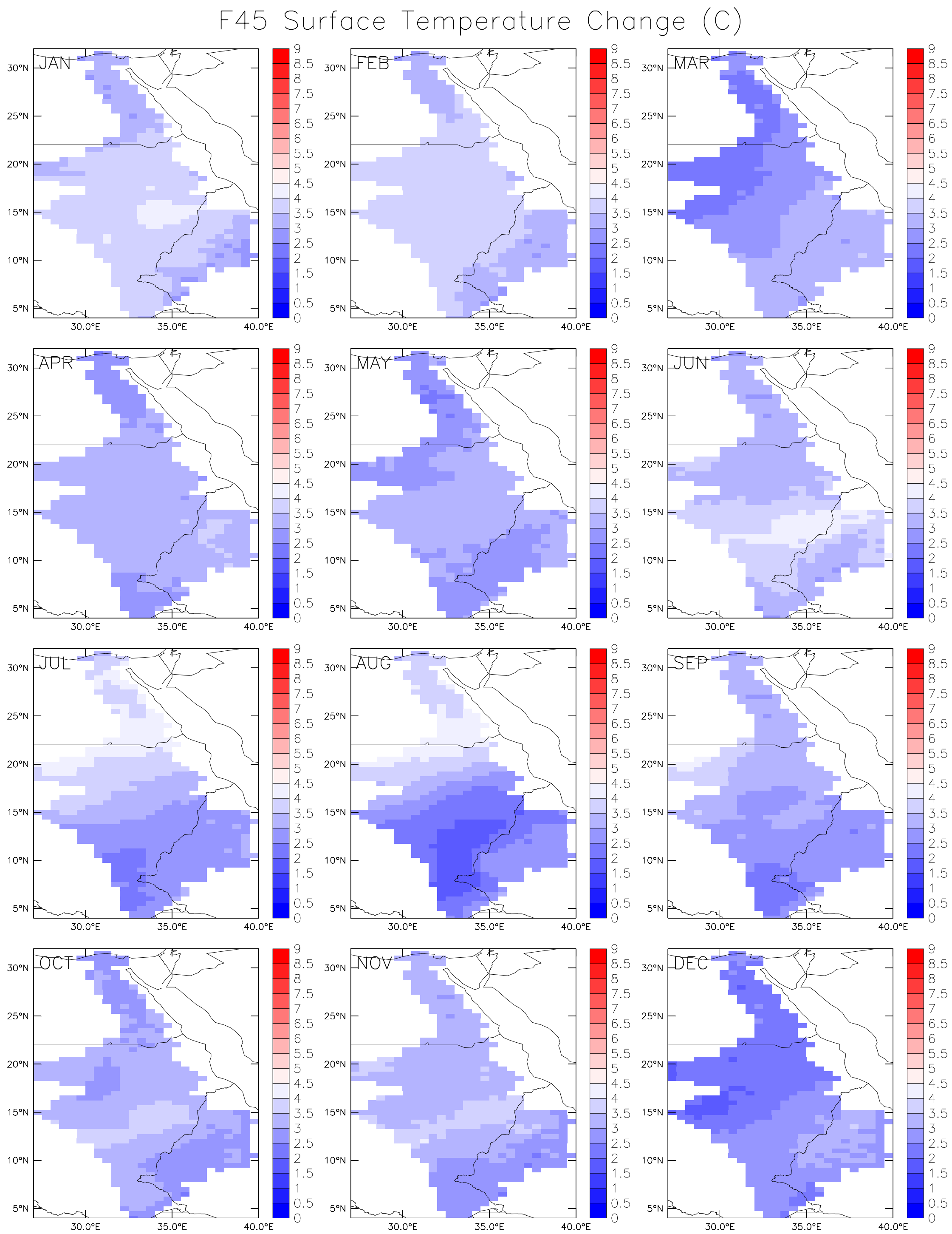

Figure 35: RCP4.5 surface temperature change (°C).

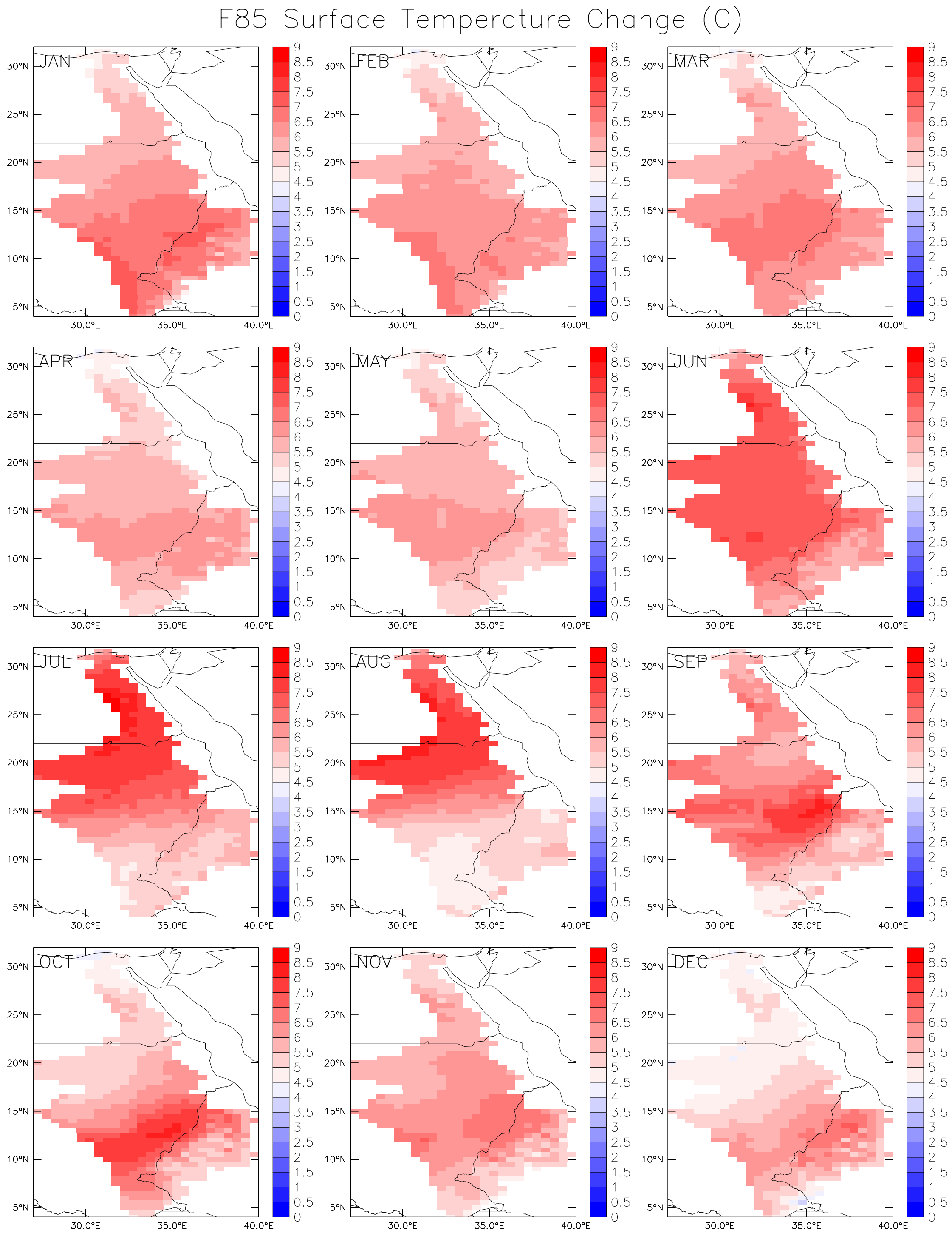

Figure 36: RCP8.5 surface temperature change (°C).

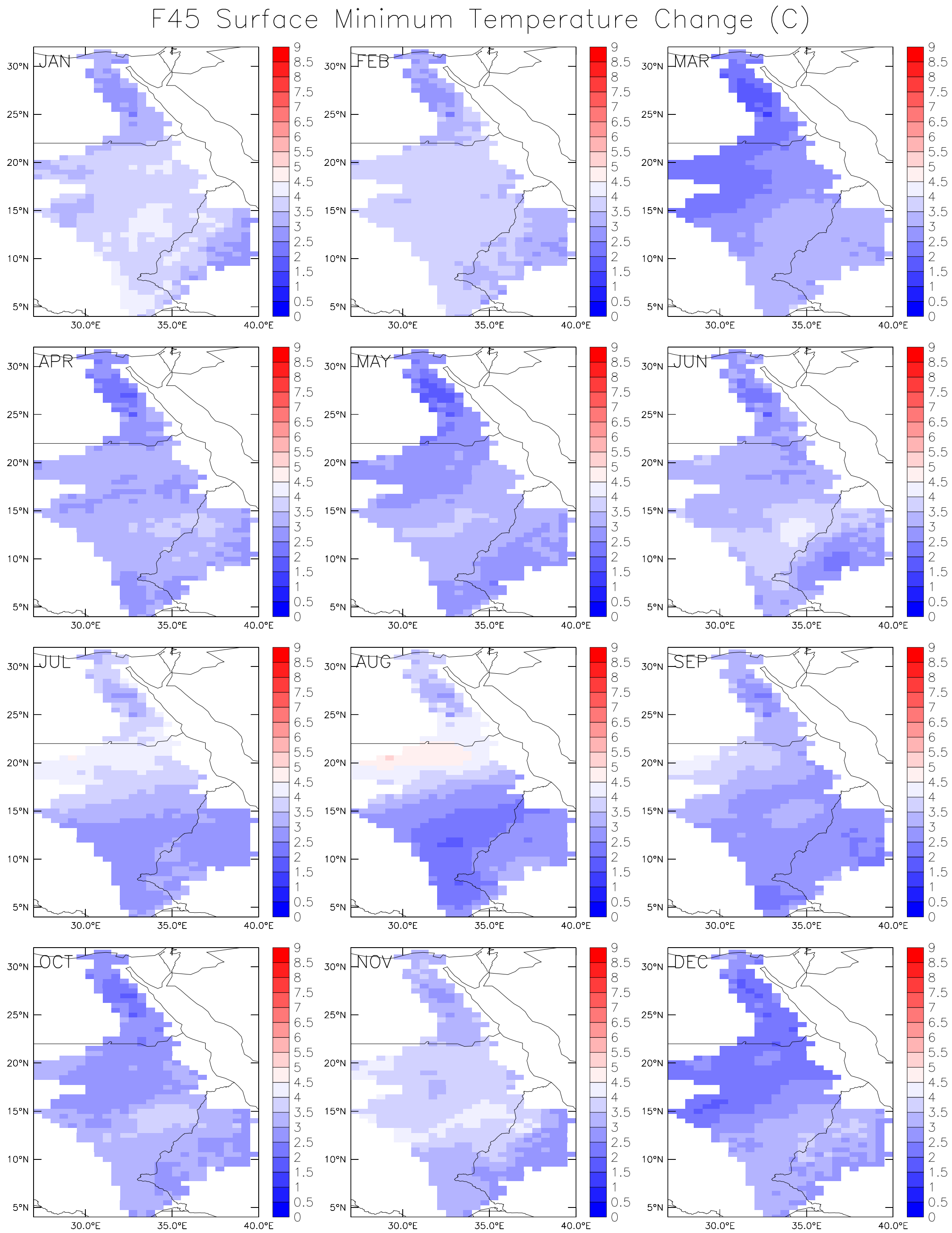

Figure 37: RCP4.5 minimum surface temperature change (°C).

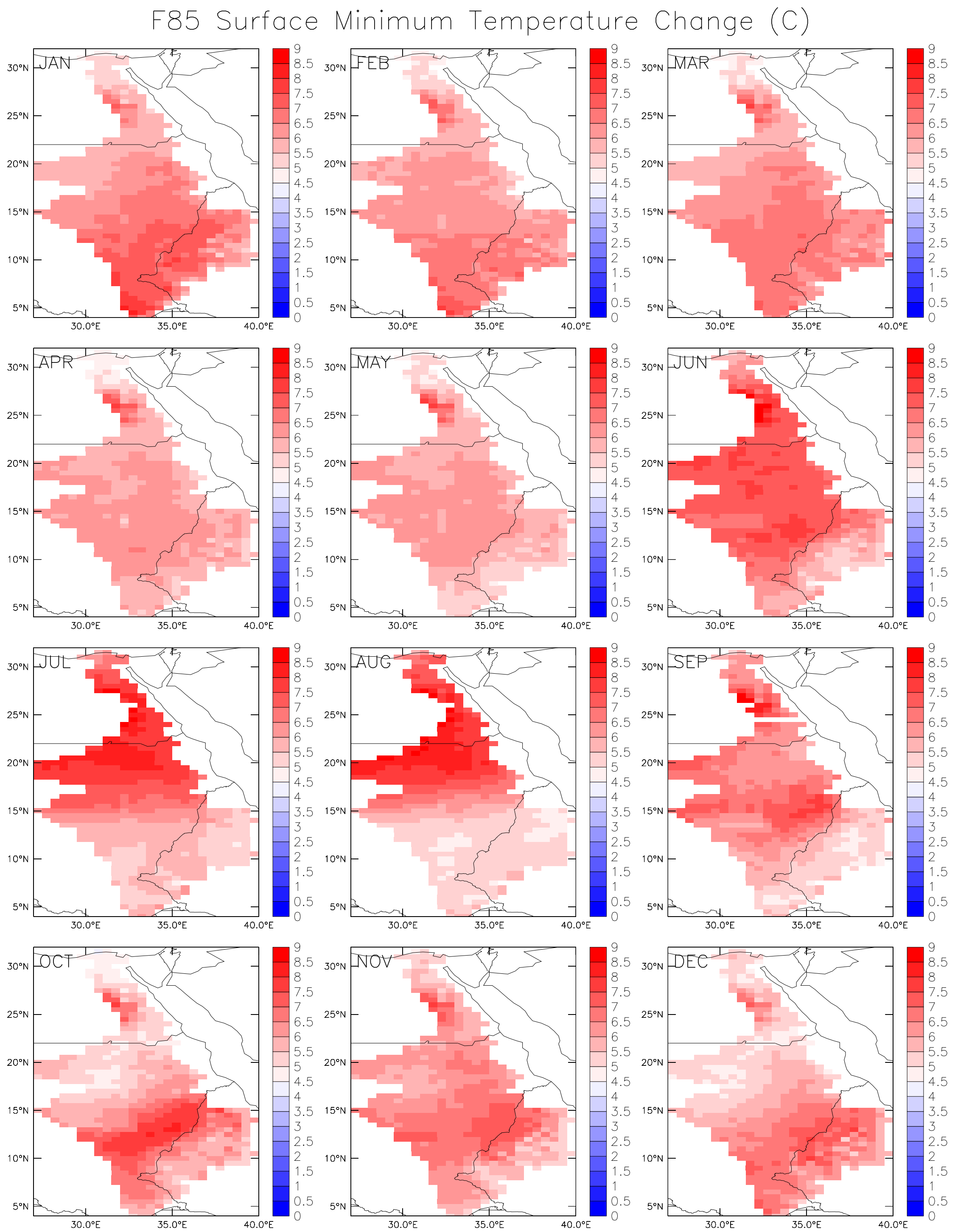

Figure 38: RCP8.5 minimum surface temperature change (°C).

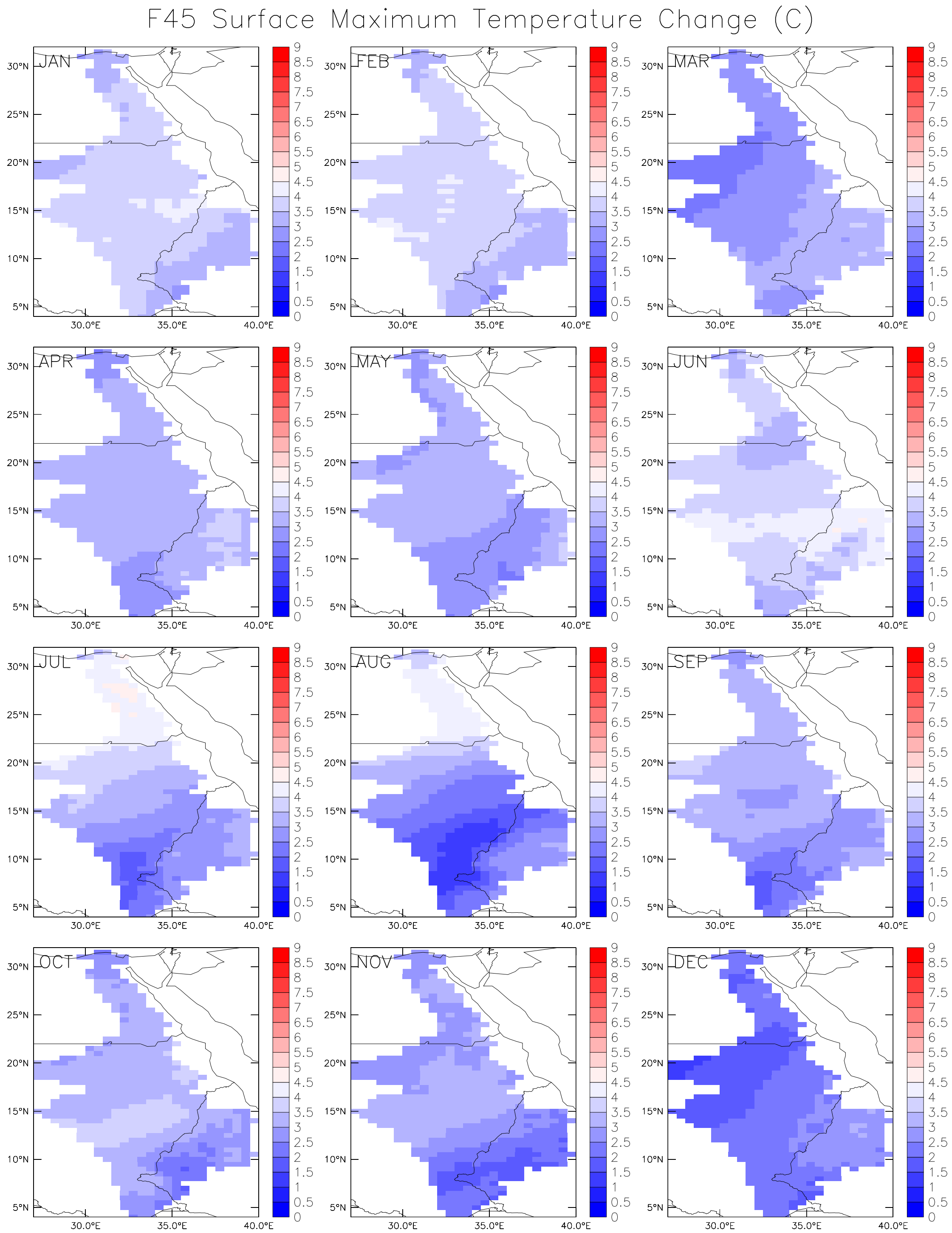

Figure 39: RCP4.5 maximum surface temperature change (°C).

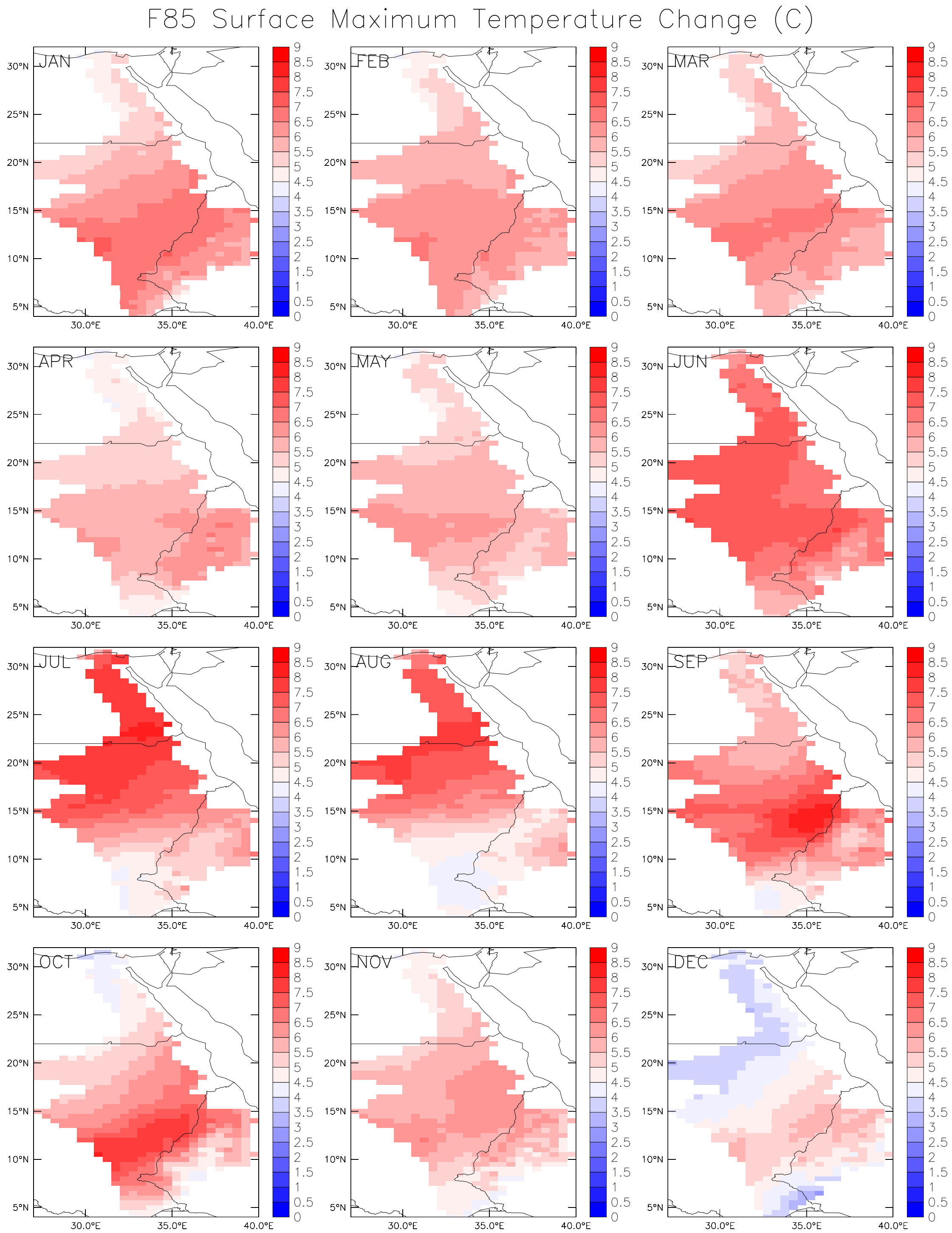

Figure 40: RCP8.5 maximum surface temperature change (°C).

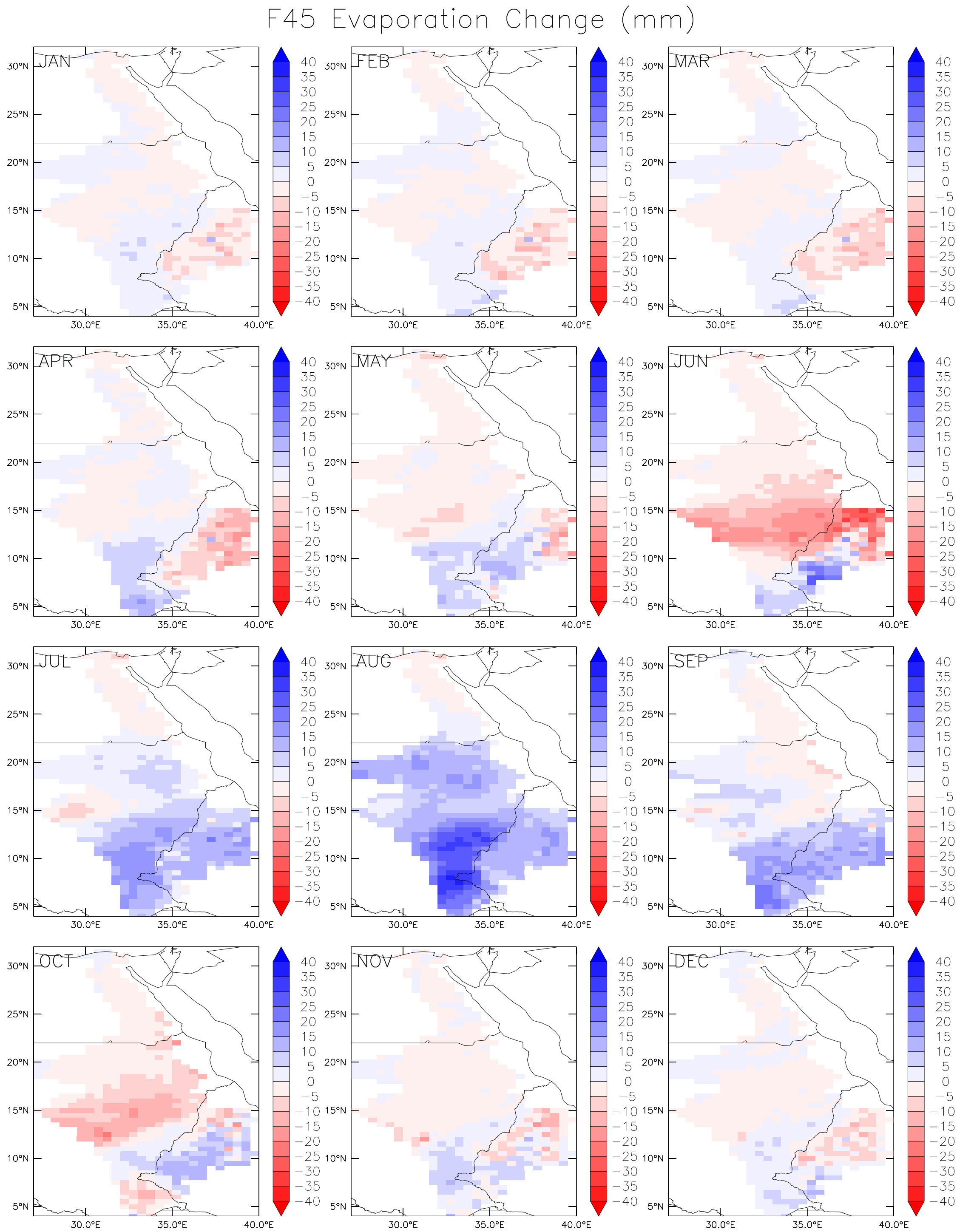

Figure 41: RCP4.5 evaporation change (mm/month).

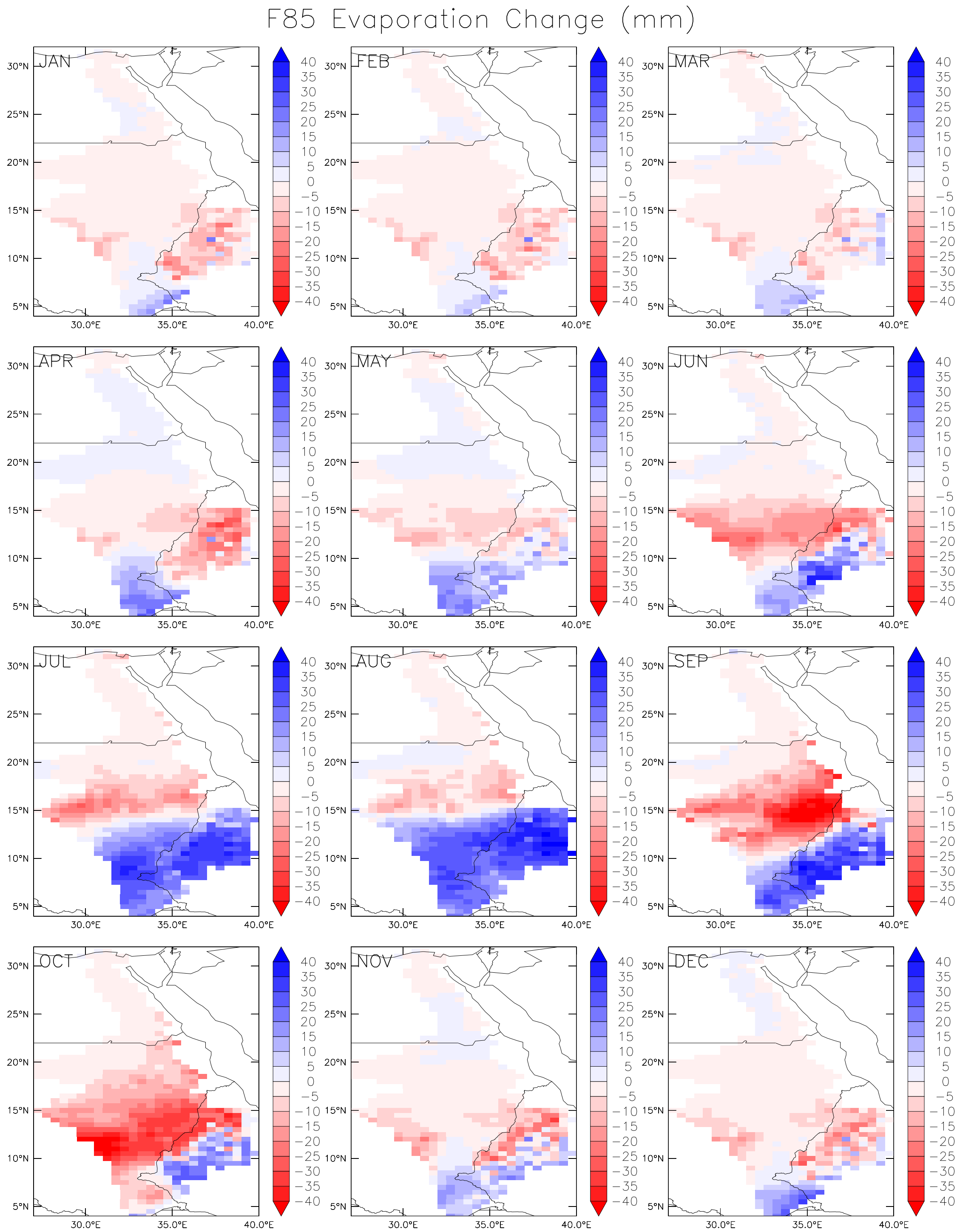

Figure 42: RCP8.5 evaporation change (mm/month).

7 Crop Suitability and Scenarios

The potential impacts of climate change on agriculture in the Eastern Nile basin include those on irrigation water requirements. The goal in this phase of the study is to determine present day and end of century projected crop suitability and irrigation requirements in the Eastern Nile basin on the 0.5-degree grid established in the observational analysis based on the CRU observations presented in Section 5 and the climate change projections based on the IPCC RCP4.5 and RCP8.5 emissions scenarios presented in Section 6. It should be noted that the UDEL observations are similar to those of CRU, and thus have similar results. In other words, inaccuracies in the methods applied are considerably greater than the differences between the datasets. As a result, only the CRU data are presented in this report, even though the UDEL data are also analyzed.

The deliverables for this phase are provided below:

1. 0.5° resolution maps of suitable regions for each crop group;
2. 0.5° resolution maps of regions suitable 80% or more years for crop growth for each group;
3. Basin plots of growing season evapotranspiration, effective rainfall, and water surplus/deficit for selected crop scenario.

7.1 Overview of Agriculture in the EN Basin

In this section, an overview of the principal crops grown in each region is discussed. Although the analysis in this study focuses primarily on the EN basin without regard to political boundaries, consideration for the individual countries within the basin is made. Furthermore, the Republic of Sudan and the Republic of South Sudan are sometimes considered one region in this study, since no disaggregated FAO agricultural data are available for the individual countries since their separation. In other words, parts of the agriculture analysis are performed for the former Sudan. Efforts, however, are made to distinguish the two countries when possible.

The top crop production for 2010 based on Profit and Metric Tons for the EN coutries except South Sudan is presented in FAOSTAT (2012). Many of these are described in further detail in the following sections. In addition, a subset of these is selected for the cropping scenarios to determine potential changes irrigation requirements.

7.1.1 Ethiopia

Agriculture in Ethiopia is primarily rainfed. The principal grain crops grown are teff, wheat, and barley, primarily cool-weather crops; and corn, sorghum, and millet, primarily warm weather crops (GAIN 2012). Wheat is mainly grown in the highlands, planted in the summer before the main rainy season, and harvested in October-November. Teff is also grown in the cooler highlands, while sorghum is the main lowland crop because it thrives well in semi-arid environments. Barley is cultivated most regions, but it performs best in cooler higher elevation regions. Finger millet is often planted in marginal areas due its resistance to drought and pests.

7.1.2 Sudan

The principal cash crops in Sudan are cotton, sesame, peanuts, sugarcane, dates, citrus fruits, mangoes, coffee, and tobacco. The principal subsistence crops are sorghum, millet, wheat, beans, cowpeas, pulses, corn, and barley. Cotton is the principal export crop and an integral part of the country's economy. According to FAOSTAT, the top three crops in terms of productivity are sugarcane, sorghum, and dry onions, respectively.

The primary source of irrigation in the Republic of Sudan comes from the Gezira Scheme, which is located between the Blue and White Niles near their confluence in Khartoum. It is one of the world's largest irrigation projects and provides a substantial portion of government revenue via exports. The scheme covers more than 800,000 hectares, producing most of the country's cotton, sugar cane, wheat, legumes, peanuts, fruits and vegetables and accounting for a substantial share of agricultural GDP (Eldaw, 2004). Cropping occurs year round. Cotton is typically sown in July, sorghum in June, and Wheat November (Plusquellec, 1990).

7.1.3 South Sudan

As mentioned above, no disaggregated FAO agricultural data are available for South Sudan since its separation from Sudan. South Sudan located in the White Nile valley has extremely fertile soils and considerably more rainfall than Sudan. The primary crops include sorghum, groundnuts, and cassava (FAO 2010). Sowing typically occurs in May and June coinciding with the start of the rainy season and harvesting between October and December depending on the crop variety.

7.1.4 Egypt

Agriculture in Egypt is primarily irrigated due to its arid climate and is confined to the Nile Valley and delta. The primary crops are cotton, sugarcane, tomatoes, clover, wheat, rice, and maize. The high humidity in the delta region best suits cotton, while the drier, hotter climate of the south favors sugarcane, onions, and lentils (Metz, 1990). Summer cereal crops are typically sown in May and harvested in September and October, and winter crops are sown in November and harvested in May (FAO Crop Calendar, 2012). Rice and Maize are planted in May and harvested in September and October. Vegetables have various plant dates throughout the year.

7.2 Crop Temperature Suitability Method

In subtropical and temperate climates, winter and summer growing periods are determined largely due to seasonal temperature changes (FAO, 1985). For example, in

Nile Delta region (Lower Egypt), temperate crops such as berseem clover, wheat, barley, and beans are grown in the winter and heat tolerant crops such as cotton, rice and maize are grown during the summer. Crops grow when temperatures fall within an operative range unique to the crop type, and cease growth when they fall outside of the range (Table 3). For optimal growth to occur, temperatures must fall within a specific range also unique to the crop type.

FAO (1985) divides crops into five adaptability groups based on their photosynthetic carbon assimilation pathways (C3, C4, and crassulacean acid metabolism (CAM)) and the effects of radiation and temperature on photosynthesis (see Table 3). Within the optimal temperature, the growth rate reaches a maximum. Outside of the range, but still within the operative range, the growth rate is reduced the further the temperature is from the optimal range. It should be noted that in many temperate climates and at high altitudes in tropical countries (such as Ethiopia), the temperature for growth is below optimal for part of the growing season. In addition, this method assumes that rainfall and/or irrigation is sufficient to meet the crop water needs. The method also assumes that soil conditions (e.g., type) and terrain (e.g., surface slope) are ideal for optimal growth, which are ignored in this study.

In this study, the suitability, based on monthly mean surface temperature for each of the crop groups, is determined. Suitability of the primary crops types of the Eastern Nile region is determined based on the FAO (1985) optimal crop suitably temperature range (see Table 3). This is done using monthly mean CRU temperature observations and temperature changes from the RCP4.5 and RCP8.5 IPCC emissions scenarios. The procedure to compute the projected temperatures is described in detail below in Subsection 7.4. The present day and future periods are considered to be 1980 through 2009 and 2080 through 2099, respectively.

The zones of suitability are based solely on temperature and do not account for other important factors relevant for crop productivity. These include soil type and ground slope. Accounting for these factors would greatly reduce the area suitable for crop production. Presumably, the regions suitable for crop growth would decrease considerably when accounting for these factors.

7.3 Description of the Crop Coefficient Method

The FAO (1985) crop coefficient method is applied to determine the total crop water requirements. This method considers crop water needs as a function of climate (temperature, photosynthetically active radiation, wind conditions, and ET_c), crop type, and crop growth state (seedlings, development, mature, etc.; see Figure 43). The crop evapotranspiration (ET_c) is determined according to the following relationship:

$$ET_c = K_c ET_O$$

where ET_O is the reference crop evapotranspiration (generally well watered grass) and K_c is the crop coefficient. ET_O represents the evaportranspiration from a large area of green gas that actively grows, completely shades the ground, and is not water limited, and represents the climate control. K_c represents both the crop type and growth stage (described below), and is what distinguishes field crops from the grass reference. ET_c

can be considered the amount of required water per unit area for a given crop type to grow optimally.

The influence of these various climatic factors on crop water needs is given by ET_O. ET_O is typically determined using evaporation pans or a theoretically approach. Given the large scale of the EN basin, the FAO theoretical approach of Blaney and Criddle (hereafter referred to as the Blaney-Criddle method) is applied in this study. In this method only observations of mean temperature and latitude to determine the percentage of daytime hours are needed, as follows:

$$ET_O = p\left(0.46T_{mean} + 8\right)$$

where T_{mean} is the mean daily temperature in degrees Celcius and p is mean daily percentage of annual daytime hours for a given latitude and time of year (see Table 6). Temperature generally determines the rate of growth and development of crops mainly due to photosynthesis as discussed in the previous section. The rate of photosynthesis is influenced by both photosynthetically active radiation and temperature, and effects crop growth and yield. Both of the temperature and radiation are considered in the Blaney-Criddle method.

Under normal conditions, the method provides reasonable results; however, under extreme conditions the method can grossly over and underestimate ET_o. While it would be preferable to use a Penman-Monteith type method, such a method requires data observations not available at the resolution and scale of this study. It should be noted, however, that both FAO and the United States Department of Agriculture (USDA)-Natural Resource Conservation Service (NRCS) recommend and use the Blaney-Criddle method.

The monthly values of ET_o are computed based on the monthly surface temperature values from CRU observations, CRU+RCP4.5 scenario, and CRU+RCP8.5 scenario (Figure 44 and Figure 45). In the present climate, the values range from approximately 80 mm/month during the winter in the Nile Delta and Ethiopian highlands and up to 250 mm/month in the summer in northern and central Sudan. Under the CRU+RCP4.5 and CRU+RCP8.5 scenarios, they increase and vary from 90 to 270 mm/month and from 100 to nearly 300 mm/month, respectively. The patterns closely follow those of temperature due to the strong dependence of temperature on ET_o (Figure 44).

While the reference crop evapotranspiration accounts for climatic influences, the influence of crop type on crop water needs must also be considered (K_c). K_c is dependent on the crop type and the growth stage of the crop (Table 5 and Table 6). Each crop species possesses differing characteristics such as leaf areas, which impact transpiration rates and resulting water needs. Fully developed crops require more water compared to a crop that has just recently been planted, thus, the dependence of K_c on growth stage. Additionally, K_c can vary to a certain extent from region to region. Certain crops grow more slowly in a cool climate than in a warm climate.

Determining K_c requires the total length of the growing season and the lengths of the various growth stages for each crop (Table 6). The total growing period in days is the period from sowing or transplanting to the last day of the harvest. It is mainly dependent on 1) the type of crop and the variant; 2) the climate; and 3) the planting date. The sowing/planting date also varies due to yearly local conditions and the customs of the farmers within a region. Such factors, however, are not considered in this study.

The total growing period is divided into four growth stages (see Figure 43, Table 5 and Table 6):

1. *Initial Stage*: This stage includes sowing or transplanting till approximately 10% ground cover.
2. *Crop Development Stage*: This period starts at the end of the initial stage and lasts until effective full ground cover has been reached (ground cover 70-80%). Plants at this stage are nearly full size.
3. *Mid-Season Stage*: This period runs from the start of effective full ground cover and until the start of maturity. It includes flowering and grain setting.
4. *Late Season Stage*: This period runs from the start of maturity through the last day of harvest. It includes ripening.

Table 6 shows the duration of the various growth stages for some of the major field crops. For each crop the minimum and maximum duration of total growing period been taken and sub-divided in the various growth stages. As can be seen, there is considerable variability of the values. Generally speaking, it can be assumed that the growing period for a certain crop is longer for cooler climates and shorter warmer climates (FAO 1986).

With the crop water requirement determined, water has to be supplied to the crops. This is done by various ways such as by rainfall, by irrigation, or by a combination of irrigation and rainfall. Water can also be supplied by the groundwater through capillary rise but for the scope of this paper the contribution of capillary rise is not taken into account. There are three cases that describe the potential supply of water to crops (FAO, 1986):

1. The water needs for optimal crop growth is provided by the effective rainfall (P_{eff}), i.e., the fraction of rainfall used to meet the plant water needs, and irrigation is not required. In this case, the irrigation water need (IN) equals zero: $IN = 0$.
2. No rainfall at all occurs during the growing season and all water needs are supplied by irrigation. Consequently, the irrigation water need equals the crop water need (ET_c): $IN = ET_c$.
3. Part of the crop water need is supplied by rainfall and the remaining part by irrigation. In such cases, the irrigation water need is the difference between the crop water need and the effective rainfall: $IN = ET_c - P_{eff}$.

To compute the irrigation needs for cases one and three, P_{eff} must be computed. P_{eff} is a function of the total rainfall, runoff, evaporation, and soil percolation: P_{eff} = *Total rainfall – runoff – evaporation – deep percolation*. Such data in most circumstances, except for total rainfall, are not available (which is the case in this study). For the purpose of this study, an approximation based on FAO (1986) is used to compute P_{eff}:

$$P_{eff} = 0.6P - 10 \text{ if } P < 75 \text{ mm/month}$$
$$P_{eff} = 0.8P - 25 \text{ if } P \geq 75 \text{ mm/month}$$

where P = rainfall or precipitation (mm/month). These formulas are applied in areas with a maximum slope of 4 to 5%. As mentioned above, slope is not considered in this study. The computed effective rainfall is presented in Figure 46 for each month and for the CRU observations and both IPCC emissions scenario.

To determine the total irrigation requirements at a location (IN_{total}), the requirements must be integrated over the entire growing season from sow date to harvest:

$$IN_{total} = \sum_{t=sow}^{harvest} IN_t$$

This provides an indication of the total water required for a successful growing cycle. Comparing these values to the precipitation occurring during the growing season establishes whether or not and how much irrigation is required.

7.4 Climate Projection Method

Under a warmer climate and an atmosphere that is richer in carbon dioxide, both potential evaporation and crop coefficients are likely to change. General speaking, potential evaporation is expected to increase due to the increase in temperature, while crop coefficients may decrease because of the carbon dioxide fertilization effect; however, the are other competing factors that impact both the signs and magnitudes of the changes. Depending on the relative magnitudes of these two changes, the overall magnitude of evaporative demand by crops may increase or decrease.

Crop suitable for the Eastern Nile region is determined based on the analysis of the modeled climate change projections (Section 6). The future climate is determined by computing the differences between the simulated future and present day climates. The simulated changes in climate are then added to the observations. For example, the following formulation would apply for future temperature:

$$T_{future} = T_{present}^{Obs} + \left(T_{projected}^{Sim} - T_{present}^{Sim}\right)$$

where $T_{present}^{Obs}$ is the observed present day temperature, $T_{present}^{Sim}$ is the simulated present day temperature, and $T_{projected}^{Sim}$ is the simulated projected temperature for the future time period and emissions scenario of interest. Applying the change in climate to the observations in this manner removes model bias.

In this analysis, the present day and future periods are considered to be 1980 through 2009 and 2080 through 2099, respectively. The present day values are based on the CRU observations (see Section 5), while the future periods are based on the RCP4.5 and RCP8.5 IPCC emissions scenarios (see Section 6). As discussed previously, RCP4.5 is considered a low emissions scenario and RCP8.5 is considered a high emissions scenario. Analyzing the two scenarios provides an indication of the uncertainties in future emission pathways.

7.5 Analysis

In this subsection, the methods described above are applied to the EN basin using the present day (CRU observations), CRU+RCP4.5, and CRU+RCP8.5 scenarios. Note that the analysis is also performed using the UDEL observations, but omitted from the report because the results are similar to the analysis using the CRU data. In addition, factors such as soil type and ground slope are not accounted for in this analysis.

Suitability is first determined where each crop group is operative and optimal for growth based on surface temperature (Figure 44). The different shading in the figures for this portion of the analysis represents the temperature zones of suitability for each of the crop groups (Figure 47, Figure 51, Figure 55, Figure 59, and Figure 63). Green represents temperatures falling within the temperature range for optimal growth. Light blue and light red represent temperatures below and above optimal, respectively, but still operative for growth. Dark blue and dark red represent temperatures below and above operative, respectively, and therefore indicate regions unsuitable for crop growth. There are 36 panels in total covering three pages, 12 for the month of each scenario. Each column represents a different scenario: Left is CRU; middle is CRU+F45; and right is CRU+F85.

Since observations of the crop types are not available over the entire basin, the water requirements for each subbasin are computed under various potential cropping scenarios. The selected crops are selected based on what is typically grown in each region of the *EN* basin (see Section 7.1).

Evapotranspiration for at least one case from each crop group is modeled using the FAO Crop Coefficient method described in Section 7.3, except for Group V (see Table 3). Sisal is the only crop from Group V that is commonly grown in that EN region. No data, however, are available from FAO for the length of each growth stage for sisal. Therefore, no results are presented for crops from Group V.

Water surplus (*IRR*) for crops typical to the EN basin is then estimated for the entire growing season using the crop coefficient method. Water surplus is defined as effective rainfall minus crop evapotranspiration. A negative value is considered the irrigation requirement. Monthly surface temperature (Figure 44) is used to compute the reference crop evapotranspiration (Figure 45), and effective precipitation (Figure 46) is used to compute the water surplus and deficit for each of the three scenarios. The data are masked for operative temperature suitably for at least 80% of the years (Table 3). All days with in the growing season must fall with in the operative range at least four out of five years or the region is considered unsuitable. For brevity only one crop from each group is considered in this analysis. Some additional cases for maize, sorghum, and millet are considered at the end of the subsection.

Similar to the figures described above, the figures displaying the total growing season crop evapotranspiration and water surplus have 36 panels: 12 for the month of each scenario. The left column displays present day climate (CRU observations) and the middle and right columns display the RCP4.5 and RCP8.5 emissions scenarios, respectively. Each row represents a different sow date starting January 15 and corresponding harvest date with one-month shifts until December 15. This is done because each region has different sow and harvest dates. In addition, a warmer climate would likely result in shifts in sow dates to cooler seasons and a change to heat tolerant crops. Lastly, in some cases Sudan and South Sudan are not distinguished from each other since the FAO has little data available separating the two countries.

7.5.1 Crop Group I

Group I crop types grow optimally between 15 and 20° C and are operative between 5 and 30° C (Table 3). These temperatures are relatively low compared to the other crop groups. Crops in this group photosynthesize through the C3 pathway and are represented by crops such as wheat, barley, and oats.

7.5.1.1 Temperature Suitability

In the present climate, this group grows optimally in region along the Sudan-Egypt border during the winter months and the higher regions of Ethiopia more or less year round (Figure 47, left panels). Temperatures in Sudan tend to be too high for these crops to grow optimally during the winter (DJF) and cease to grow from more or less April through October. In South Sudan, from February through April, temperatures are too hot crop growth. The rest of the year the high temperatures allow for crop growth, but not under optimal conditions.

Temperature changes from the climate change scenarios have the greatest impact on Group I crops because of the group's low range of operative temperature suitability (5 to 30° C; Figure 47, middle and right panels). Under the RCP4.5 and RCP85 scenarios, most of Sudan, South Sudan, and southern Egypt are unsuitable for crop growth. The Ethiopian Highlands, which had temperatures optimal for growth under the present day conditions, are mostly operative under the future scenarios. The temperature increase in Northern Egypt, on the other hand, shifts the region into optimal growing conditions during the winter. This change would likely result in an increase in productivity in the region.

7.5.1.2 Wheat

Wheat is cultivated in all of the countries of the EN basin. It is most common in Ethiopia and Egypt where temperatures are cooler. The growing season is relative long at 150 days and the crop coefficients vary from 0.30 during the initial period to 1.15 during the mid period to 0.40 at harvest (see Figure 48, Table 5, and Table 6).

In Ethiopia wheat is typically sown during the spring and harvested in the summer coinciding with the rainier portion of the year (FAO Crop Calendar, 2012). In some cases, it is grown as the second crop in a rotation where it is planted in the late summer and harvested in the late fall and early winter. In Egypt, wheat is typically planted in November and harvested in May when temperatures are cooler.

In the present climate, wheat is suitable for operative cropping in Ethiopia and the Nile Delta region regardless of the sow date (Figure 49). In South Sudan, wheat is suitable when sown during the summer months. Wheat is not suitable in most of Sudan.

The evapotranspiration losses from wheat in the present climate are relatively low despite the long growing season (Figure 49, left column). As a result, the irrigation requirements are relatively low for wheat ranging from a water surplus in parts of Ethiopia during the rainy season to approximately a 1 meter deficit in Egypt during the summer over the entire growing season (Figure 50, left column). It should be noted that wheat is typically not grown in the summer in Egypt, and in winter the growing season water requirements are approximate 0.5 meters.

In a warmer climate, the regions suitable for wheat shrink dramatically (Figure 49, middle and right columns). Wheat is no longer be suitable for growth in Egypt except when sown in the late fall in along the Mediterranean. In South Sudan, no months are be suitable for wheat growth. Wheat shifts to the higher regions of the Ethiopian Highlands. Although the crop evapotranspiration increases in with the warmer climate, the increase in effective precipitation tends to compensate (not shown). As a result, the total irrigation requirements do not change considerably change in Ethiopia (Figure 50).

7.5.2 Crop Group II

Group II crop types (e.g., tropical lowland soybean, groundnut, and rice) grow optimally between 25 and 30° C, are operative between 10 and 35° C (Table 3), and follow the C3 photosynthetic pathway. In this analysis, only rice is considered from this group, which is commonly grown in the EN region.

7.5.2.1 Temperature Suitability

Temperatures in the present climate in all regions fall with in the Group II operative range during all months of all years, except for a relatively small region in northern Sudan during the summer months (Figure 51, left column). Crops in this group grow optimally in Nile Delta region during the summer months and South Sudan during most months except from February through May. Generally, temperatures exceed the Group II optimal range in Ethiopia except in the lower elevation regions along the Sudanese border.

When considering climate change, some regions during some seasons improve in productivity, while others decline (Figure 51, middle and right columns). For example, productivity Sudan increases during the winter. During the late spring, summer, and early autumn, however, temperatures in Sudan are too high for Group II crops. In South Sudan, which had optimal temperatures for Group II crops, warmer temperatures decrease in productivity in all months. The warmer temperatures, however, improve productivity in the Ethiopian Highlands and Northern Egypt during most months. In southern Egypt, suitability decreases except during the winter months.

7.5.2.2 Rice

Rice is cultivated in all of the countries in the EN basin. Depending on the region and variety (irrigated versus flooded), it is generally planted in the late spring and early summer and harvested in autumn (FAO Crop Calendar, 2012). Like wheat, rice has a relatively long growing season of 150 days. Unlike wheat, its evapotranspiration losses are considerably higher with crop coefficients starting at 1.05 in the initial crop phase to 1.20 in the mature phase to 0.75 at harvest (see Figure 52, Table 5, and Table 6).

Typical present day values of estimated evapotranspiration for rice in the growing season range from approximately 0.5 m in Ethiopian highlands (where rice is not commonly grown) to in excess of 1 meter in central Sudan (Figure 53, left column). Similarly, all regions where rice is grown in the EN basin require irrigation due to the high evapotranspiration (Figure 54, left column). Since rainfall is low in much of Sudan and Egypt, close to 100% of the evaporative losses for rice are met through irrigation. Consequentially, the irrigation requirements are similar to the evapotranspiration losses. In the low lands of Ethiopia where rice is grown, a considerable portion of the irrigation needs is met by rainfall.

In a warmer climate, much of EN region that suitable for rice growth in the present climate is no longer suitable (Figure 53, middle and right columns). Of particular note, Sudan is no longer suitable for rice in the high emissions RCP8.5 scenario, except for a few localized regions. In Egypt, remains suitable when sown in autumn and early winter, the rest of the year is no longer suitable. Since little rainfall occurs in Egypt, the increase in evapotranspiration with the warmer climate must be compensated with additional irrigation (Figure 54). If rice were to be cultivated in the Ethiopian Highlands, irrigation requirements would be relatively low due to lower temperatures and higher rainfall.

7.5.3 Crop Group III

Group III crops are the most common southern Egypt, Sudan, and South Sudan. They are operative between 15 and 45° C and are thus suitable for the high temperatures observed in these regions (Table 3). The main crop types are maize, millet, sorghum, and sugarcane. In this section, sugarcane is presented. Since maize, millet, and sorghum are also part of Group IV, they are presented in Section 7.5.6 with the operative temperatures combined.

7.5.3.1 Temperature Suitability

In the present climate, crops associated with Group III are suitable for growing in all regions except the Nile Delta region during the winter months where temperatures are too cool (Figure 55, left column). In Northern Sudan (except the central portion of the region) and southern Egypt, crops in Group III grow optimally in the late spring and summer months. The other regions of the EN basin are too cool for optimal growth, however, still suitable for sub-optimal growth.

A warmer climate makes this crop group operative in all months of the year (Figure 55, middle and right columns). While some regions and seasons that are optimal for growth are only operative with warmer temperatures, others that are currently operative are optimal. For example, for the current climate the region of optimal growth centered over Sudan for much the year except winter, shifts northward into Egypt and southward into South Sudan. This implies a decrease in productivity in Sudan and an increase in Egypt and South Sudan. The suitability in Ethiopia remains more or less the same expect in the lowlands where suitability is improved.

7.5.3.2 Sugarcane (Ratoon)

Ratooned sugarcane requires the most water and has the longest growing season of the crops considered in this study. The crop coefficient varies from 0.45 in the initial phase to 1.25 in the mature phase to 0.75 at harvest (Figure 56). The growing season length is 320 days, and therefore requires suitability for nearly 11 months. Since average winter temperatures in Egypt are below 15° C, ratooned sugarcane not suitable there. It is, however, suitable for growth in Sudan, South Sudan, and Ethiopia.

Although the growing season is nearly 11 months, the crop evapotranspiration varies considerably depending on the planting date (Figure 57, left column). The summer months are associated with sow dates with the lowest total crop evapotranspiration (~1.8 m) since the maximum crop coefficient (which last for 180 days) coincides with the cooler months. For the same reason, the highest crop evapotranspiration values (> 2.0 m) are associated with sow dates occurring in winter months and hence the maximum crop coefficient in the summer. The irrigation requirements for sugarcane are extremely high. Values in Sudan where rainfall is low exceed 2 m, almost double that of any other crop considered in this study (Figure 58, left column).

Unlike wheat and rice, the region suitable for sugarcane expands in range with a warmer climate (Figure 57, middle and right columns). With the RCP8.5 scenario, the entire EN basin is suitable for sugarcane growth. Evapotranspiration increases by approximately by 0.3 m over the growing season, resulting in a similar corresponding increase in irrigation requirements (Figure 58, middle and right columns). While a warmer climate would likely result in an increase in rice productivity, the irrigation requirements would increase substantially.

7.5.4 Crop Group IV

Group IV crops are best suited for the temperate zone of the Nile Delta region and the tropical highlands of Ethiopia, due to their suitability at lower temperatures and wide range of temperature suitability (10 to 35 °C; Table 3). In this section, teff is analyzed. As mentioned above, Maize, millet, and sorghum are considered in Section 7.5.6 where the operative temperatures from Groups III and IV are combined.

7.5.4.1 Temperature Suitability

In the present climate crops in this group are operative in all regions and all months except in central northern Sudan (Figure 55, left column). The crops are best suited (i.e., optimal) for Sudan from November through March; South Sudan from May through February; and the Nile Delta region from April through October.

The impacts of climate change on Group IV crops are substantial (Figure 55, middle and right columns). While more of the EN basin is suitable for growth in all months and optimal in many of the months, a warmer climate shifts many of the regions into suboptimal or unsuitable. For example, crops southern Sudan and South Sudan shift from optimal to suboptimal in winter and from suboptimal to optimal in summer. In Egypt, warmer climate benefits crops in winter, but damage them in summer. Crops in Ethiopia, on the contrary, benefit from a warmer climate in all regions, implying increases in agricultural productivity.

7.5.4.2 Teff

Teff is commonly grown in Ethiopia. At 90 days, the growing season is relatively short, thus requiring little rainfall for cultivation. The crop coefficient values initiate at 0.9, then increase to 1.00 at maturity, and decrease to 0.50 at harvest (Figure 60).

In the present climate, due to the short growing season for teff, the growing season crop evapotranspiration does not exceed 0.5 m except in Sudan during the summer (Figure 61, left column). As a result, the irrigation requirements are also low (Figure 62, left column). In fact, if planted during the rainy season in Ethiopia, irrigation is not required in most regions.

Although the regions suitable for teff shrink considerably with a warmer climate, Ethiopia remains suitable for teff when sown any of the months (Figure 61, middle and right columns). Despite the warming resulting increased evapotranspiration, irrigation requirements remain similar and in some cases decrease (Figure 62).

7.5.5 Crop Group V

Group V crops, have the largest range of temperature suitability and greatest tolerance to heat (10 to 45° C for operative conditions and 20 – 30° C for optimal conditions; Table 3). This group is associated with sisal and pineapple, which follow the CAM photosynthetic pathway.

Given this large range of temperature suitability, crops in the group are suitable for growth in all regions and all months in the present climate (Figure 63, left column). Optimal growth occurs in South Sudan in all months; most of Sudan from March through November; and in most of Egypt from May through September. Although operative, Group V crops are never optimal in Ethiopia. The core of this zone lies in Sudan from April to October when temperatures are higher.

Group V crops, which have the greatest area of optimal suitability, also see significant changes with a warmer climate (Figure 63, middle and right columns). Much of Sudan, which has optimal temperatures for growth in spring and summer months, shifts to suboptimal, but still operative; suitability in winter months, on the contrary, shifts from suboptimal to optimal. South Sudan, which in the present climate is optimal for growth in all months, remains optimal in most months, except the spring where it shifts to suboptimal. Temperature changes in Egypt generally tend improve the suitability of agriculture in summer. Temperatures in the Ethiopian Highlands remain optimal regardless of climate change.

7.5.6 Group III and IV Combined

Maize, sorghum, and millet are represented in both Group III and Group IV (Table 3). The difference between individual crops is strictly based on temperature suitability and thus regional (temperate and tropical highland cultivars versus tropical lowland cultivars). As a result, the operative temperature ranges expand for this analysis to cover a range from 10 to 45° C (Table 3). This combines tropical lowland cultivars with temperate and tropical highland cultivars. The crop coefficient values and growing stage lengths are the same regardless of the region, at least for the purposes of this study. In this subsection, grain maize, sweet sorghum, and millet are considered. Sweet maize and grain sorghum are also considered but not presented in this report for brevity.

7.5.6.1 Grain Maize

Grain maize has a wide range of crop coefficient values starting at 0.30 in the initial phase, increasing to 1.20 during development phase, and decreasing to 0.40 at harvest (Figure 64). The growing season length is 180 days, the longest of the crop analyzed in this study except for ratooned sugarcane. Sweet maize has a shorter growing season, but is not shown in the analysis. Maize is typically sown in May in Egypt, July and September in former Sudan, and February through May in Ethiopia (FAO Crop Calendar, 2012).

In the present climate, grain maize is suitable for growth regardless of the month in which it is sown (Figure 65, left column). Evapotranspiration and corresponding irrigation requirements are lowest for grain maize when it is sown in late summer and early fall (Figure 65 and Figure 66, left columns). The reason for this is that the peak crop coefficient value (1.2) occurs 80 days after planting and persists 60 days (Figure 64). When the peak values coincide with the coolest months, evapotranspiration over the growing season is lowest. Similarly the highest evapotranspiration when grain maize is sown in late winter and earlier spring, which coincides with the highest crop coefficient values in summer.

In warmer climate, grain maize remains suitable for growth in all months over the growing season. Evapotranspiration and corresponding irrigation requirements increases by 0.1 m in RCP4.5 and 0.2 m in RCP8.5 over the growing season (Figure 65 and Figure 66, middle and right columns).

7.5.6.2 Sweet Sorghum

Sweet sorghum has a 130-day growing season. The crop coefficient initiates at 0.30, increases to 1.20 at maturity, and decreases to 1.05 at harvest (Figure 67). In Ethiopia, sorghum is typically planted in Ethiopia in March, April, and May and harvested sometime between July and September (FAO Crop Calendar 2012). In the former Sudan, it is typically planted in July and August and harvested in October and November, except in irrigated zones where it is planted in March and harvested in December. In Egypt, it is planted in May and June and harvested in September and October.

Sweet sorghum in the present climate, like grain maize, is suitable for growth in all regions regardless of the sow date (Figure 68, left column). Sweet sorghum, however, transpires considerably less that grain maize (Figure 69, left column). As a result, the corresponding irrigation requirements are also considerably lower. Values for growing season evapotranspiration range from 0.5 m up to slightly below 1.0 m. In Sudan, the optimal time to sow is in autumn due to the lower temperatures when evapotranspiration is highest. This, however, is a period with low rainfall in Sudan, requiring nearly 100% of the water needs to be met by irrigation. In the Ethiopian highlands, if sown in the late spring, irrigation requirements for sweet sorghum are close to zero.

In a warmer climate, sweet sorghum remains suitable growth in all regions regardless of the sow date (Figure 68, left column). Growing season evapotranspiration and corresponding irrigation requirements increase by slightly less 0.1 m in the CRU+RCP8.5 scenario due to the higher surface temperatures (Figure 69, middle and right columns). In the Ethiopian highlands, if sown in the late spring, irrigation requirements for sweet sorghum are close to zero. In the Ethiopian highlands, the irrigation requirements remain close to zero due to the increase in growing season rainfall.

7.5.6.3 Millet

Millet is not commonly grown in Egypt. It is, however, grown in Ethiopia and the former Sudan. In Ethiopia, it is typically sown in March and April and harvested in July, August, and September (FAO Crop Calendar 2012). It is sometimes planted for a second season in July and harvested in October, November, and December. In the former Sudan, it is typically planted in July and August and harvested in October and November. In irrigated regions in Sudan, it is planted in early September and harvested in late November, when evapotranspiration is lower. Millet initiates its 140-day growing season with a crop coefficient of 0.30. The crop coefficient increases to 1.00 at maturity and decreases to back to 0.30 at harvest (Figure 70).

In the present climate, millet is suitable for growth regardless of the date it is sown, as is the case for all Group III/IV combined crops (Figure 71, left column). Crop evapotranspiration over the growing season is relatively low due to its small crop coefficient values. When sown in the late summer and early autumn, evapotranspiration values are less than 0.5 m. When sown in the spring, values are at their highest but do not exceed 0.8 m. Correspondingly, the irrigation requirements for millet are relatively low except in northern Sudan (Figure 72, left column). In the

Ethiopian Highlands, when sown in the late spring, the irrigation requirements are close to zero, similar to sweet sorghum.

In a warmer climate, as also is the case for all Group III/IV combined crops, millet remains suitable for cultivation (Figure 71, middle and right columns). The growing season evapotranspiration increases by approximately 0.05 and 0.1 in the CRU+RCP4.5 and CRU+RCP8.5 scenarios, respectively. The irrigation requirements increase by a similar amount (Figure 72, middle and right columns). The exception is the Ethiopian Highlands when millet is sown in the late spring, since effective rainfall tends to increase in the summer corresponding to the highest crop coefficient values, which occur 50 to 105 days after the sow date.

7.6 Summary

The projected changes in temperature, regardless of the emissions scenario result in large changes in crop suitability. In general, there are both spatial and temporal shifts in suitability. Crops suited for cooler climates shift north and south out of Sudan and southern Egypt to higher elevations such as the Ethiopian Highlands and north to the Nile Delta. In addition, crops suitable in warmers months shift to the cooler winter months. The largest decreases are to Group I crops (e.g., wheat, barley, oats, and potatoes) and Group II crops (e.g., rice, cotton, cassava, and groundnut), which become unsuitable in much of the region due to their lower temperature suitability range. On the contrary, Group III crops (e.g., maize, sorghum, and millet) tend to benefit in terms total area suitable for cultivation due to their higher temperature suitability range.

Although the Eastern Nile region remains suitable for crop growth, the areas of optimal growth reduce considerably regardless of whether or not farmers shift to crops better suited for warmer climates and shift the growing season to cooler periods. The resulting decrease in productivity with a warmer climate would to some extent likely be compensated by improvements in agricultural technologies and by fertilization effect from the increased atmospheric carbon dioxide. However, populations are also expected to grow substantially, which would increase agricultural demand.

Crop evapotranspiration increases substantially over the entire region due to the increases in temperature and resulting increases in reference evapotranspiration. This results in a substantial increase in irrigation required to meet the crops needs (except in summer in the Ethiopian Highlands where rainfall increases). Shifting the primary growing season to cooler periods can help compensate the additional irrigation requirements; however Nile flow are lowest during the cooler portions of the year. As a result, additional storage (e.g., reservoirs) in the upstream portions of the basin would be required.

Table 2: Top crop production 2010 based on profit and metric tons. Data from FAOSTAT (2012).

Commodity	Egypt	Sudan	Ethiopia
Bananas	x	x	x
Barley			x
Beans, dry			x
Broad beans, horse beans, dry			x
Cabbages and other brassicas	x		x
Cereals, nes			x
Chick peas			x
Coffee, green			x
Dates	x	x	
Eggplants (aubergines)	x		
Fruit Fresh Nes		x	
Grapes	x		
Groundnuts, with shell		x	
Maize	x		x
Mangoes, mangosteens, guavas		x	
Millet		x	x
Okra		x	
Onions, dry	x	x	
Oranges	x		
Potatoes	x	x	x
Rice, paddy	x		
Roots and Tubers, nes			x
Sorghum	x	x	x
Sugar beet	x		
Sugar cane	x	x	x
Sweet potatoes			x
Tangerines, mandarins, clem.	x		
Tomatoes	x	x	
Vegetables fresh nes		x	x
Watermelons	x	x	
Wheat	x	x	x
Yams			x

Table 3: Crop adaptability groups, based on photosynthetic pathway and response to radiation and temperature. Adapted from FAO (1978a, 1980c and 1985).

Crop adaptability group	I	II	III	IV	V
Photosynthetic pathway	C3	C3	C4	C4	CAM
Optimal photosynthesis temperature range (°C)	15-20	25-30	30-35	20-30	25-35
Operative photosynthesis temperature range (°C)	5-30	10-35	15-45	10-35	10-45
	Sugarbeet Phaseolus Wheat Barley Oats Potato Bean TE Chickpea	Soybean TR Phaseolus Rice Cassava Sweet Potato Yams Bean TR Groundnut Cotton Tobacco Banana Coconut Rubber Oil palm	Sorghum TR Maize TR Pearl millet Panicum Millet TR Finger millet Setaria Sugarcane	Panicum Millet TE,TH Sorghum TE,TH Maize TE,TH Setaria Teff	Sisal Pineapple

TE = Temperate cultivars; TR = Tropical (lowland) cultivars; TH = Tropical (highland) cultivars.

Table 4: Mean Daily Percentage (p) of Annual Daytime Hours for Different Latitudes. Table from FAO (1986).

Latitude	North	Jan	Feb	Mar	Apr	May	June	July	Aug	Sept	Oct	Nov	Dec
	South	July	Aug	Sept	Oct	Nov	Dec	Jan	Feb	Mar	Apr	May	June
60		0.15	0.20	0.26	0.32	0.38	0.41	0.40	0.34	0.28	0.22	0.17	0.13
55		0.17	0.21	0.26	0.32	0.36	0.39	0.38	0.33	0.28	0.23	0.18	0.16
50		0.19	0.23	0.27	0.31	0.34	0.36	0.35	0.32	0.28	0.24	0.20	0.18
45		0.20	0.23	0.27	0.30	0.34	0.35	0.34	0.32	0.28	0.24	0.21	0.20
40		0.22	0.24	0.27	0.30	0.32	0.34	0.33	0.31	0.28	0.25	0.22	0.21
35		0.23	0.25	0.27	0.29	0.31	0.32	0.32	0.30	0.28	0.25	0.23	0.22
30		0.24	0.25	0.27	0.29	0.31	0.32	0.31	0.30	0.28	0.26	0.24	0.23
25		0.24	0.26	0.27	0.29	0.30	0.31	0.31	0.29	0.28	0.26	0.25	0.24
20		0.25	0.26	0.27	0.28	0.29	0.30	0.30	0.29	0.28	0.26	0.25	0.25
15		0.26	0.26	0.27	0.28	0.29	0.29	0.29	0.28	0.28	0.27	0.26	0.25
10		0.26	0.27	0.27	0.28	0.28	0.29	0.29	0.28	0.28	0.27	0.26	0.26
5		0.27	0.27	0.27	0.28	0.28	0.28	0.28	0.28	0.28	0.27	0.27	0.27
0		0.27	0.27	0.27	0.27	0.27	0.27	0.27	0.27	0.27	0.27	0.27	0.27

Table 5: Tabulated Crop Coefficient Values. Data from FAO (1998).

Commodity	Specific Distinction	kc ini	kc mid	kc end
Barley		0.30	1.15	0.25
Maize	Grain	0.30	1.20	0.60,0.35
	Sweet	0.30	1.15	1.05
Millet		0.30	1.00	0.30
Rice, paddy		1.05	1.20	0.90-0.60
Sisal		0.35	0.4-0.7	0.4-0.7
Sorghum	Grain	0.30	1.00-1.10	0.55
	Sweet	0.30	1.20	1.05
Sugar cane		0.40	1.25	0.75
Teff		0.90	1.0	0.45
Wheat	Winter with non-frozen soils	0.70	1.15	0.25-0.4

Table 6: Approximate Duration of Growth Stages for Various Field Crops. Adapted from FAO (1986).

	Total Length	Initial stage	Crop Development stage	Mid season stage	Late season stage	Region
Barley, Oats, Wheat	150	15	30	65	40	East Africa
Maize, sweet	80	20	25	25	10	Med.
Maize, grain	180	30	50	60	40	East Africa
Millet	140	20	30	55	35	Central U.S.
Sorghum	120	20	30	40	30	Med.
Sugarcane, Ratoon	280	30	50	180	60	Tropics
Teff	85	15	20	35	15	

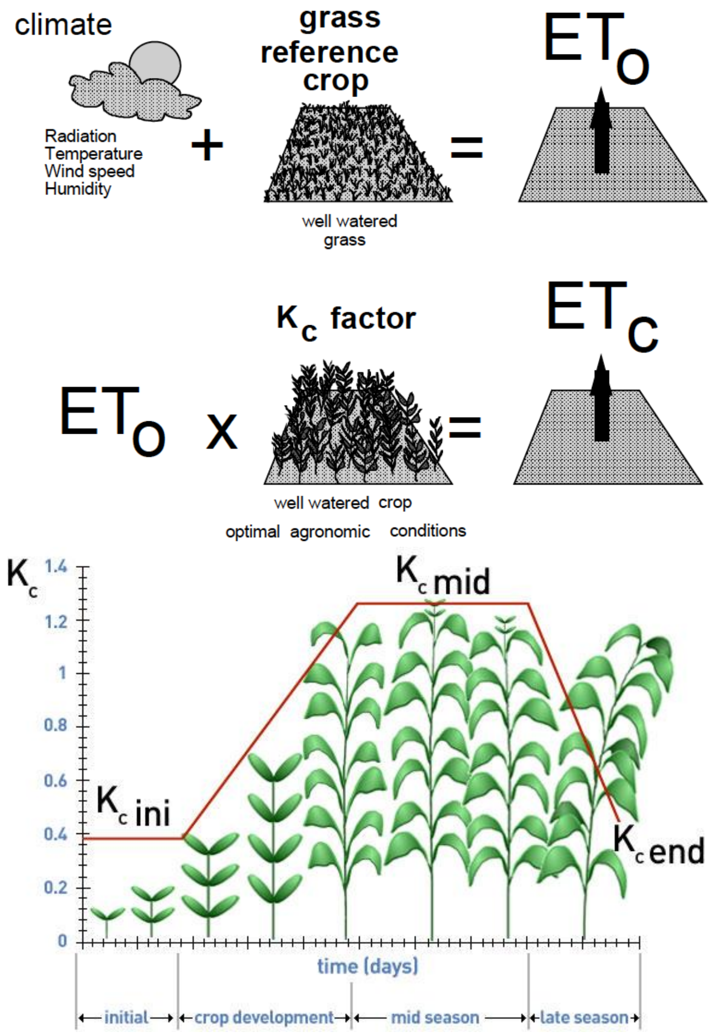

Figure 43: Crop coefficient method for calculating crop evapotranspiration. Figures from FAO (1998).

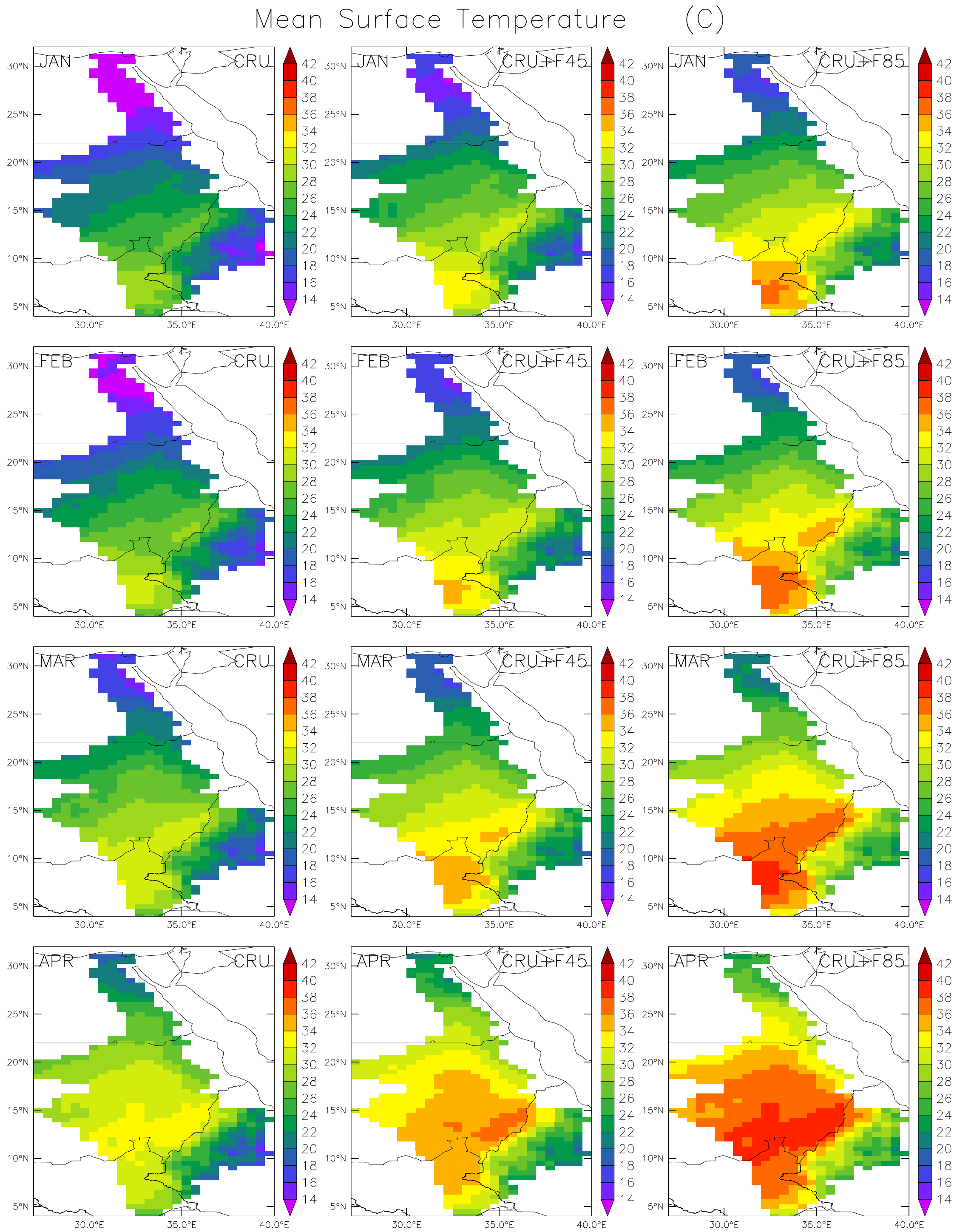
Mean Surface Temperature (C)
JAN
CRU
CRU+F45
CRU+F85
FEB
MAR
APR
42 40 38 36 34 32 30 28 26 24 22 20 18 16 14
30°N 25°N 20°N 15°N 10°N 5°N
30.0°E 35.0°E 40.0°E

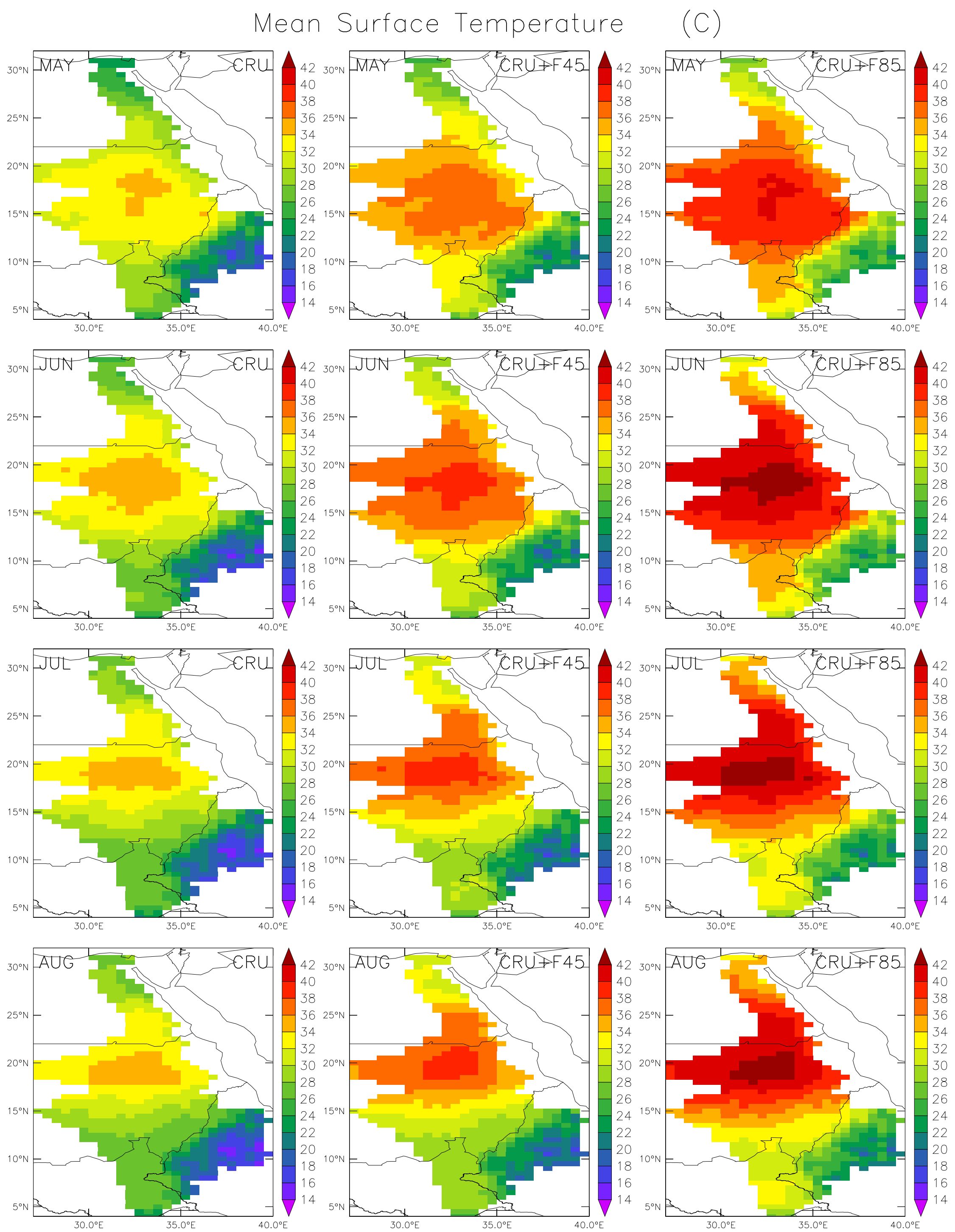
Mean Surface Temperature (C)
MAY
CRU
CRU+F45
CRU+F85
JUN
JUL
AUG
42 40 38 36 34 32 30 28 26 24 22 20 18 16 14
30°N 25°N 20°N 15°N 10°N 5°N
30.0°E 35.0°E 40.0°E

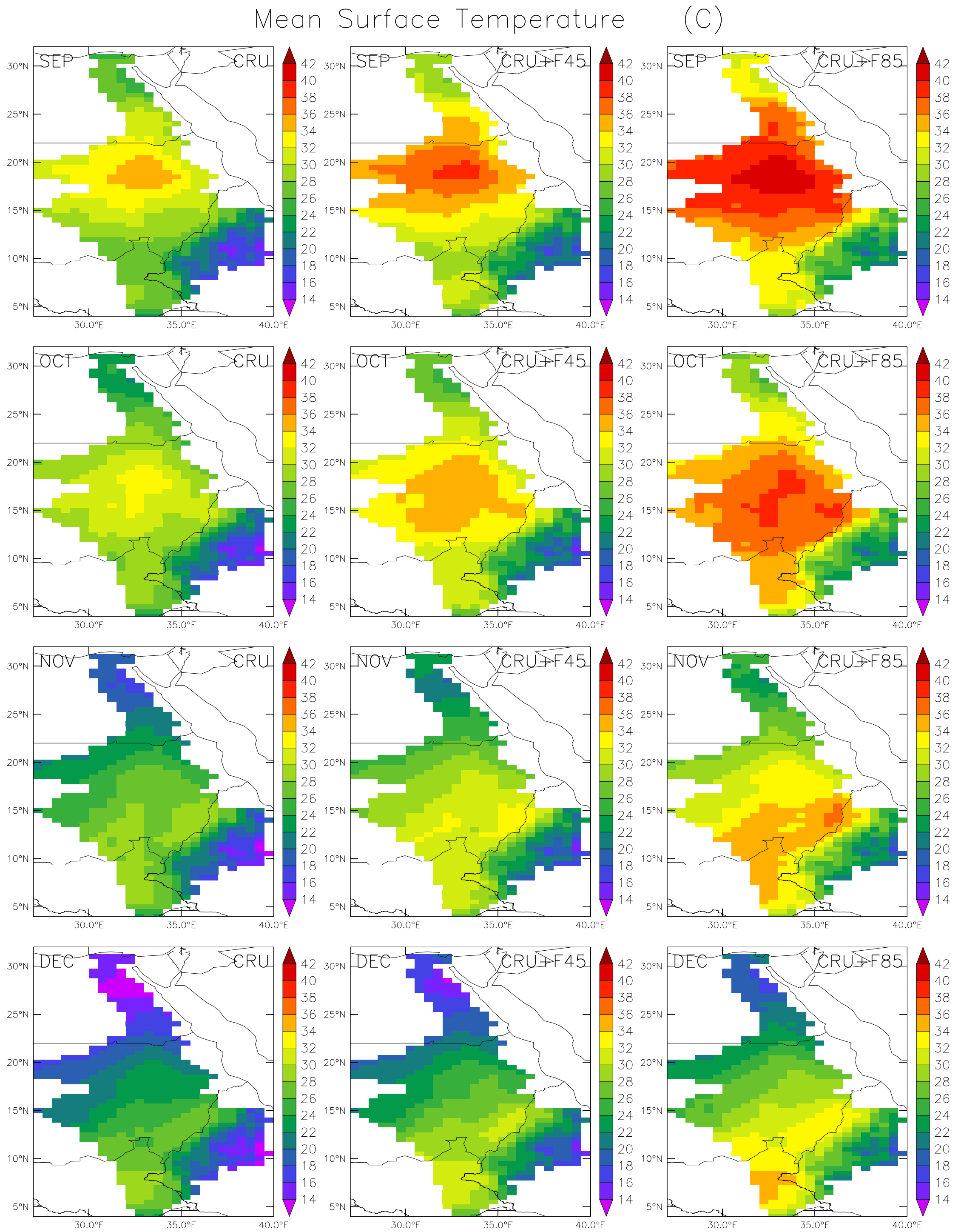

Figure 44: Monthly surface temperature (°C) used for the crop group suitability analysis and reference crop evapotranspiration. Each row represents a different months starting in January. Each column represents a different scenario: Left is CRU; middle is CRU+F45; and right is CRU+F85.

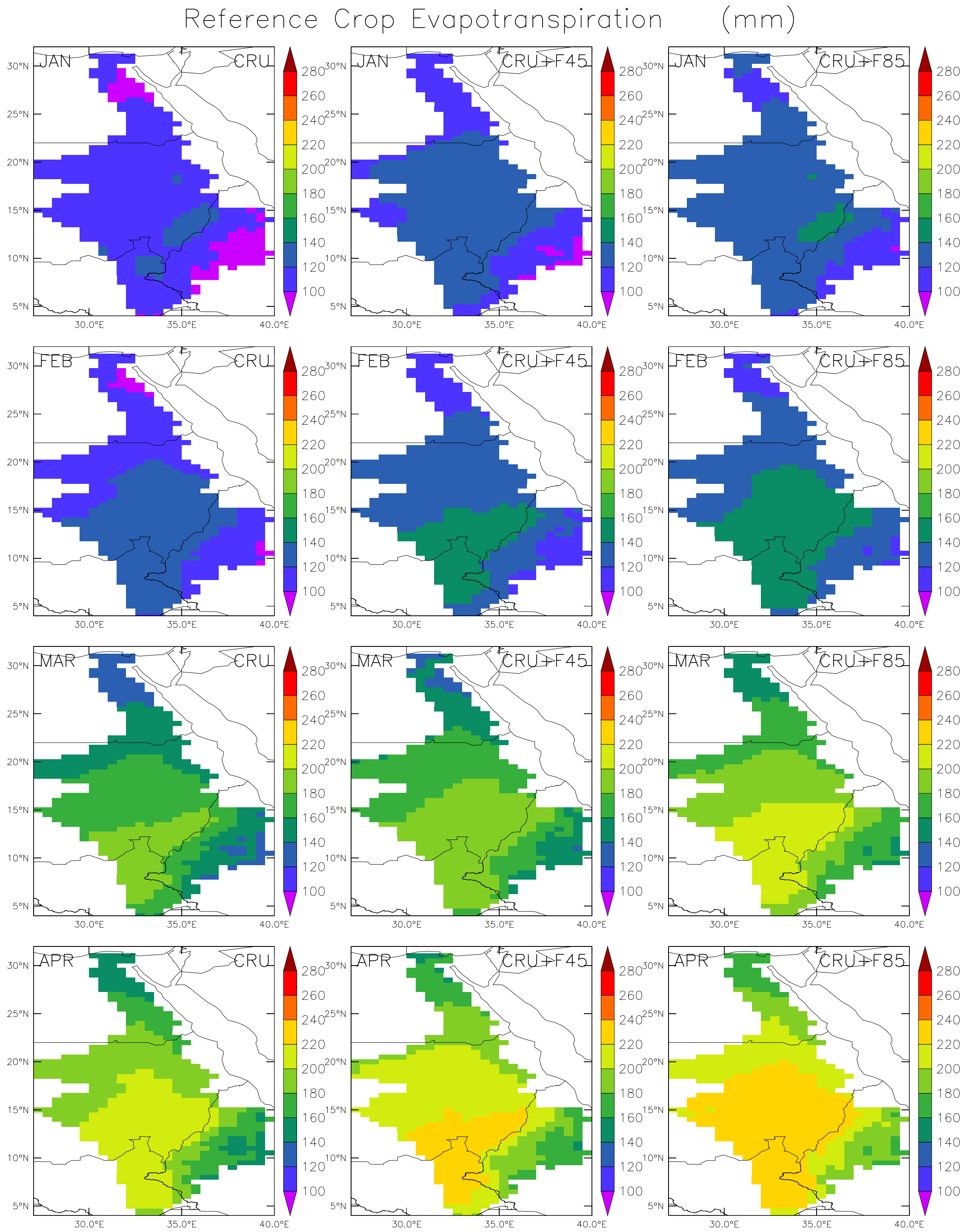
Reference Crop Evapotranspiration (mm)
JAN
CRU
CRU+F45
CRU+F85
FEB
MAR
APR
280
260
240
220
200
180
160
140
120
100
30°N
25°N
20°N
15°N
10°N
5°N
30.0°E
35.0°E
40.0°E

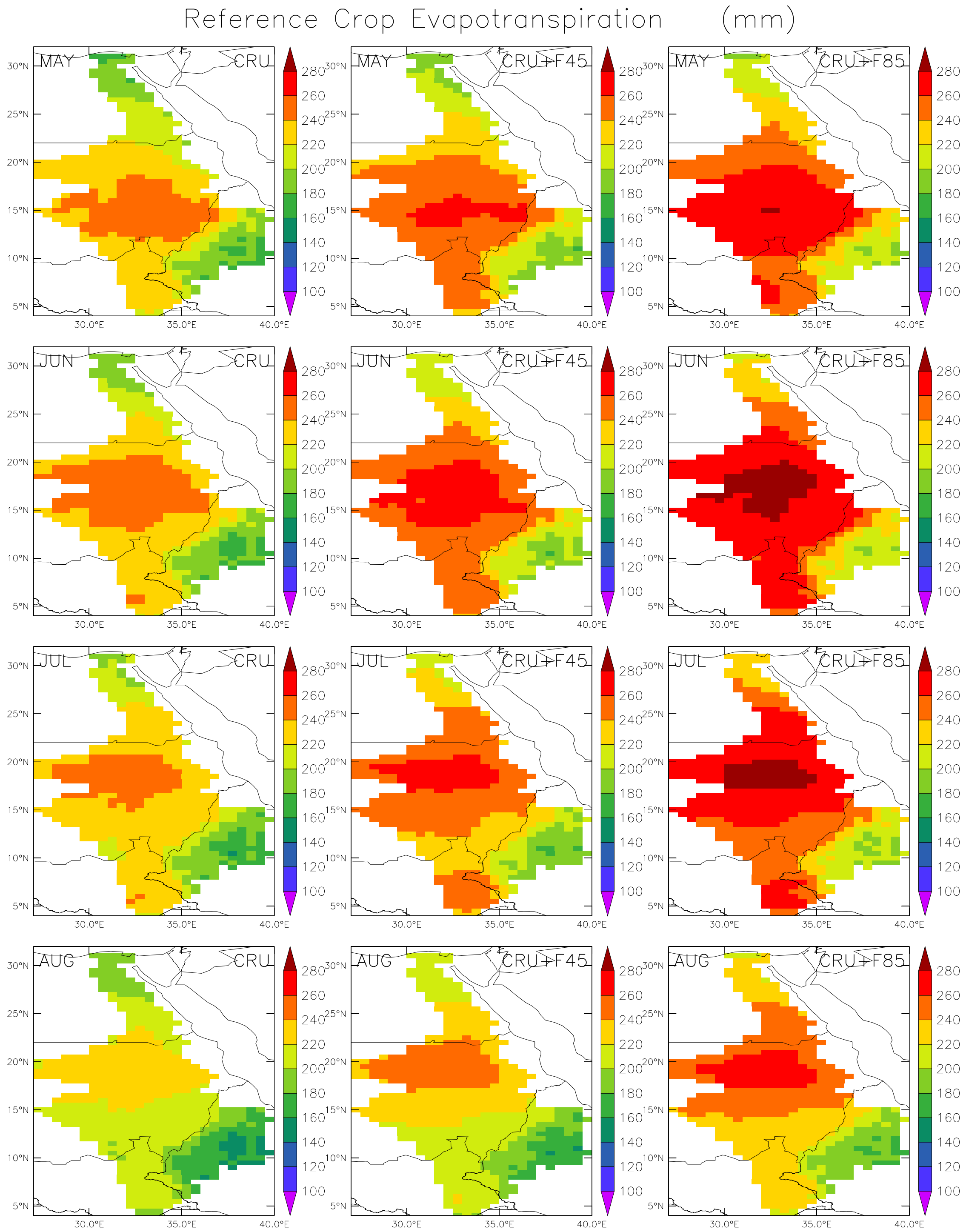
Reference Crop Evapotranspiration (mm)
MAY
CRU
CRU+F45
CRU+F85
JUN
JUL
AUG
280
260
240
220
200
180
160
140
120
100
30°N
25°N
20°N
15°N
10°N
5°N
30.0°E
35.0°E
40.0°E

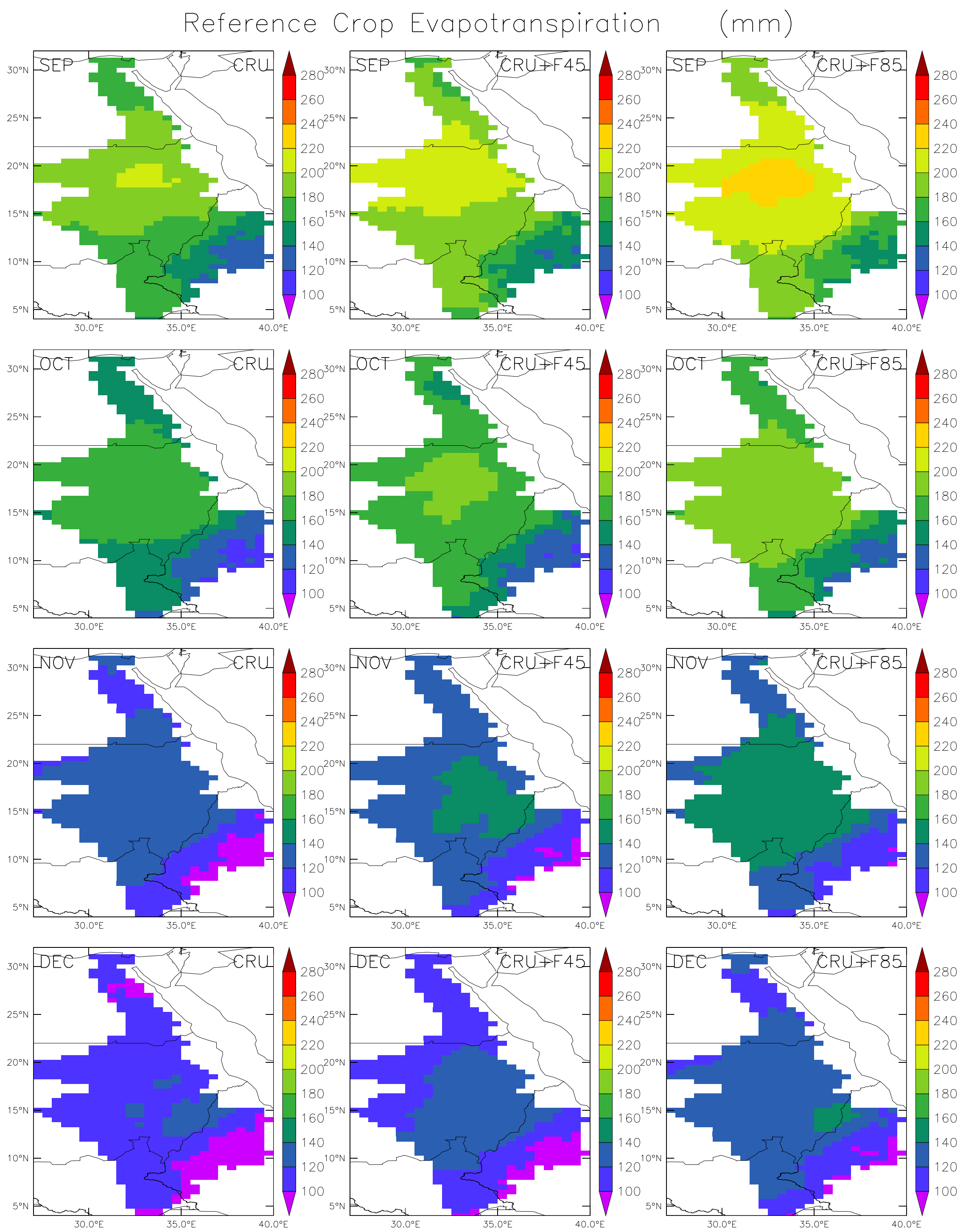

Figure 45: Reference crop evapotranspiration (mm/month) used for the crop group suitability analysis and reference crop evapotranspiration. Each row represents a different months starting in January. Each column represents a different scenario: Left is CRU; middle is CRU+F45; and right is CRU+F85.

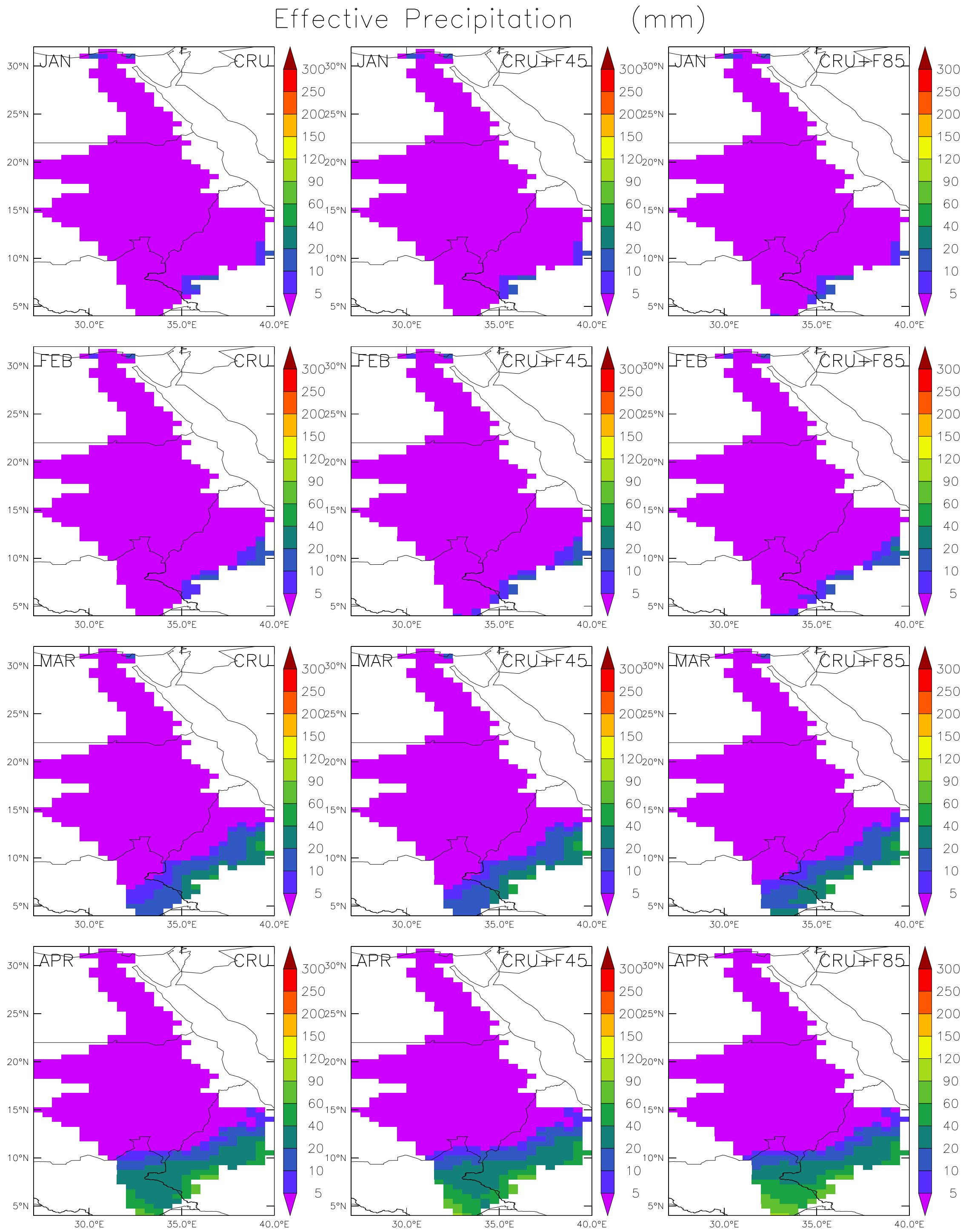
Effective Precipitation (mm)
JAN
CRU
CRU+F45
CRU+F85
FEB
MAR
APR
300
250
200
150
120
90
60
40
20
10
5
30°N
25°N
20°N
15°N
10°N
5°N
30.0°E
35.0°E
40.0°E

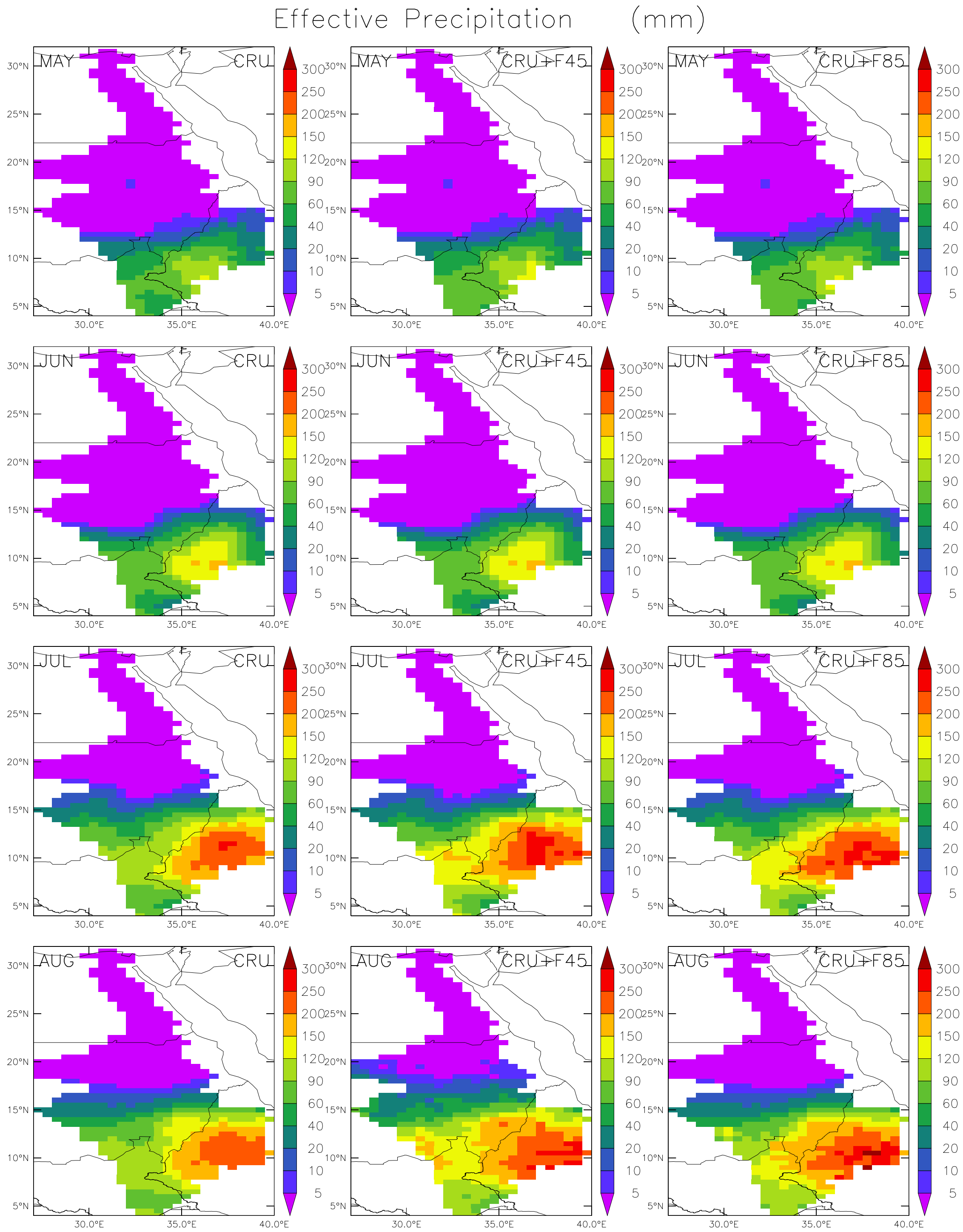
Effective Precipitation (mm)
MAY
CRU
CRU+F45
CRU+F85
JUN
JUL
AUG
300
250
200
150
120
90
60
40
20
10
5
30°N
25°N
20°N
15°N
10°N
5°N
30.0°E
35.0°E
40.0°E

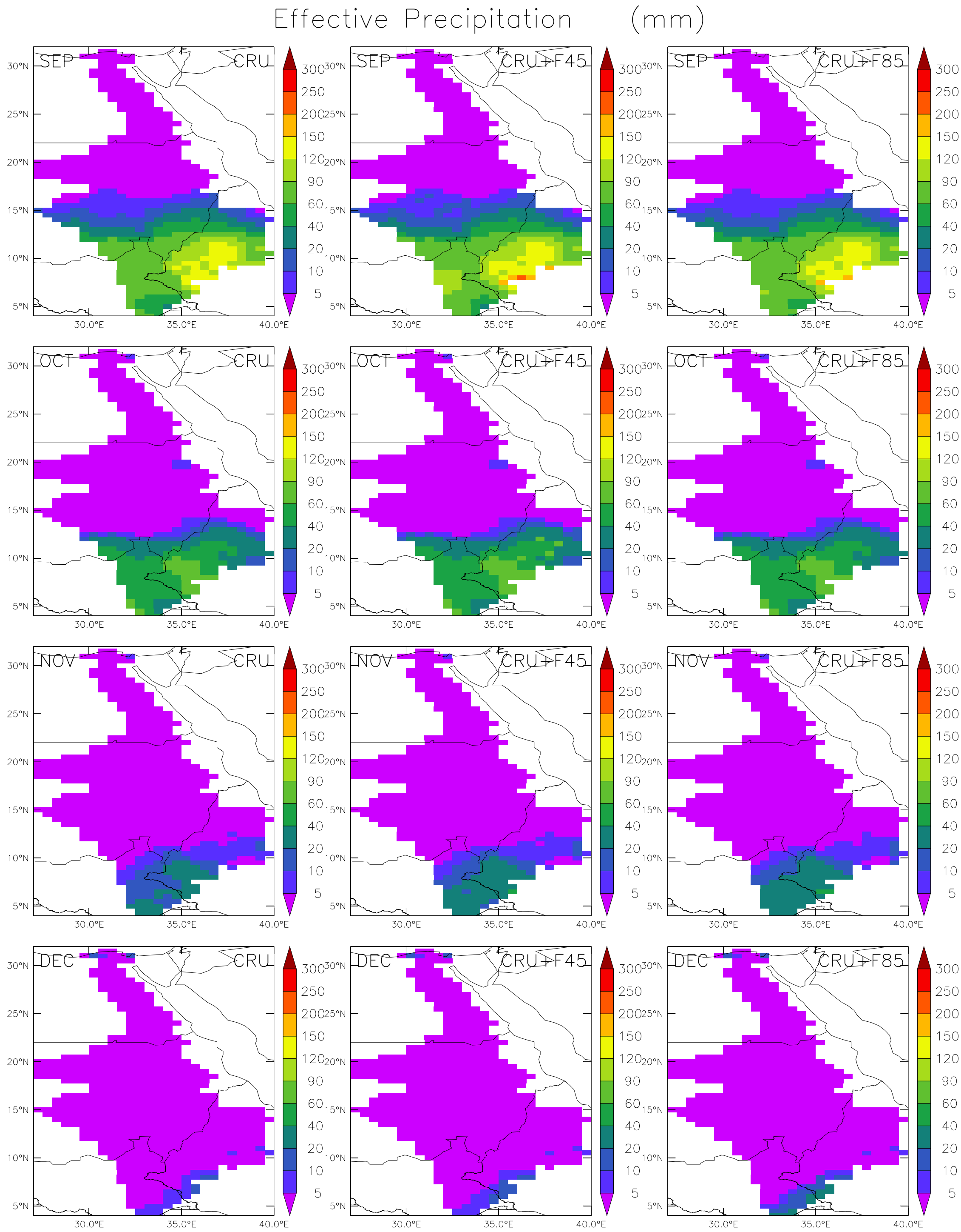

Figure 46: Effective precipitation (mm/month) used for the crop group suitability analysis and reference crop evapotranspiration. Each row represents a different months starting in January. Each column represents a different scenario: Left is CRU; middle is CRU+F45; and right is CRU+F85.

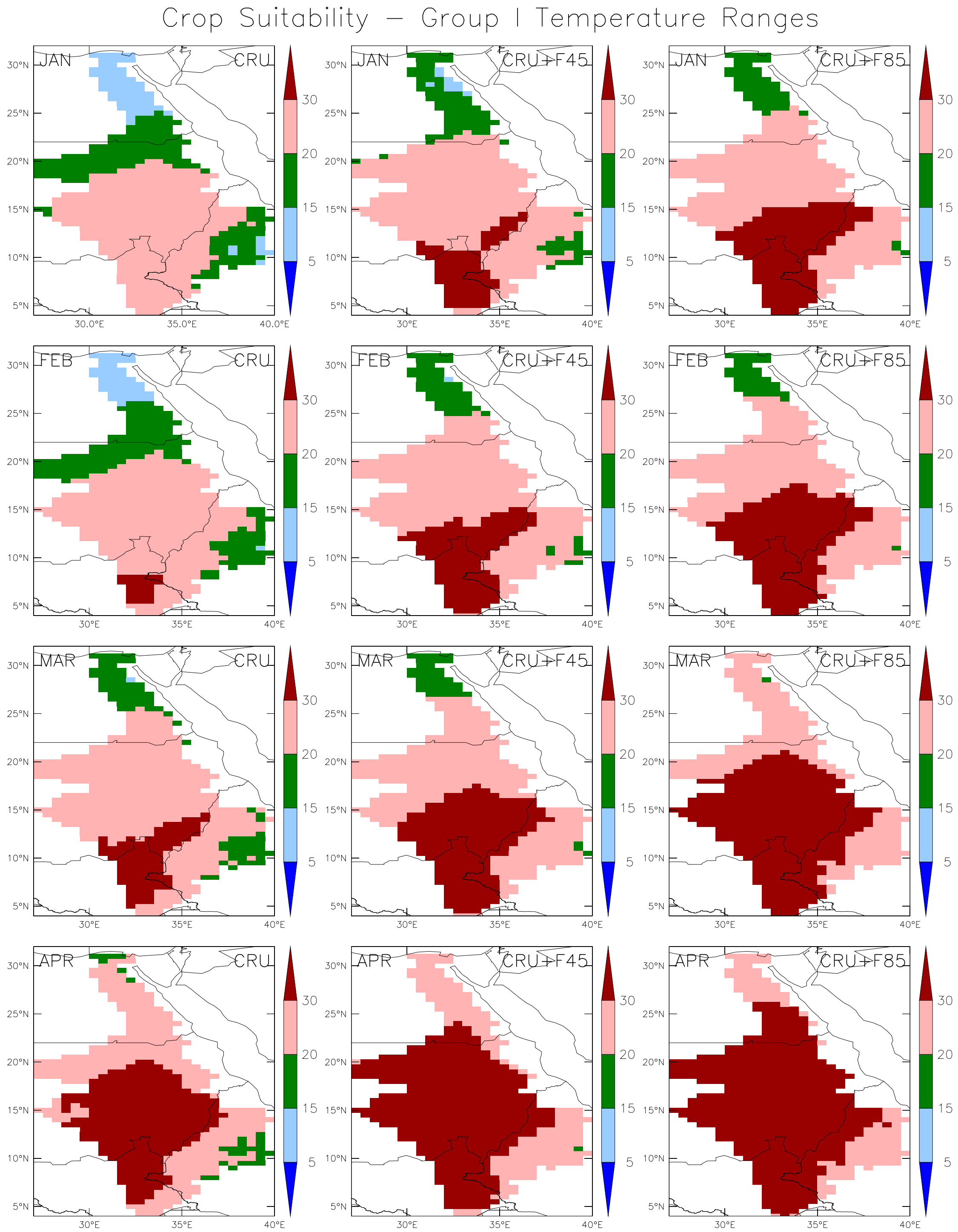
Crop Suitability – Group I Temperature Ranges
JAN
CRU
JAN
CRU+F45
JAN
CRU+F85
FEB
CRU
FEB
CRU+F45
FEB
CRU+F85
MAR
CRU
MAR
CRU+F45
MAR
CRU+F85
APR
CRU
APR
CRU+F45
APR
CRU+F85
30
20
15
5
30°N
25°N
20°N
15°N
10°N
5°N
30.0°E
35.0°E
40.0°E
30°E
35°E
40°E

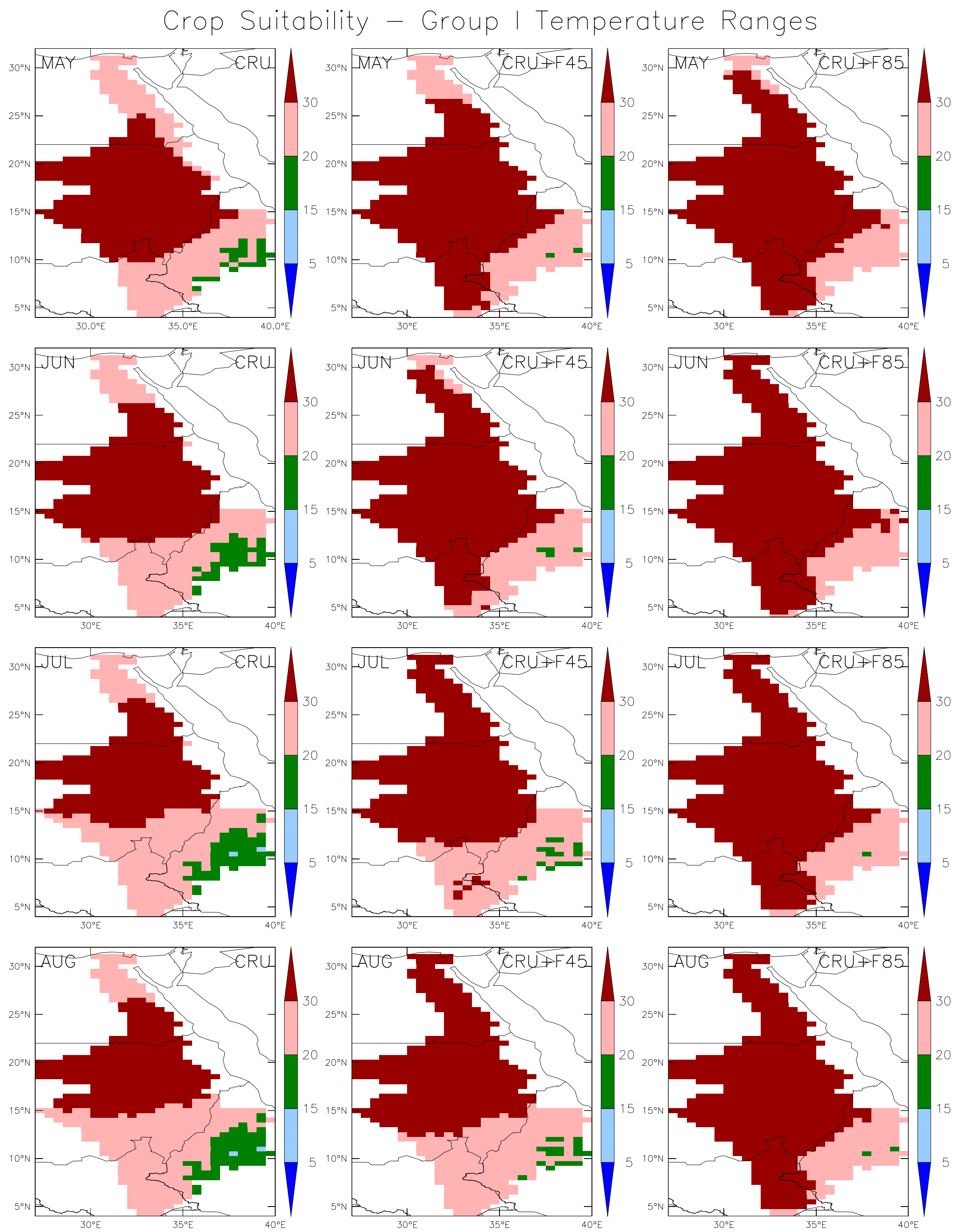
Crop Suitability – Group I Temperature Ranges
MAY
CRU
CRU+F45
CRU+F85
JUN
JUL
AUG
30
20
15
5
30°N
25°N
20°N
15°N
10°N
5°N
30.0°E
35.0°E
40.0°E
30°E
35°E
40°E

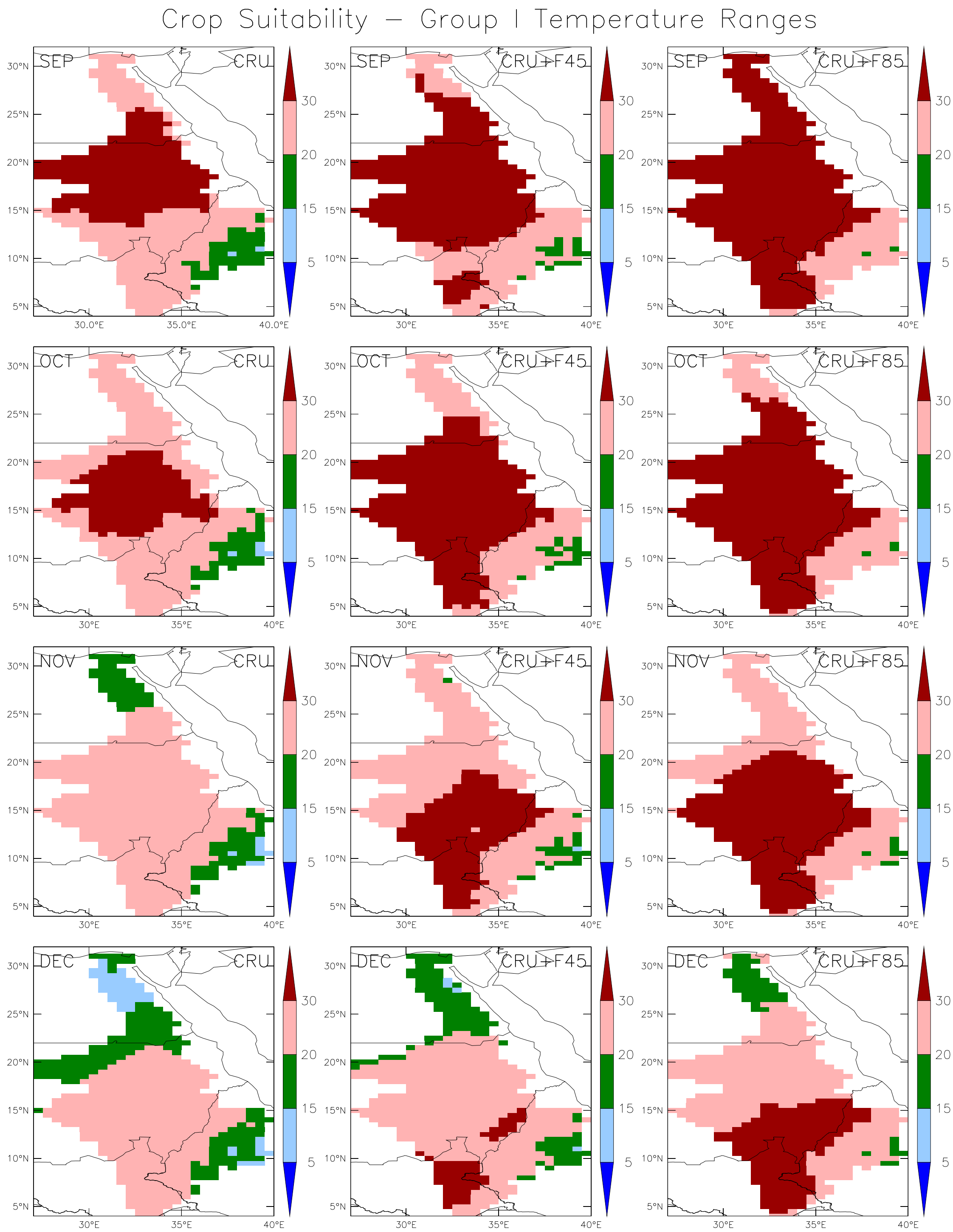

Figure 47: Monthly suitability for Group I crops based on surface temperature. Left column: CRU; middle column: CRU+F45; and right column: CRU+F85. Areas in green fall indicate temperatures for optimal growth; areas in light blue indicate temperatures below optimal but operative; areas in pink indicated temperatures above optimal but operative; and areas with in the basin that are white fall outside of the operative temperature range.

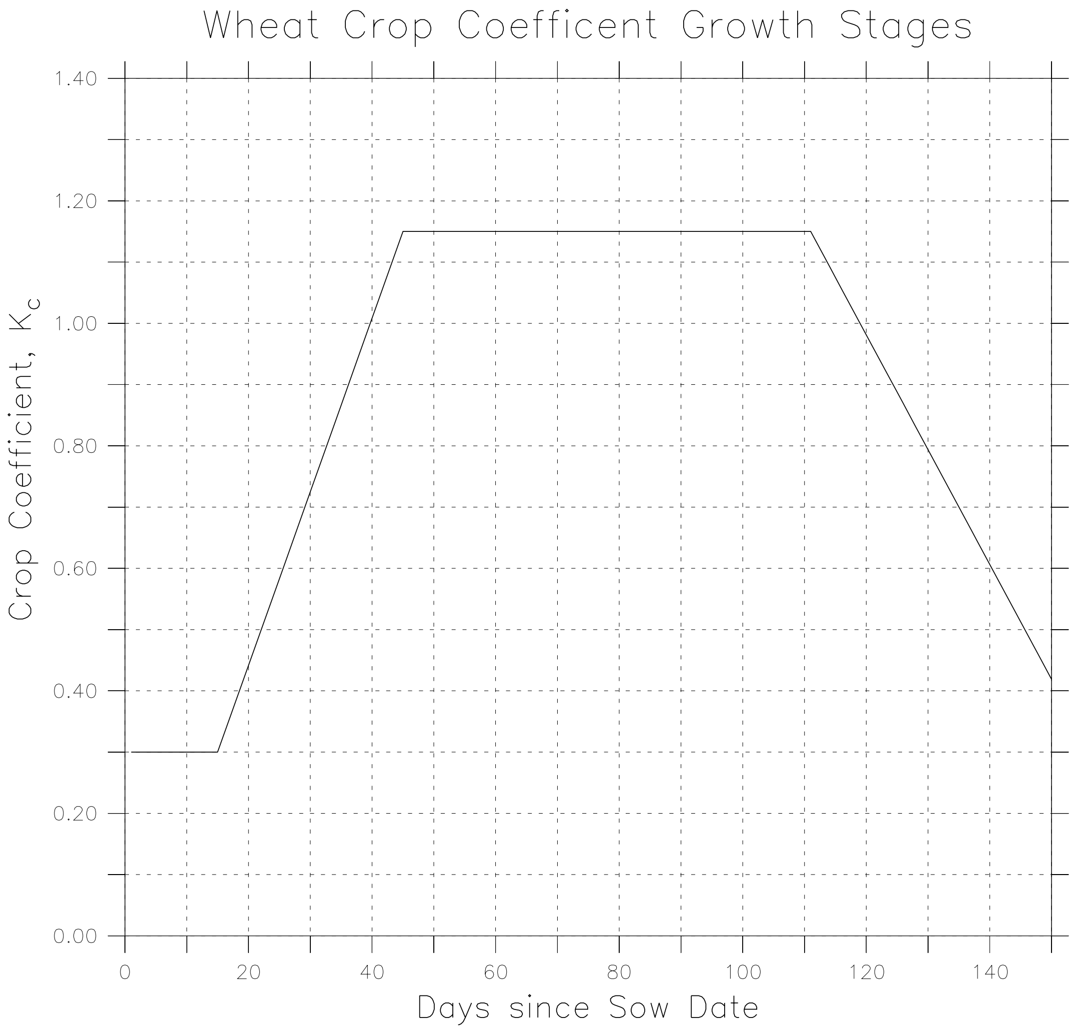

Figure 48: Wheat crop coefficients and growth stages. Data adapted from on FAO (1998).

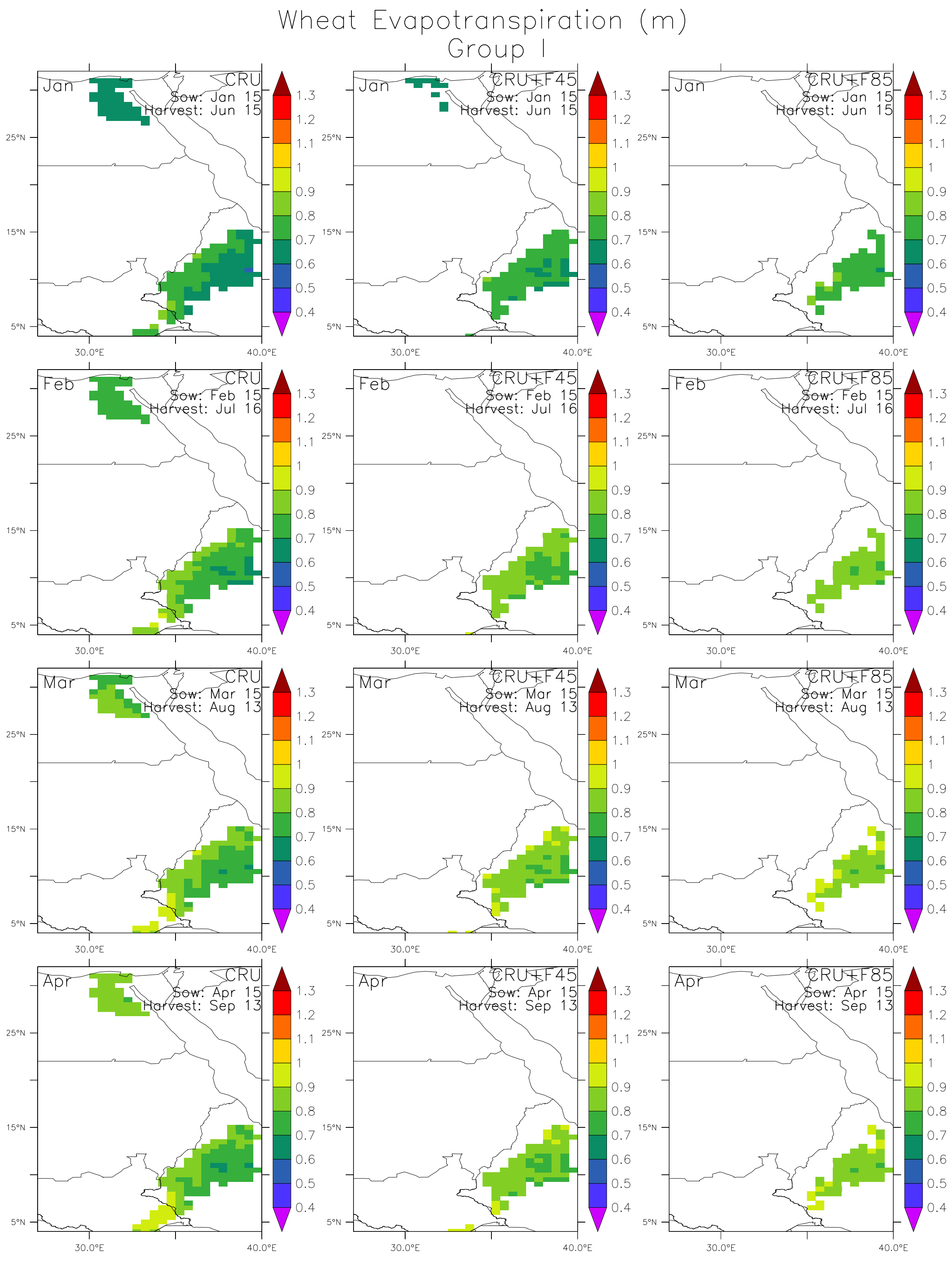
Wheat Evapotranspiration (m)
Group I
Jan
CRU
Sow: Jan 15
Harvest: Jun 15
CRU+F45
CRU+F85
Feb
Sow: Feb 15
Harvest: Jul 16
Mar
Sow: Mar 15
Harvest: Aug 13
Apr
Sow: Apr 15
Harvest: Sep 13
25°N
15°N
5°N
30.0°E
40.0°E
1.3
1.2
1.1
1
0.9
0.8
0.7
0.6
0.5
0.4

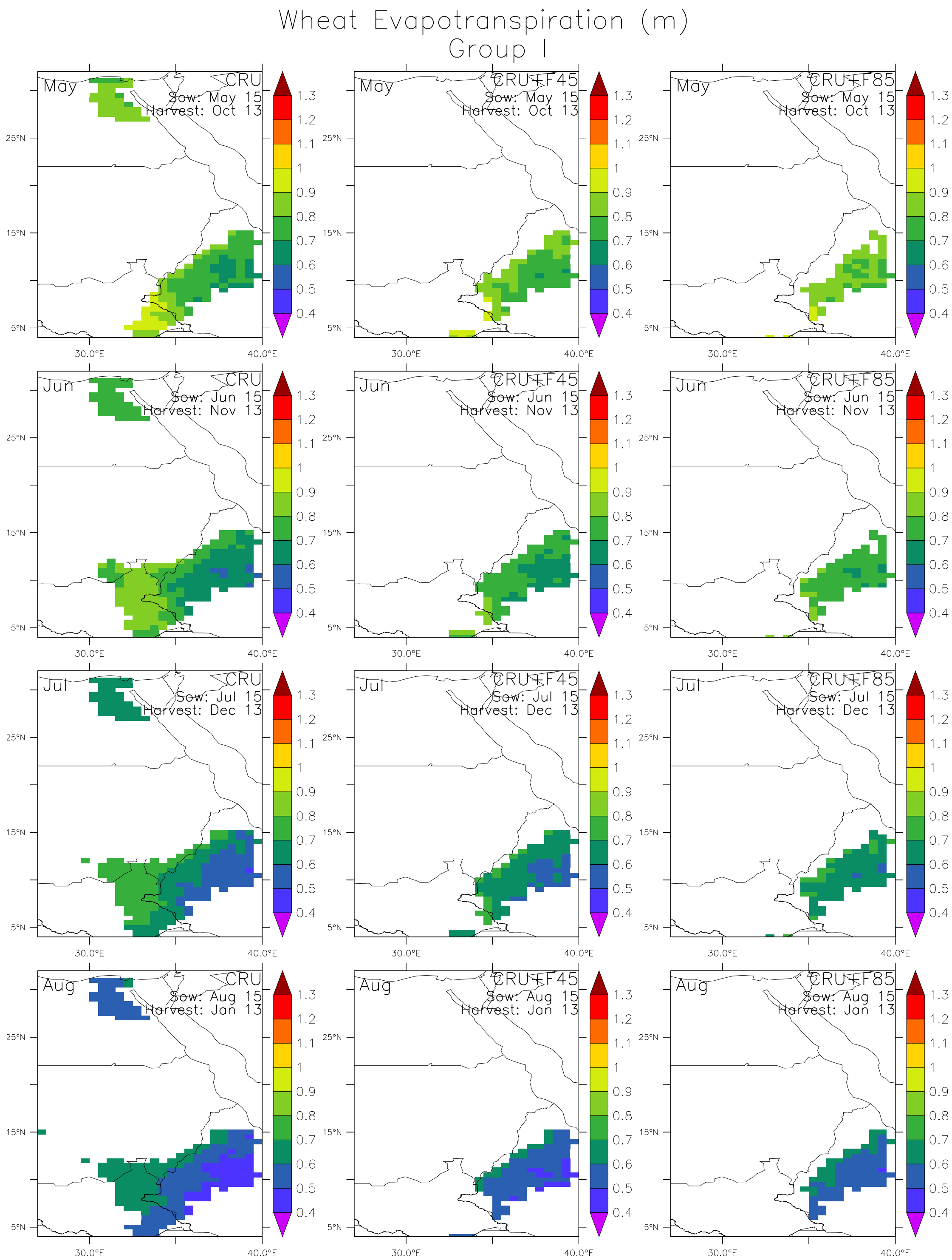
Wheat Evapotranspiration (m)
Group I
May
CRU
Sow: May 15
Harvest: Oct 13
CRU+F45
CRU+F85
Jun
Sow: Jun 15
Harvest: Nov 13
Jul
Sow: Jul 15
Harvest: Dec 13
Aug
Sow: Aug 15
Harvest: Jan 13
1.3
1.2
1.1
1
0.9
0.8
0.7
0.6
0.5
0.4
25°N
15°N
5°N
30.0°E
40.0°E

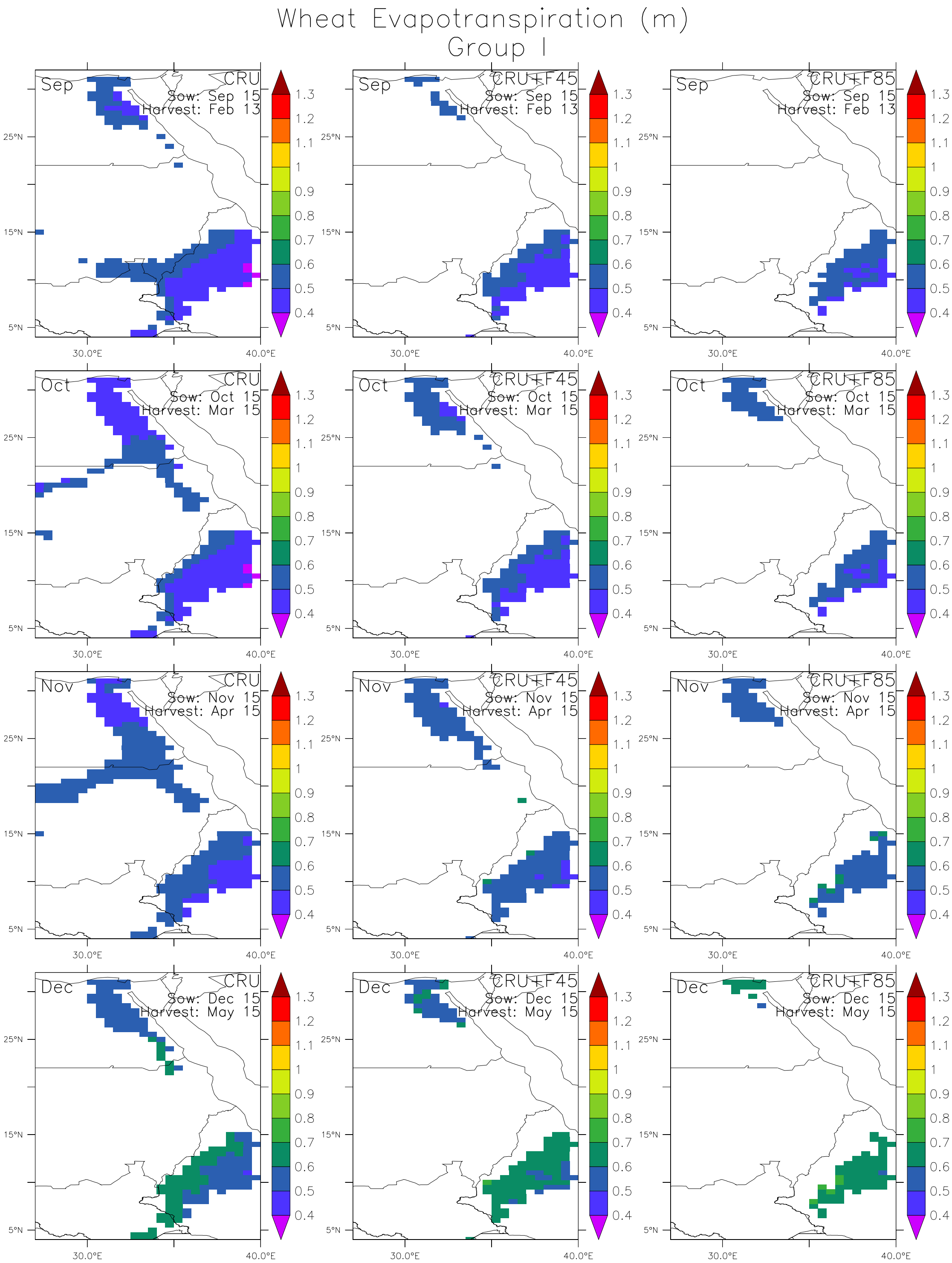

Figure 49: Wheat evapotranspiration in m based on surface temperature. Left column: CRU; middle column: CRU+F45; and right column: CRU+F85. The values are masked for temperature suitability for Group I operative conditions over the entire growing season. Each panel represents a different sow date starting January 15 with one-month shifts.

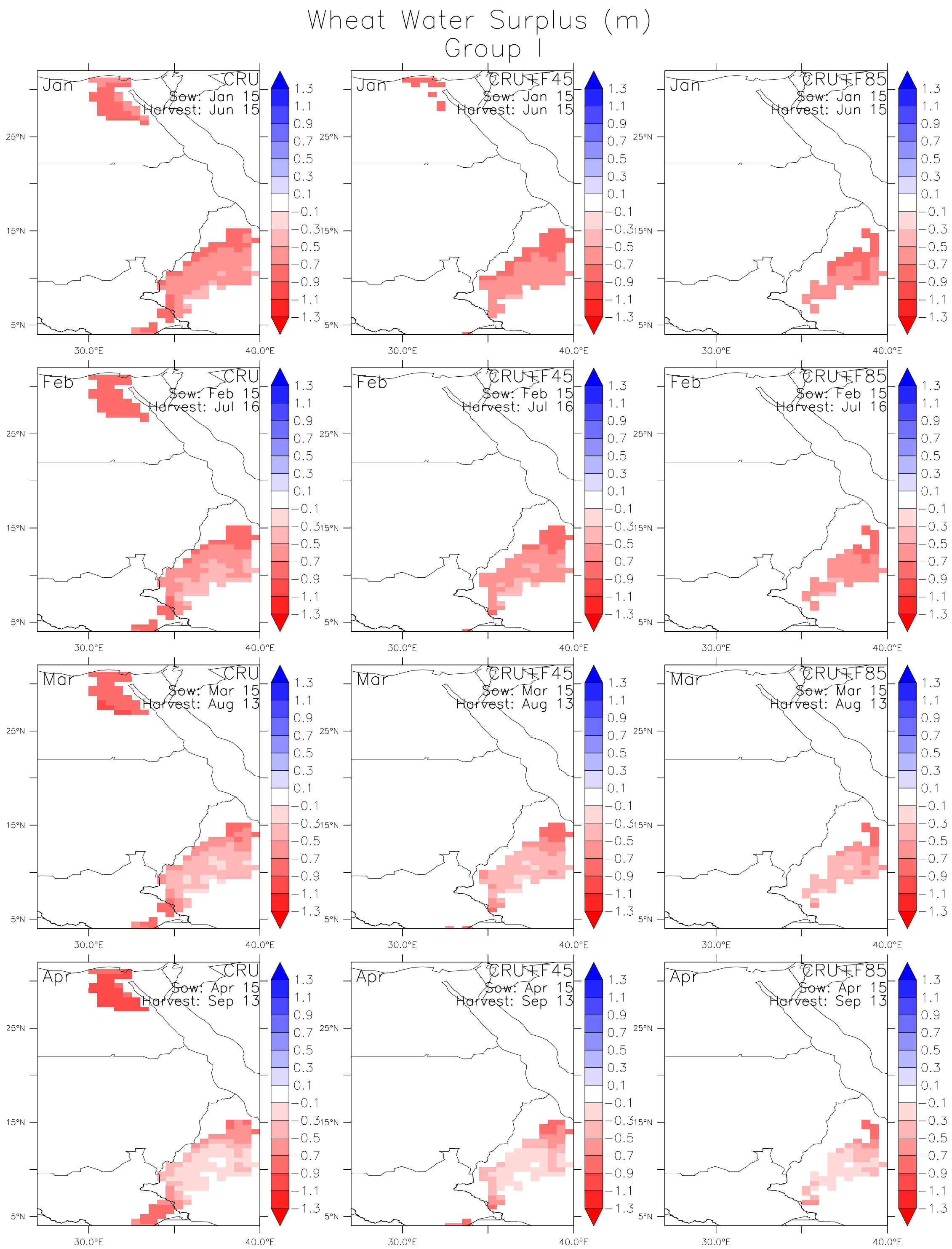
Wheat Water Surplus (m)
Group I
Jan
CRU
Sow: Jan 15
Harvest: Jun 15
CRU+F45
CRU+F85
Feb
Sow: Feb 15
Harvest: Jul 16
Mar
Sow: Mar 15
Harvest: Aug 13
Apr
Sow: Apr 15
Harvest: Sep 13
1.3
1.1
0.9
0.7
0.5
0.3
0.1
-0.1
-0.3
-0.5
-0.7
-0.9
-1.1
-1.3
25°N
15°N
5°N
30.0°E
40.0°E

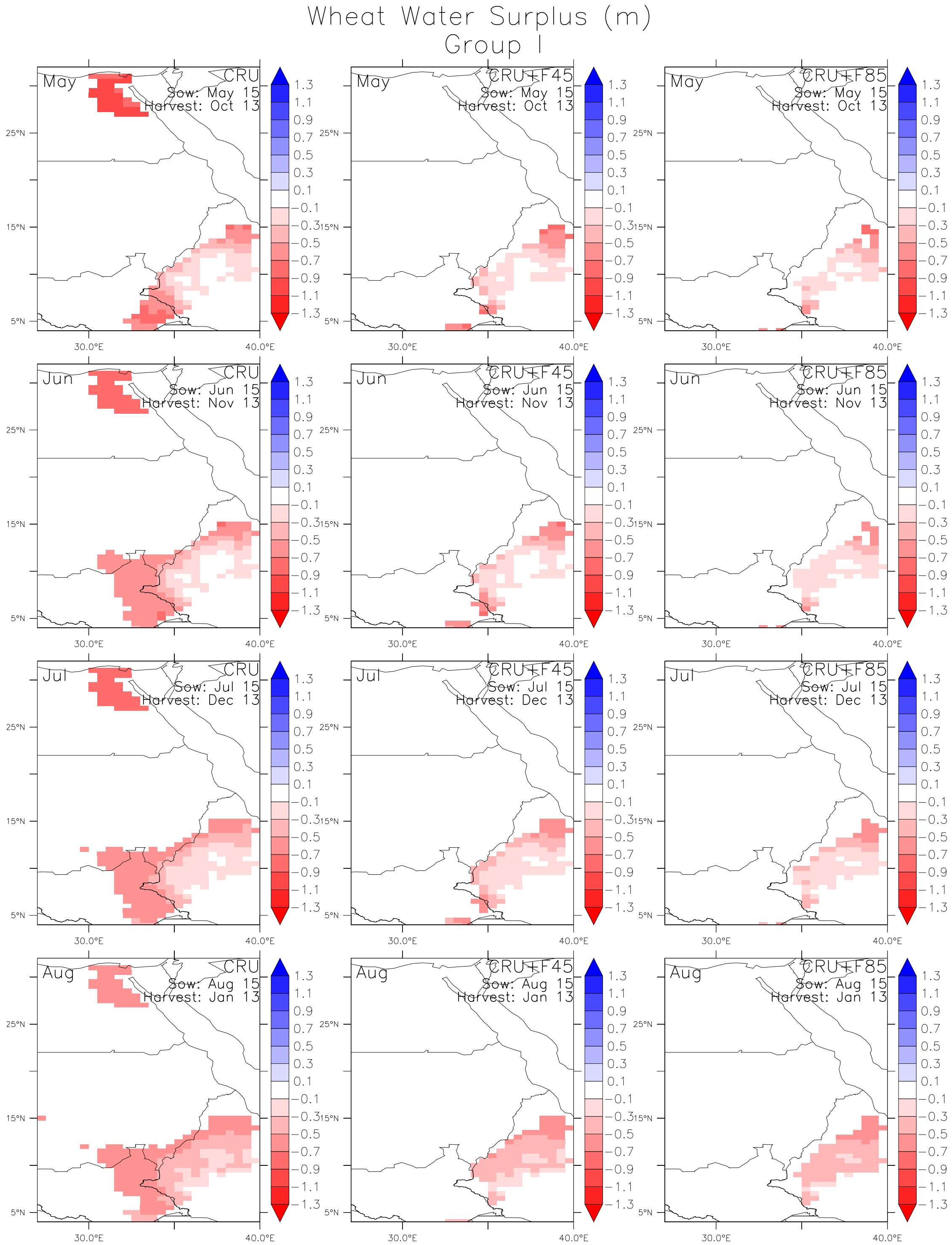
Wheat Water Surplus (m)
Group I
May
CRU
Sow: May 15
Harvest: Oct 13
CRU+F45
CRU+F85
Jun
Sow: Jun 15
Harvest: Nov 13
Jul
Sow: Jul 15
Harvest: Dec 13
Aug
Sow: Aug 15
Harvest: Jan 13
1.3
1.1
0.9
0.7
0.5
0.3
0.1
−0.1
−0.3
−0.5
−0.7
−0.9
−1.1
−1.3
25°N
15°N
5°N
30.0°E
40.0°E

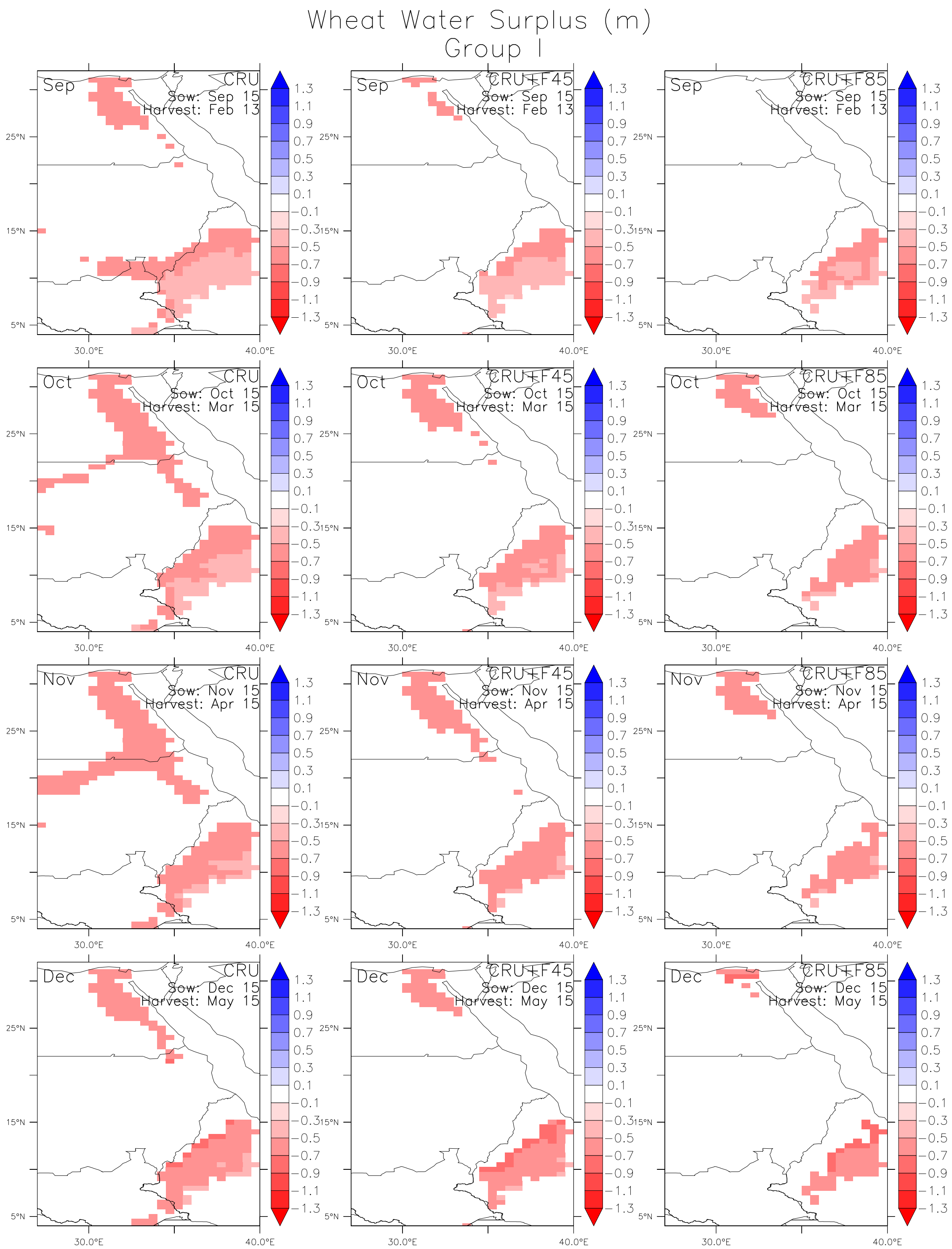

Figure 50: Wheat water surplus in m based on surface temperature. Left column: CRU; middle column: CRU+F45; and right column: CRU+F85. The values are masked for temperature suitability for Group I operative conditions over the entire growing season. Each panel represents a different sow date starting January 15 with one-month shifts. Blue shading indicates a surplus, while red shading indicates a deficit.

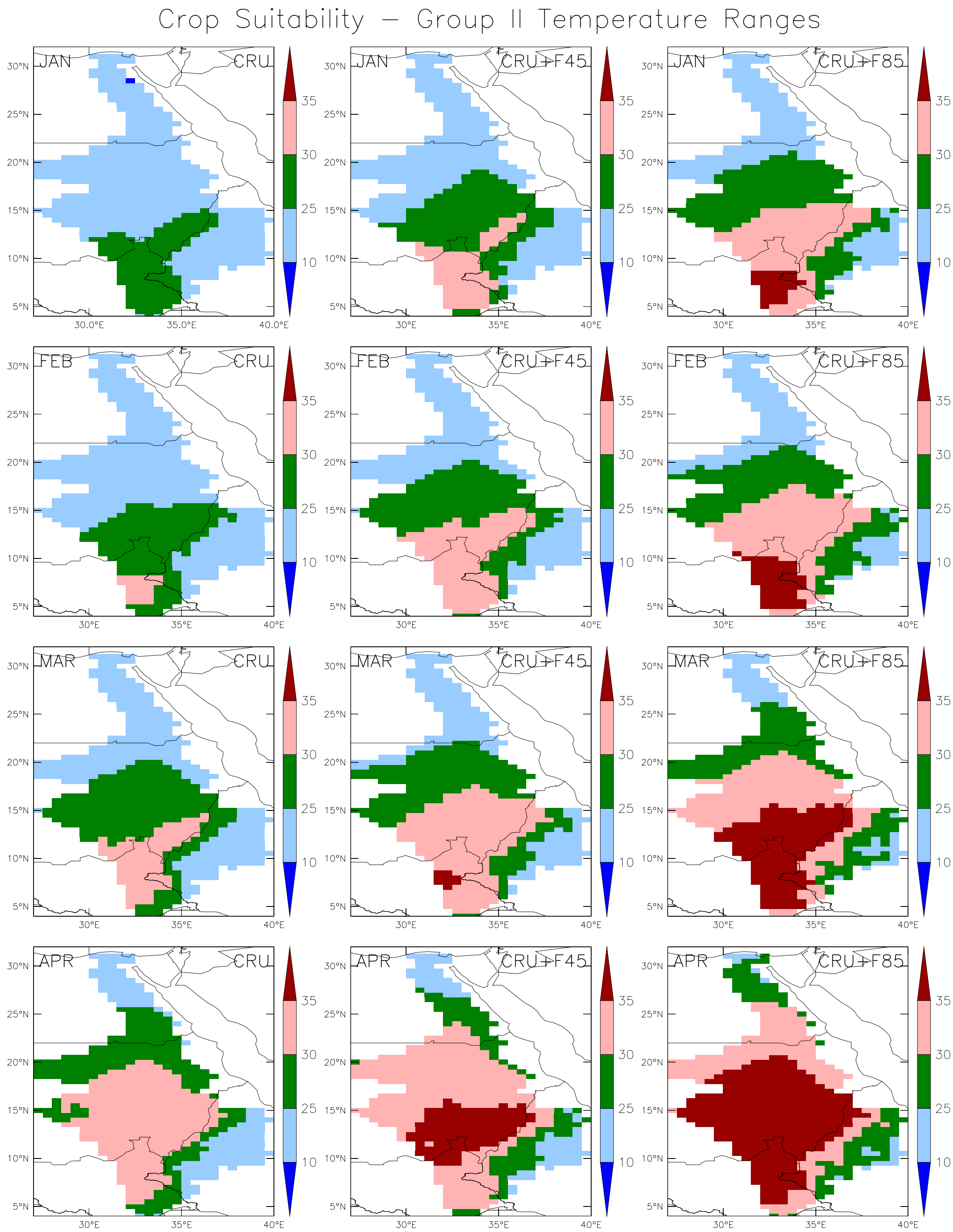
Crop Suitability – Group II Temperature Ranges
JAN
CRU
CRU+F45
CRU+F85
FEB
MAR
APR
35
30
25
10
30°N
25°N
20°N
15°N
10°N
5°N
30.0°E
35.0°E
40.0°E
30°E
35°E
40°E

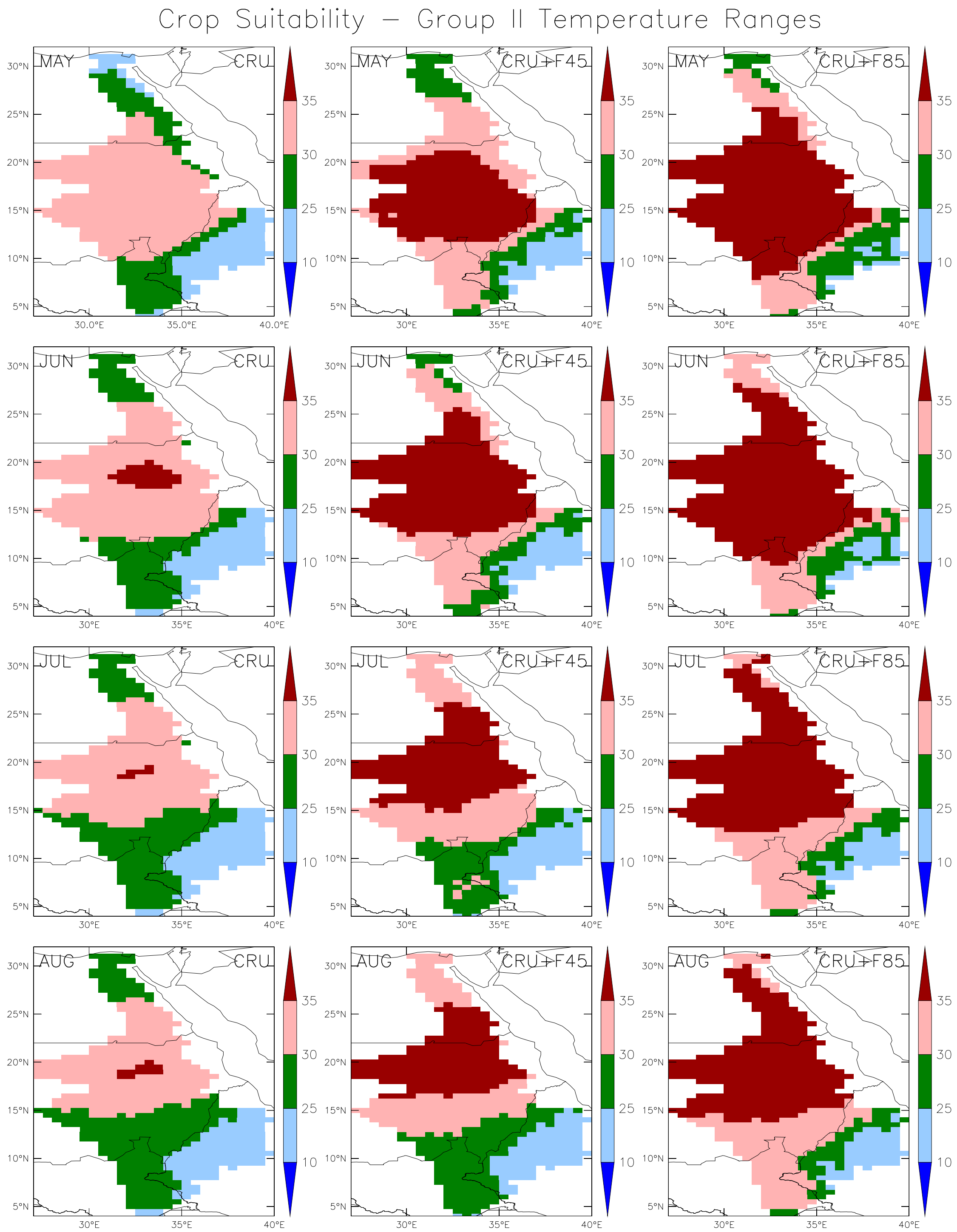
Crop Suitability – Group II Temperature Ranges
MAY
CRU
CRU+F45
CRU+F85
JUN
JUL
AUG
35
30
25
10
30°N
25°N
20°N
15°N
10°N
5°N
30.0°E
35.0°E
40.0°E
30°E
35°E
40°E

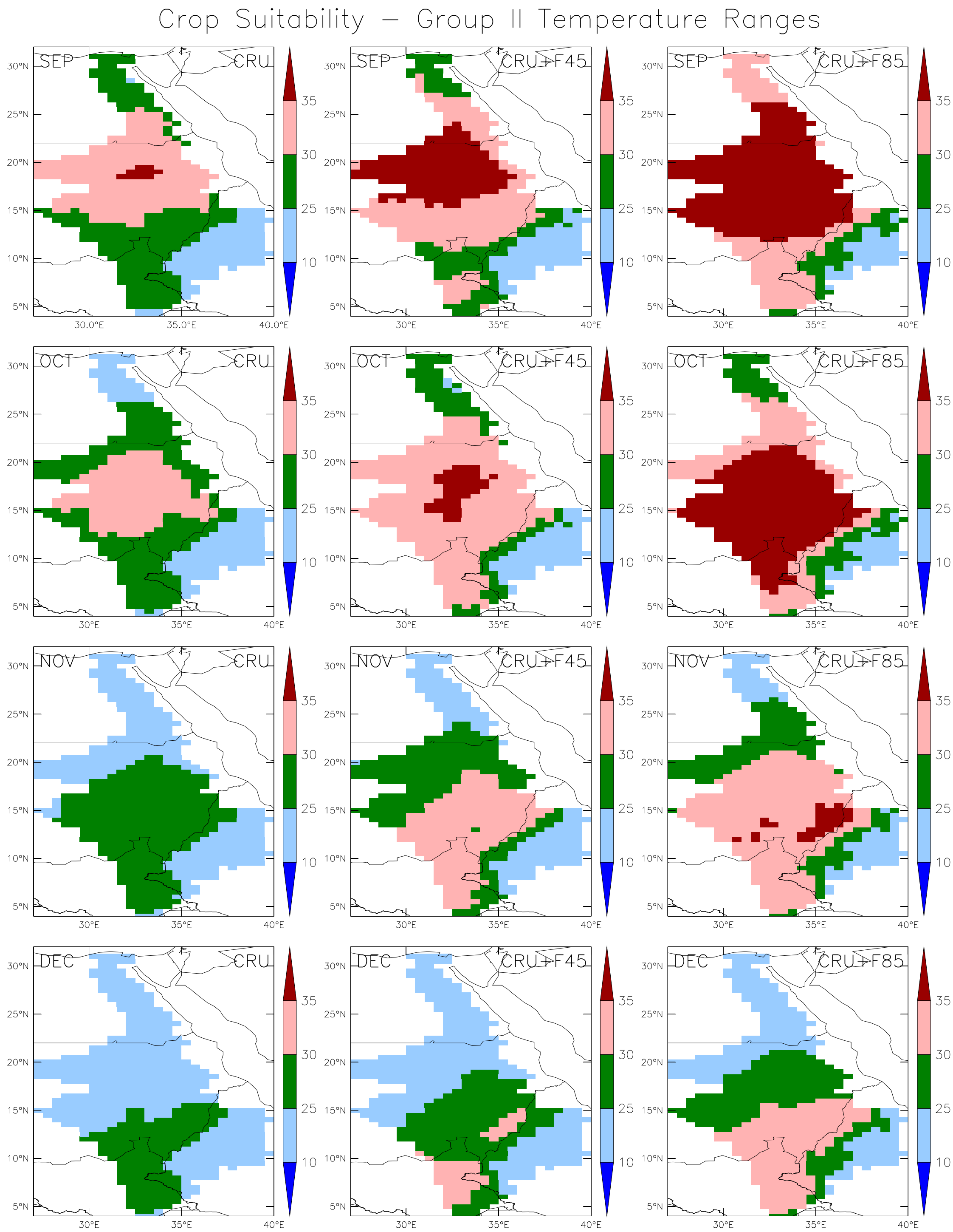

Figure 51: Monthly suitability for Group II crops based on surface temperature. Left column: CRU; middle column: CRU+F45; and right column: CRU+F85. Areas in green fall indicate temperatures for optimal growth; areas in light blue indicate temperatures below optimal but operative; areas in pink indicated temperatures above optimal but operative; and areas with in the basin that are white fall outside of the operative temperature range.

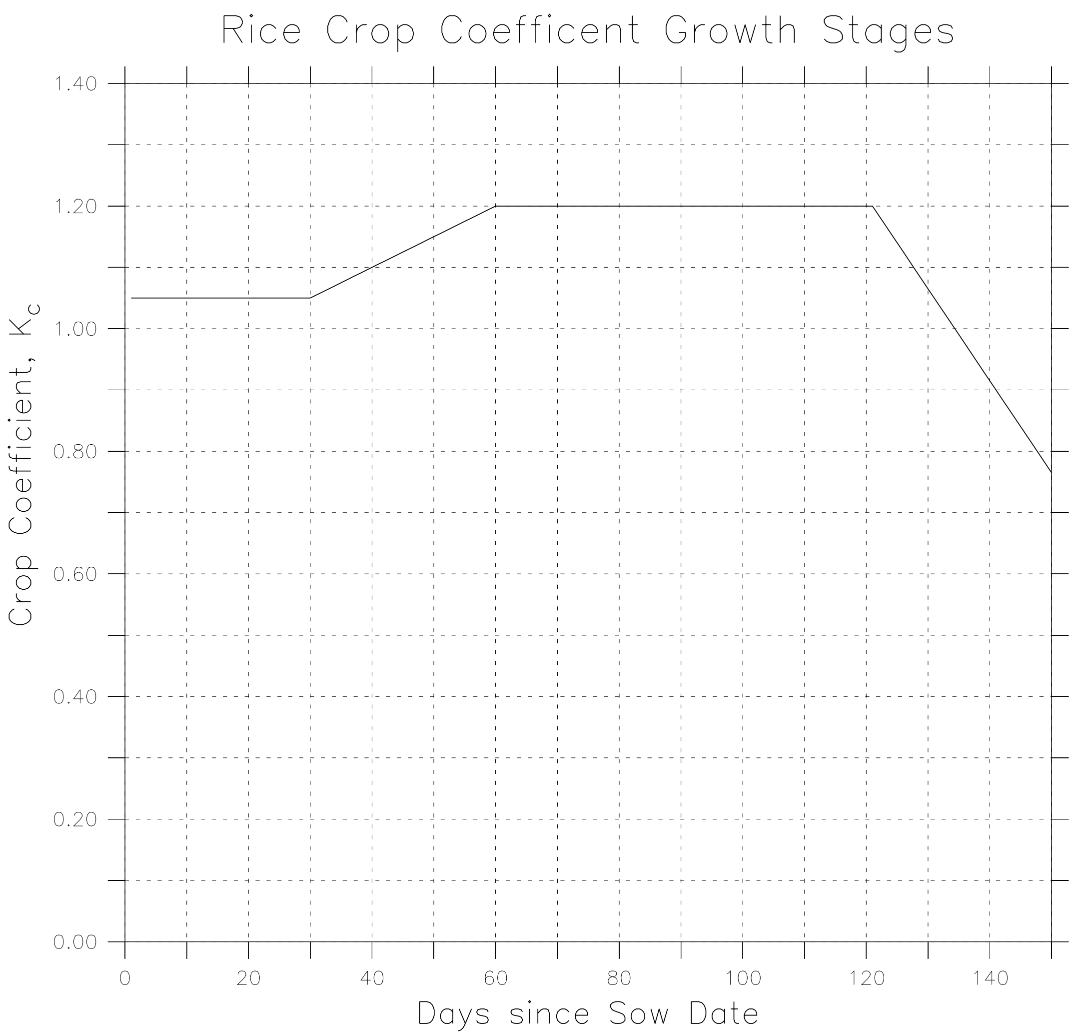

Figure 52: Rice crop coefficients and growth stages. Data adapted from on FAO (1998).

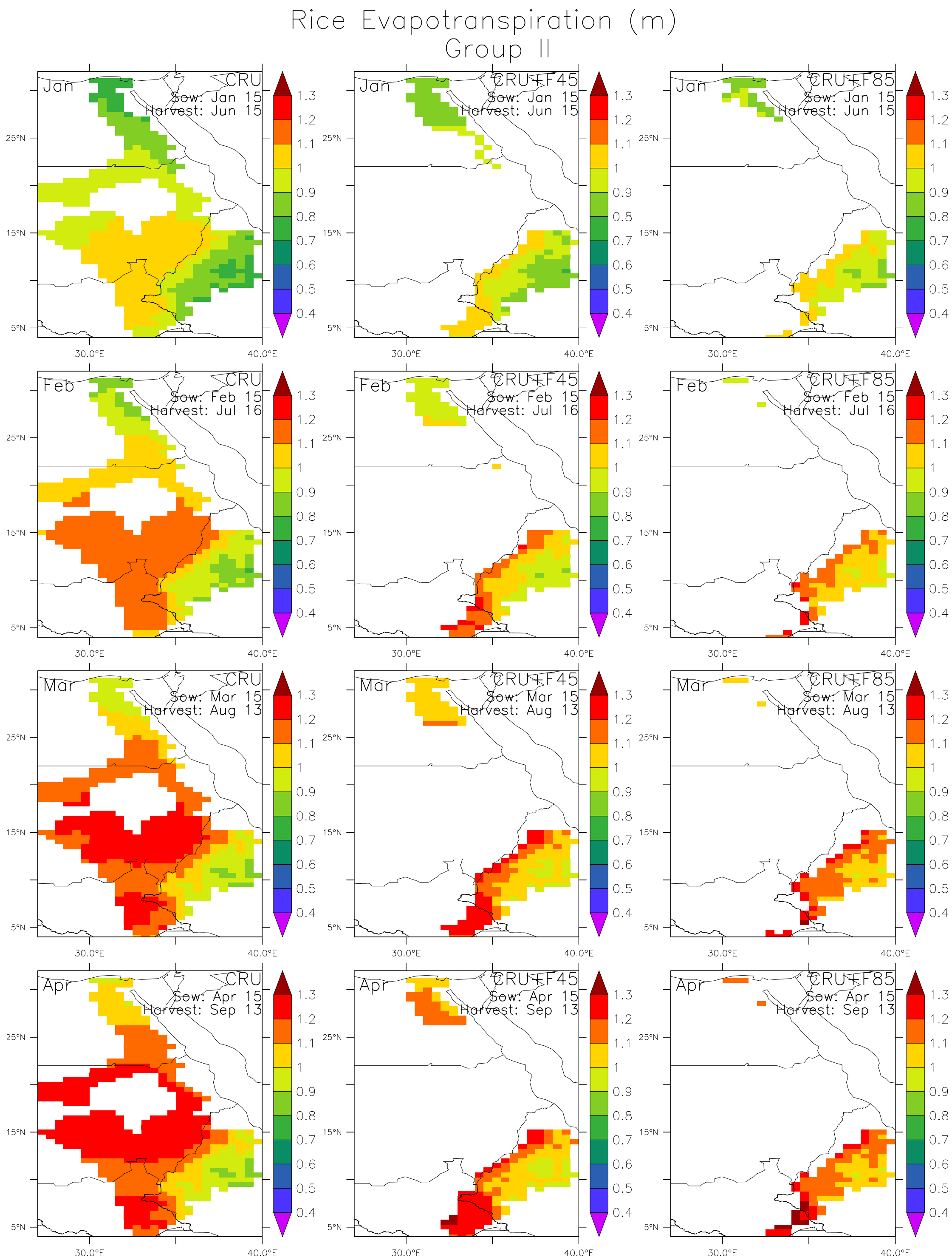
Rice Evapotranspiration (m)
Group II
Jan
CRU
Sow: Jan 15
Harvest: Jun 15
CRU+F45
CRU+F85
Feb
Sow: Feb 15
Harvest: Jul 16
Mar
Sow: Mar 15
Harvest: Aug 13
Apr
Sow: Apr 15
Harvest: Sep 13
1.3
1.2
1.1
1
0.9
0.8
0.7
0.6
0.5
0.4
25°N
15°N
5°N
30.0°E
40.0°E

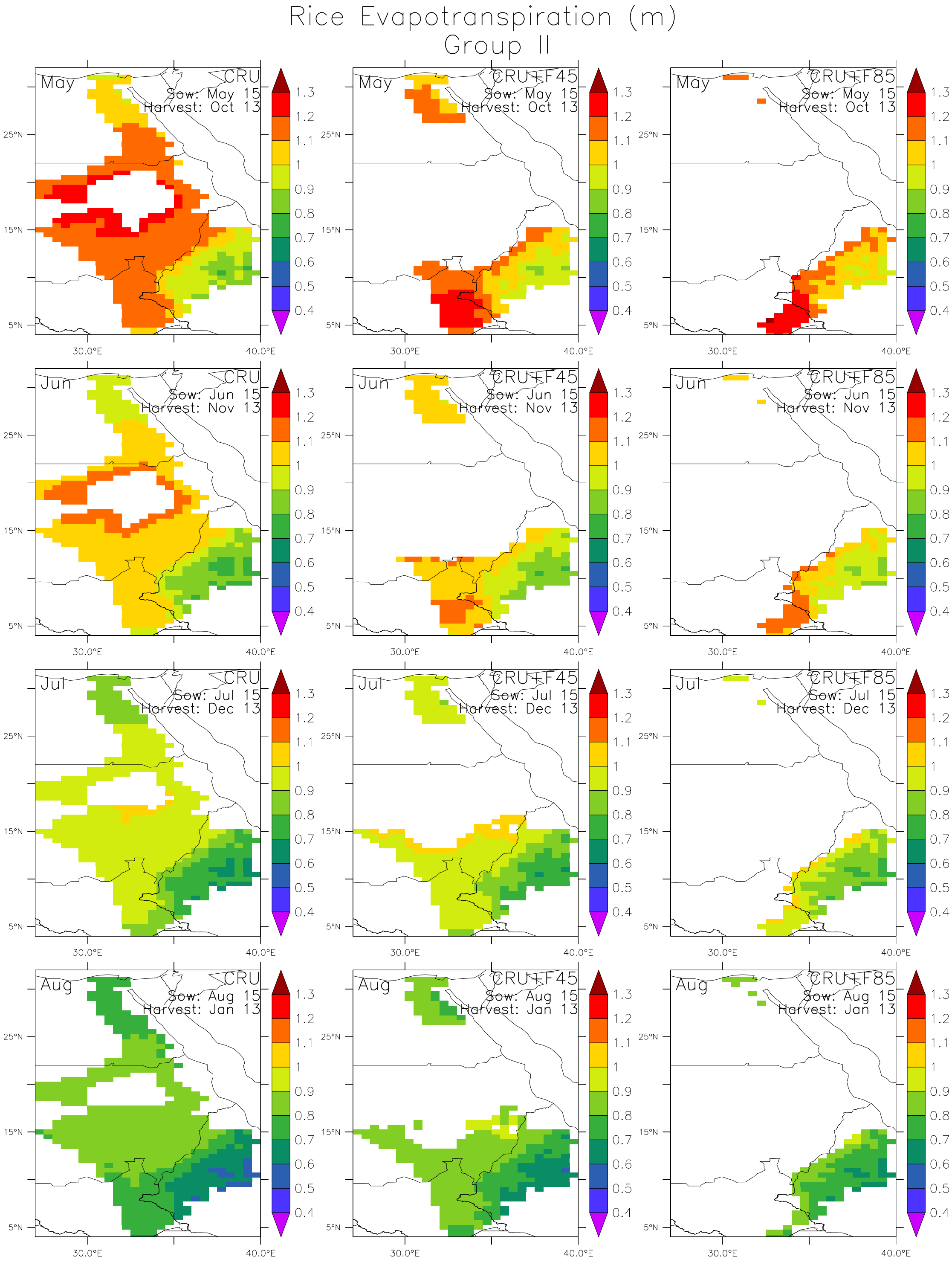
Rice Evapotranspiration (m)
Group II
May
CRU
Sow: May 15
Harvest: Oct 13
CRU+F45
CRU+F85
Jun
Sow: Jun 15
Harvest: Nov 13
Jul
Sow: Jul 15
Harvest: Dec 13
Aug
Sow: Aug 15
Harvest: Jan 13
1.3
1.2
1.1
1
0.9
0.8
0.7
0.6
0.5
0.4
25°N
15°N
5°N
30.0°E
40.0°E

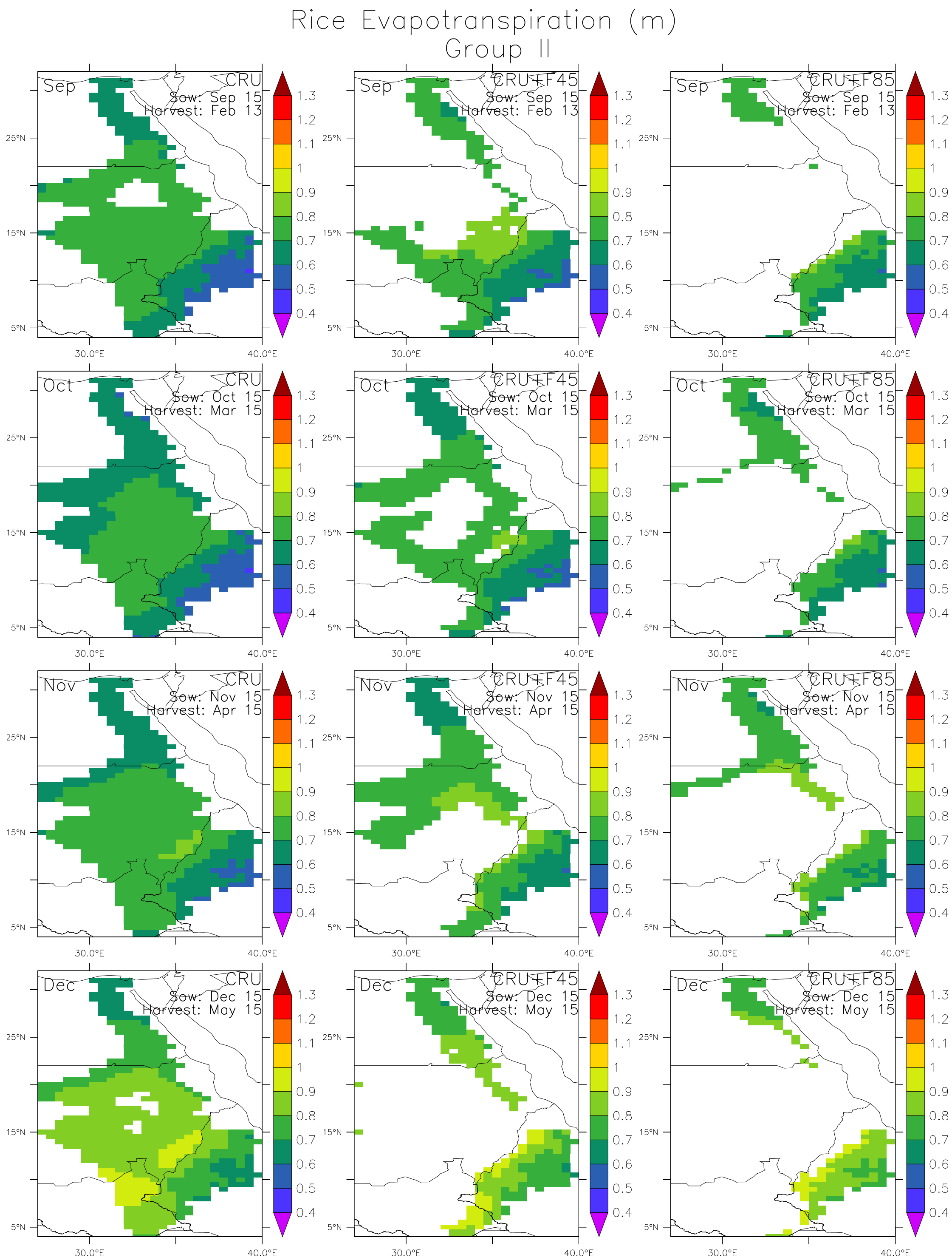

Figure 53: Rice evapotranspiration in m based on surface temperature. Left column: CRU; middle column: CRU+F45; and right column: CRU+F85. The values are masked for temperature suitability for Group II operative conditions over the entire growing season. Each panel represents a different sow date starting January 15 with one-month shifts.

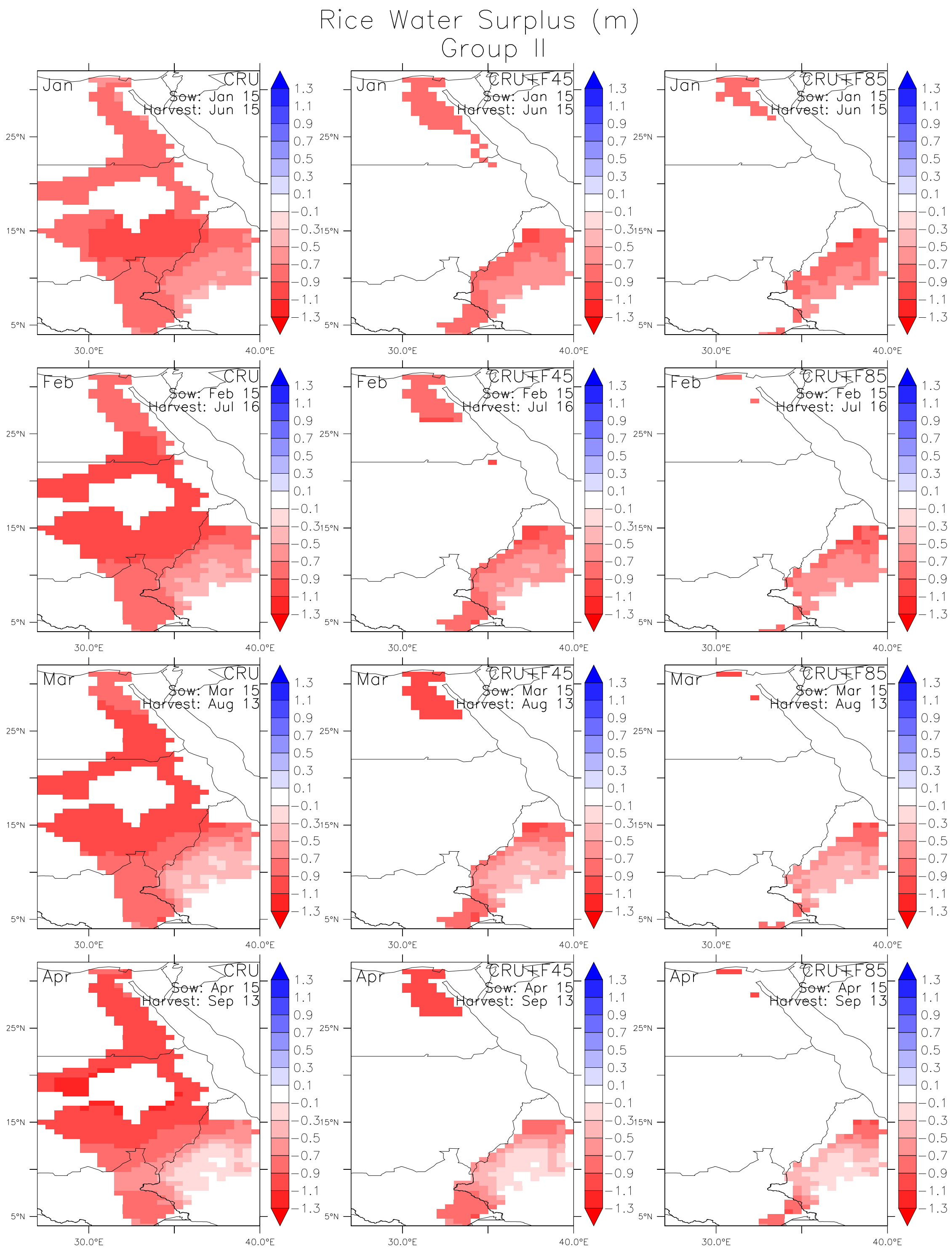
Rice Water Surplus (m)
Group II
Jan
CRU
Sow: Jan 15
Harvest: Jun 15
CRU+F45
CRU+F85
Feb
Sow: Feb 15
Harvest: Jul 16
Mar
Sow: Mar 15
Harvest: Aug 13
Apr
Sow: Apr 15
Harvest: Sep 13
25°N
15°N
5°N
30.0°E
40.0°E
1.3
1.1
0.9
0.7
0.5
0.3
0.1
-0.1
-0.3
-0.5
-0.7
-0.9
-1.1
-1.3

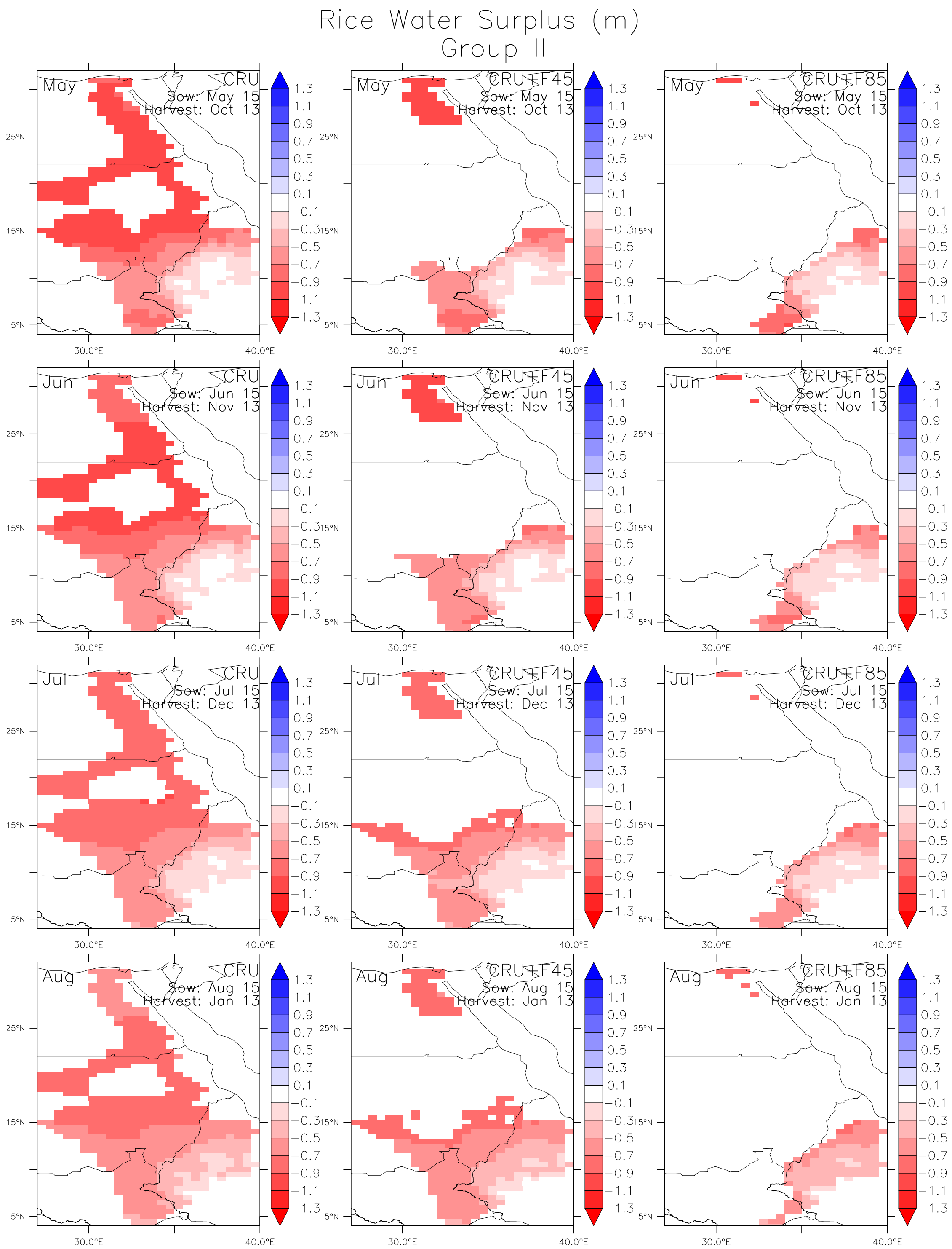
Rice Water Surplus (m)
Group II
May
CRU
Sow: May 15
Harvest: Oct 13
CRU+F45
CRU+F85
Jun
Sow: Jun 15
Harvest: Nov 13
Jul
Sow: Jul 15
Harvest: Dec 13
Aug
Sow: Aug 15
Harvest: Jan 13
25°N
15°N
5°N
30.0°E
40.0°E
1.3
1.1
0.9
0.7
0.5
0.3
0.1
-0.1
-0.3
-0.5
-0.7
-0.9
-1.1
-1.3

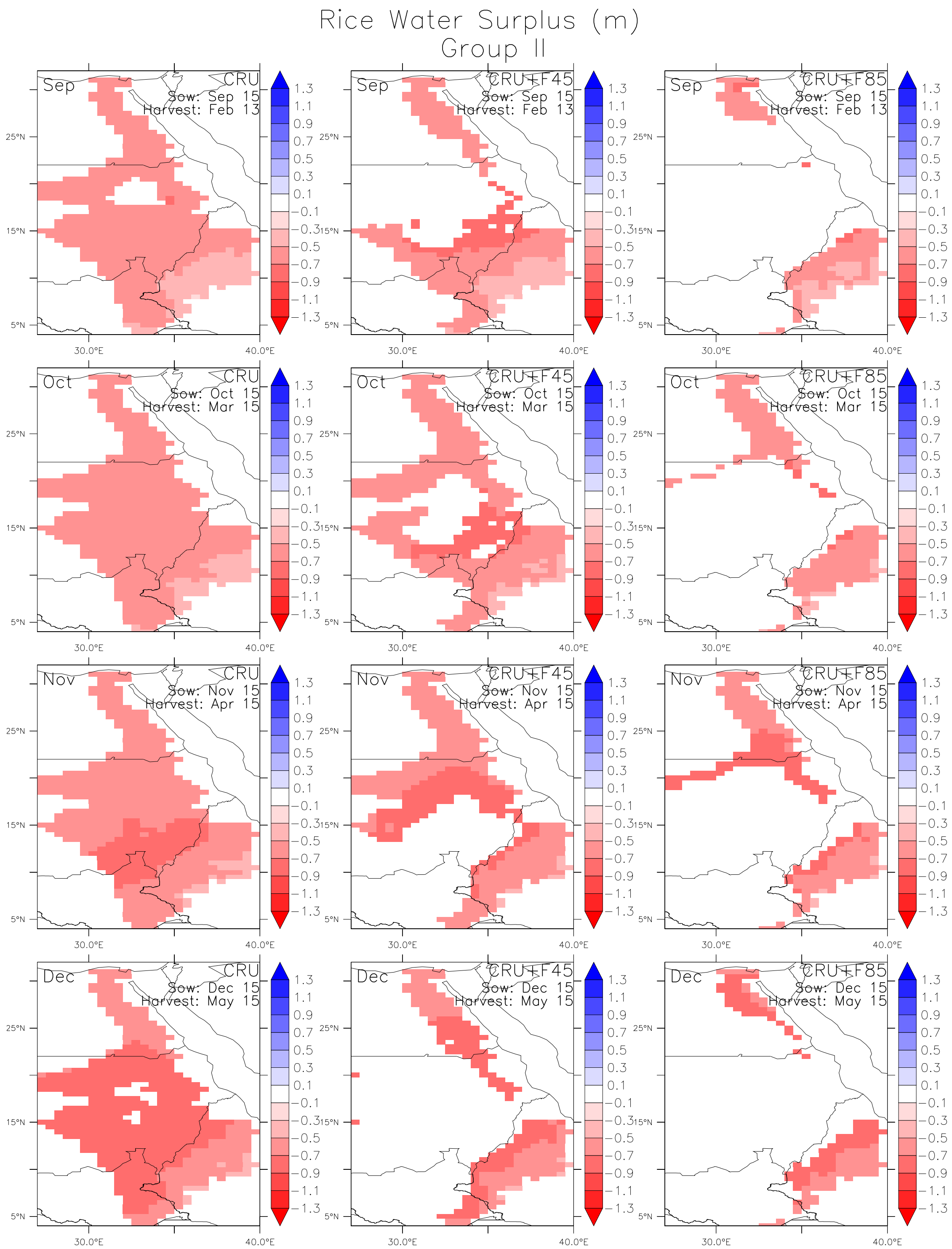

Figure 54: Rice water surplus in m based on surface temperature. Left column: CRU; middle column: CRU+F45; and right column: CRU+F85. The values are masked for temperature suitability for Group II operative conditions over the entire growing season. Each panel represents a different sow date starting January 15 with one-month shifts. Blue shading indicates a surplus, while red shading indicates a deficit.

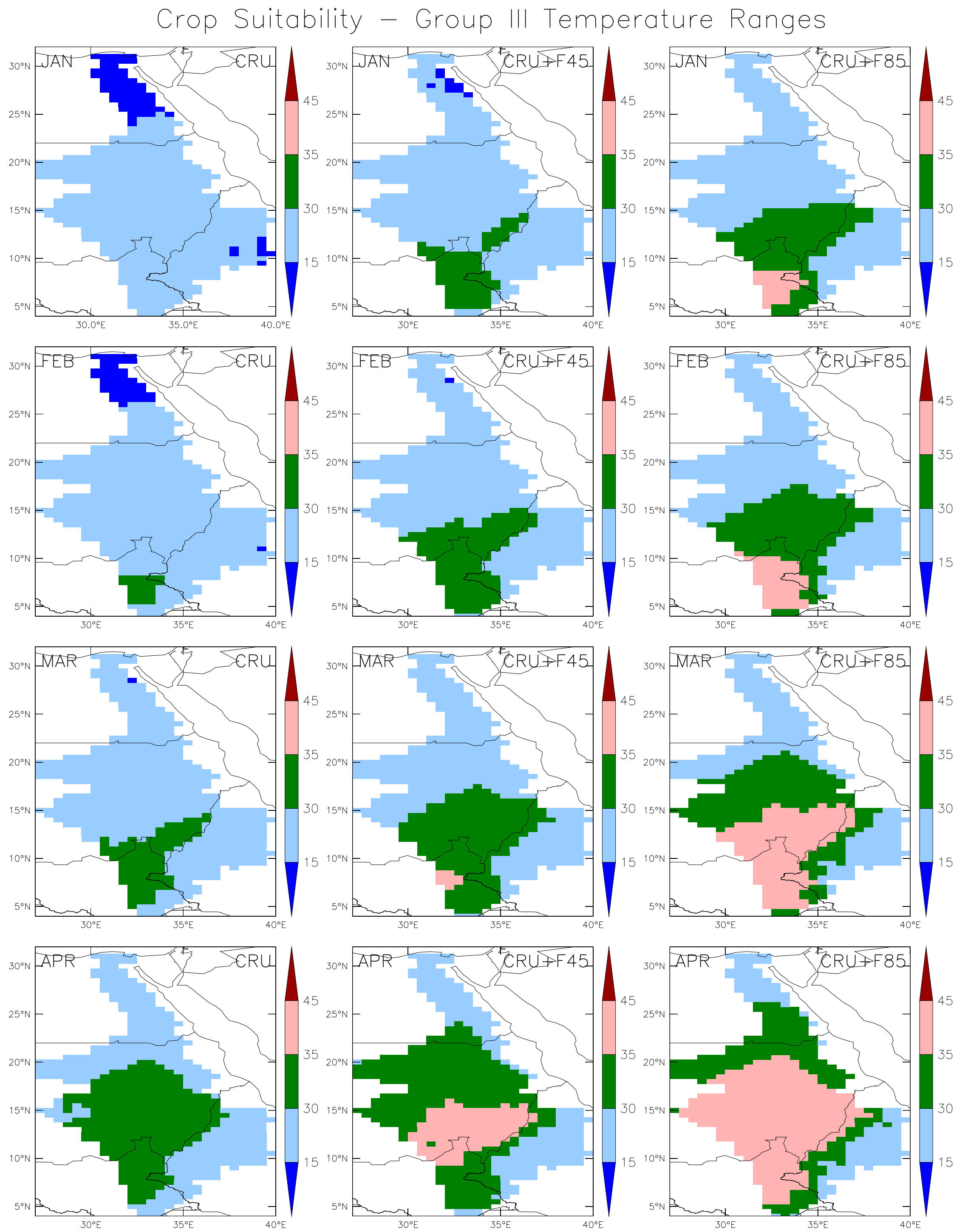
Crop Suitability – Group III Temperature Ranges
JAN
CRU
CRU+F45
CRU+F85
FEB
MAR
APR
45
35
30
15
30°N
25°N
20°N
15°N
10°N
5°N
30°E
35°E
40°E

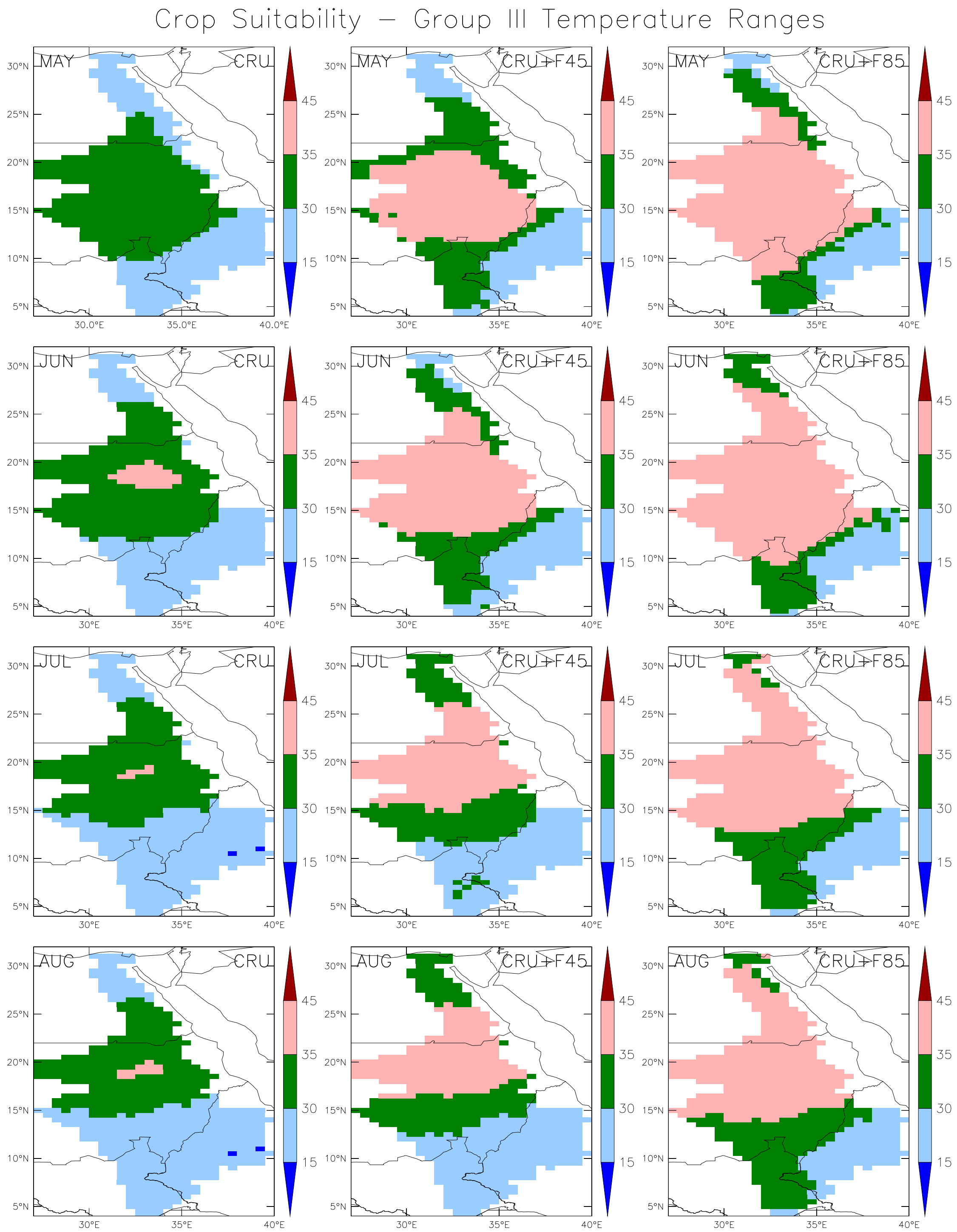
Crop Suitability – Group III Temperature Ranges
MAY
CRU
CRU+F45
CRU+F85
JUN
JUL
AUG
45
35
30
15
30°N
25°N
20°N
15°N
10°N
5°N
30°E
35°E
40°E

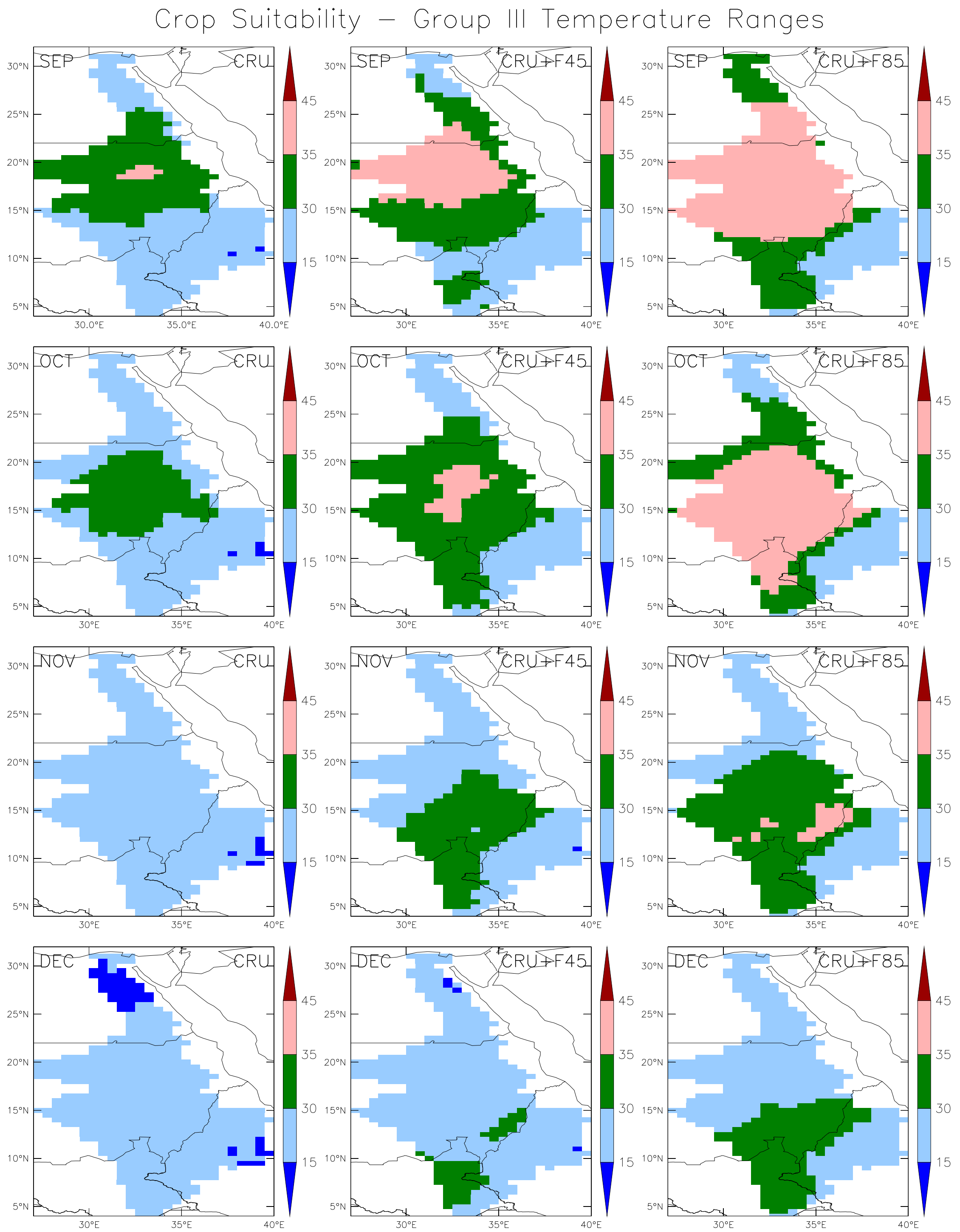

Figure 55: Monthly suitability for Group III crops based on surface temperature. Left column: CRU; middle column: CRU+F45; and right column: CRU+F85. Areas in green fall indicate temperatures for optimal growth; areas in light blue indicate temperatures below optimal but operative; areas in pink indicated temperatures above optimal but operative; and areas with in the basin that are white fall outside of the operative temperature range.

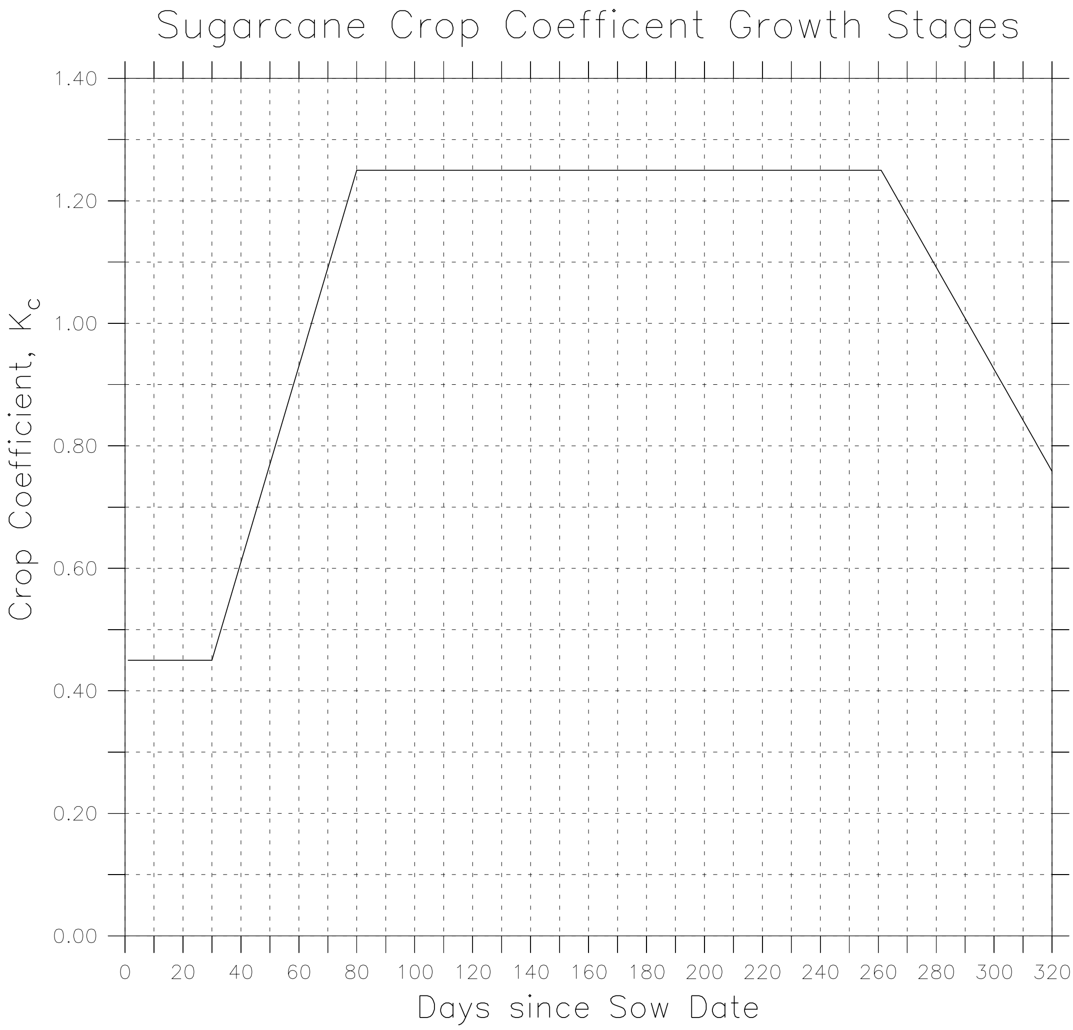

Figure 56: Ratoon sugarcane crop coefficients and growth stages. Data adapted from on FAO (1998).

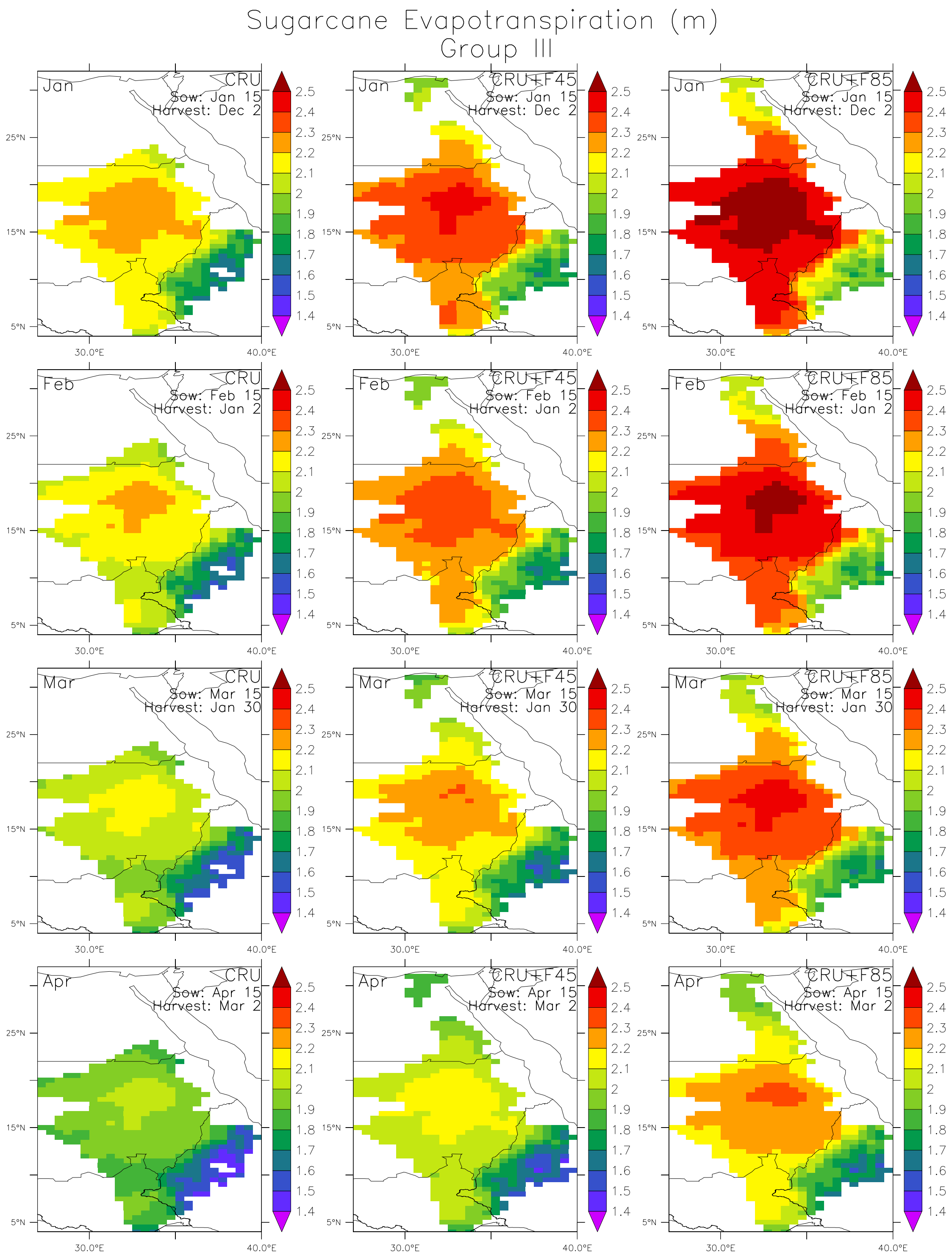
Sugarcane Evapotranspiration (m)
Group III
Jan
CRU
Sow: Jan 15
Harvest: Dec 2
CRU+F45
CRU+F85
Feb
Sow: Feb 15
Harvest: Jan 2
Mar
Sow: Mar 15
Harvest: Jan 30
Apr
Sow: Apr 15
Harvest: Mar 2
2.5
2.4
2.3
2.2
2.1
2
1.9
1.8
1.7
1.6
1.5
1.4
25°N
15°N
5°N
30.0°E
40.0°E

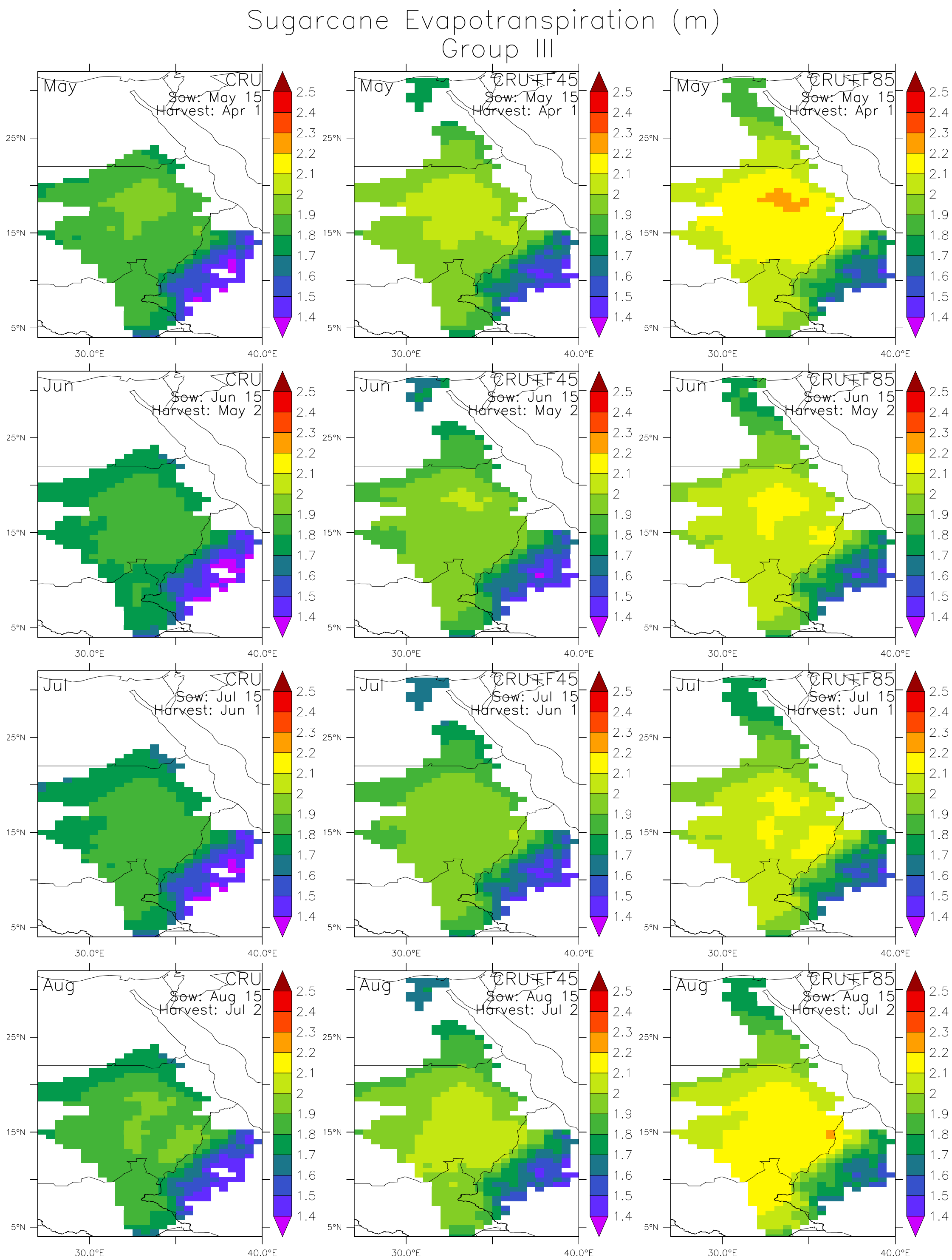
Sugarcane Evapotranspiration (m)
Group III
May
CRU
Sow: May 15
Harvest: Apr 1
CRU+F45
CRU+F85
Jun
Sow: Jun 15
Harvest: May 2
Jul
Sow: Jul 15
Harvest: Jun 1
Aug
Sow: Aug 15
Harvest: Jul 2
2.5
2.4
2.3
2.2
2.1
2
1.9
1.8
1.7
1.6
1.5
1.4
25°N
15°N
5°N
30.0°E
40.0°E

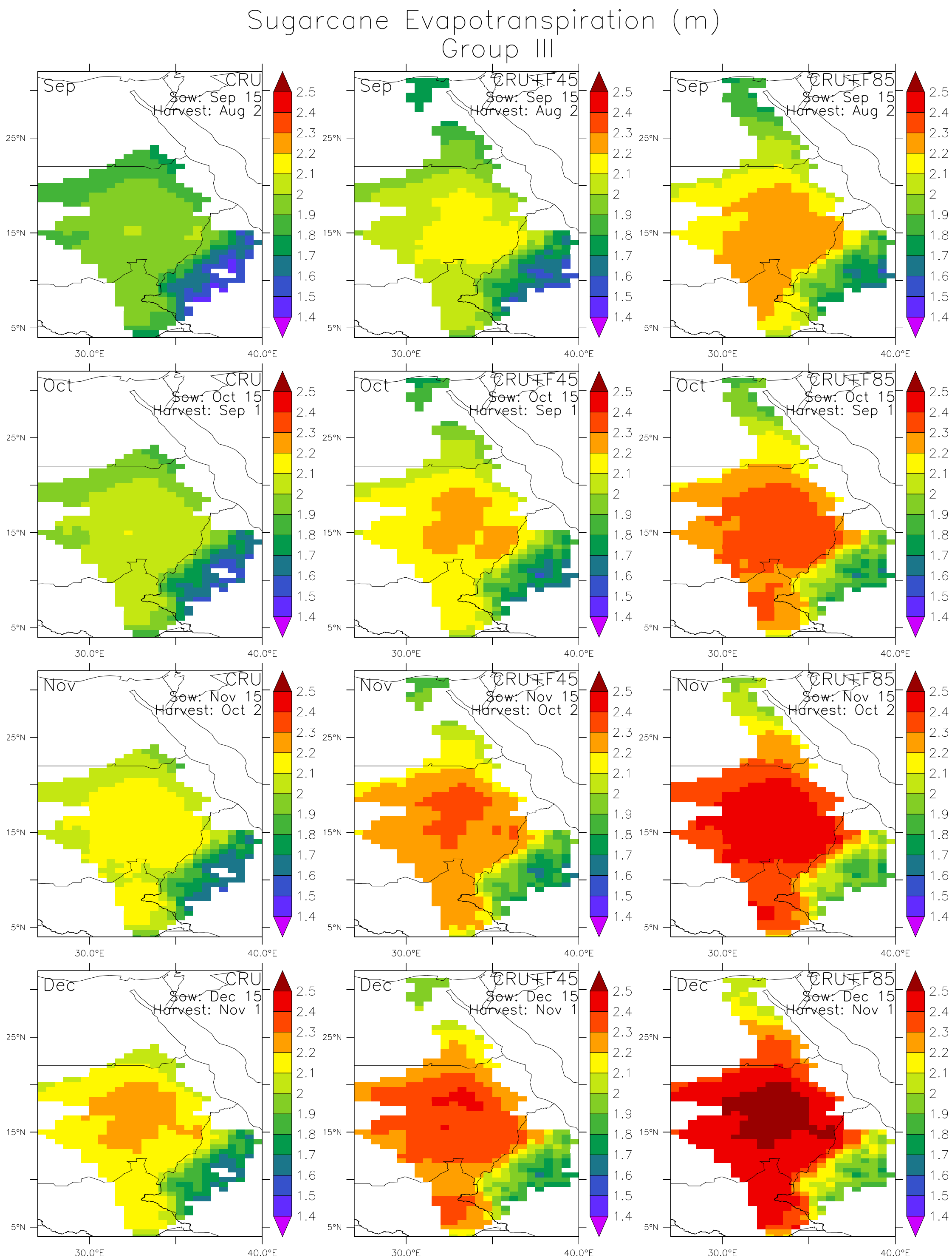

Figure 57: Ratoon sugarcane evapotranspiration in based on surface temperature. Left column: CRU; middle column: CRU+F45; and right column: CRU+F85. The values are masked for temperature suitability for Group III operative conditions over the entire growing season. Each panel represents a different sow date starting January 15 with one-month shifts.

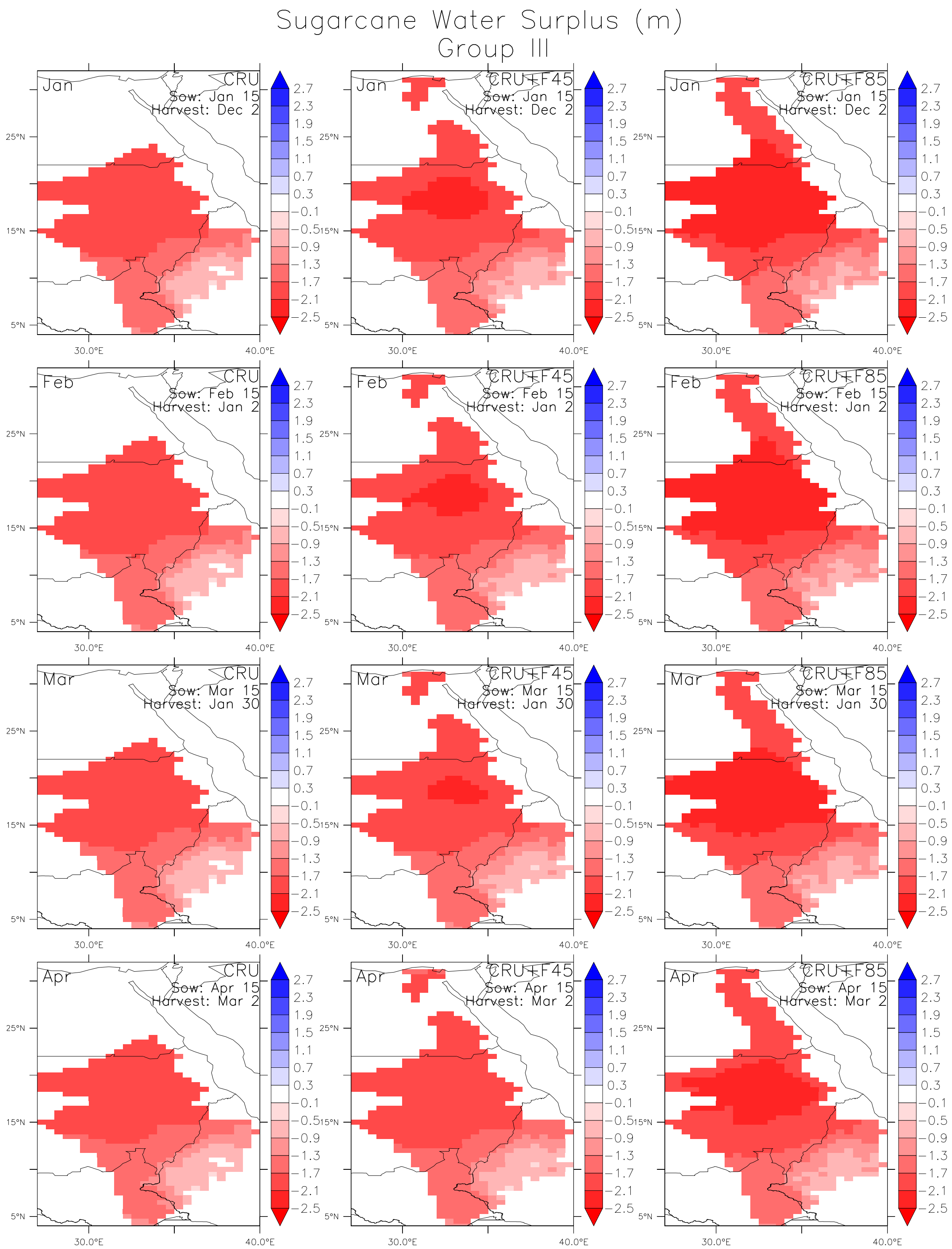
Sugarcane Water Surplus (m)
Group III
Jan
CRU
Sow: Jan 15
Harvest: Dec 2
CRU+F45
CRU+F85
Feb
Sow: Feb 15
Harvest: Jan 2
Mar
Sow: Mar 15
Harvest: Jan 30
Apr
Sow: Apr 15
Harvest: Mar 2
2.7
2.3
1.9
1.5
1.1
0.7
0.3
-0.1
-0.5
-0.9
-1.3
-1.7
-2.1
-2.5
25°N
15°N
5°N
30.0°E
40.0°E

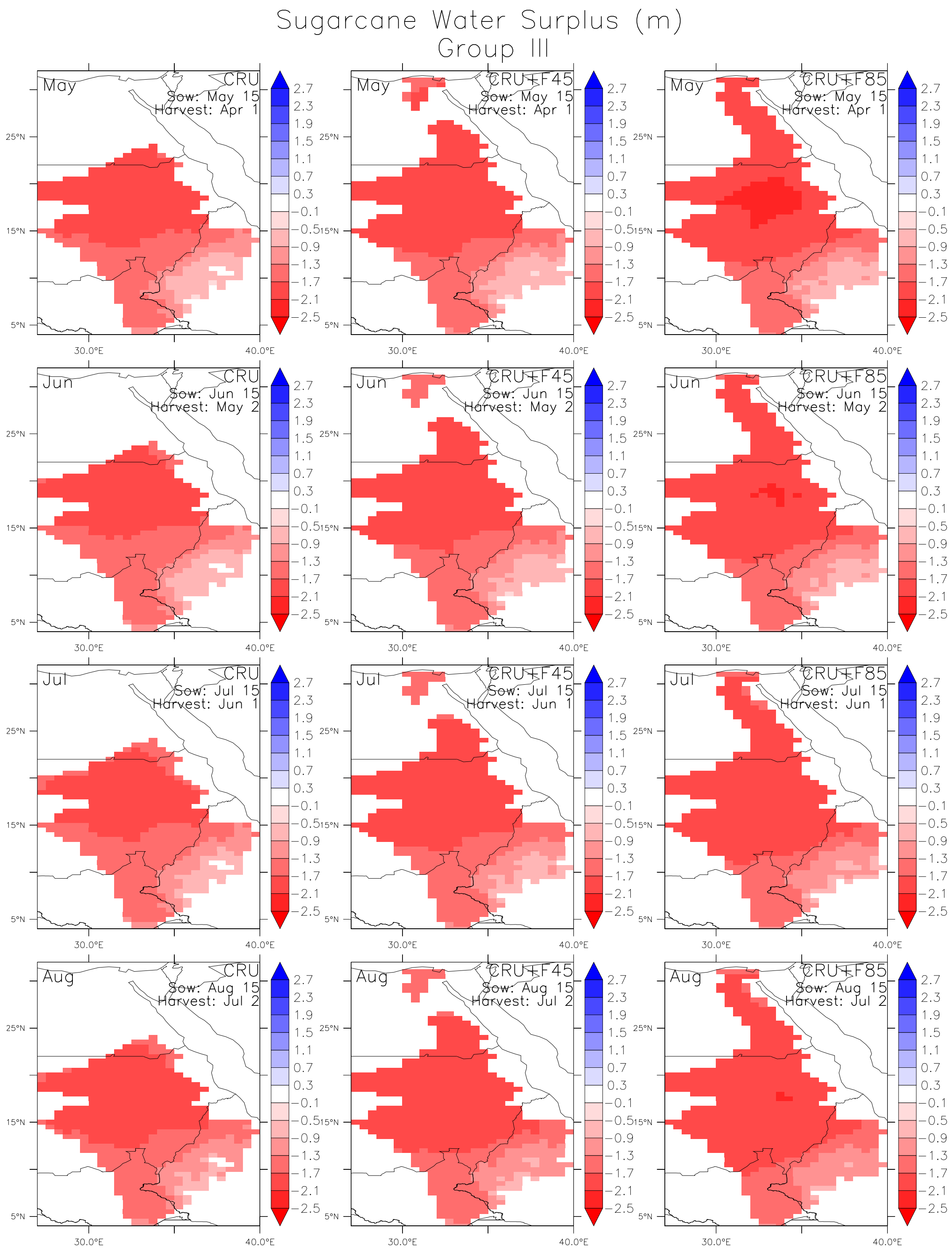
Sugarcane Water Surplus (m)
Group III
May
Jun
Jul
Aug
CRU
CRU+F45
CRU+F85
Sow: May 15
Harvest: Apr 1
Sow: Jun 15
Harvest: May 2
Sow: Jul 15
Harvest: Jun 1
Sow: Aug 15
Harvest: Jul 2
2.7
2.3
1.9
1.5
1.1
0.7
0.3
−0.1
−0.5
−0.9
−1.3
−1.7
−2.1
−2.5
25°N
15°N
5°N
30.0°E
40.0°E

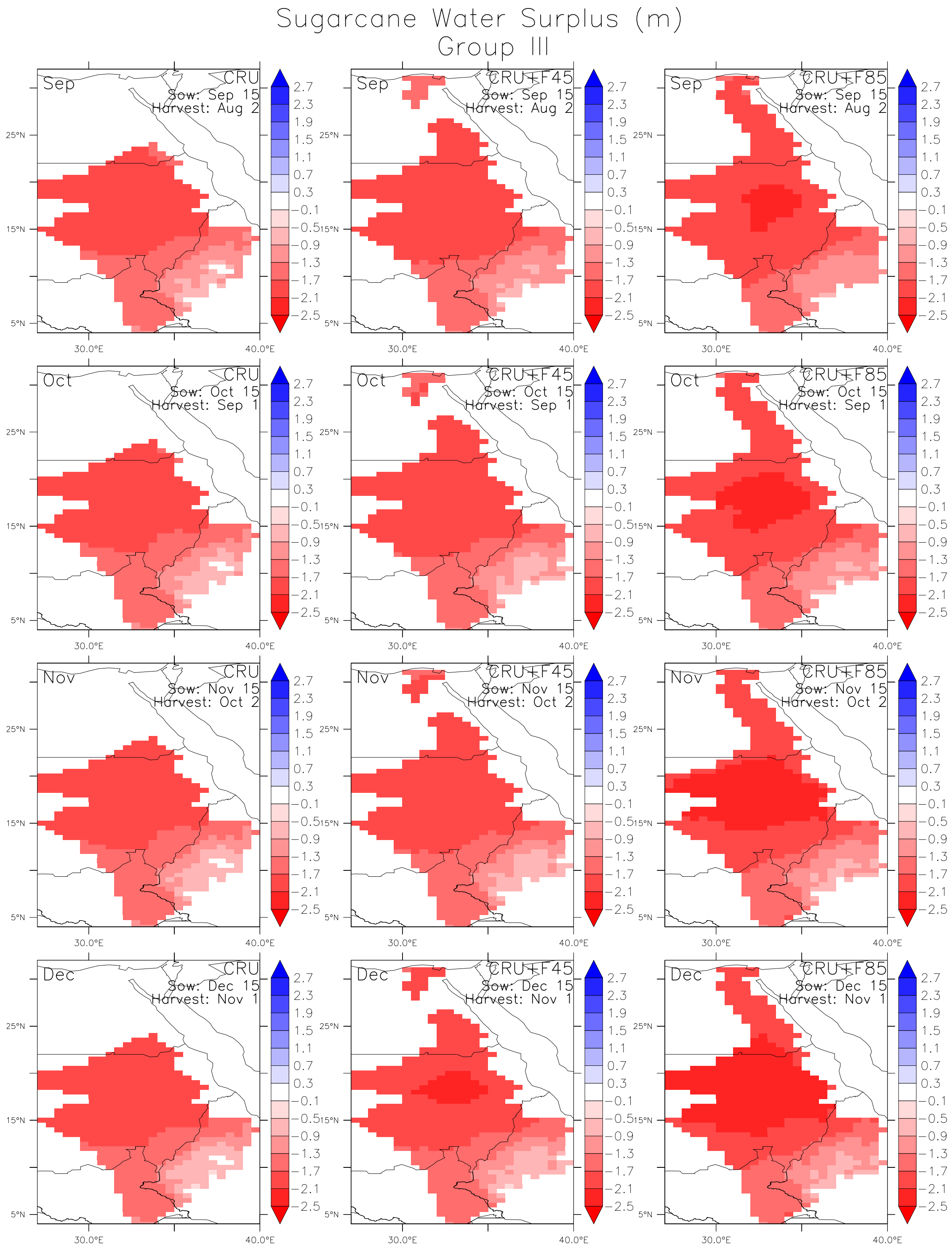

Figure 58: Ratoon sugarcane water surplus in m based on surface temperature. Left column: CRU; middle column: CRU+F45; and right column: CRU+F85. The values are masked for temperature suitability for Group III operative conditions over the entire growing season. Each panel represents a different sow date starting January 15 with one-month shifts. Blue shading indicates a surplus, while red shading indicates a deficit.

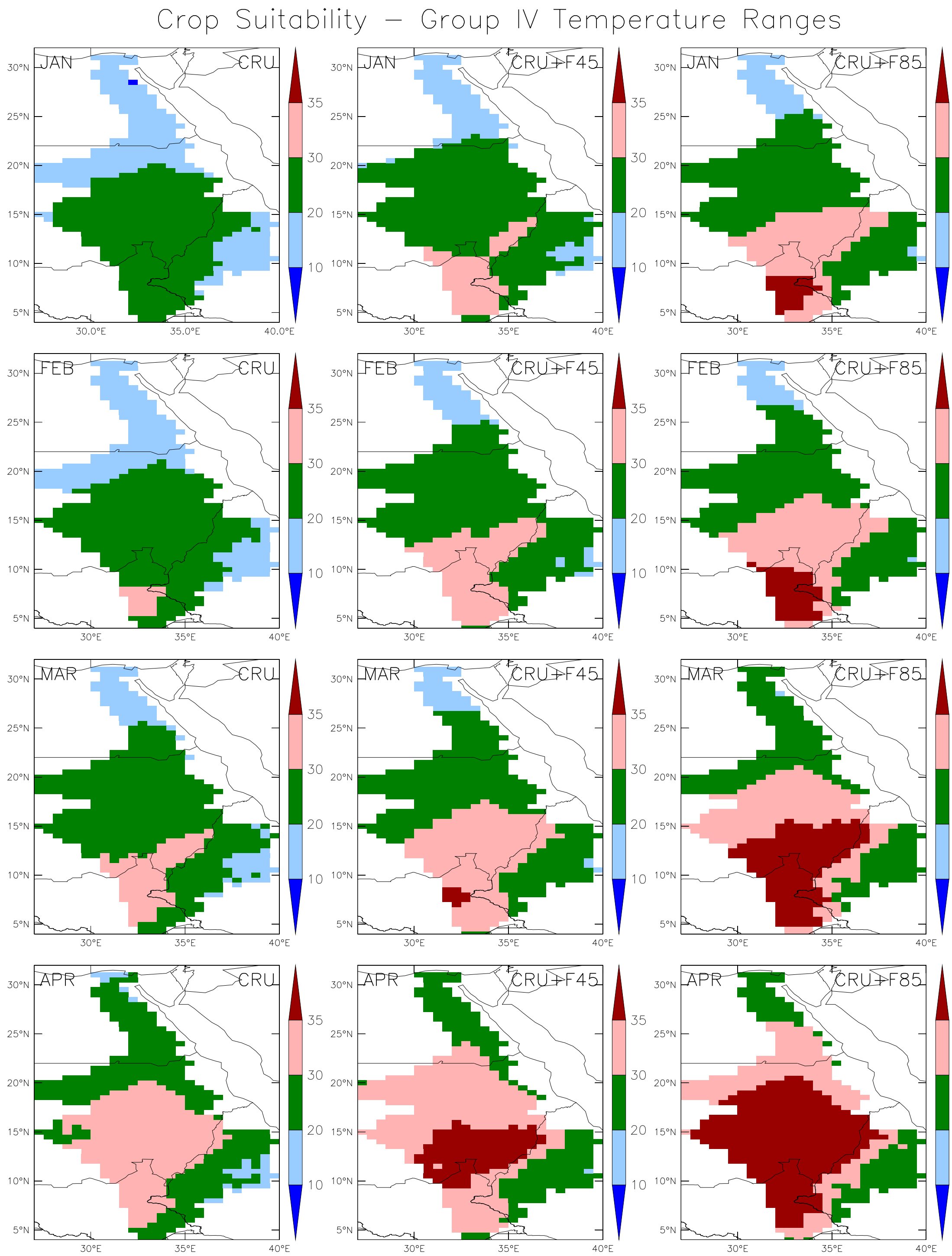
Crop Suitability – Group IV Temperature Ranges
JAN
CRU
CRU+F45
CRU+F85
FEB
MAR
APR
35
30
20
10
30°N
25°N
20°N
15°N
10°N
5°N
30°E
35°E
40°E
30.0°E
35.0°E
40.0°E

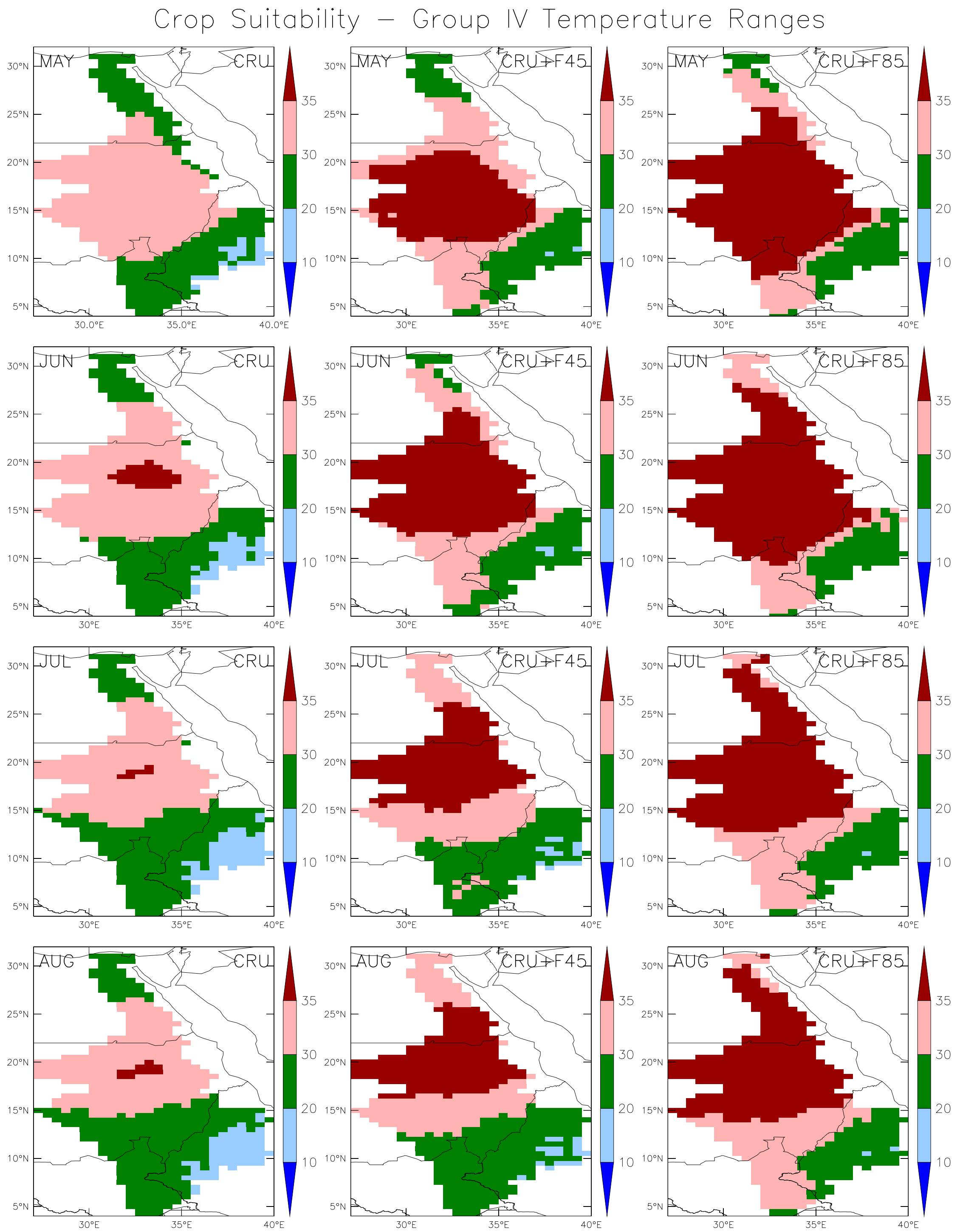
Crop Suitability – Group IV Temperature Ranges
MAY
CRU
CRU+F45
CRU+F85
JUN
JUL
AUG
35
30
20
10
30°N
25°N
20°N
15°N
10°N
5°N
30.0°E
35.0°E
40.0°E
30°E
35°E
40°E

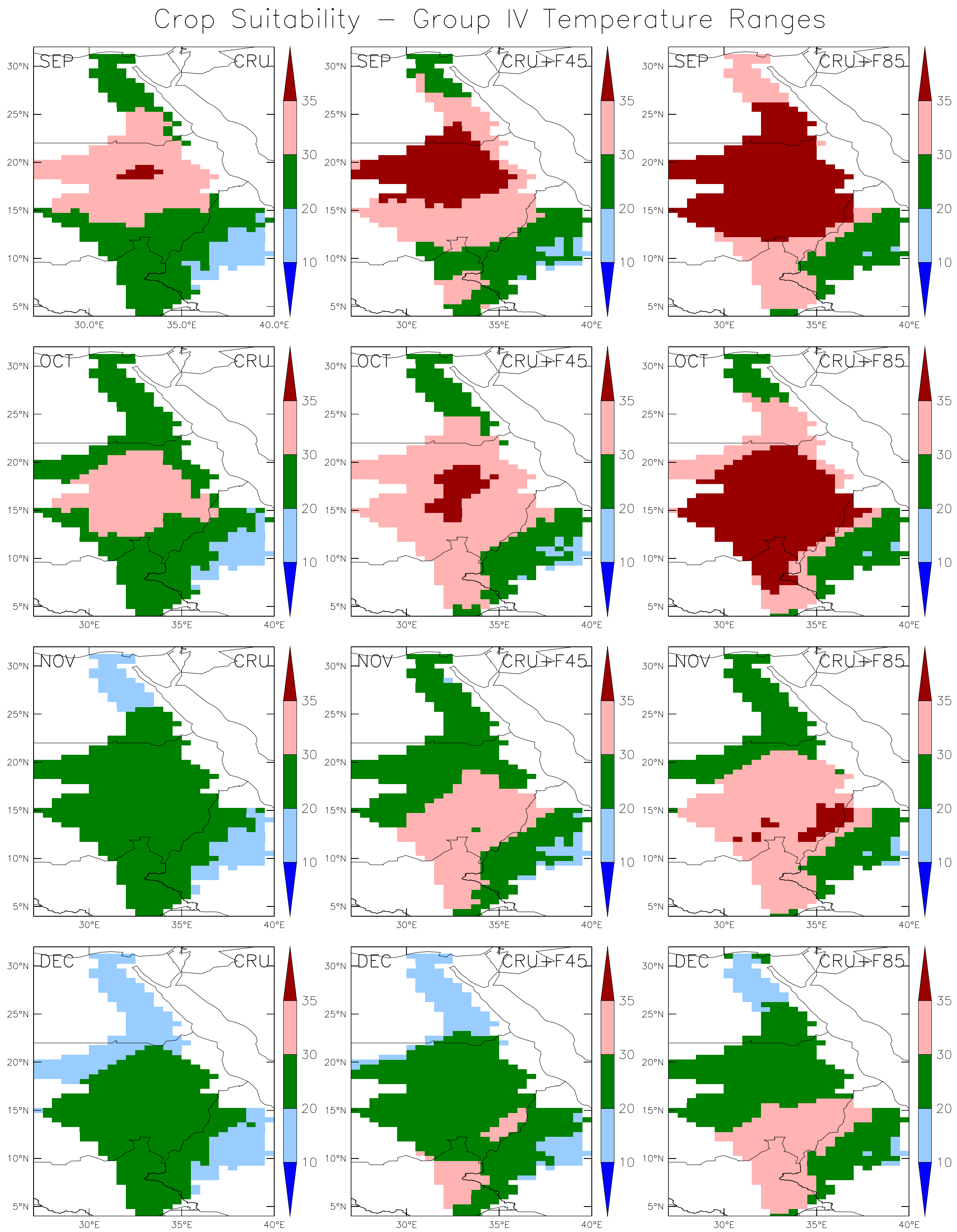

Figure 59: Monthly suitability for Group IV crops based on surface temperature. Left column: CRU; middle column: CRU+F45; and right column: CRU+F85. Areas in green fall indicate temperatures for optimal growth; areas in light blue indicate temperatures below optimal but operative; areas in pink indicated temperatures above optimal but operative; and areas with in the basin that are white fall outside of the operative temperature range.

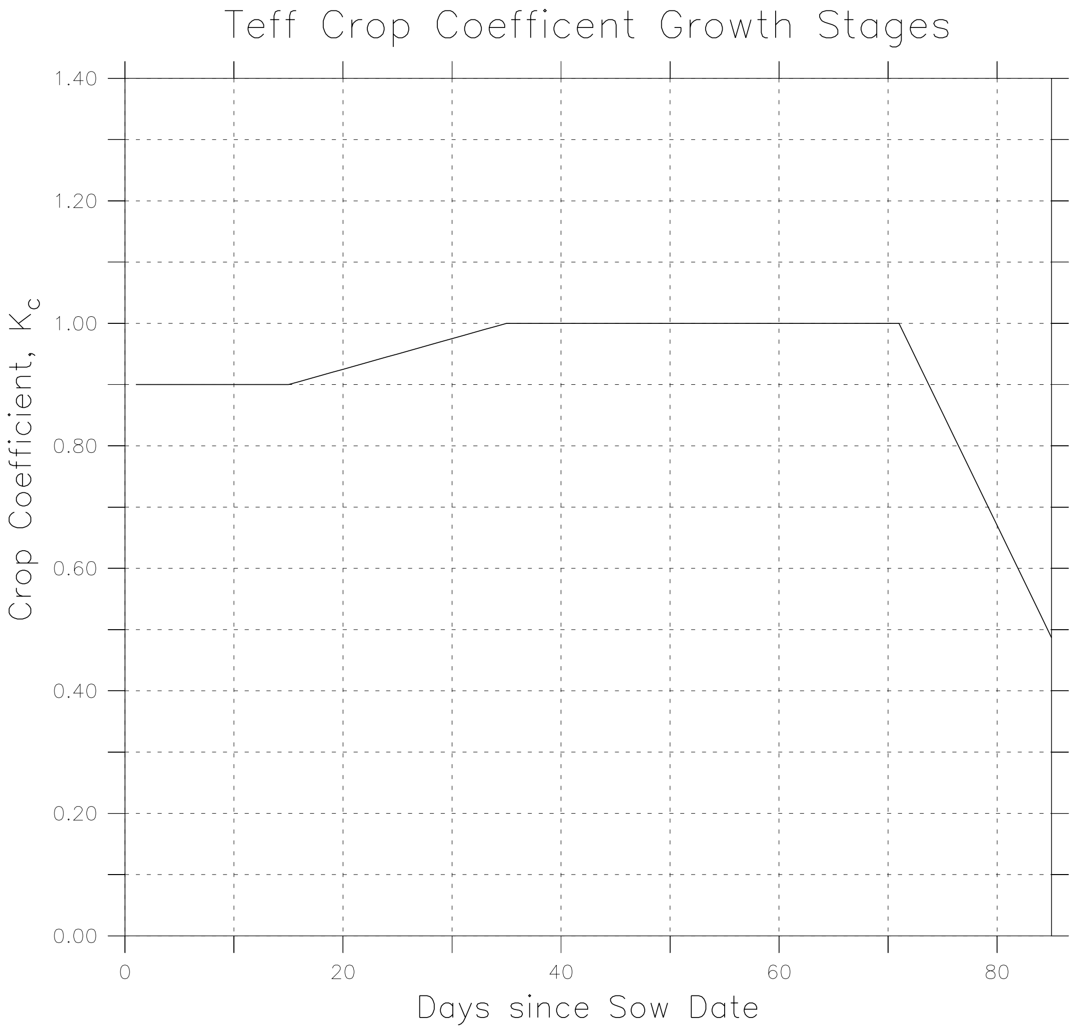

Figure 60: Teff crop coefficients and growth stages. Data adapted from on Araya et al (2011).

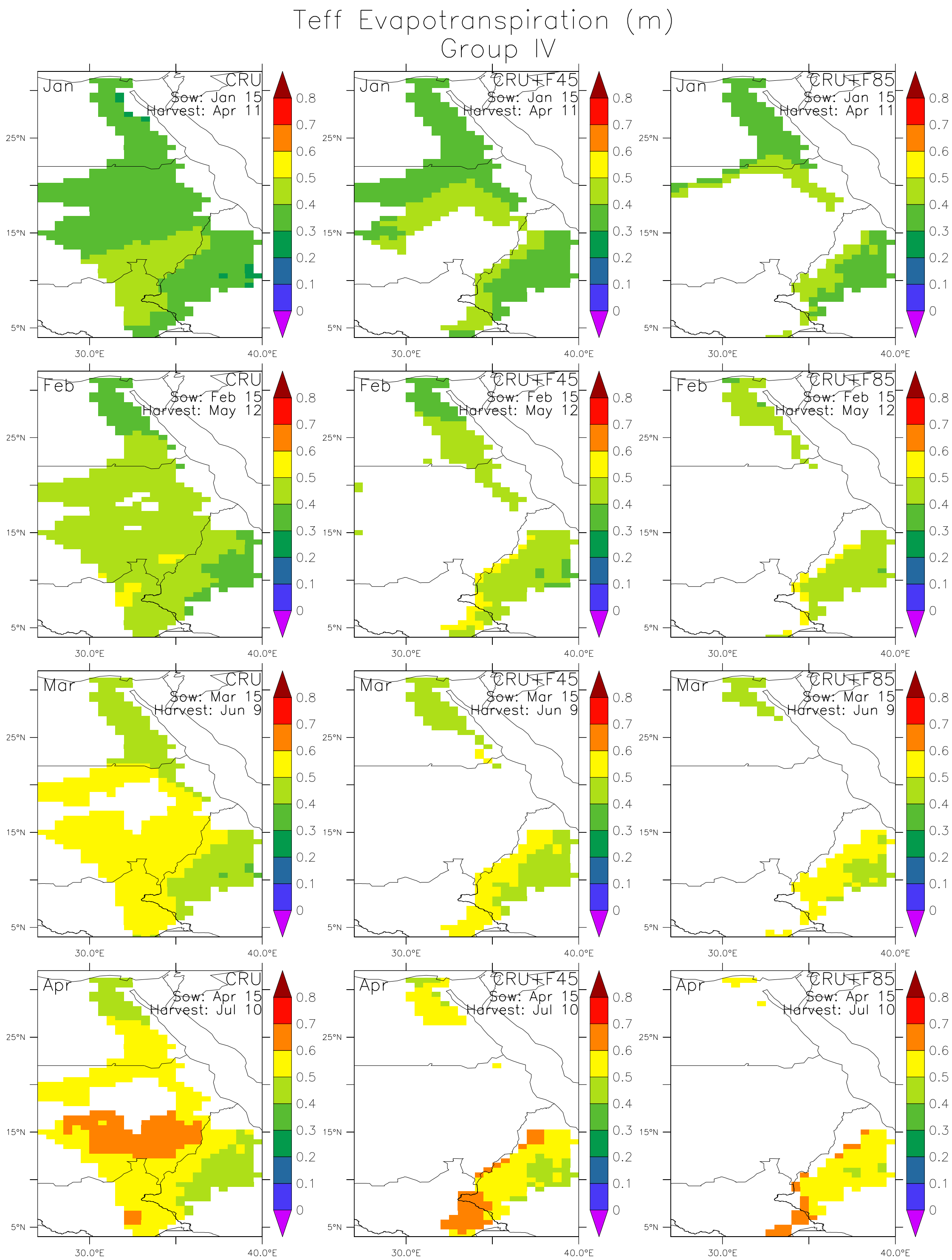
Teff Evapotranspiration (m)
Group IV
Jan
CRU
Sow: Jan 15
Harvest: Apr 11
CRU+F45
CRU+F85
Feb
Sow: Feb 15
Harvest: May 12
Mar
Sow: Mar 15
Harvest: Jun 9
Apr
Sow: Apr 15
Harvest: Jul 10
0.8
0.7
0.6
0.5
0.4
0.3
0.2
0.1
0
25°N
15°N
5°N
30.0°E
40.0°E

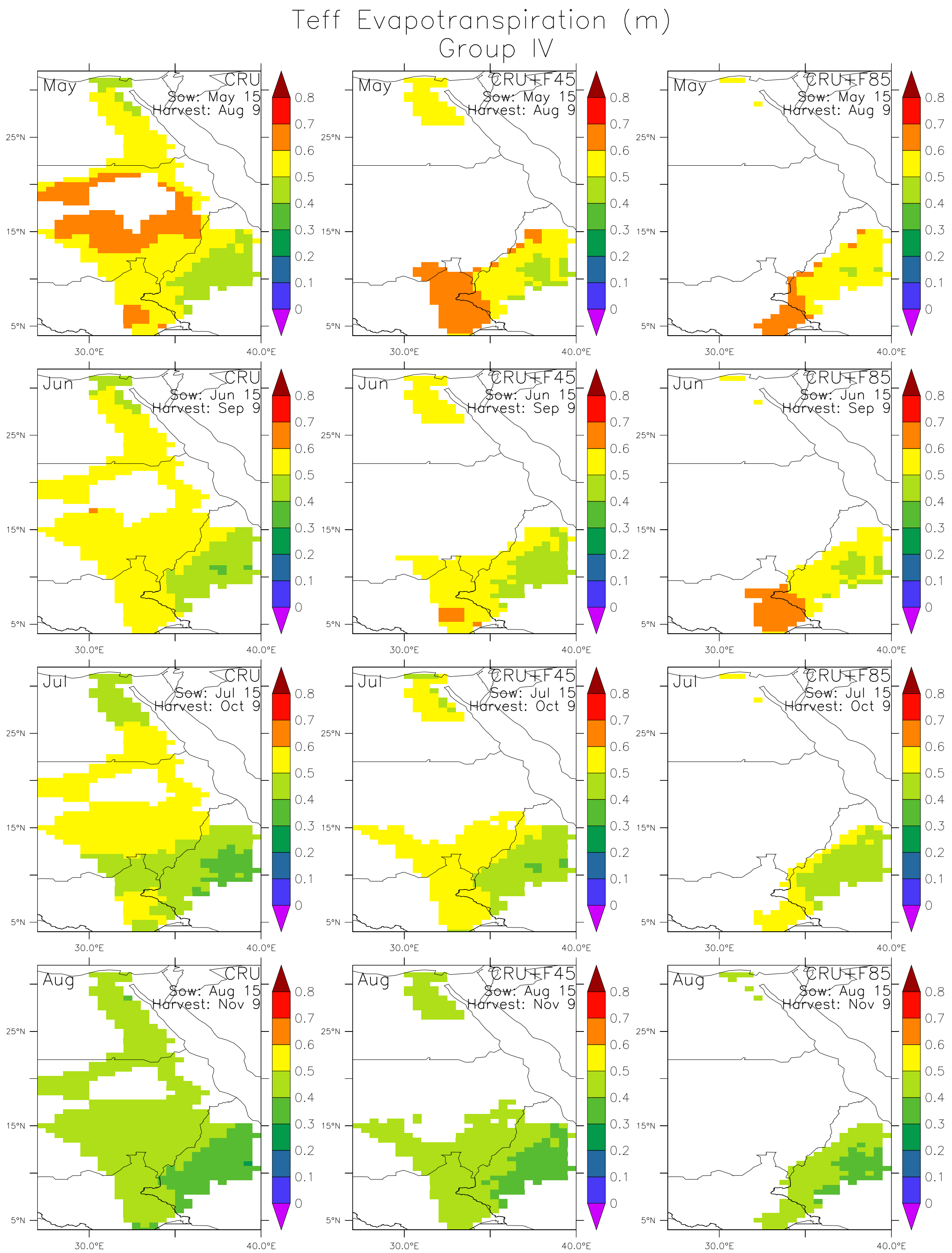
Teff Evapotranspiration (m)
Group IV
May
CRU
Sow: May 15
Harvest: Aug 9
CRU+F45
CRU+F85
Jun
Sow: Jun 15
Harvest: Sep 9
Jul
Sow: Jul 15
Harvest: Oct 9
Aug
Sow: Aug 15
Harvest: Nov 9
0.8
0.7
0.6
0.5
0.4
0.3
0.2
0.1
0
25°N
15°N
5°N
30.0°E
40.0°E

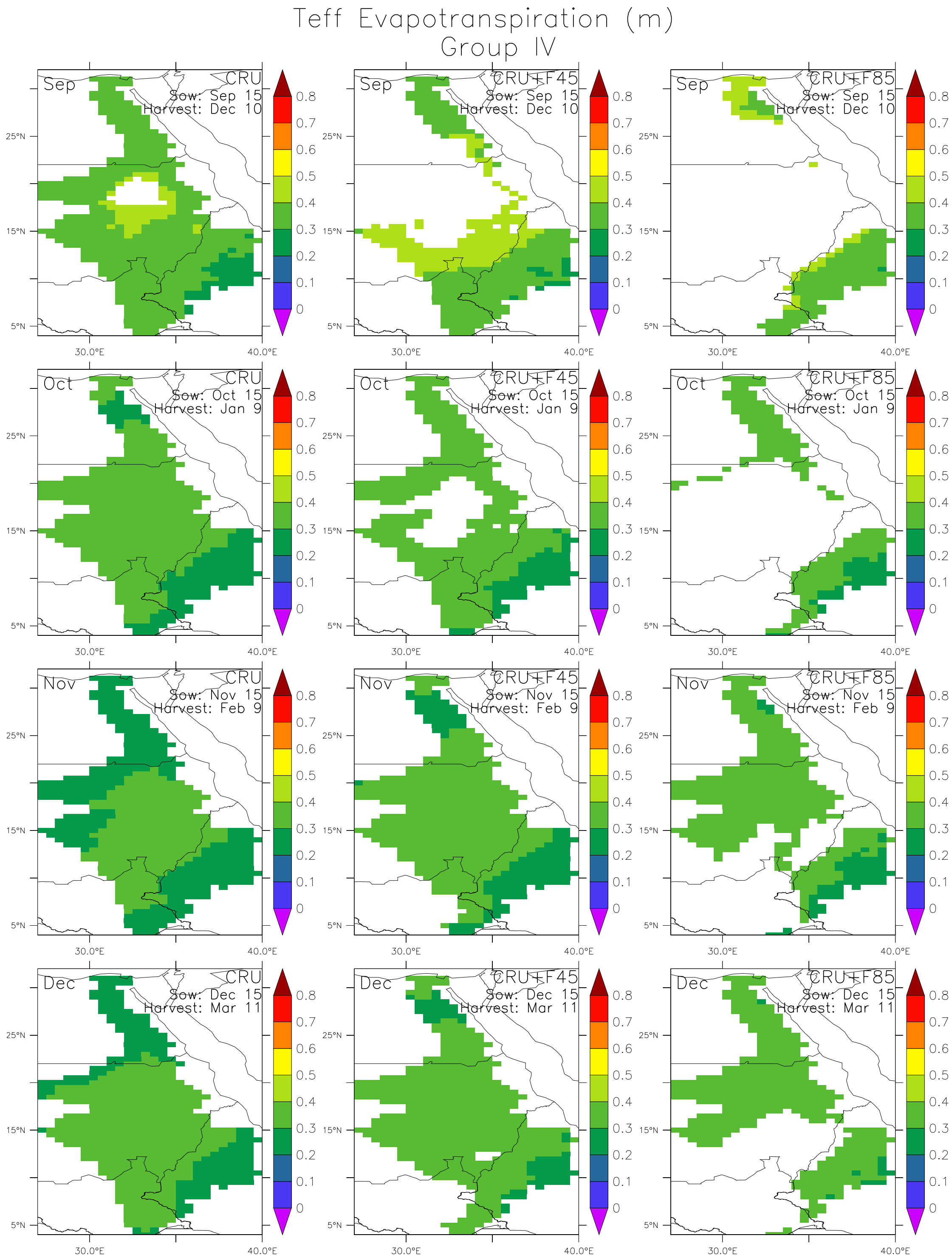

Figure 61: Teff evapotranspiration in m based on surface temperature. Left column: CRU; middle column: CRU+F45; and right column: CRU+F85. The values are masked for temperature suitability for Group IV operative conditions over the entire growing season. Each panel represents a different sow date starting January 15 with one-month shifts.

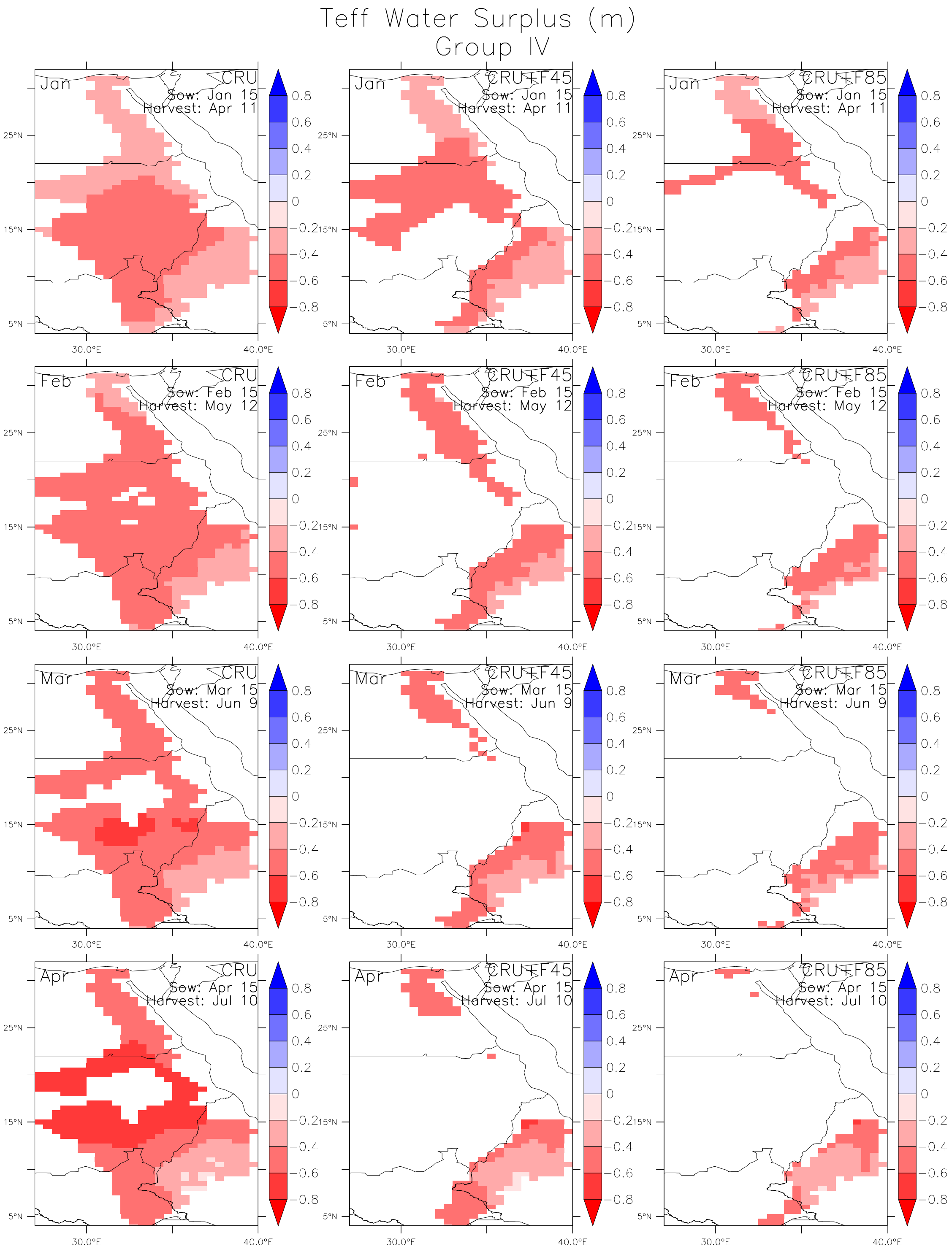
Teff Water Surplus (m)
Group IV
Jan
CRU
Sow: Jan 15
Harvest: Apr 11
CRU+F45
CRU+F85
Feb
Sow: Feb 15
Harvest: May 12
Mar
Sow: Mar 15
Harvest: Jun 9
Apr
Sow: Apr 15
Harvest: Jul 10
0.8
0.6
0.4
0.2
0
-0.2
-0.4
-0.6
-0.8
25°N
15°N
5°N
30.0°E
40.0°E

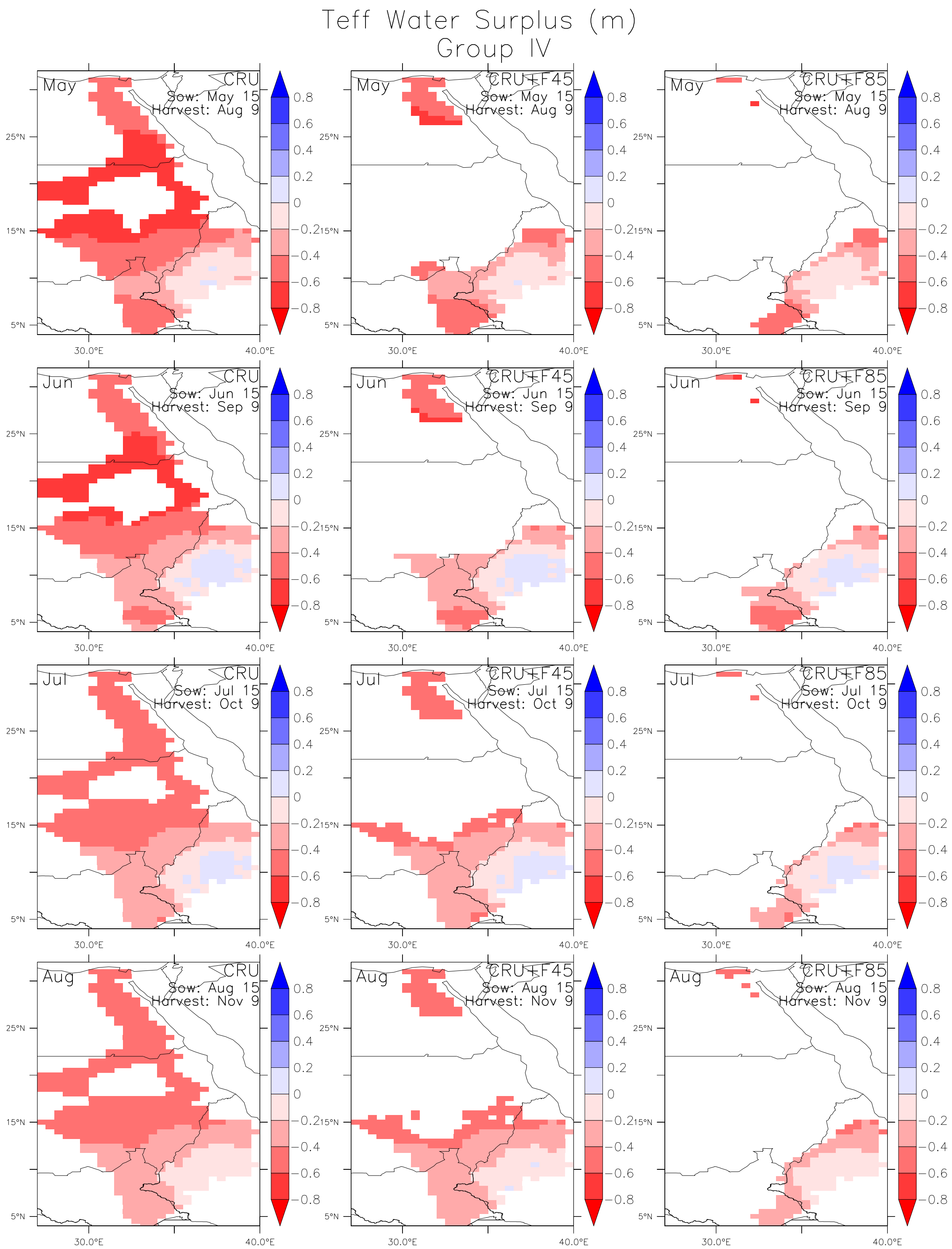
Teff Water Surplus (m)
Group IV
May
CRU
Sow: May 15
Harvest: Aug 9
CRU+F45
CRU+F85
Jun
Sow: Jun 15
Harvest: Sep 9
Jul
Sow: Jul 15
Harvest: Oct 9
Aug
Sow: Aug 15
Harvest: Nov 9
0.8
0.6
0.4
0.2
0
-0.2
-0.4
-0.6
-0.8
25°N
15°N
5°N
30.0°E
40.0°E

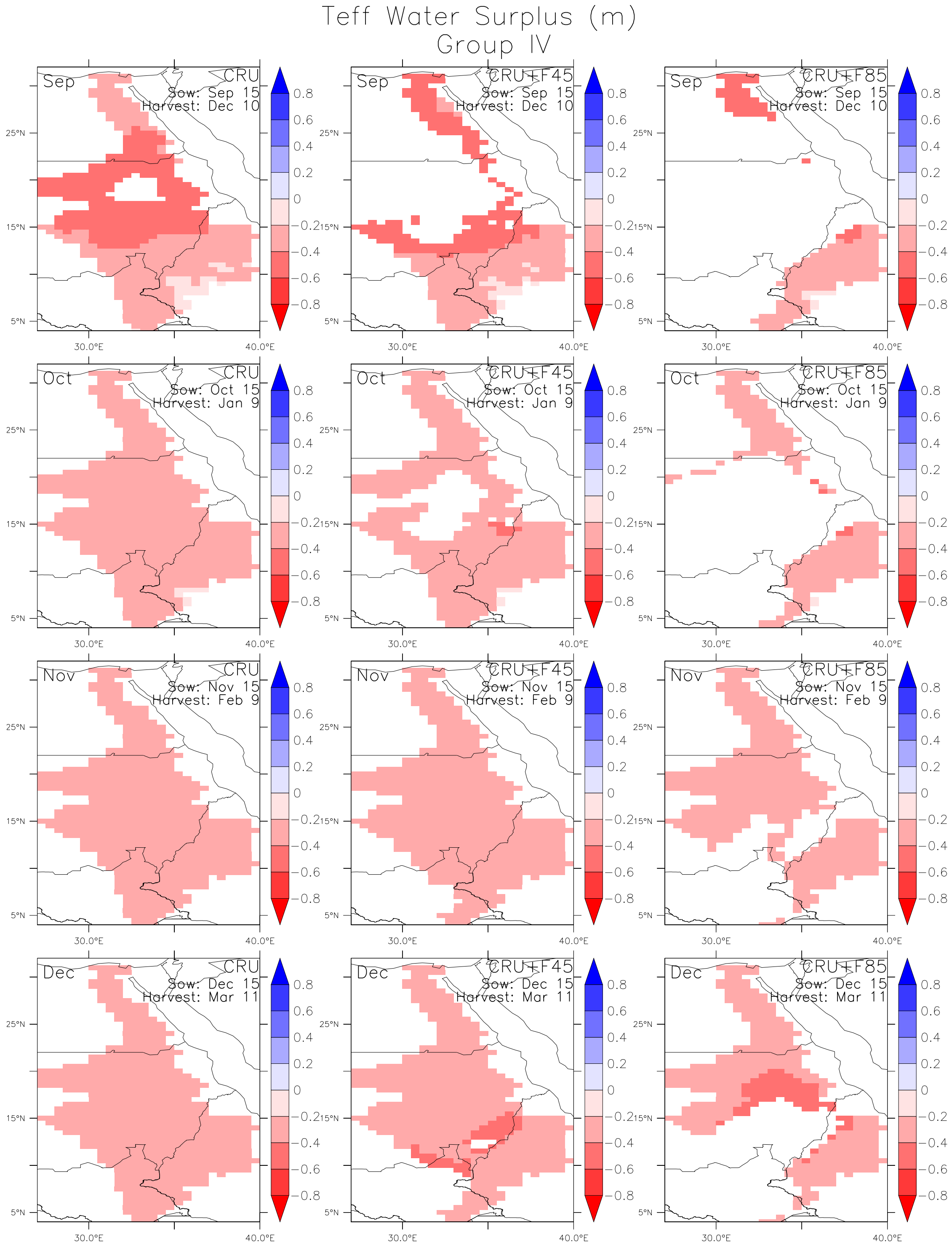

Figure 62: Teff water surplus in m based on surface temperature. Left column: CRU; middle column: CRU+F45; and right column: CRU+F85. The values are masked for temperature suitability for Group IV operative conditions over the entire growing season. Each panel represents a different sow date starting January 15 with one-month shifts. Blue shading indicates a surplus, while red shading indicates a deficit.

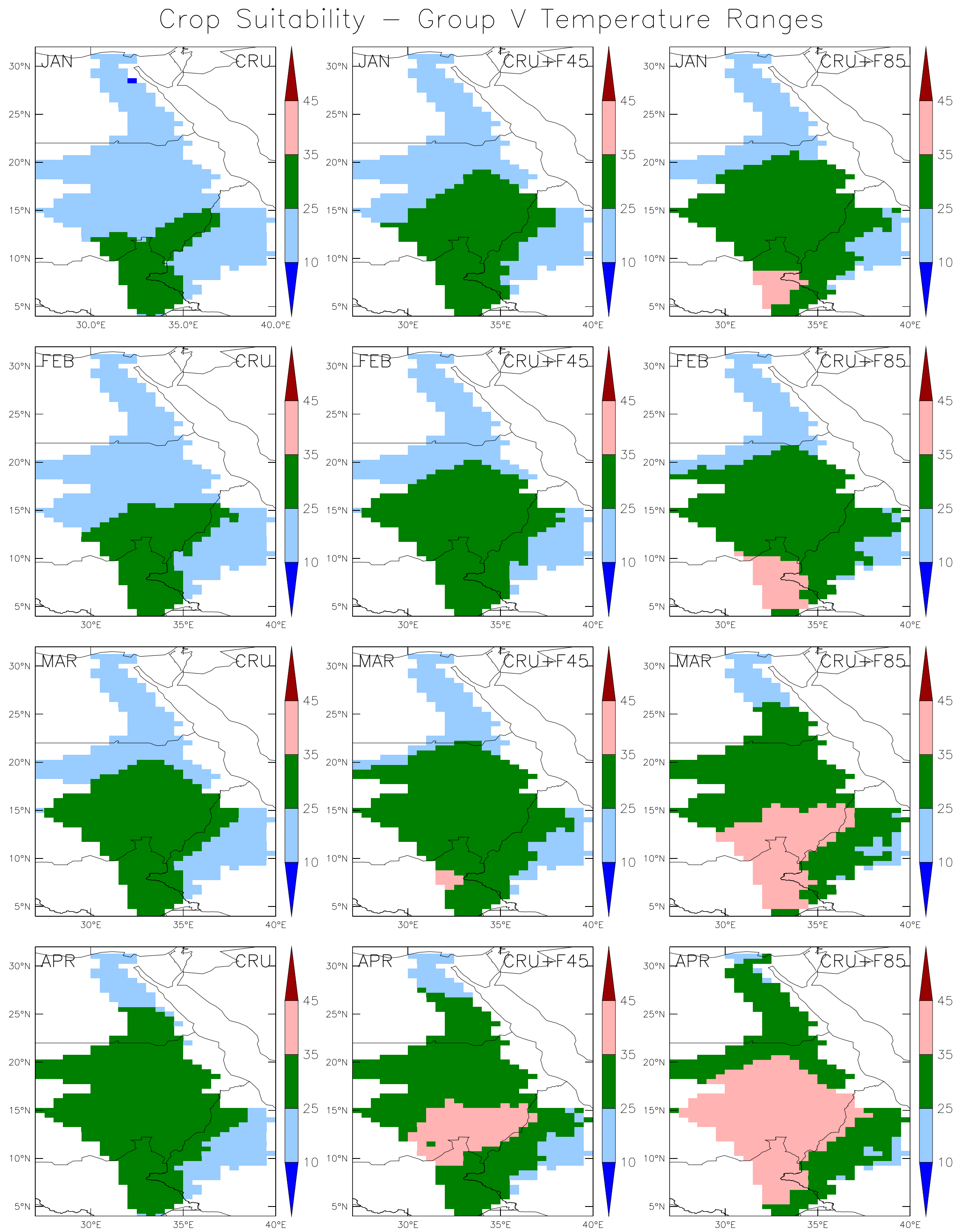
Crop Suitability – Group V Temperature Ranges
JAN
CRU
CRU+F45
CRU+F85
FEB
MAR
APR
45
35
25
10
30°N
25°N
20°N
15°N
10°N
5°N
30°E
35°E
40°E

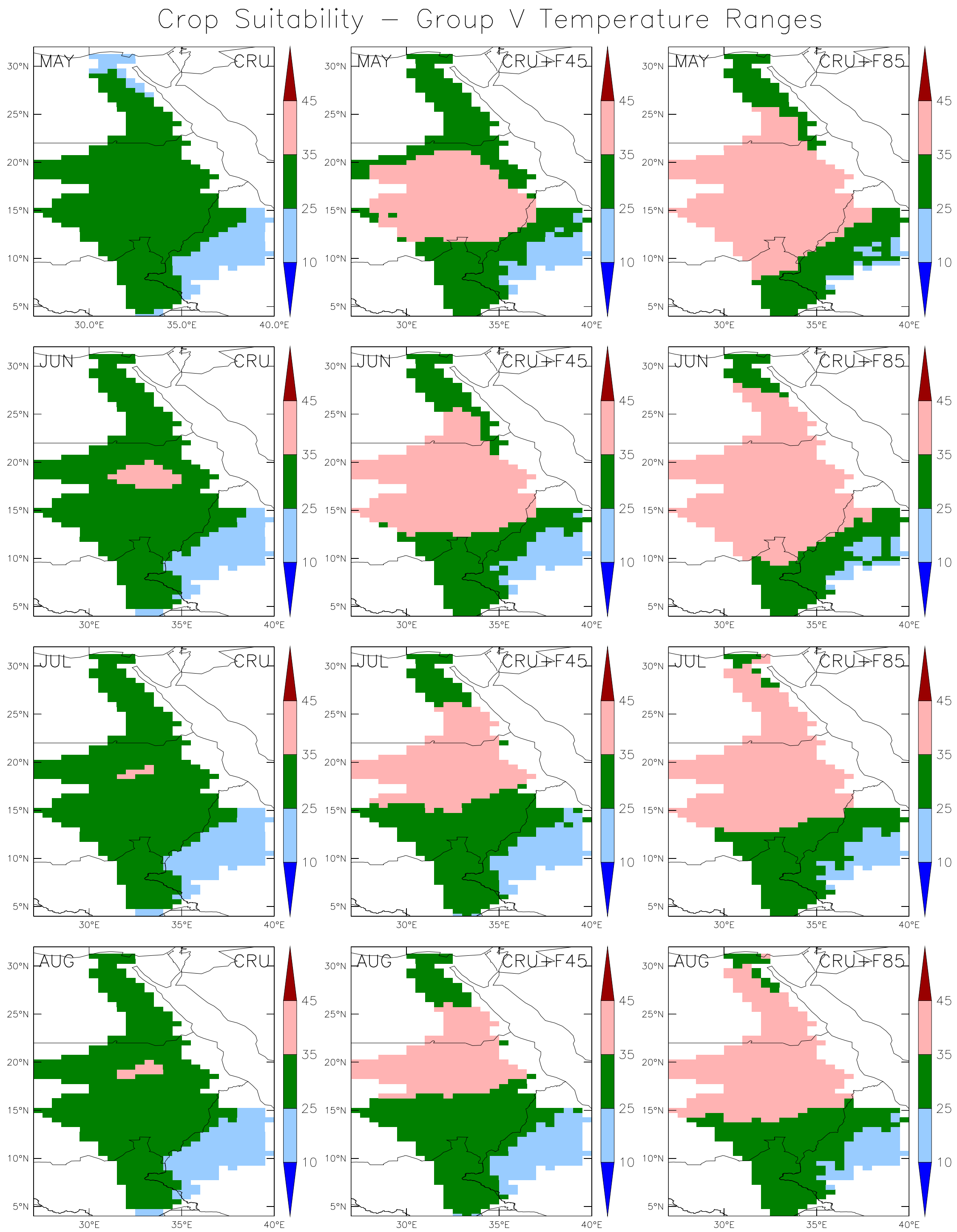
Crop Suitability – Group V Temperature Ranges
MAY
CRU
CRU+F45
CRU+F85
JUN
JUL
AUG
45
35
25
10
30°N
25°N
20°N
15°N
10°N
5°N
30.0°E
35.0°E
40.0°E
30°E
35°E
40°E

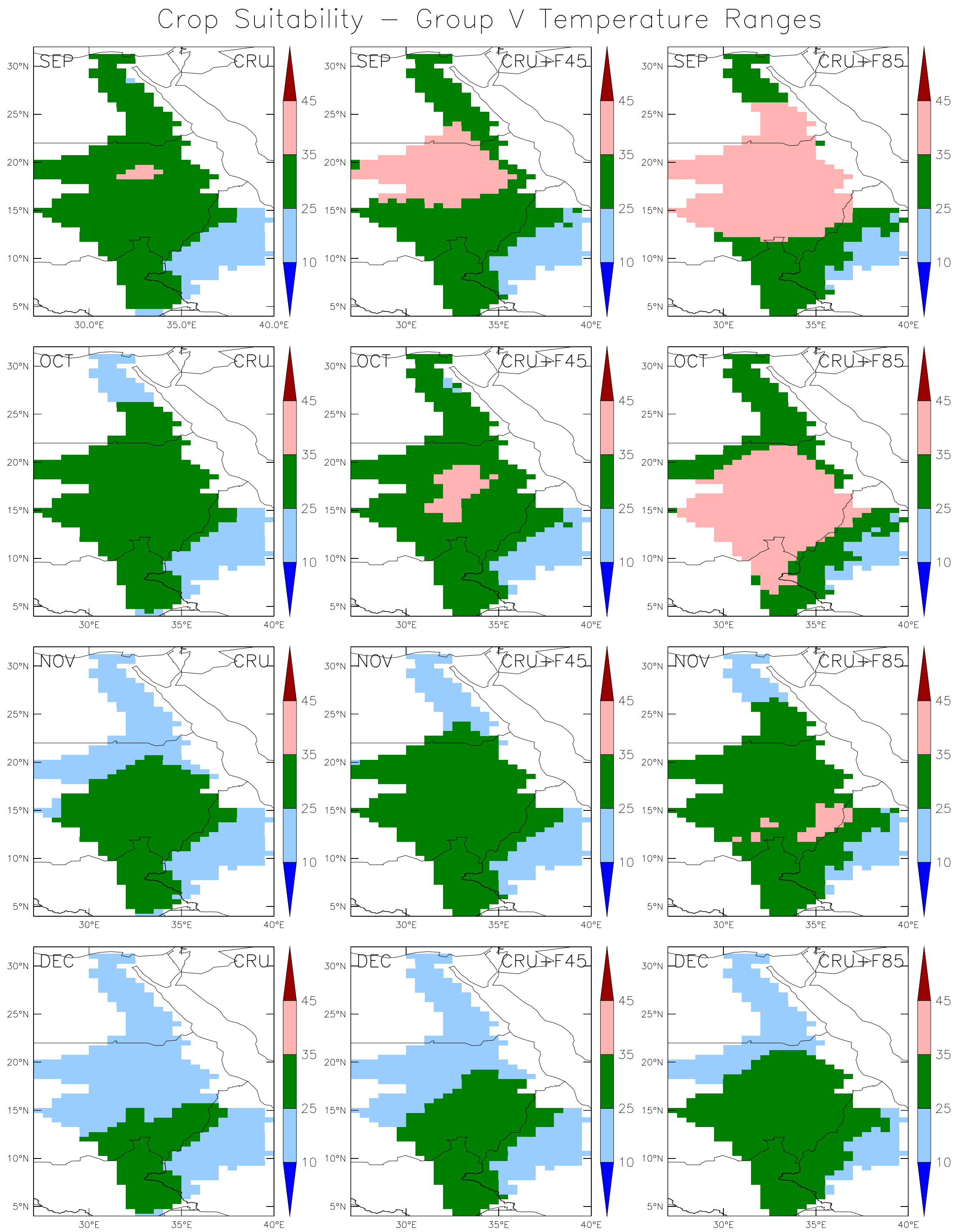

Figure 63: Monthly suitability for Group V crops based on surface temperature. Left column: CRU; middle column: CRU+F45; and right column: CRU+F85. Areas in green fall indicate temperatures for optimal growth; areas in light blue indicate temperatures below optimal but operative; areas in pink indicated temperatures above optimal but operative; and areas with in the basin that are white fall outside of the operative temperature range.

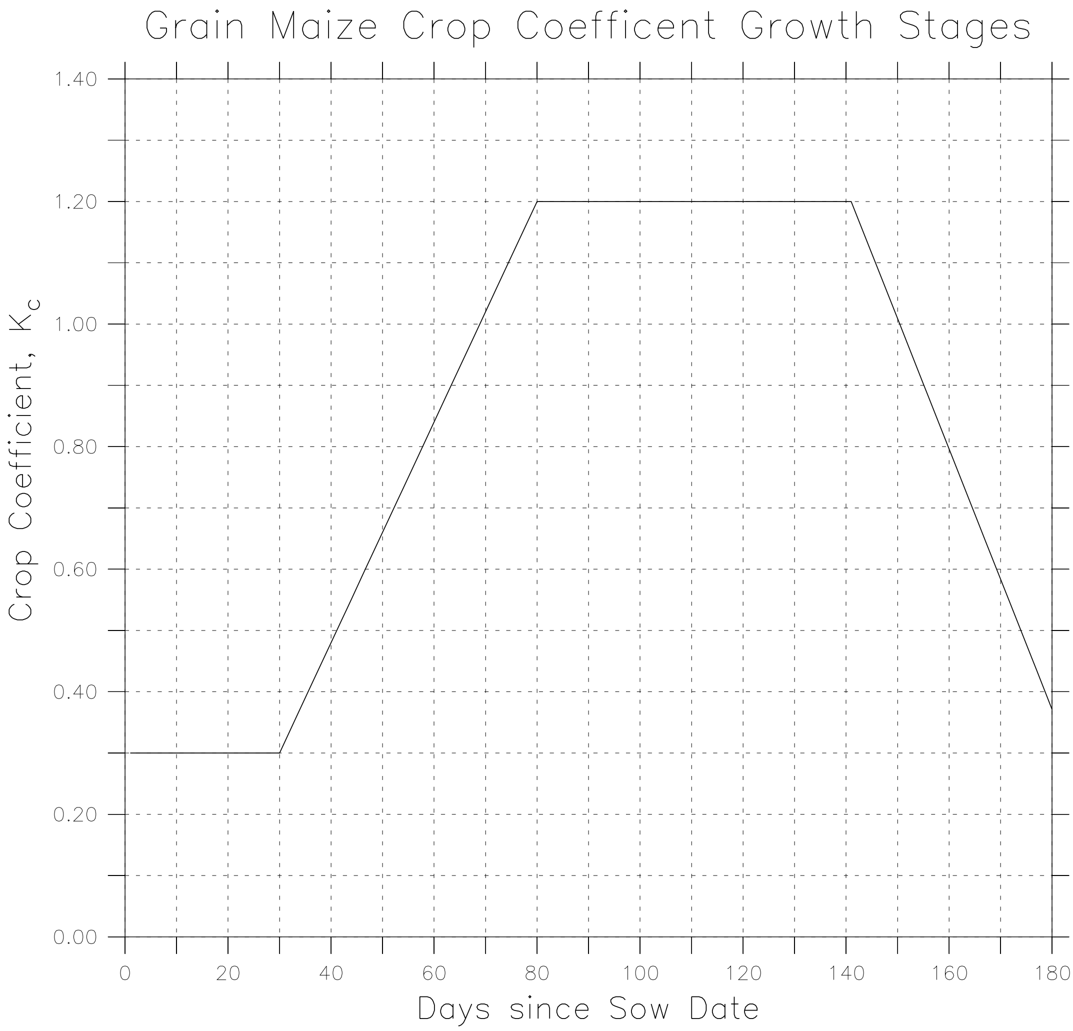

Figure 64: Grain maize crop coefficients and growth stages. Data adapted from on FAO (1998).

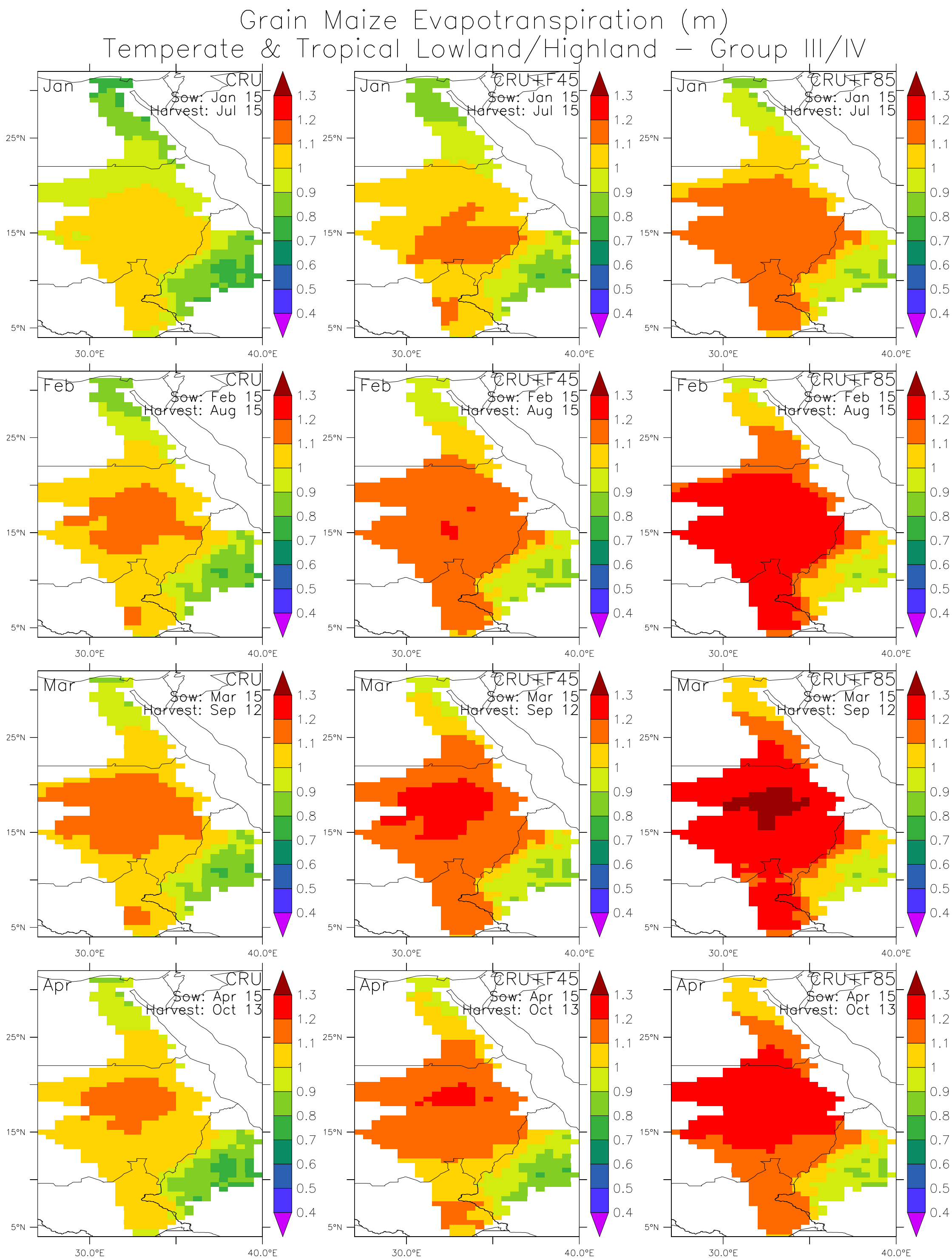
Grain Maize Evapotranspiration (m)
Temperate & Tropical Lowland/Highland – Group III/IV
Jan
CRU
Sow: Jan 15
Harvest: Jul 15
CRU+F45
CRU+F85
Feb
Sow: Feb 15
Harvest: Aug 15
Mar
Sow: Mar 15
Harvest: Sep 12
Apr
Sow: Apr 15
Harvest: Oct 13
1.3
1.2
1.1
1
0.9
0.8
0.7
0.6
0.5
0.4
25°N
15°N
5°N
30.0°E
40.0°E

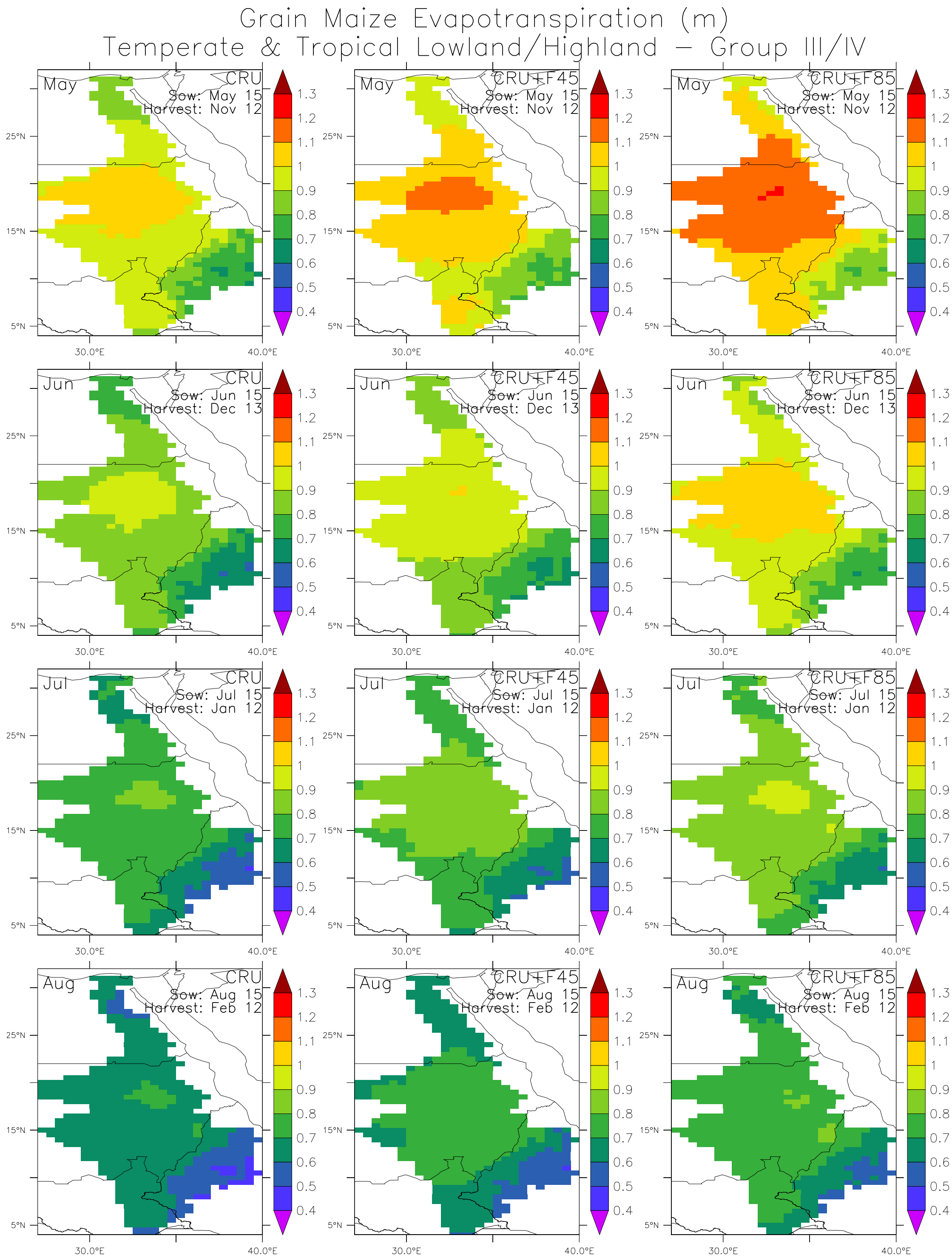

Grain Maize Evapotranspiration (m)
Temperate & Tropical Lowland/Highland – Group III/IV
May
CRU
Sow: May 15
Harvest: Nov 12
CRU+F45
CRU+F85
Jun
Sow: Jun 15
Harvest: Dec 13
Jul
Sow: Jul 15
Harvest: Jan 12
Aug
Sow: Aug 15
Harvest: Feb 12
1.3
1.2
1.1
1
0.9
0.8
0.7
0.6
0.5
0.4
25°N
15°N
5°N
30.0°E
40.0°E

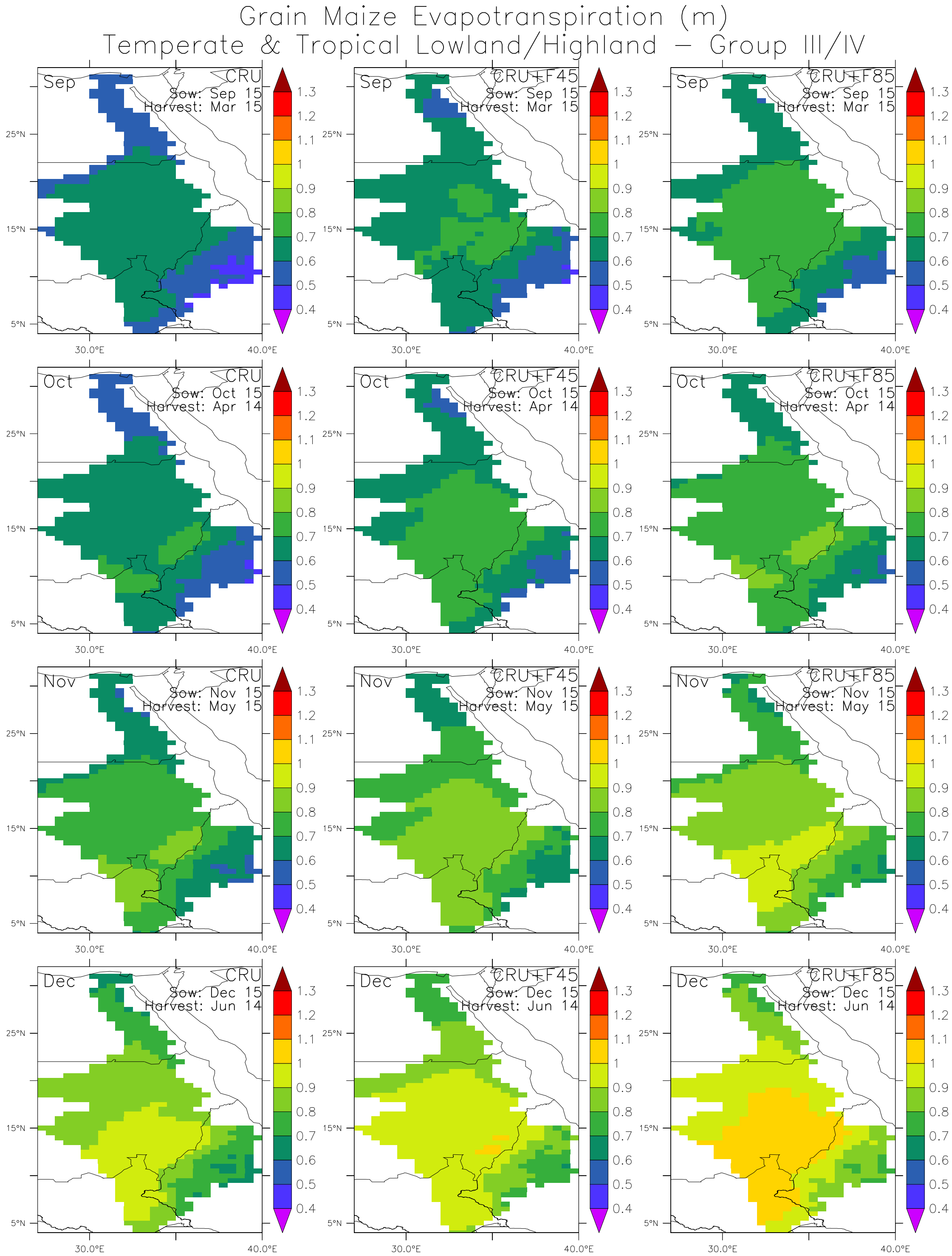

Figure 65: Temperate and tropical lowland/highland grain maize evapotranspiration in m based on surface temperature. Left column: CRU; middle column: CRU+F45; and right column: CRU+F85. The values are masked for temperature suitability for Group III/IV operative conditions over the entire growing season. Each panel represents a different sow date starting January 15 with one-month shifts.

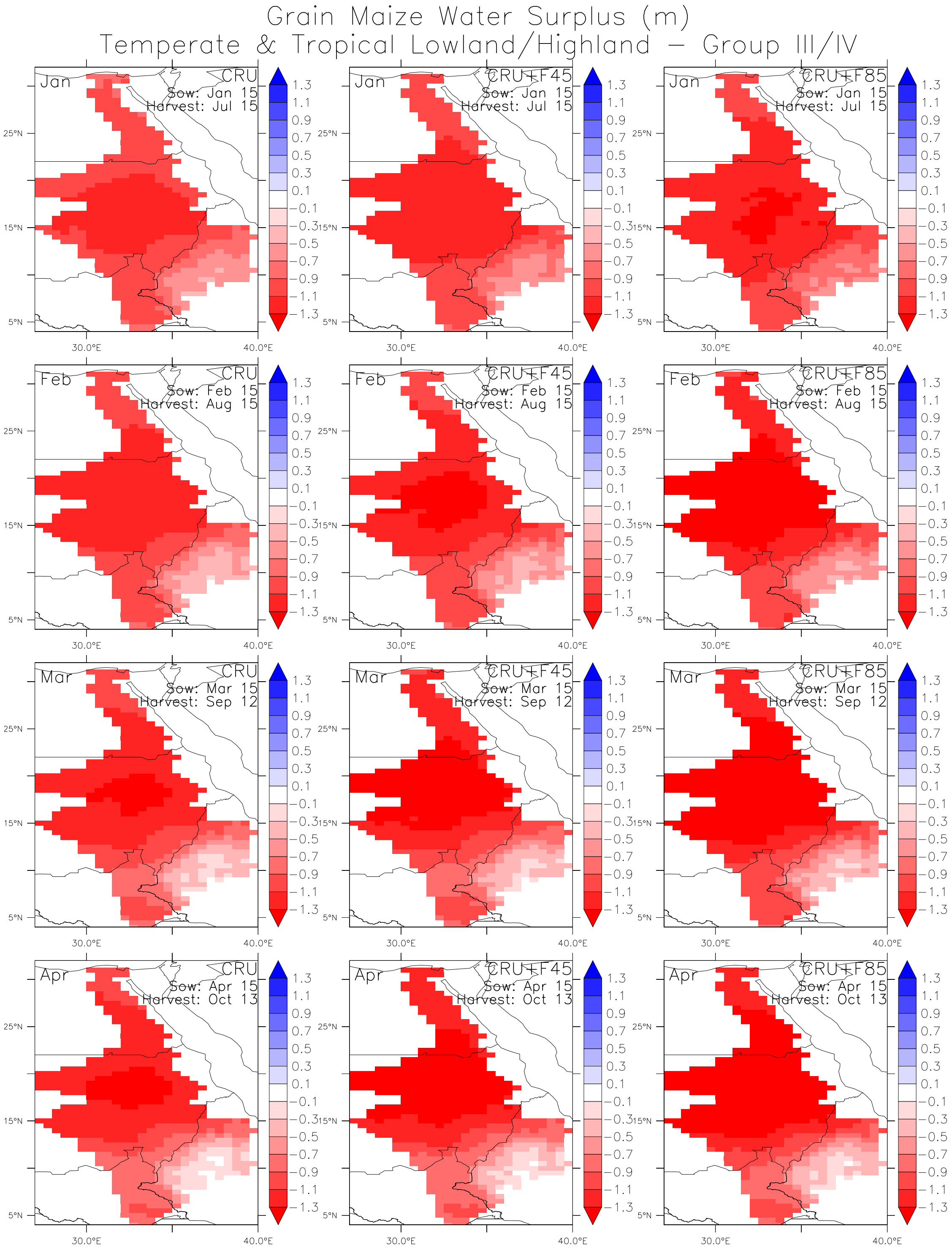
Grain Maize Water Surplus (m)
Temperate & Tropical Lowland/Highland – Group III/IV
Jan
CRU
Sow: Jan 15
Harvest: Jul 15
CRU+F45
CRU+F85
Feb
Sow: Feb 15
Harvest: Aug 15
Mar
Sow: Mar 15
Harvest: Sep 12
Apr
Sow: Apr 15
Harvest: Oct 13
1.3
1.1
0.9
0.7
0.5
0.3
0.1
-0.1
-0.3
-0.5
-0.7
-0.9
-1.1
-1.3
25°N
15°N
5°N
30.0°E
40.0°E

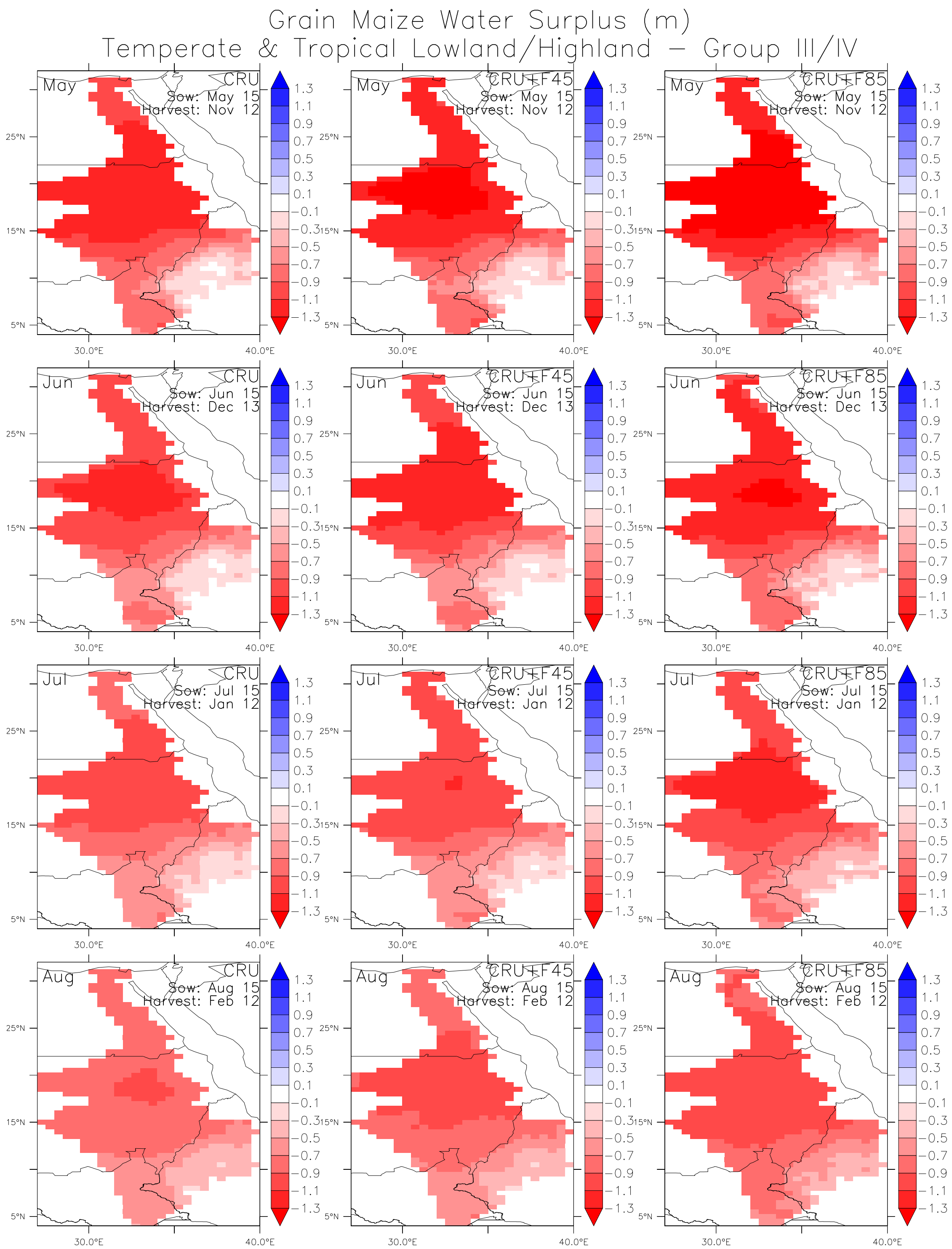
Grain Maize Water Surplus (m)
Temperate & Tropical Lowland/Highland – Group III/IV
May
CRU
Sow: May 15
Harvest: Nov 12
CRU+F45
CRU+F85
Jun
Sow: Jun 15
Harvest: Dec 13
Jul
Sow: Jul 15
Harvest: Jan 12
Aug
Sow: Aug 15
Harvest: Feb 12
25°N
15°N
5°N
30.0°E
40.0°E
1.3
1.1
0.9
0.7
0.5
0.3
0.1
-0.1
-0.3
-0.5
-0.7
-0.9
-1.1
-1.3

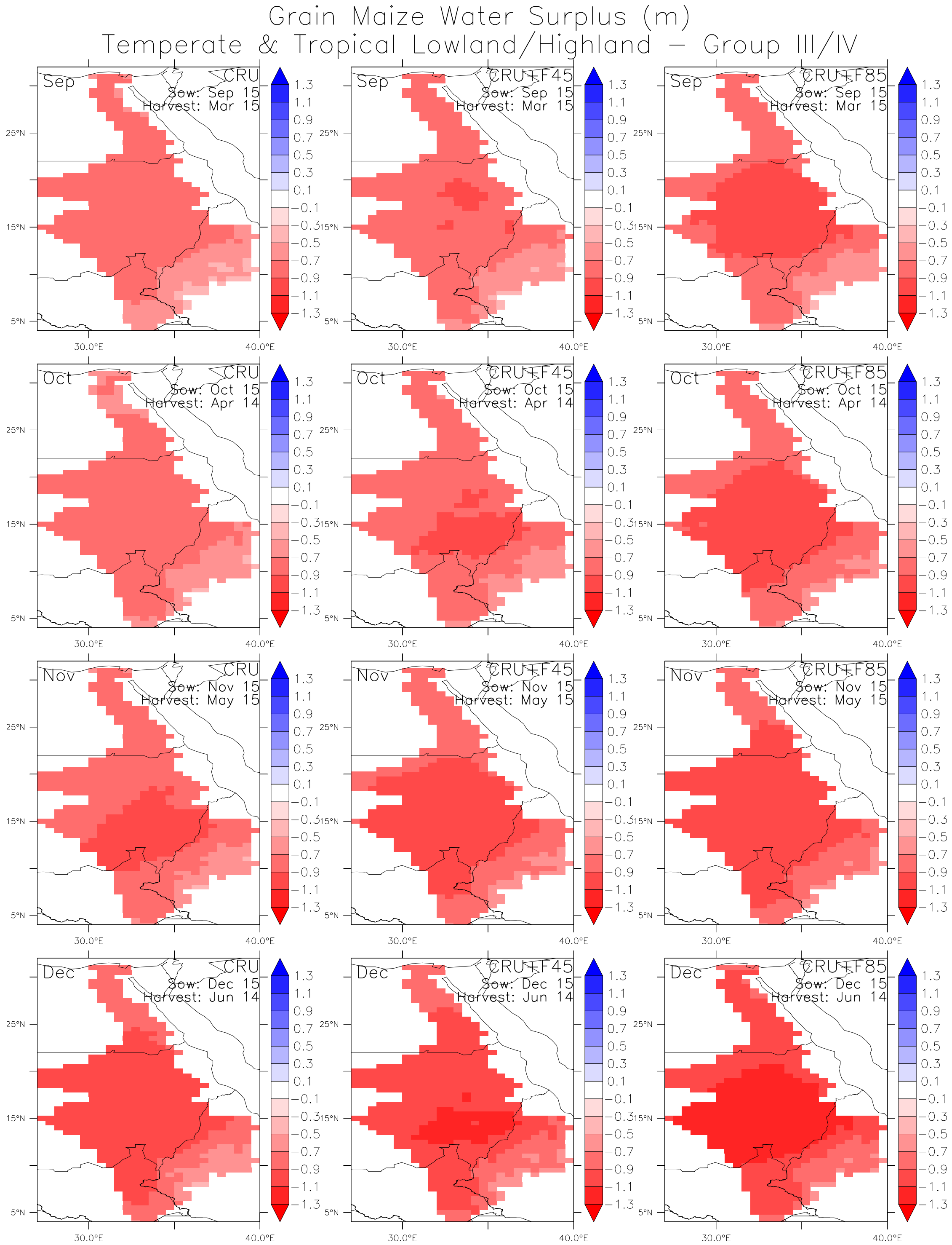

Figure 66: Temperate and tropical lowland/highland grain maize water surplus in m based on surface temperature. Left column: CRU; middle column: CRU+F45; and right column: CRU+F85. The values are masked for temperature suitability for Group III/IV operative conditions over the entire growing season. Each panel represents a different sow date starting January 15 with one-month shifts. Blue shading indicates a surplus, while red shading indicates a deficit.

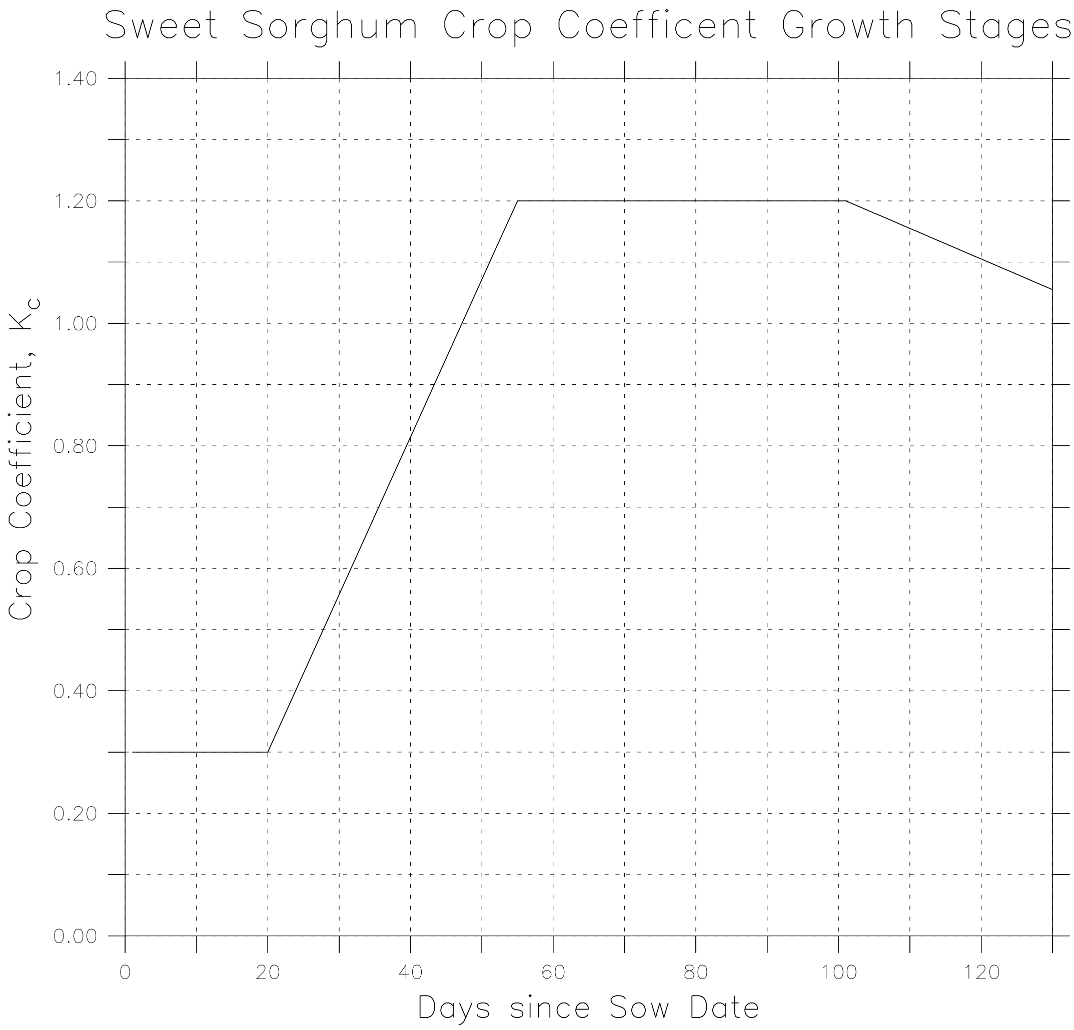

Figure 67: Sweet sorghum crop coefficients and growth stages. Data adapted from on FAO (1998).

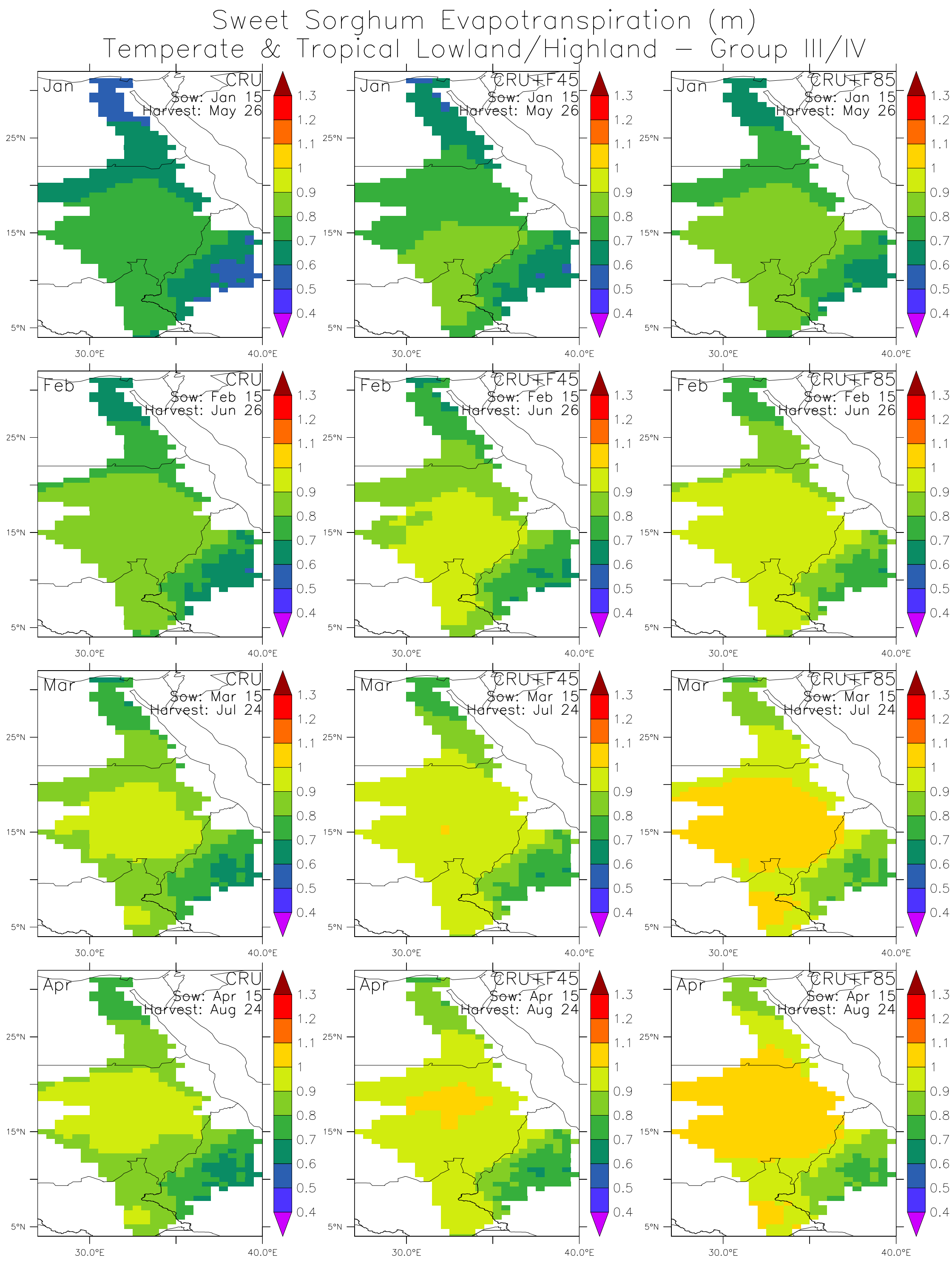
Sweet Sorghum Evapotranspiration (m)
Temperate & Tropical Lowland/Highland – Group III/IV
Jan
CRU
Sow: Jan 15
Harvest: May 26
CRU+F45
CRU+F85
Feb
Sow: Feb 15
Harvest: Jun 26
Mar
Sow: Mar 15
Harvest: Jul 24
Apr
Sow: Apr 15
Harvest: Aug 24
1.3
1.2
1.1
1
0.9
0.8
0.7
0.6
0.5
0.4
25°N
15°N
5°N
30.0°E
40.0°E

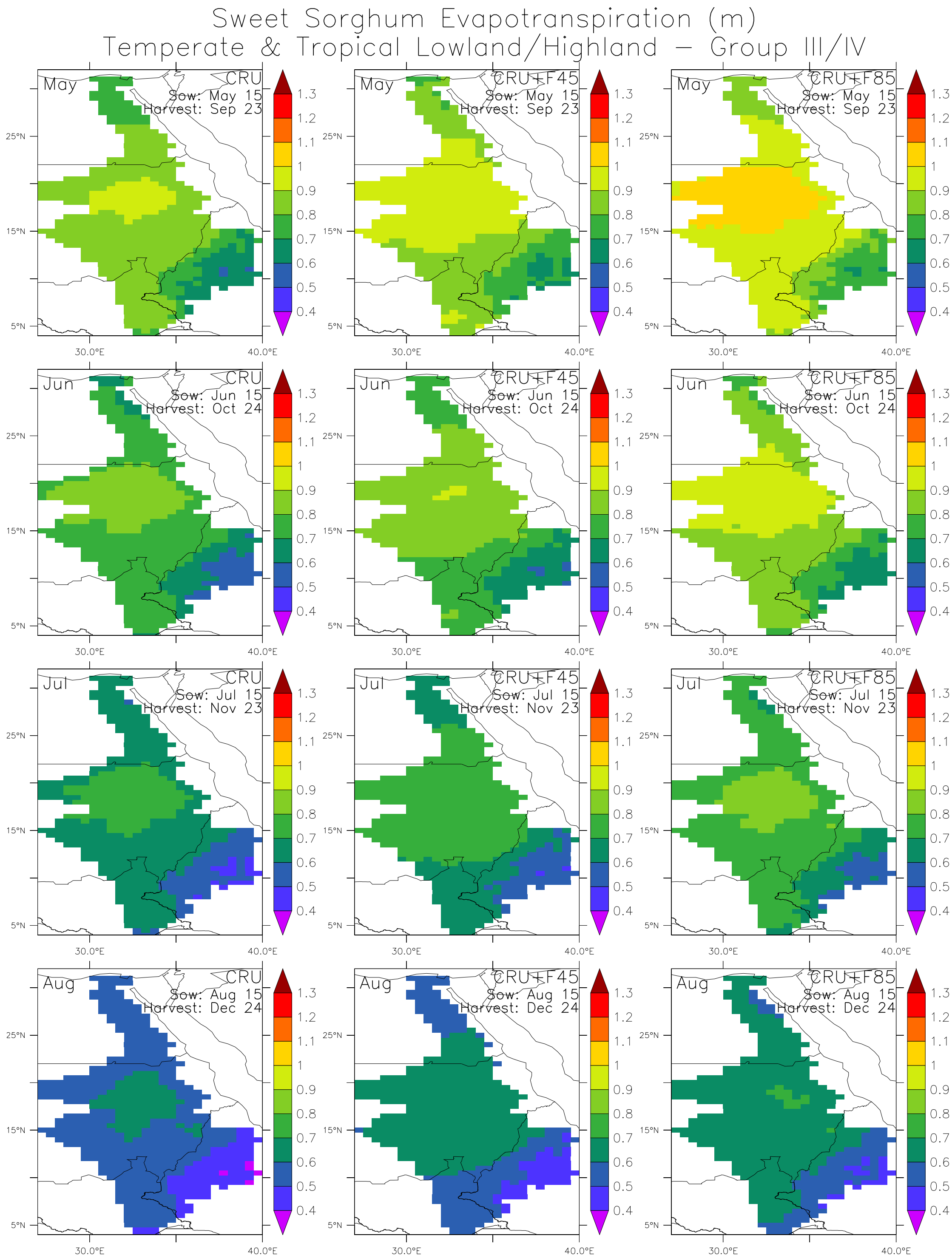
Sweet Sorghum Evapotranspiration (m)
Temperate & Tropical Lowland/Highland – Group III/IV
May
CRU
Sow: May 15
Harvest: Sep 23
CRU+F45
CRU+F85
Jun
Sow: Jun 15
Harvest: Oct 24
Jul
Sow: Jul 15
Harvest: Nov 23
Aug
Sow: Aug 15
Harvest: Dec 24
1.3
1.2
1.1
1
0.9
0.8
0.7
0.6
0.5
0.4
25°N
15°N
5°N
30.0°E
40.0°E

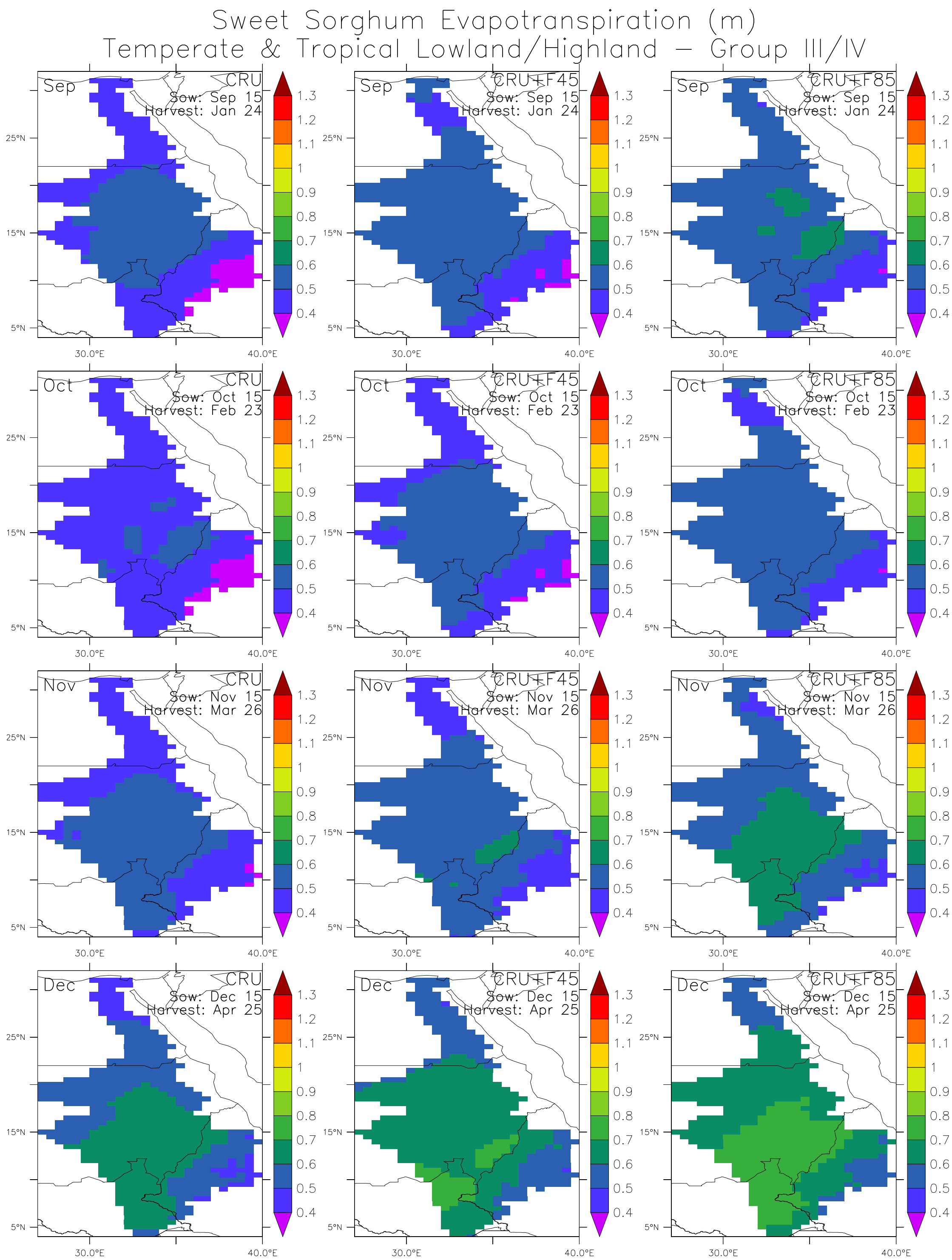

Figure 68: Temperate and tropical lowland/highland sweet sorghum evapotranspiration in m based on surface temperature. Left column: CRU; middle column: CRU+F45; and right column: CRU+F85. The values are masked for temperature suitability for Group III/IV operative conditions over the entire growing season. Each panel represents a different sow date starting January 15 with one-month shifts.

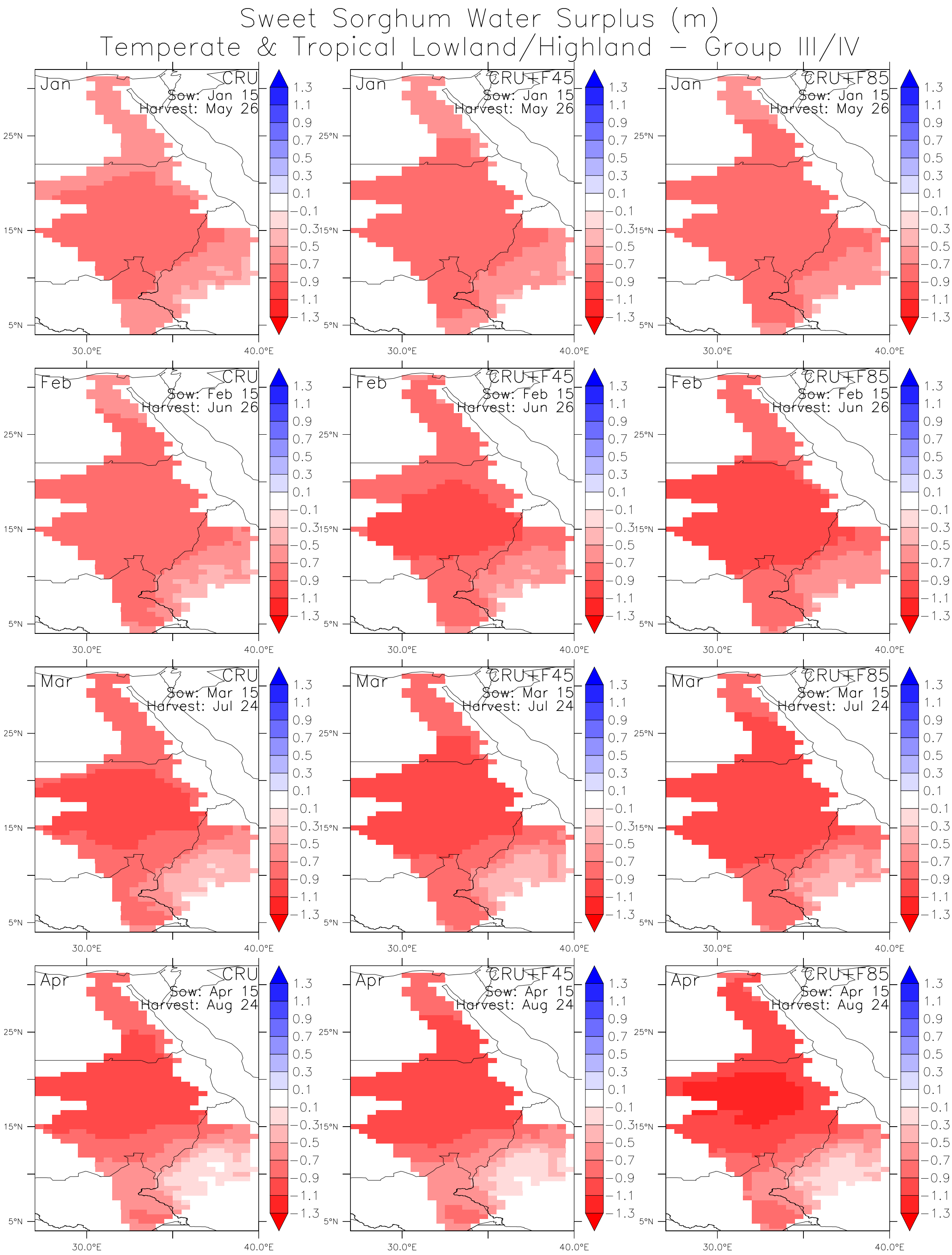
Sweet Sorghum Water Surplus (m)
Temperate & Tropical Lowland/Highland – Group III/IV
Jan
CRU
CRU+F45
CRU+F85
Sow: Jan 15
Harvest: May 26
Feb
Sow: Feb 15
Harvest: Jun 26
Mar
Sow: Mar 15
Harvest: Jul 24
Apr
Sow: Apr 15
Harvest: Aug 24
1.3
1.1
0.9
0.7
0.5
0.3
0.1
-0.1
-0.3
-0.5
-0.7
-0.9
-1.1
-1.3
25°N
15°N
5°N
30.0°E
40.0°E

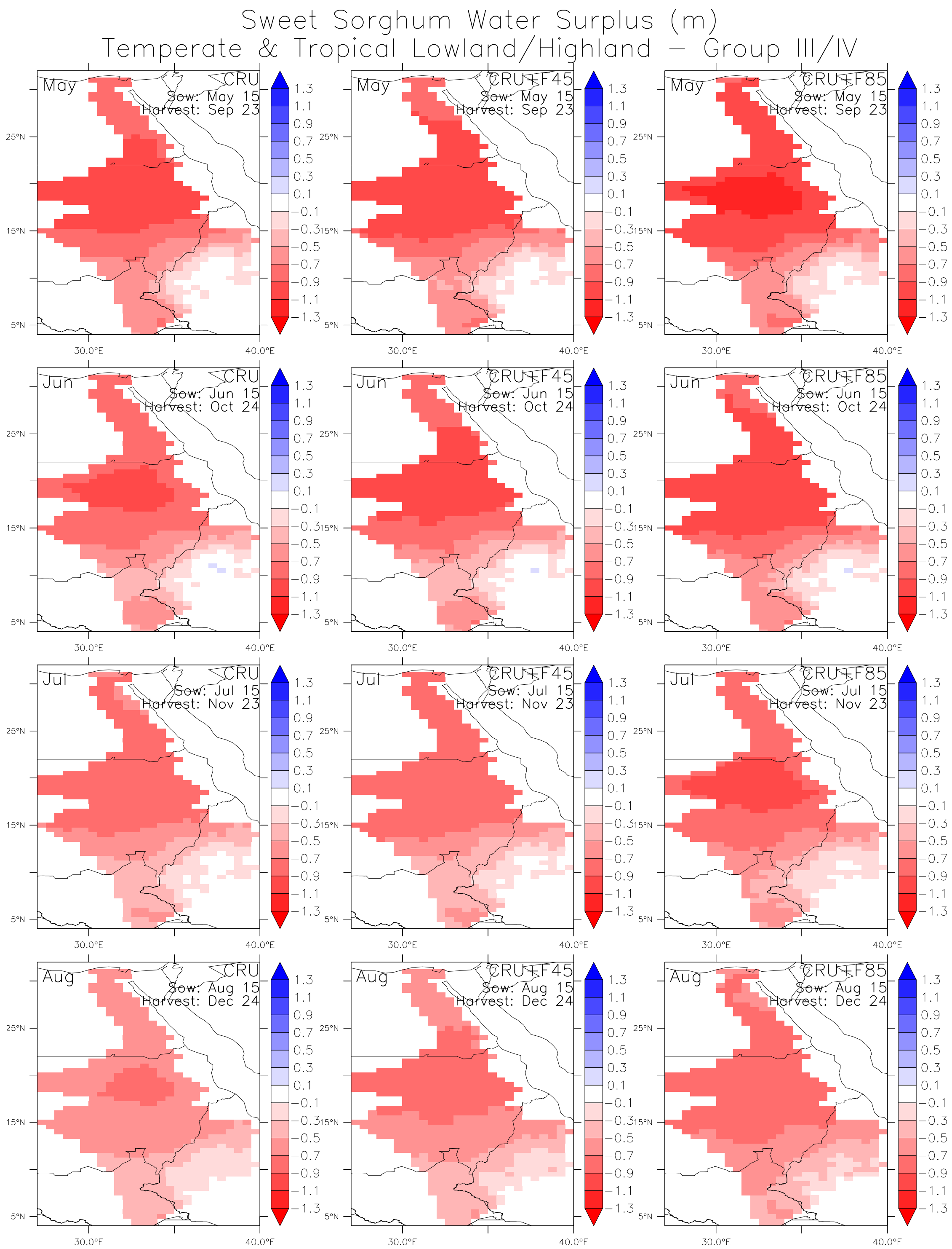
Sweet Sorghum Water Surplus (m)
Temperate & Tropical Lowland/Highland – Group III/IV
May
CRU
Sow: May 15
Harvest: Sep 23
CRU+F45
CRU+F85
Jun
Sow: Jun 15
Harvest: Oct 24
Jul
Sow: Jul 15
Harvest: Nov 23
Aug
Sow: Aug 15
Harvest: Dec 24
1.3
1.1
0.9
0.7
0.5
0.3
0.1
−0.1
−0.3
−0.5
−0.7
−0.9
−1.1
−1.3
25°N
15°N
5°N
30.0°E
40.0°E

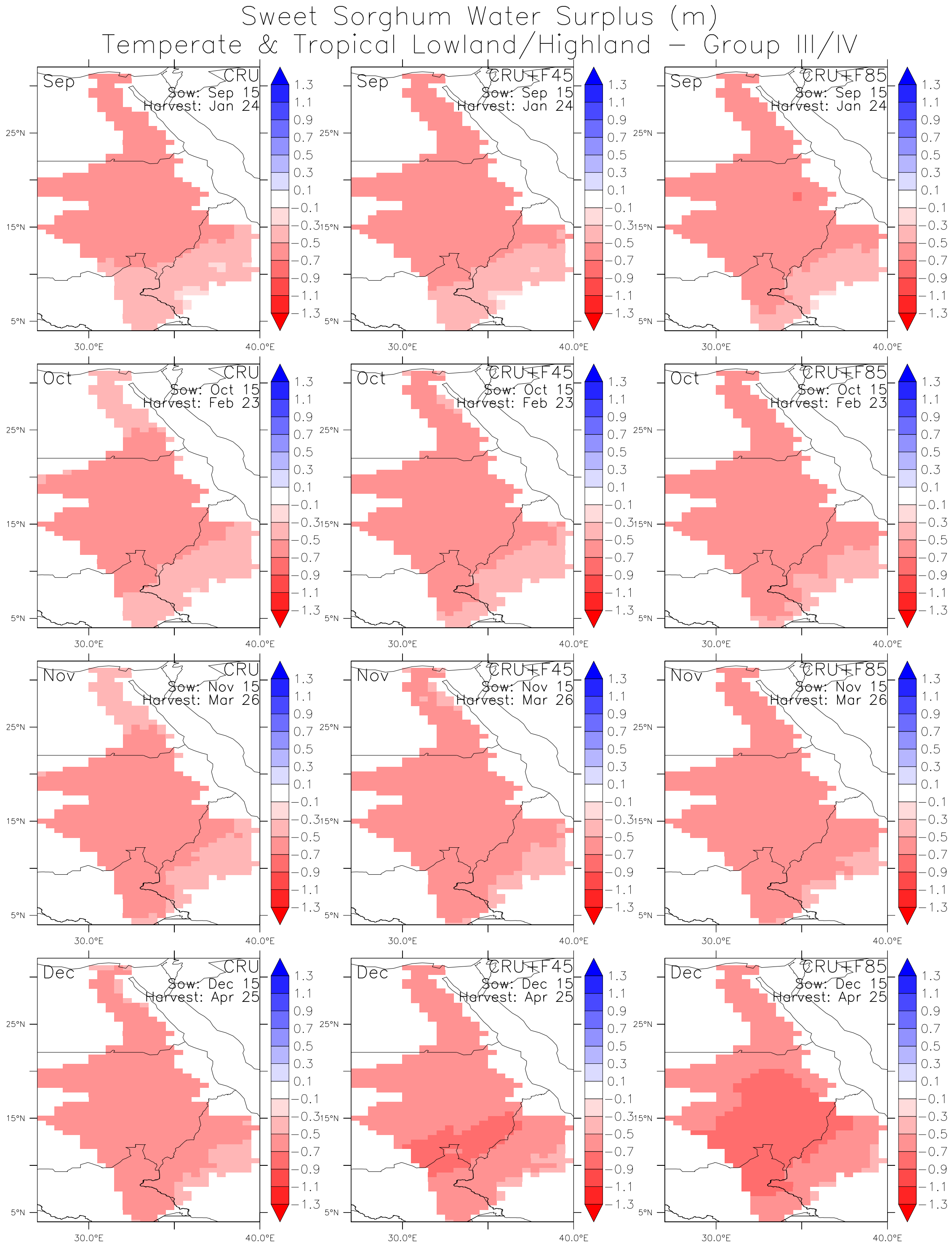

Figure 69: Temperate and tropical lowland/highland sweet sorghum water surplus in m based on surface temperature. Left column: CRU; middle column: CRU+F45; and right column: CRU+F85. The values are masked for temperature suitability for Group III/IV operative conditions over the entire growing season. Each panel represents a different sow date starting January 15 with one-month shifts. Blue shading indicates a surplus, while red shading indicates a deficit.

Figure 70: Millet crop coefficients and growth stages. Data adapted from on FAO (1998).

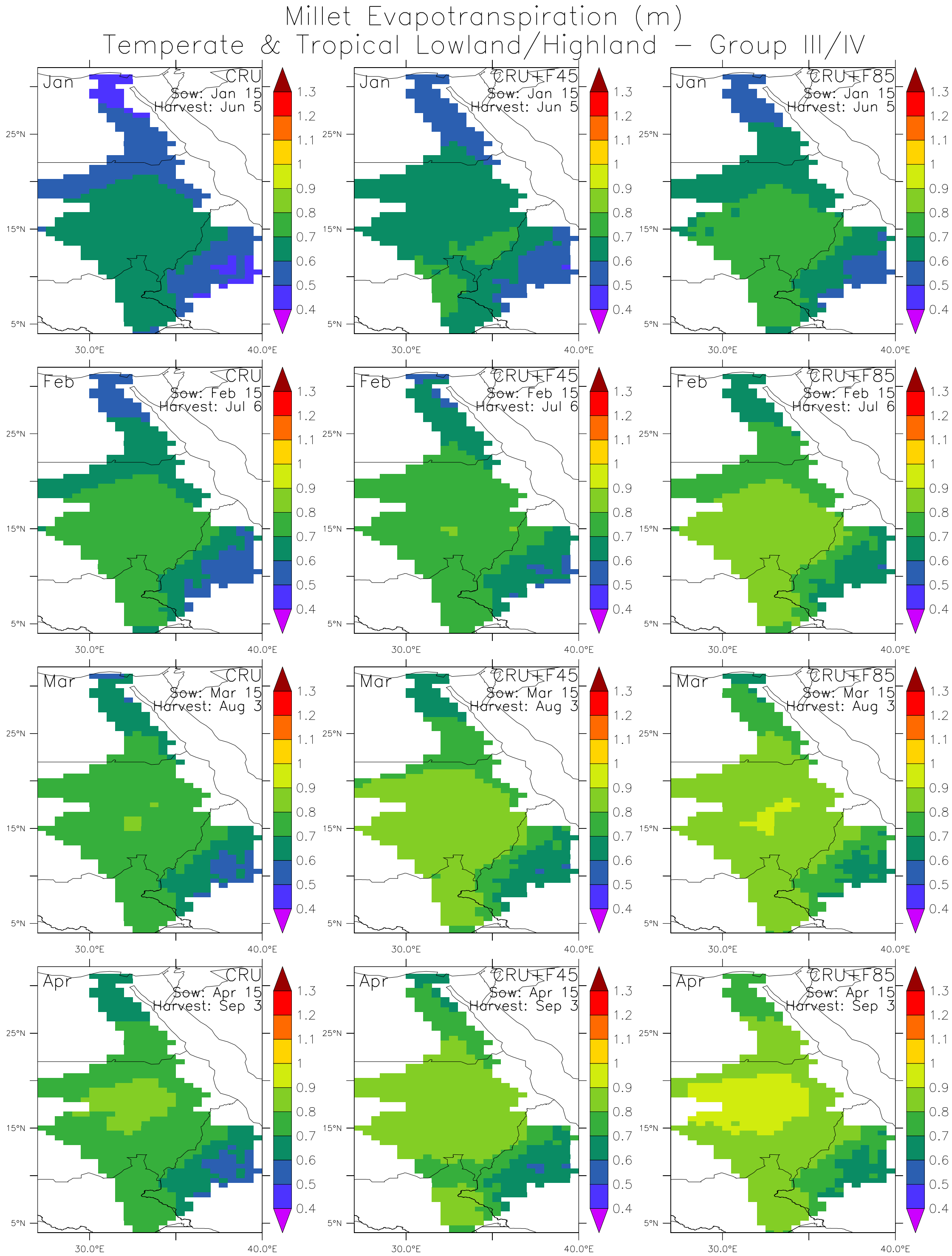
Millet Evapotranspiration (m)
Temperate & Tropical Lowland/Highland – Group III/IV
Jan
CRU
Sow: Jan 15
Harvest: Jun 5
CRU+F45
CRU+F85
Feb
Sow: Feb 15
Harvest: Jul 6
Mar
Sow: Mar 15
Harvest: Aug 3
Apr
Sow: Apr 15
Harvest: Sep 3
1.3
1.2
1.1
1
0.9
0.8
0.7
0.6
0.5
0.4
25°N
15°N
5°N
30.0°E
40.0°E

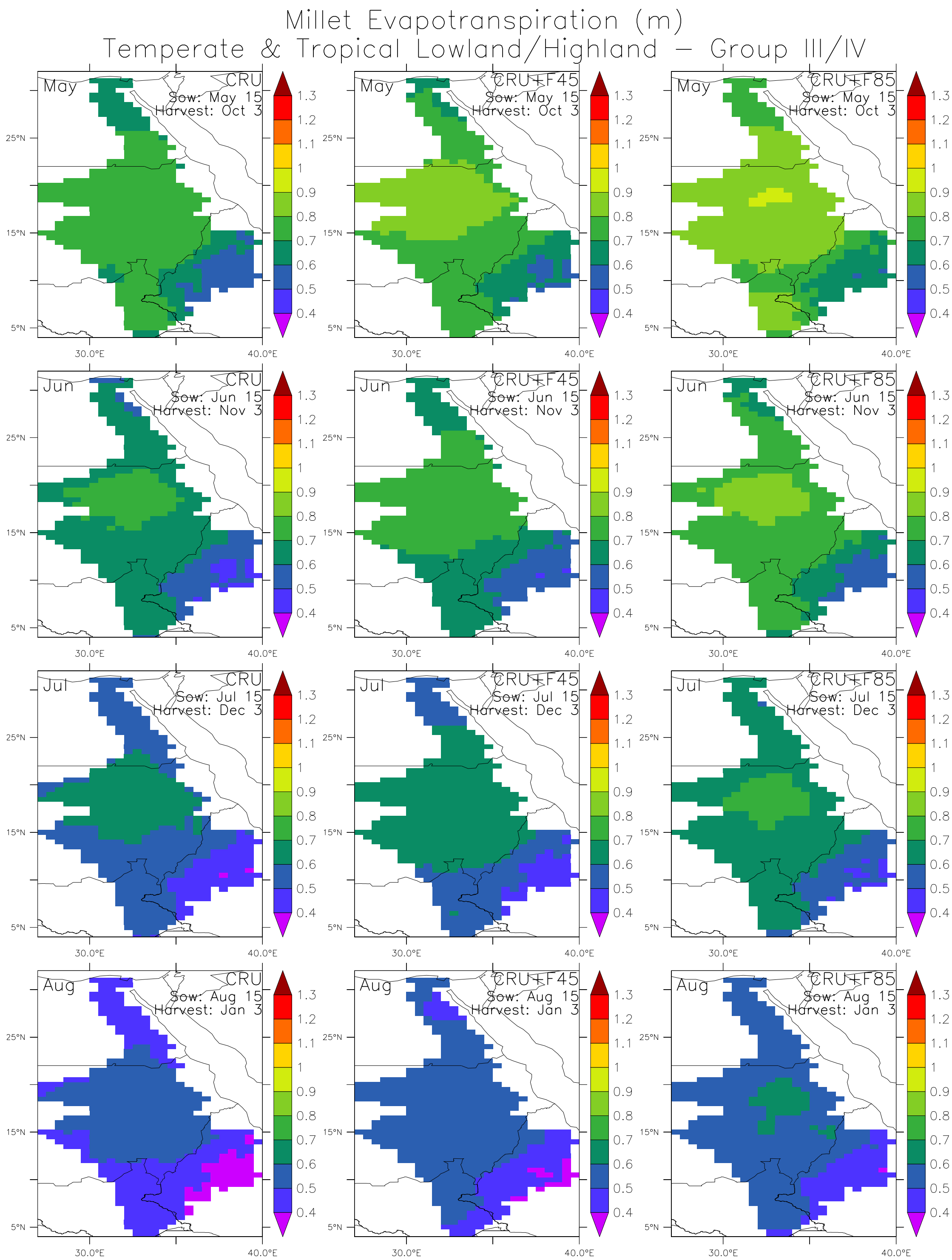
Millet Evapotranspiration (m)
Temperate & Tropical Lowland/Highland – Group III/IV
May
CRU
Sow: May 15
Harvest: Oct 3
CRU+F45
CRU+F85
Jun
Sow: Jun 15
Harvest: Nov 3
Jul
Sow: Jul 15
Harvest: Dec 3
Aug
Sow: Aug 15
Harvest: Jan 3
1.3
1.2
1.1
1
0.9
0.8
0.7
0.6
0.5
0.4
25°N
15°N
5°N
30.0°E
40.0°E

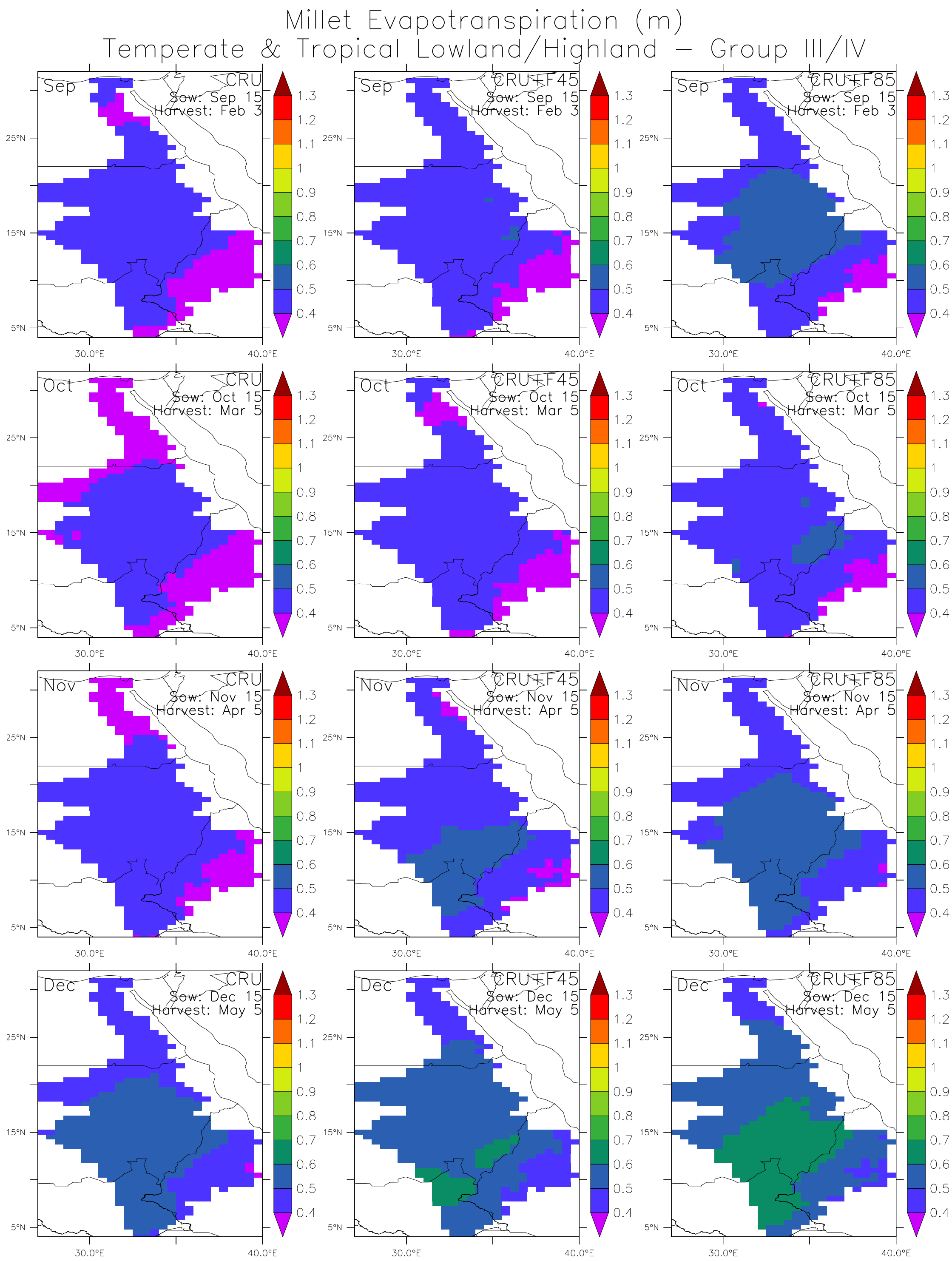

Figure 71: Temperate and tropical highland millet evapotranspiration in m based on surface temperature. Left column: CRU; middle column: CRU+F45; and right column: CRU+F85. The values are masked for temperature suitability for Group I operative conditions over the entire growing season. Each panel represents a different sow date starting January 15 with one-month shifts.

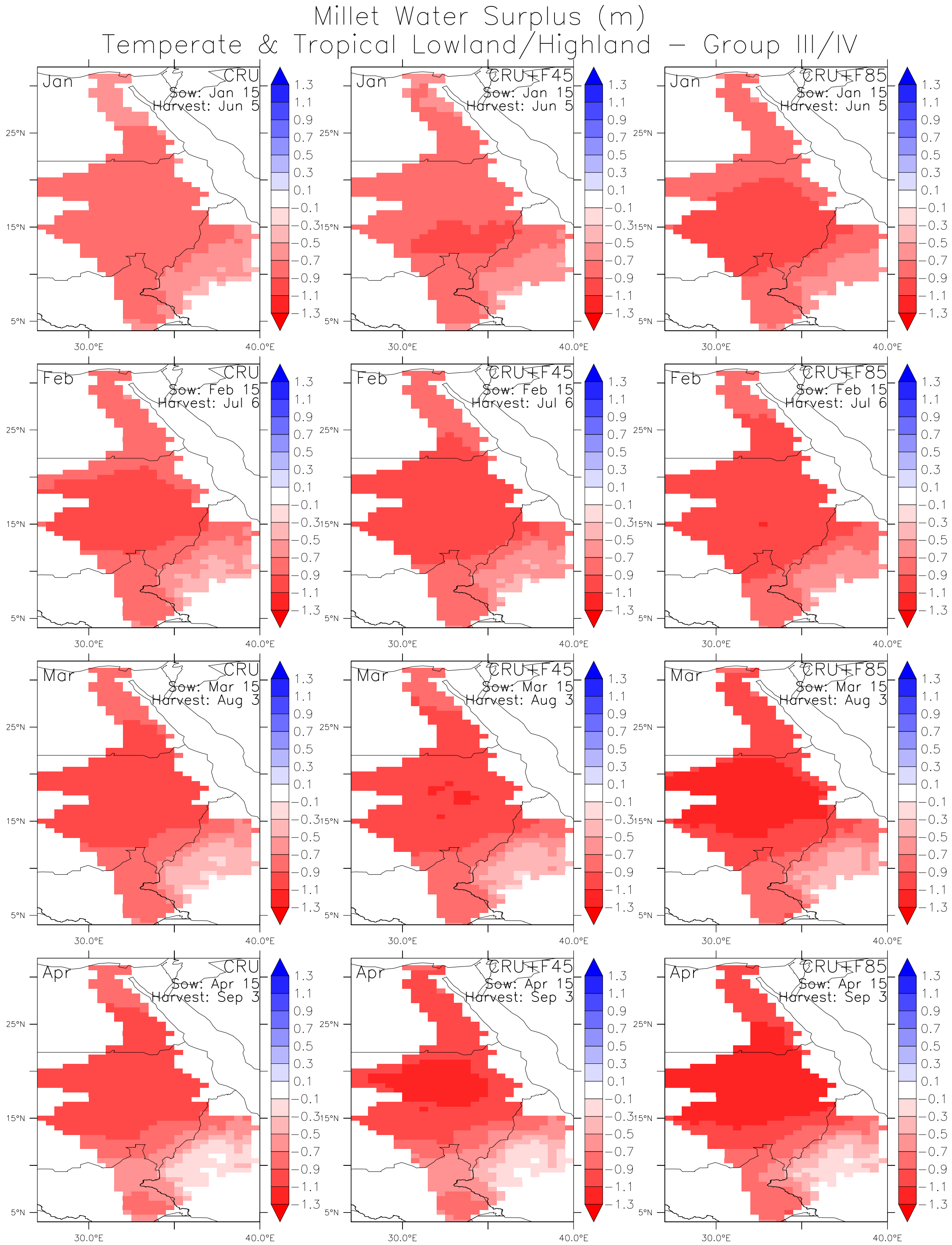
Millet Water Surplus (m)
Temperate & Tropical Lowland/Highland – Group III/IV
Jan
CRU
Sow: Jan 15
Harvest: Jun 5
CRU+F45
CRU+F85
Feb
Sow: Feb 15
Harvest: Jul 6
Mar
Sow: Mar 15
Harvest: Aug 3
Apr
Sow: Apr 15
Harvest: Sep 3
1.3
1.1
0.9
0.7
0.5
0.3
0.1
-0.1
-0.3
-0.5
-0.7
-0.9
-1.1
-1.3
25°N
15°N
5°N
30.0°E
40.0°E

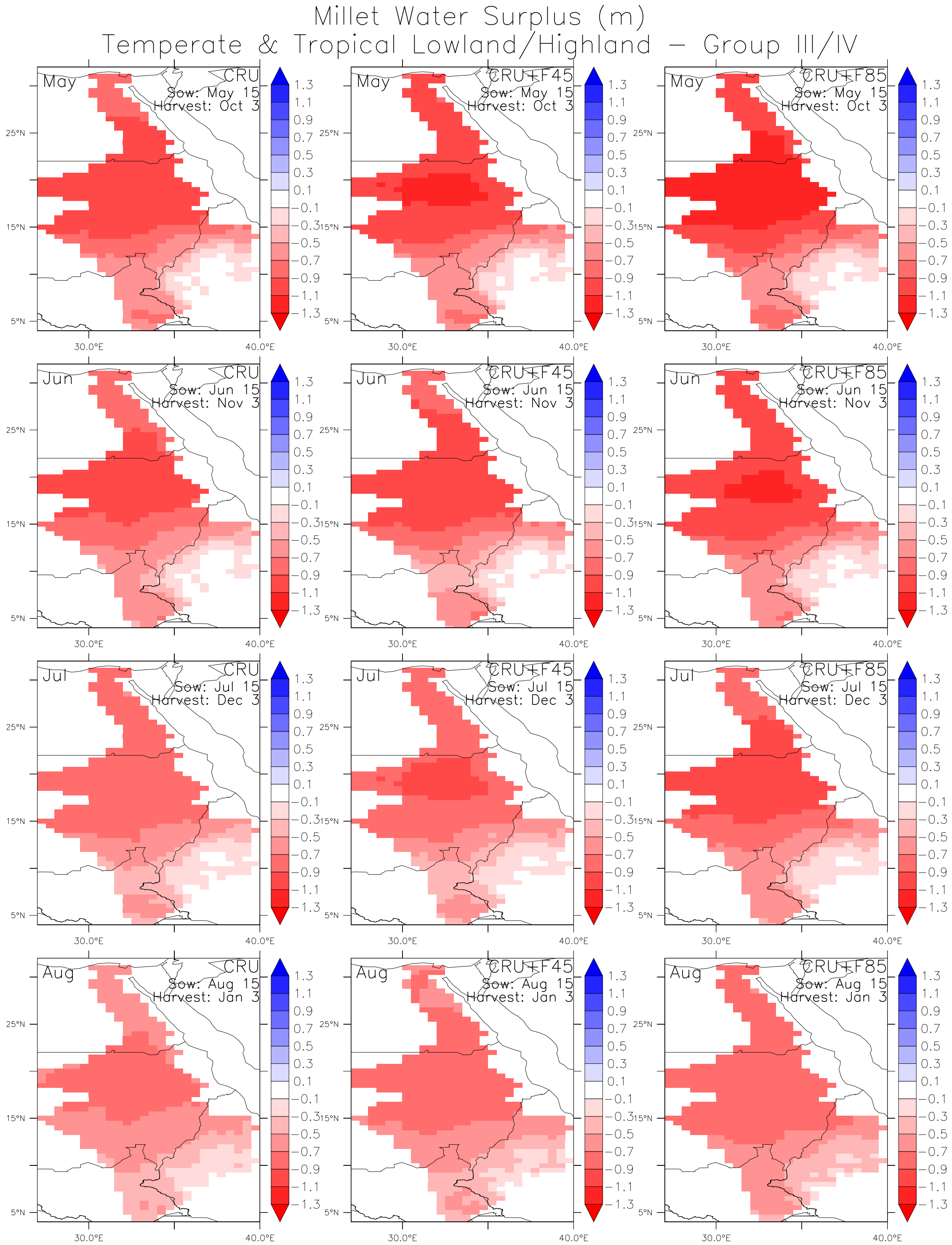
Millet Water Surplus (m)
Temperate & Tropical Lowland/Highland – Group III/IV
May
CRU
Sow: May 15
Harvest: Oct 3
CRU+F45
CRU+F85
Jun
Sow: Jun 15
Harvest: Nov 3
Jul
Sow: Jul 15
Harvest: Dec 3
Aug
Sow: Aug 15
Harvest: Jan 3
25°N
15°N
5°N
30.0°E
40.0°E
1.3
1.1
0.9
0.7
0.5
0.3
0.1
−0.1
−0.3
−0.5
−0.7
−0.9
−1.1
−1.3

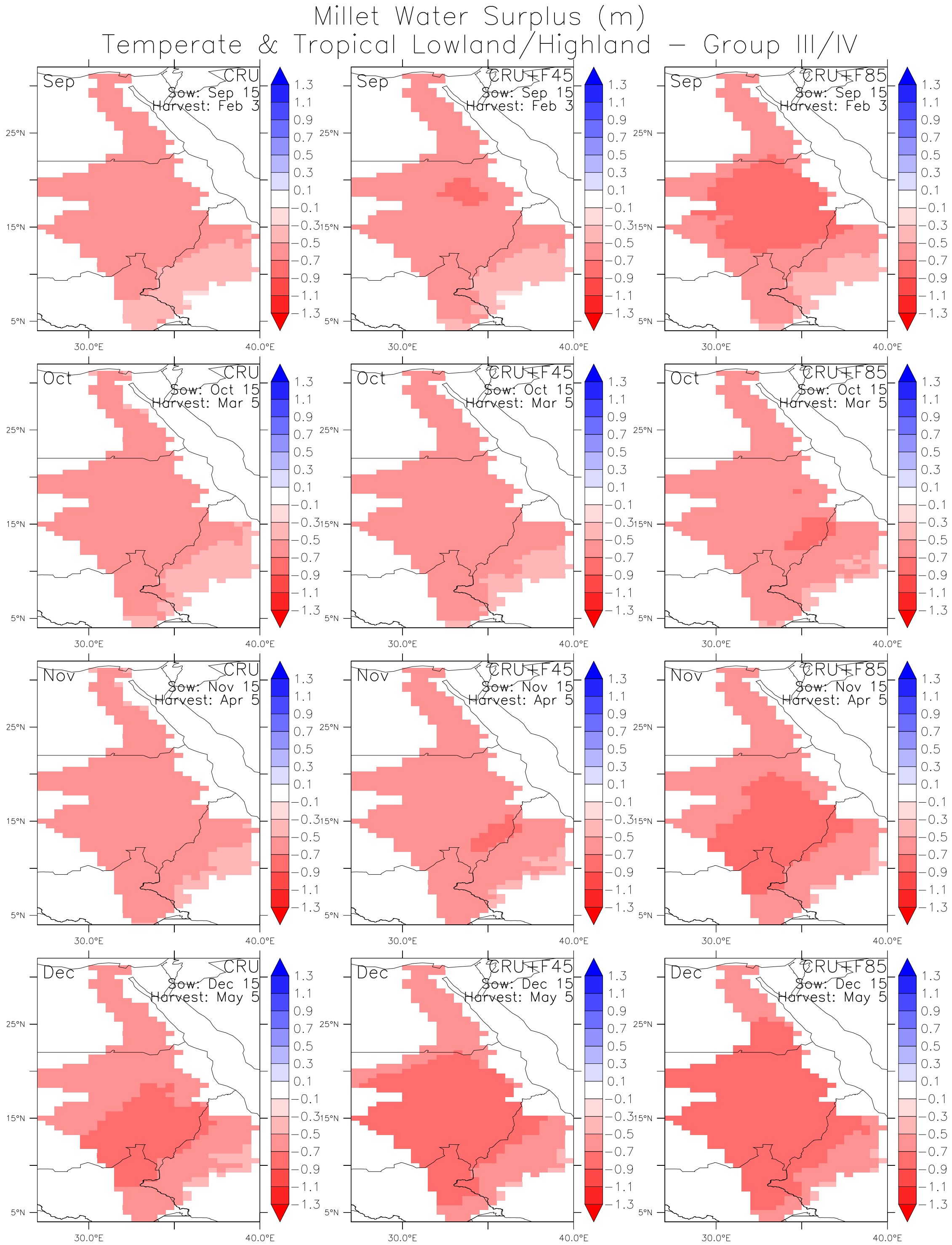

Figure 72: Temperate and tropical highland millet water surplus in m based on surface temperature. Left column: CRU; middle column: CRU+F45; and right column: CRU+F85. The values are masked for temperature suitability for Group I operative conditions over the entire growing season. Each panel represents a different sow date starting January 15 with one-month shifts. Blue shading indicates a surplus, while red shading indicates a deficit.

8 Recommendations

In this final phase, recommendations are made based on the above findings. This includes possible adjustments in crop types and cropping patterns as well as other measures to adapt to these impacts.

The projected changes in temperature, regardless of the emissions scenario result in large changes in crop suitability. In general, there are both spatial and temporal shifts in suitability. Crops suited for cooler climates shift north and south out of Sudan and southern Egypt to higher elevations such as the Ethiopian Highlands and north to the Nile Delta. In addition, crops suitable in warmers months shift to the cooler winter months. The largest decreases are to Group I crops (e.g., wheat, barley, oats, and potatoes) and Group II crops (e.g., rice, cotton, cassava, and groundnut), which become unsuitable in much of the region due to their lower temperature suitability range. On the contrary, Group III crops (e.g., maize, sorghum, and millet) tend to benefit in terms total area suitable for cultivation due to their higher temperature suitability range.

The Eastern Nile region remains suitable for crop growth; however, the areas of optimal growth reduce considerably. The resulting decrease in productivity with a warmer climate would to some extent likely be compensated by improvements in agricultural technologies and by fertilization effect from the increased atmospheric carbon dioxide. However, populations are also expected to grow substantially, which would increase agricultural demand.

Crop evapotranspiration increases substantially over the entire region due to the increases in temperature and resulting increases in reference evapotranspiration. This results in a substantial increase in irrigation required to meet the crops needs (except in summer in the Ethiopian Highlands where rainfall increases).

Based on these findings, the following five recommendations should be considered as long-term adaptation measures:

1. In Sudan, South Sudan, and Egypt, the primary growing season should be shifted to cooler periods so that the primary crops in the region can remain suitable.
2. Group I and II crops (e.g., wheat, barley, oats, rice, and cotton) should be phased out in Sudan, South Sudan, and Egypt in favor of heat tolerant Group III crops (e.g., maize, sorghum, and millet).
3. To meet the additional irrigation requirements in Sudan, South Sudan, and Egypt, additional reservoirs should be considered in Ethiopia and perhaps South Sudan.
4. High water demand crops such as rice, sugarcane, and grain maize should be phased out in favor of lower demand crops such as sorghum and millet.
5. Efforts to increase agricultural productivity in Ethiopia where crops remain optimal for growth should be made to compensate for potential reductions in productivity in Sudan and Ethiopia. This would require fair trade agreements between the countries (if they do not already exist) and better land management practices in Ethiopia.

9 References

Adar (2007): Kenya's Foreign Policy and Geopolitical Interests: The Case of the Nile River Basin. African Sociological Review 11 (1): 63-80.

Anyah R. O., F. H. M. Semazzi and L. Xie (2006): Simulated physical mechanisms associated with multiscale climate variability over Lake Victoria Basin in East Africa. Mon. Wea. Rev., 134, 3588-3609.

Arayaa, A., L. Stroosnijderb, G. Girmayc, and S.D. Keesstrab (2011): Crop coefficient, yield response to water stress and water productivity of teff (Eragrostis tef (Zucc.). Agricultural Water Management, 98, 775–783, doi:10.1016/j.agwat.2010.12.001.

Arnell N.W (1999): Climate change and global water resources. Global Environmental Change 9: S31–S50.

Beltrando G. and P.Camberlin (1993): Interannual variability of rainfall in the Eastern Horn of Africa and indicators of atmospheric circulation. International Journal of Climatology 13: 533-546.

Beyene Tazebe, Dennis P. Lettenmaier, and Pavel Kabat (2007): Hydrologic Impacts of Climate Change on the Nile River Basin: Implications of the 2007 IPCC Climate Change. UW Land Surface Hydrology Research Group.

Beyene T., Lettenmaier D. P., and Kabat P (2010): Hydrologic impacts of climate change on the Nile River Basin: implications of the 2007 IPCC scenarios. Clim. Change 100: 433–461.

Boko M., I. Niang, A. Nyong, C. Vogel, A. Githeko, M. Medany, B. Osman-Elasha, R. Tabo, and P. Yanda (2007): Africa. Climate Change 2007: Impacts, Adaptation and Vulnerability. Contribution of Working Group II to the Fourth Assessment Report of the Intergovernmental Panel on Climate Change, M. L. Parry, O. F. Canziani, J. P. Palutikof, P. J. van der Linden, and C. E. Hanson, Eds., Cambridge University Press, 433-467.

Buontempo, C. J.K. Lørup, M.A. Antar, M. Sanderson, M.B. Butts, E. Palin, R. McCarthy, R. Jones, R Betts. (2009): Assessing the impacts of climate change on the water resources in the Nile Basin using a regional climate model ensemble, Climate change: Global Risks, Challenges & Decisions. Copenhagen 10-12 March, 2009. IOP Conf. Ser.: Earth Environ. Sci. 6 292017 http://iopscience.iop.org/1755-1315/6/29

Burke M., Jorde K., Buffington K.M. (2009): Application of a hierarchical framework for assessing environmental impacts of dam operation: changes in streamflow, bed mobility and recruitment of riparian trees in a western North American river. Journal of Environmental Management 90 (S3), S224–S236.

Camberlin P. (1997): Rainfall anomalies in the source region of the Nile and their connection with the Indian summer monsoon. Journal of Climate 10: 1380-1392.

Camberlin P. (2009): Nile Basin Climates. In "The Nile: Origin, Environments, Limnology and Human Use", Dumont, Henri J. (Ed.), Monographiae Biologicae, Springer, 307-333.

Challinor AJ, Wheeler TR, Slingo JM, Hemming D (2005): Quantification of physical and biological uncertainty in the simulation of the yield of a tropical crop using present day and doubled CO2 climates. Phil Trans Roy Soc Lond, B 360(1463):1981-2194.

Cline, W.R., 2007: Global Warming and Agriculture: Impact Estimates by Country. Washington: Center for Global Development and Peterson Institute for International Economics.

Conway D. (1997): A water balance model of the upper Blue Nile in Ethiopia, Hydrological Sciences (42) 265-282.

Conway D. (2000): The climate and hydrology of the Upper Blue Nile River, The Geographical Journal 166: 49-62.

Conway, D. (2005): From headwater tributaries to international river: Observing and adapting to climate variability and change in the Nile basin, Global Environ. Change Part A 15: 99-114.

Conway D. and M. Hulme (1993): Recent fluctuations in precipitation and runoff over the Nile sub-basins and their impact on main Nile discharge, Climatic Change 25: 127-151.

Conway D. and M. l. Hulme (1996): The impacts of climate variability and future climate change in the Nile Basin on water resources in Egypt, Water Resources Development 12: 277-296.

Davidson O., K. Halsnaes, S. Huq, M. Kok, B. Metz, Y. Sokona and J. Verhagen (2003): The development and climate nexus: the case of sub-Saharan Africa. Climate Policy 3: 97-113.

Dee, D.P., with 35 co-authors, 2011: The ERA-Interim reanalysis: configuration and performance of the data assimilation system. Quart. J. R. Meteorol. Soc., 137, DOI: 10.1002/qj.828.

Domroes M and El-Tantawi A. (2005): Recent temporal and spatial temperature changes in Egypt. International Journal of Climatology 25: 51-63.

Dumont HJ (2009): The Cnidaria of the Nile Basin. In: Dumont HJ (ed), The Nile: Origin, environments, limnology and human use. Springer, 495-498.

Eldaw, A.M. (2004): The Gezira Scheme: Perspectives for Sustainable Development. German Development Institute, ISBN 3-88985-262-9.

Elshamy M. E. A. M. (2000): Impacts of climate change on Nile flows, Diploma of Imperial College (DIC), Civil and Environmental Engineering, Imperial College London, London, UK.

Elshamy M. E., Seierstad I. A., and Sorteberg A. (2009): Impacts of climate change on Blue Nile flows using bias-corrected GCM scenarios, Hydrol. Earth Syst. Sci. 13: 551-565, doi:10.5194/hess-13-551-2009.

Evans T. (1990): History of Nile Flows. In: H.P. P. and A. J.A. (Editors), The Nile: Resource Evaluation, Resource Management, Hydropolitics and Legal Issues. SOAS-RGS, London, pp. 5-39.

FAO; 1978: Report on the Agro-ecological Zones Project. Vol. 1. Methodology and results for Africa. World Soil Resources Report 48/1, FAO, Rome. http://ufdc.ufl.edu/UF00085364/00001

FAO, 1980: Land Resources for Populations of the Future. Report of the Second FAO/UNFPA Expert Consultation. FAO, Rome. http://books.google.com/books?id=X2mIrSVbrucC&pg=PA315&source=gbs_selected_pages&cad=3#v=onepage&q&f=false

FAO, 1985: Guidelines: land evaluation for irrigated agriculture. FAO Soils Bulletin 55. http://www.fao.org/docrep/X5648E/X5648E00.htm

FAO, 1986: Irrigation Water Management: Irrigation Water Needs. Irrigation Water Management Training manual no. 3. FAO, Rome. http://www.fao.org/docrep/S2022E/s2022e00.htm#Contents

FAO, 1993: Agro-Ecological Land Resources Assessment For Agricultural Development Planning: A Case Study of Kenya Resources Data Base and Land Productivity Main Report.
http://www.fao.org/docrep/009/t0737e/t0737e00.htm
http://www.fao.org/docrep/009/t0741e/T0741E00.htm#TOC

FAO, 1998: Crop evapotranspiration - Guidelines for computing crop water requirements. FAO Irrigation and Drainage Papers, 56, Retrieved from http://www.fao.org/docrep/X0490E/X0490E00.htm

FAO, 2000: Irrigation and Drainage Paper 56. Crop Evapotranspiration. http://www.kimberly.uidaho.edu/ref-et/fao56.pdf

FAO, 2010: Plan of Action for Southern Sudan: Emergency response and rehabilitation for food and agriculture. Food and Agriculture Organization of the United Nations. Emergency Operations and Rehabilitation Division. http://www.fao.org/fileadmin/templates/tc/tce/pdf/SSudan_PoA.pdf

FAO Crop Calendar, 2012: Crop Calendar – An information Tool for Seed Security. http://www.fao.org/agriculture/seed/cropcalendar/cropcalendar.do

FAOSTAT, 2012: Statistical Database Production. Food and Agriculture Organization of the United Nations (FAO), Rome. Retrieved from http://faostat.fao.org/

Funk C., Senay G., Asfaw A., Verdin J., Rowland J., Korecha D., Eilerts G., Michaelsen J., Amer S. and Choularton R. (2005): Recent Drought Tendencies in Ethiopia and Equatorial Subtropical Eastern Africa, Famine Early Warning System, US Agency for International Development.

Flohn H. (1987): East African rains of 1961/62 and the abrupt change of the White Nile discharge. Palaeoecology of Africa 18: 3-18.

GAIN, 2010: Ethiopia grain and feed annual report, GAIN Report ET 1201.

Gleick PH (1991): The vulnerability of runoff in the Nile Basin to climate changes. Environ Prof 13:66-73.

Gornall, J., R. A. Betts, Eleanor Burke, R. A. Clark, J. Camp, K. Willett, and A. Wiltshire. (2010): Implications of Climate Change for Agricultural Productivity in the Early Twenty-First Century. Philosophical Transactions of the Royal Society B 365: 2973-89.

Hasanean H.M. and H. Abdel-Basset (2006): Variability of Summer temperature over Egypt. International journal of Climatology 26: 1619 -1634.

Hulme M., R. Doherty, T. Ngara and M. New (2005): Global warming and African climate change. Climate Change and Africa, P.S Low, Ed., Cambridge University Press, Cambridge, 29-40.

Hulme M., R. Doherty, T. Ngara, M. New and D. Lister, 2001: African Climate Change: 1900-2100. Climate Research 17: 145-168.

Ibrahim, A. M. (1984): The Nile-Description, hydrology, control and utilization, Hydrobiologia, 110, 1-13.

IPCC, 2000: Special Report on Emissions Scenarios, 570 pp., Cambridge University Press, Cambridge, U.K.

IPCC (2007): Climate Change 2007: The Physical Science Basis. Contribution of Working Group I to the Fourth Assessment Report of the Intergovernmental Panel on Climate Change [Solomon, S., D. Qin, M. Manning, Z. Chen, M. Marquis, K.B. Averyt, M. Tignor and H.L. Miller (eds.)]. Cambridge University Press, Cambridge, United Kingdom and New York, NY, USA, 996 pp.

Jaramillo J, Muchugu E, Vega FE, Davis A, Borgemeister C, et al. (2011): Some Like It Hot: The Influence and Implications of Climate Change on Coffee Berry Borer (Hypothenemus hampei) and Coffee Production in East Africa. PLoS ONE 6(9): e24528. doi:10.1371/journal.pone.0024528

King'uyu S.M., L.A. Ogallo and E.K. Anyamba (2000): Recent trends of minimum and maximum surface temperatures over Eastern Africa. J. Climate 13: 2876-2886.

Knox J. W., Rodríguez Díaz J. A., Nixon D. J., and Mkhwanazi M. (2010): A preliminary assessment of climate change impacts on sugarcane in Swaziland. Agricultural Systems 103: 63–72.

Kurukulasuriya, P., and Mendelsohn, R. (2008): Crop switching as a strategy for adapting to climate change, African Journal of Agricultural and Resource Economics, Volume 2, No. 1 (March), Pretoria

Lobell DB, Burke MB, Tebaldi C, Mastrandrea MD, Falcon WP, Naylor RL. 2008: Prioritizing climate change adaptation needs for food security in 2030. Science 319: 607-610.

McCarthy J.J., Canziani O., Leary N., Kokken D. and White K., 2001: Climate Change 2001: Impacts, Adaptation, and Vulnerability. New York, NY: Cambridge University Press.

Metz, H.C., 1990: Egypt: A Country Study. Washington: GPO for the Library of Congress, 1990.

Mitchell, T.D., Carter, T.R., Jones, P.D., Hulme, M., and New, M., 2003: A comprehensive set of climate scenarios for Europe and the globe. Tyndall Centre Working Paper 55.

Mitchell T.D., Carter T.R., Jones PD, Hulme M, New M., 2004: A Comprehensive Set of High-Resolution Grids of Monthly Climate for Europe and the Globe: The Observed Record (1901-2000) and 16 Scenarios (2001-2100). Tyndall Centre for Climate Change Research, Norwich, U.K., Working Paper 55.

Mohamed Y.A., van den Hurk B., Savenije H.H.G., and Bastiaanssen W.G.M., 2005: Hydroclimatology of the Nile: results from a regional climate model, Hydrol. Earth Syst. Sci. 9: 263-278.

Moss R. H., Edmonds J. A., Hibbard K. A., Manning M. R., Rose S. K., van Vuuren D. P., Carter T. R., Emori S., Kainuma M., Kram T., Meehl G. A., Mitchell J. F., Nakicenovic N., Riahi K., Smith S. J., Stouffer R. J., Thomson A. M., Weyant J. P., Wilbanks T. J. (2010): The next generation of scenarios for climate change research and assessment. Nature. 463(7282):747-56.

Mu, Q., M. Zhao, S. W. Running, 2011: Remote Sensing of Environment, 115 doi:10.1016/j.rse.2011.02.019.

Nakicenovic N. and Swart R.J. (2000): Emissions Scenarios 2000 - Special Report of the Intergovernmental Panel on Climate Change, Cambridge University Press, Cambridge.

Osman M. and P. Sauerborn (2002): A preliminary assessment of characteristics and long-term variability of rainfall in Ethiopia-basis for sustainable land use and resource management. Conference in International Agriculture Research, Deutscher.Tropentag, Witzenhausen, 9-11 October.

Pal JS, Giorgi F, Bi X, Elguindi N, Solmon F, Gao X, Rauscher SA, Francisco R, Zakey A, Winter J, Ashfaq M, Syed FS, Bell JL, Diffenbaugh NS, Karmacharya J, Konare A, Martinez D, Da Rocha RP, Sloan LC, Steiner A (2007) Regional climate modeling for the developing world: the ICTP RegCM3 and RegCNET. Bull Am Meteorol Soc 89:1395–1409. doi:10.1175/ BAMS-88-9-1395.

Parry M. L., Rosenzweig C., Iglesias A., Livermore M. and Fischer G. (2004): Effects of climate change on global food production under SRES emissions and socio-economic scenarios. Global Environmental Change-Human and Policy Dimensions 14: 53-67.

Parry M. L., Canziani O. F., Palutikof J. P., Van Der Linden P. J., Hanson C. E. (2007): Contribution of Working Group II to the Fourth Assessment Report of the Intergovernmental Panel on Climate Change, 2007. Cambridge University Press, Cambridge, United Kingdom and New York, NY, USA.

Pierce CI, Rasmussen JB, Legget WC (1996): Back-calculation of fish length from scales: empirical comparison of proportional methods. Trans. Am. Fish. Soc. 125: 889-898.

Plusquellec, H. (1990): The Gezira Irrigation Scheme in Sudan: Objectives, Design, and Performance. World Bank Technical Paper Number 120, ISSN 0253-749.

Roeckner, E., G. Bäuml, L. Bonaventura, R. Brokopf, M. Esch, M. Giorgetta, S. Hagemann, I. Kirchner, L. Kornblueh, E. Manzini, A. Rhodin, U. Schlese, U. Schulzweida, and A. Tompkins, 2003: The atmospheric general circulation model ECHAM5. Part I: Model description. Max Planck Institute for Meteorology Rep. 349, 127 pp.

Said R. (1993): The River Nile: Geology, Hydrology and Utilization, 320pp. Elsevier, New York.

Sayed MAA (2004): Lake Nasser Management, Integration with Risks Posed by Floods and Droughts Hazards, for Achieving Food Security in Egypt, Invited to World Water Week, Stockholm Water Symposium, Stockholm, 15-21 August, 2004.

Seleshi Y. and Demarée G. R. (1995): Rainfall variability in the Ethiopian and Eritrean highlands and its links with the Southern Oscillation Index. Journal of Biogeography 22: 945-952.

Seleshi Y., U. Zanke, 2004: Recent changes in rainfall and rainy days in Ethiopia. International Journal of Climatology 24, 973-983.

Stern N (2007): The Economics of Climate Change: The Stern Review. Cambridge University Press, Cambridge, 692 pp.

Strzepek K., Yates D., and El Quosy, D. (1996): Vulnerability assessment of water resources in Egypt to climate changes in the Nile Basin. Clim. Res. 6: 89-95.

Strzepek K., Yates D.N., Yohe G., Tol R.J.S., Mader N. (2001): Constructing 'not implausible' climate and economic scenarios for Egypt. Integrated Assessment 2, 139-157. In Conway, D. 2003, From headwater tributaries to international river: observing and adapting to climate variability and change in the Nile basin/ Global Environmental Change, PP16.

Tafesse T. (2001): The Nile Question: Hydropolitics, Legal Wrangling, Modus Vivendi and Perspectives. LIT Verlag, London.

Tate E., Sutcliffe J., Conway D., and Farquharson F. (2004): Water balance of Lake Victoria: update to 2000 and climate change modeling to 2100. Hydrol. Sci. J. 49: 563-574.

Tesemma Z.K., Mohamed Y.A. and Steenhuis T.S. (2010): Trends in rainfall and runoff in the Blue Nile Basin: 1964-2003. Hydrological Processes 24: 3747-3758.

Thornton PK, Jones PG, Owiyo T, Kruska RL, Herrero M, Orindi V, Bhadwal S, Kristjanson P, Notenbaert A, Bekele N, Omolo A (2008): Climate change and povert in Africa: mapping hotspots of vulnerability. African Journal of Agricultural and Resource Economics 2(1):24–44

Willmott CJ, Matsuura K, 2001: Terrestrial air temperature and precipitation: monthly and annual time series (1950–1999). University of Delaware, Newark.

Yates, D.N. and K.M. Strzepek (1998): Modeling the Nile basin under climatic change. Journal of Hydrologic Engineering 3(2): 98-108.

Yates, David N. and Kenneth M. Strzepek (1998a) Assessment of integrated climate change impacts on the agricultural economy of Egypt. Climatic Change 38:261-287.